VOLUME 38 MARCH 1960 NUMBER 3

Canadian Journal of Chemistry

Editor: LÉO MARION

Associate Editors:

HERBERT C. BROWN, *Purdue University*
A. R. GORDON, *University of Toronto*
C. B. PURVES, *McGill University*
SIR ERIC RIDEAL, *Imperial College, University of London*
J. W. T. SPINKS, *University of Saskatchewan*
E. W. R. STEACIE, *National Research Council of Canada*
H. G. THODE, *McMaster University*
A. E. VAN ARKEL, *University of Leiden*

Published by THE NATIONAL RESEARCH COUNCIL

OTTAWA CANADA

Canadian Journal of Chemistry

Under the authority of the Chairman of the Committee of the Privy Council on Scientific and Industrial Research, the National Research Council issues THE CANADIAN JOURNAL OF CHEMISTRY and five other journals devoted to the publication, in English or French, of the results of original scientific research. Matters of general policy concerning these journals are the responsibility of a joint Editorial Board consisting of: members representing the National Research Council of Canada; the Editors of the Journals; and members representing the Royal Society of Canada and four other scientific societies.

The Chemical Institute of Canada has chosen the Canadian Journal of Chemistry as its medium of publication for scientific papers.

EDITORIAL BOARD

Representatives of the National Research Council

I. McT. Cowan, *University of British Columbia*
A. Gauthier, *University of Montreal*
H. G. Thode (Chairman), *McMaster University*
D. L. Thomson, *McGill University*

Editors of the Journals

D. L. Bailey, *University of Toronto*
T. W. M. Cameron, *Macdonald College*
H. E. Duckworth, *McMaster University*
Léo Marion, *National Research Council*
J. F. Morgan, *Department of National Health and Welfare, Ottawa*
R. G. E. Murray, *University of Western Ontario*
J. A. F. Stevenson, *University of Western Ontario*

Representatives of Societies

D. L. Bailey, *University of Toronto*
Royal Society of Canada
T. W. M. Cameron, *Macdonald College*
Royal Society of Canada
H. E. Duckworth, *McMaster University*
Royal Society of Canada
Canadian Association of Physicists
P. R. Gendron, *University of Ottawa*
Chemical Institute of Canada
J. F. Morgan, *Department of National Health and Welfare, Ottawa*
Canadian Biochemical Society
R. G. E. Murray, *University of Western Ontario*
Canadian Society of Microbiologists
J. A. F. Stevenson, *University of Western Ontario*
Canadian Physiological Society
T. Thorvaldson, *University of Saskatchewan*
Royal Society of Canada

Ex officio

Léo Marion (Editor-in-Chief), *National Research Council*
J. B. Marshall (Administration and Awards), *National Research Council*

Manuscripts for publication should be submitted to Dr. Léo Marion, Editor-in-Chief, Canadian Journal of Chemistry, National Research Council, Ottawa 2, Canada.
(For instructions on preparation of copy, see **Notes to Contributors** (inside back cover).)

Proof, correspondence concerning proof, and orders for reprints should be sent to the Manager, Editorial Office (Research Journals), Division of Administration and Awards, National Research Council, Ottawa 2, Canada.

Subscriptions, renewals, requests for single or back numbers, and all remittances should be sent to Division of Administration and Awards, National Research Council, Ottawa 2, Canada. Remittances should be made payable to the Receiver General of Canada, credit National Research Council.

The journals published, frequency of publication, and subscription prices are:

Canadian Journal of Biochemistry and Physiology	Monthly	$9.00 a year
Canadian Journal of Botany	Bimonthly	$6.00 a year
Canadian Journal of Chemistry	Monthly	$12.00 a year
Canadian Journal of Microbiology	Bimonthly	$6.00 a year
Canadian Journal of Physics	Monthly	$9.00 a year
Canadian Journal of Zoology	Bimonthly	$5.00 a year

The price of regular single numbers of all journals is $2.00.

Canadian Journal of Chemistry

Issued by THE NATIONAL RESEARCH COUNCIL OF CANADA

VOLUME 38 MARCH 1960 NUMBER 3

MAGNETIC PROPERTIES OF MESONAPHTHODIANTHRENE[1]

YOSHIO MATSUNAGA[2]

ABSTRACT

Electron spin resonance absorption was detected in mesonaphthodianthrene and mesonaphthodianthrone. The spectra of both of these compounds consist of, at least, seven lines with a separation of 4.4 oersteds and the central line has a *g*-value of 2.0024±0.0002. The growth of the central line by admission of air was observed in the case of the hydrocarbon. Some suggestions are presented as to the nature of the unpaired electrons in these compounds. The magnitude of the molar diamagnetic susceptibility of mesonaphthodianthrene, after correction for the paramagnetic contribution from the unpaired electrons, is discussed in relation to the molecular structure.

INTRODUCTION

The appearance of unpaired electrons has been reported in crystals of some highly conjugated molecules, namely metal-free phthalocyanine (1, 2), violanthrone (3, 4), violanthrene (3, 4), and binaphthoquinones (5). Here we wish to present the results of a study of mesonaphthodianthrene (I) and mesonaphthodianthrone (II) by the electron spin resonance method. The hydrocarbons studied are compounds which have anomalously small values of diamagnetic susceptibility (6). This anomaly was found to be characteristic of perylene (III) and its analogues. In the sense of the valence-bond theory the central single bonds in perylene, violanthrone (IV), and mesonaphthodianthrene can be doubled only in the excited states.

EXPERIMENTAL

Mesonaphthodianthrone was prepared by photodehydrogenation of bianthraquinone dissolved in pyridine (7). The hydrocarbon was obtained by the zinc-dust fusion of the quinone (8). The latter was found to be reactive towards oxygen, therefore our sample was stored in an evacuated tube after repeated sublimation in high vacuum.

The electron spin resonance was examined at a frequency of 9 kMc/s at room temperature, and at 77° K.

RESULTS

Unlike the spectra of the other paramagnetic polycyclic aromatic compounds, the spectra of mesonaphthodianthrene and its quinone show some structure and this can be modified by admission of air. The spectra of these two compounds consist of at least seven lines with a separation of 4.4 oersteds and spread over 50 oersteds as shown in Fig. 1. The *g*-value of the central peak, estimated by comparison with D.P.P.H. (2.0036), was found to be 2.0024±0.0002. The spin concentration was about 3×10^{21} per mole

[1]*Manuscript received October 16, 1959.*
Contribution from Department of Chemistry, University of British Columbia, Vancouver 8, B.C., Canada.
[2]*N.R.C. Postdoctoral Fellow 1957–59. On leave of absence from Department of Chemistry, University of Tokyo, Tokyo, Japan.*

in the hydrocarbon. This value was not affected by further sublimation nor by cooling to liquid-nitrogen temperature. The spin concentration in the quinone was about one-third of that of the hydrocarbon.

In contact with air the central peak in the spectrum of mesonaphthodianthrene grew slowly. After a few days the intensity of this sharp absorption reached its maximum. The line width of the signal from this oxygen-containing radical was about one oersted at half height. In Fig. 2, a higher magnetic-field modulation was used to detect the broad main absorption, so the central line is artificially broadened. The ratio of the number of unpaired electrons contributing to the sharp absorption to that contributing to the broad one was estimated as about one-tenth at its maximum. By evacuation for a few minutes the intensity of this sharp absorption was decreased considerably; however, only a slow decrease was observed by further prolonged evacuation at room temperature.

No electron spin resonance absorption was detected in bianthraquinone. However, samples heated to 194° C or higher show resonance absorption (9). No structure was observed and the line width at a half height was about twelve oersteds.

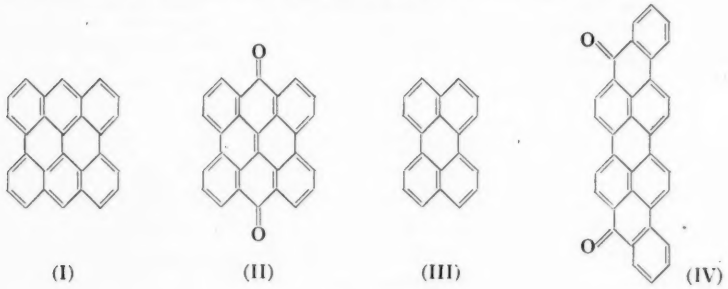

(I) (II) (III) (IV)

DISCUSSION

The nature of the broad absorption found in the hydrocarbon and quinone seems not to be simple. Winslow *et al.* (2) suggested that enough thermal energy is absorbed at room temperature to produce unpaired electrons in crystals of highly conjugated, metal-free phthalocyanine. Although the electron spin resonance absorption of naphthalene in a triplet state is too broad to be observed in a randomly orientated system (10), the dipolar interaction, which contributes to line broadening, is proportional to the inverse cube of the electron–electron distance, therefore the resonance absorption of the unpaired electrons in excited states might be detectable in large aromatic molecules like the present hydrocarbon. However, the spin concentration in our samples was found to be independent of temperature as in violanthrone (4).

FIG. 1. Derivative of electron spin resonance absorption of mesonaphthodianthrene in vacuum.

Polycyclic aromatic compounds have been known as intrinsic semiconductors and the activation energy for semiconduction was considered as the energy gap between the full

band and the empty band (11, 12, 13). Consequently the unpaired electrons in the present compounds cannot be considered charge carriers and must be trapped somewhere. It has been shown that crystals of highly conjugated aromatic molecules contain the imperfections which can behave as traps for charge carriers. Although the nature of the imperfections in molecular crystals is not well known, this term includes not only chemical impurities but also some kinds of lattice defects (14, 15). Because our hydrocarbon and quinone give the same hyperfine structure in resonance absorption, the unpaired electrons must be in a common situation in these compounds. The presence of hyperfine structure can be attributed to the dipolar interaction between an unpaired electron and several ring protons. The line splitting can be given approximately by $28/r^3$ where r is the electron–proton distance (16). The presence of seven or more lines with a separation of 4.4 oersteds suggests that the unpaired electron is surrounded by six or more protons at a distance of about 1.8 Å.

It seems highly likely that the unpaired electrons in our compounds are associated with some common impurity. If the impurity molecule has originally an unpaired electron, this free-radical molecule must be extraordinarily stable and survive through the processes of zinc-dust fusion and repeated vacuum sublimations. Besides, it seems to be unlikely that such a free-radical molecule, which must be formed in the process of photodehydrogenation of bianthraquinone, has six nearly equivalent protons at a distance of about 1.8 Å from the unpaired electron. It is more probable that the impurity molecules which have originally no unpaired electrons can create favorable sites to trap electrons by interaction with the semiconductive host lattice. In this case an unpaired electron may be shared by neighboring molecules and find six or more nearly equivalent protons at a distance as small as 1.8 Å. This situation may be similar to that in aromatic hydrocarbon – iodine complexes which show strong resonance absorption. Therefore, we extended our low-temperature measurements to molecular complexes. For example, perylene–iodine (2 : 3) complex gives a resonance absorption with a g-value of 2.0033. At room temperature the line width at a half power was about eight oersteds and the ratio of the number of unpaired electrons to that of perylene molecules was about 0.07 (17). On cooling to 77° K the line width decreases to about 2.5 oersteds and the spin concentration is estimated as 0.06. Similar decreases of line width were observed in pyranthrene– and violanthrene–iodine complexes. The spin concentration in the latter two is also found to be independent of temperature within the limit of experimental error. If unpaired electrons in these highly conductive molecular complexes are charge carriers, the spin concentration must be decreased by a factor of hundreds by cooling to liquid-nitrogen temperature (18). The appearance of unpaired electrons in hydrocarbon–iodine complexes is apparently related to the complex formation by strong intermolecular charge-transfer forces. However, the whole mechanism is not yet clear.

It is interesting to point out that if we compare the spin concentrations in violanthrone and its hydrocarbon (3, 4) and mesonaphthodianthrene and its quinone, in each pair the member which is of perylene type shows stronger resonance absorption than the other. This fact suggests the importance of the role of the host molecules in the appearance of unpaired electrons. Therefore, it might be possible that without impurity molecules the host molecules associated with some kind of lattice defects can form traps for unpaired electrons; however, at present we have no detailed knowledge of such lattice defects in molecular crystals.

The nature of the unpaired electrons in the other polycyclic aromatic compounds may be similar to those in the present hydrocarbon and quinone. We can hope to resolve

FIG. 2. Derivative of electron spin resonance absorption of mesonaphthodianthrene in air.

broad component lines from dipolar interaction in a randomly orientated solid sample only when the interaction is with equivalent protons. The absence of hyperfine structure in resonance absorption in the other cases may be due to non-equivalence of the interacting protons.

Oxygen molecules, which contribute to the appearance of a sharp line, seem to be combined loosely on the surface of crystals of the hydrocarbon, but the presence of slow diffusion in the formation and dissociation of this free radical is likely. Absence of detectable asymmetry in the sharp absorption line suggests that the new free radical has no axial symmetry; therefore the formation of a peroxide radical is not probable. The effect of oxygen on electron spin resonance absorption has been observed in a number of organic free radicals and carbonaceous materials; however, the effect in most cases is line broadening or disappearance. Similar appearance of a symmetric absorption by admission of air or oxygen has been reported only in the case of tri-*p*-nitrophenylmethyl where the *g*-value is as high as 2.006 (19). Therefore, the present case seems to be an entirely new kind of oxygen effect. Our oxygen-containing free radical, which gives a sharp line with a *g*-value as low as 2.0024, may be some kind of molecular complex formed by interaction between oxygen and the hydrocarbon molecule.

The effect of oxygen on the semiconductivity and the photoconductivity of some highly conjugated aromatic compounds is known (20, 21). Therefore, a study of the effect on the electrical properties of mesonaphthodianthrene might be fruitful in order to elucidate the nature of the oxygen-containing free radical. The semiconductivity of the present hydrocarbon was studied by Inokuchi but the oxygen effect was not considered (12).

Using London's molecular orbital theory for diamagnetic anisotropy of aromatic molecules, Hazato predicted that the conjugation between two naphthalene nuclei in a perylene molecule brings about a decrease of diamagnetic anisotropy from twice that of naphthalene (22). This prediction is qualitatively in agreement with the experimental results. We shall examine here whether or not the same relation is valid for mesonaph-

thodianthrene and violanthrone after the correction for the paramagnetic contribution from the unpaired electrons. The diamagnetic anisotropy ΔK is defined by the following equation,

$$\Delta K = 3(\chi_m - K_i),$$

where χ_m is the mean molar susceptibility and K_i is the isotropic part of molar susceptibility. The latter can be estimated by empirical rules (23, 24). Following our previous paper (6), the isotropic part will be estimated by

$$K_i \times 10^6 = -3.36 \times N_C - 2.93 \times N_H + 1.73 \times N_O,$$

where N_C, N_H, N_O are the numbers of aromatic carbon atoms, hydrogen atoms, and quinone oxygen atoms in a molecule. The results are summarized in Table I. All the

TABLE I

Diamagnetic susceptibilities and anisotropies of mesonaphthodianthrene and related compounds

Compound	Molar susceptibility (multiplied by 10^6)				
	Total by static method	Paramagnetic part by ESR	Diamagnetic part	Isotropic part	Anisotropy
Naphthalene	−91.9	0	−91.9	−57.0	−105
Perylene	−166.8	0	−166.8	−102.4	−193
Anthracene	−129.4	0	−129.4	−76.3	−159
Mesonaphthodianthrene	−214.6	+6	−220.6	−135.1	−257
Benzanthrone	−142.9	0	−142.9	−84.7	−175
Violanthrone	−204.8	+25 to +63*	−230 to −268	−157.7	−217 to −331

*See reference 4.

necessary values of susceptibility were taken from our previous paper. Although there is uncertainty in the values of the total molar susceptibility and the paramagnetic part because different preparations were used for the measurements with a Gouy balance and with an electron spin resonance spectrometer, it appears that the diamagnetic anisotropy of mesonaphthodianthrene is far less than twice that of anthracene even after the correction for the paramagnetic contribution from the unpaired electrons. A similar relation was found in violanthrone. The large difference between the anisotropy of mesonaphthodianthrene and twice that of anthracene suggests the presence of strong conjugation between two anthracene nuclei in a mesonaphthodianthrene molecule. This conclusion is in accordance with the fact that the difference between the calculated π-electron energy for mesonaphthodianthrene and twice that for anthracene is nearly twice as large as the similar difference for perylene and naphthalene as cited in Table II (25).

TABLE II

Total π-electron energies and average radii of π-electron orbitals in mesonaphthodianthrene and related compounds

Compound	Total π-electron energy by LCAO*	Average radius of π-electron orbital (Å)
Naphthalene	$3.68\,\beta$	1.57
Perylene	$8.24\,\beta$	1.51
Anthracene	$5.31\,\beta$	1.64
Mesonaphthodianthrene	$12.1\,\beta$	1.47

*See reference 25.

The diamagnetic anisotropy is correlated with the average radius of the π-electron orbital $\sqrt{\bar{r}^2}$ by the two-dimensional Langevin's equation,

$$\Delta K = -(Ne^2/4mc^2) \sum \bar{r}^2 = -4.248\times10^{10}\, p\bar{r}^2,$$

where p is the number of π-electrons in a molecule and the other symbols have the usual physical meanings (26). Therefore, as shown in Table II, we must conclude that, on the average, the π-electrons in the mesonaphthodianthrene molecule are less mobile than those in the anthracene molecule.

ACKNOWLEDGMENTS

The author would like to thank Professor C. A. McDowell for his interest and guidance throughout the course of this research. This work was supported by grants from the National Research Council of Canada, and we wish to thank that body for its generosity.

REFERENCES

1. D. J. E. Ingram and J. E. Bennett. J. Chem. Phys. **22**, 1136 (1954).
2. F. H. Winslow, W. O. Baker, and W. A. Yager. J. Am. Chem. Soc. **77**, 4751 (1955).
3. Y. Yokozawa and I. Tatsuzaki. J. Chem. Phys. **22**, 2087 (1954).
4. H. Akamatu, S. Mrozowski, and D. Wobschall. Proceedings of the Third Conference on Carbon. Pergamon Press, Inc., New York. 1959. p. 129.
5. Y. Matsunaga. Can. J. Chem. **37**, 1003 (1959).
6. H. Akamatu and Y. Matsunaga. Bull. Chem. Soc. Japan, **26**, 364 (1953).
7. H. Brockmann and R. Mühlmann. Chem. Ber. **82**, 348 (1949).
8. E. Clar. Ber. **72**, 1645 (1939).
9. W. G. Nielsen and G. K. Fraenkel. J. Chem. Phys. **21**, 1619 (1953).
10. C. A. Hutchison and B. W. Mangum. J. Chem. Phys. **29**, 952 (1958).
11. H. Akamatu and H. Inokuchi. J. Chem. Phys. **18**, 810 (1950); **20**, 1481 (1952).
12. H. Inokuchi. Bull. Chem. Soc. Japan, **24**, 222 (1951); **27**, 22 (1954).
13. D. D. Eley and G. D. Parfitt. Trans. Faraday Soc. **51**, 1529 (1955).
14. J. Kommandeur and W. G. Schneider. J. Chem. Phys. **28**, 590 (1958).
15. D. M. J. Compton, W. G. Schneider, and T. C. Waddington. J. Chem. Phys. **28**, 741 (1958).
16. D. J. E. Ingram. Free radicals as studied by electron spin resonance. Butterworth Scientific Publications, London. 1958. p. 117.
17. Y. Matsunaga. J. Chem. Phys. **30**, 855 (1959).
18. H. Akamatu, H. Inokuchi, and Y. Matsunaga. Bull. Chem. Soc. Japan, **29**, 213 (1956).
19. F. M. Schimmel and F. W. Heineken. Physica, **28**, 781 (1957).
20. H. Pick and W. Wissman. Z. Physik, **138**, 436 (1954).
21. T. C. Waddington and W. G. Schneider. Can. J. Chem. **36**, 789 (1958); and references cited there.
22. G. Hazato. Bull. Chem. Soc. Japan, **22**, 151 (1949).
23. H. Shiba and G. Hazato. Bull. Chem. Soc. Japan, **22**, 92 (1949).
24. A. Pacault. Bull. soc. chim. France, D, 40 (1949).
25. C. A. Coulson, L. J. Schaad, and L. Burnelle. Proceedings of the Third Conference on Carbon. Pergamon Press, Inc., New York. 1959. p. 27.
26. K. Lonsdale. Proc. Roy. Soc. (London), A, **159**, 149 (1937).

THE REACTIONS OF ACTIVE NITROGEN WITH CYANOGEN AND CN RADICALS[1]

CATHERINE HAGGART[2] AND C. A. WINKLER

ABSTRACT

Cyanogen is destroyed by active nitrogen at temperatures of 80° to 400° C, and nitrogen pressures of 0.34 to 3.1 mm, with the formation of polymer. At 400° C and sufficiently high flow rates of cyanogen, a constant amount is destroyed, which apparently corresponds to practically complete consumption of the available nitrogen atoms.

The formation of CN radicals in the reaction of cyanogen with active nitrogen was established by the production of HCN and CH_3CN when hydrogen or methane was added to the reaction mixture. The rate of destruction of cyanide radicals, when they were transported through a reaction vessel, was determined by introducing hydrogen below the site of reaction, and found to follow first order kinetics.

INTRODUCTION

The reactions of active nitrogen with saturated and unsaturated hydrocarbons have been studied and found generally to produce small amounts of cyanogen in addition to hydrogen cyanide as the main product. The behavior of cyanogen with active nitrogen has therefore been investigated, to assess, if possible, the significance of its presence in the reaction products, in relation to the mechanism of formation of hydrogen cyanide in the hydrocarbon – active nitrogen systems.

EXPERIMENTAL

The apparatus used in this investigation was similar to those described in previous papers from this laboratory (1, 2). A spherical reaction vessel was employed in preliminary experiments to study the reactions of CN radicals, but subsequently a cylindrical vessel made of 28-mm O.D. pyrex tubing was used. Since the results were essentially similar, regardless of the reaction vessel employed, only those results obtained with the cylindrical vessel are reported in detail.

Three nitrogen flow rates were used, 14, 130, and 315 μmoles per second, corresponding to nitrogen pressures of 0.34, 1.4, and 3.1 mm in the reaction vessel. In the experiments in which the nitrogen flow rate was 14 μmoles per second, the total pressure in the reaction vessel was maintained constant at 1.43 mm, by the addition of argon to the nitrogen prior to its introduction into the discharge tube.

As in previous studies, the active nitrogen concentration in the system (assumed to be nitrogen atoms) was estimated from the maximum amount of HCN produced in the ethylene – active nitrogen reaction at 300° C (3).

Cyanogen was analyzed by hydrolysis followed by estimation of the cyanide thus formed. Since the hydrolysis proceeds slowly in water but rapidly and almost quantitatively in sodium hydroxide (4) to produce sodium cyanide and sodium cyanate, the unreacted cyanogen was collected in 10 to 20 ml 10% NaOH and the cyanide was then analyzed by the Liebig–Dénigès method (5).

When methane was added to the cyanogen – active nitrogen reaction mixture, the

[1]*Manuscript received November 4, 1959.*
Contribution from the Upper Atmosphere Chemistry Research Group, the Physical Chemistry Laboratory, McGill University, Montreal, with financial assistance from Canadian Industries Limited and the National Research Council of Canada.
[2]*Holder of a C.I.L. Fellowship 1958–59.*

HCN and CH_3CN formed, as well as the unreacted cyanogen, were collected in a known volume of 10% NaOH which was then separated into three equal portions. The cyanide content of the first portion, consisting of HCN and the cyanide from the hydrolysis of cyanogen, was determined by the Liebig–Dénigès method. To the second portion, dilute sulphuric acid was added to expel the HCN, and after this solution was heated for 2 hours, the nitrogen content was determined by a Kjeldahl distillation (5). The value so obtained corresponded to the amount of cyanate present in the original solution due to the hydrolysis of the cyanogen. The difference between the amounts of cyanide and cyanate was equal to the HCN present in the original solution. Since Ouillemard (6) reported that methyl cyanide was quantitatively hydrolyzed by the action of concentrated sulphuric acid to form ammonia and acetic acid, concentrated sulphuric acid was carefully added to the third portion, which had been previously frozen in liquid air, and then the solution was digested at 150° C for 8 hours. After the digestion, the total nitrogen content of the solution was determined by a Kjeldahl distillation. The difference between the total nitrogen content of this last solution and the total cyanide content of the first portion of the original solution provided a measure of the methyl cyanide formed in the reaction.

In the experiments in which hydrogen was added as a second reactant, HCN and cyanogen were present in the reaction products and were separated and analyzed by the method described by Wallis (7) and Rhodes (8). Since HCN, but not cyanogen, reacts with acidified silver nitrate solution, both products were collected in a known volume of standard silver nitrate solution to which a few drops of dilute nitric acid had been added. Cyanogen was quantitatively recovered from the mixture by bubbling nitrogen through the absorber and then into three scrubbers (Wallis bubblers), one containing acidified silver nitrate and two containing 10% sodium hydroxide solution. The excess silver nitrate was titrated with potassium thiocyanate using ferrous ammonium sulphate indicator (5) and the amount of cyanide in the last two bubblers was estimated by the Liebig–Dénigès method (5).

RESULTS AND DISCUSSION

The introduction of even small amounts of cyanogen into the stream of yellow active nitrogen immediately quenched the afterglow and caused the emission of a bright red reaction flame accompanied by the accumulation of a black polymer.

The extent to which cyanogen was destroyed by active nitrogen was determined under various conditions of temperature and pressure and over a wide range of cyanogen flow rates, Fig. 1. At 100° C, and a nitrogen pressure of 1.4 mm, with an active nitrogen concentration of 19.5 μmoles per second, the amount of cyanogen destroyed increased slowly to a constant or plateau value of about 9.5 μmoles per second when the cyanogen flow rate was 90 μmoles per second. Although an increase of temperature to 400° C increased somewhat the rate of destruction of cyanogen, the plateau value, which approximated one-half the nitrogen atom concentration, still was reached only at cyanogen flow rates greater than 85 μmoles per second.

To substantiate these observations, the nitrogen pressure was decreased to 0.34 mm and 7.6 μmoles per second respectively, with the total pressure in the system maintained at 1.4 mm by the addition of argon to the nitrogen prior to its introduction into the discharge tube. The results obtained were similar to those outlined previously, i.e. the amount of cyanogen destroyed increased slowly as the cyanogen flow rate was increased and at 400° C the plateau value for the amount of cyanogen destroyed corresponded to one-half the nitrogen atom concentration.

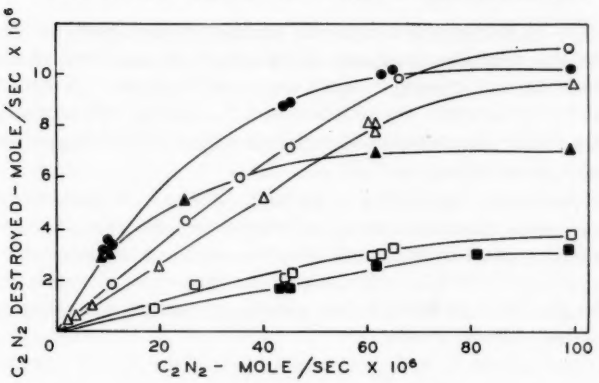

FIG. 1. Relation between amount of cyanogen destroyed by active nitrogen and the cyanogen flow rate. ○ P_{N_2} = 1.4 mm; T = 405° C. ● P_{N_2} = 3.1 mm; T = 410° C. △ P_{N_2} = 1.4 mm; T = 100° C. ▲ P_{N_2} = 3.1 mm; T = 115° C. □ P_{N_2} = 0.34 mm; T = 395° C. ■ P_{N_2} = 0.34 mm; T = 80° C.

The results obtained under the various experimental conditions suggested that NC radicals were formed in the cyanogen – active nitrogen reaction mixture. Since the NC radical, but not cyanogen itself, apparently reacts with hydrogen to produce HCN (9), while hydrogen does not react appreciably with active nitrogen, it seemed that the presence of CN radicals might be detected by the addition of hydrogen to the reaction mixture. Similarly, the addition of methane, which also reacts to a negligible extent with active nitrogen at lower temperatures, might be expected to cause reaction with CN radicals to produce HCN and CH_3CN.

A constant flow rate of hydrogen, 10 μmoles per second, was added to cyanogen prior to its introduction into the stream of active nitrogen. HCN was isolated from the reaction products in amounts which increased with increase of temperature. At flow rates of cyanogen below 6 μmoles per second, all the CN radicals produced in the cyanogen – active nitrogen mixture reacted with hydrogen to form HCN, and polymer formation was virtually eliminated. There was no evidence of a chain reaction, since the amount of HCN isolated was never greater than the amount of CN radicals formed, assuming that two CN radicals were produced for each cyanogen molecule destroyed. As the flow rate of cyanogen was increased, the presence of hydrogen was no longer able to eliminate the formation of polymer at either 124° or 440° C and the yield of HCN reached a plateau value, corresponding to about 30% reaction of the CN radicals with hydrogen.

To determine the amount of hydrogen necessary to react completely with all the CN radicals formed, experiments were made in which the cyanogen flow rate was maintained constant and the flow rate of hydrogen was varied. In this way it was found that at least 90% of the CN radicals produced could be isolated at 100° C as HCN when the hydrogen flow rate was some twenty-five times that of the flow rate of CN radicals, while at 400° C the hydrogen flow rate had to be about fifteen times that of the CN radicals for their complete conversion to HCN.

As an alternative to the large amounts of hydrogen necessary to react effectively with all the CN radicals formed, the use of methane as addend was investigated, since the abstraction of a hydrogen atom by a CN radical would result in the formation of a CH_3 radical which might be expected to combine easily with a second CN radical. When a constant flow rate of 40 μmoles per second of methane was added to the cyanogen at room

temperature, prior to its introduction into the reaction vessel, both HCN and CH_3CN were isolated from the reaction products. Both products attained plateau values at sufficiently high flow rates of cyanogen when about 60% of the CN radicals were consumed by methane. Unfortunately, the reaction of CN radicals with methane was limited to lower temperatures since the reaction of methane with active nitrogen becomes significant at temperatures above about 250° C.

Since the use of hydrogen permitted a measure of the CN radicals present in the cyanogen – active nitrogen mixture, it was possible to study the rate at which CN radicals were lost in being transported through the reaction vessel. A cylindrical reaction vessel was used so that cyanogen could be introduced into the active nitrogen stream through one inlet and hydrogen through other inlets placed at various distances, 3.1, 7.3, 11.3, and 26.6 cm, below the cyanogen inlet.

When 90 μmoles per second of hydrogen was added to the active nitrogen – cyanogen mixture through the second inlet, it was found that, at low flow rates of cyanogen, the majority of the CN radicals formed reacted with hydrogen to produce HCN. Hence, this amount of hydrogen was introduced through the third, fourth, and fifth inlets and the amount of HCN produced was determined to follow the destruction of CN radicals as they were transported through the reaction vessel.

The rate of destruction of CN radicals appears to follow first order kinetics, Table I. The rate constant at 95° C was 220 ± 10 sec^{-1} and at 400° C 125 ± 10 sec^{-1}. On this basis,

TABLE I

Rate of destruction of CN radicals

N_2 pressure (mm)	T (° C)	Flow rate (μmoles/sec)					
				HCN produced (inlet)			
		C_2N_2	CN produced	1	2	3	4
1.4	100	2.0	0.8	0.8	0.25	0.09	Nil
		5.5	1.6	1.6		0.15	0.1
		6.0	1.6	1.6	0.7	0.18	0.1
0.34	80	20.0	1.6	1.5		0.3	Traces
		45.0	3.5	1.7		0.3	0.02
1.4	400	5.0	2.2	2.1	1.1	0.8	0.2
		11.5	4.6	4.4		1.3	0.2
0.34	400	44.1	4.4	4.3		2.2	0.68
		45.0	4.3	4.3		2.2	0.7
3.1	410	9.0	6.4	4.5		1.0	Nil

$k_{av} = 220\pm10$ sec^{-1} at low temperature. $k_{av} = 125\pm10$ sec^{-1} at 400° C.

the process responsible for the destruction of CN radicals would have a negative activation energy of roughly -1.5 kcal and might be assumed to involve a wall reaction.

Since small amounts of cyanogen were sufficient to quench the active nitrogen afterglow, it was of interest to determine, if possible, the extent to which nitrogen atoms were destroyed in the process. Since ethylene is known to react rapidly with active nitrogen (3) to produce HCN, the introduction of ethylene into the reaction vessel below the site of the cyanogen – active nitrogen reaction should produce substantial amounts of HCN if relatively little destruction of nitrogen atoms by cyanogen occurred, whereas the formation of relatively small amounts of HCN should indicate that practically all the nitrogen atoms were destroyed by cyanogen. Cyanogen at the rate of 10 μmoles per second was

admitted into the reaction vessel and the amount of ethylene was varied from 20 to 50 μmoles per second. HCN was formed but the amount isolated was always less than the amount of CN radicals produced, corresponding to reaction of not more than 5% of the nitrogen atoms with ethylene.

Some, at least, of this HCN might have been formed by reaction of CN radicals with ethylene, since a small amount of liquid, possibly acrylonitrile, was formed during the reaction, perhaps by abstraction of a hydrogen atom from ethylene by CN radicals. It may therefore be assumed that at least 95% of the nitrogen atoms were destroyed by small amounts of cyanogen, even though only about 10% of the cyanogen was destroyed in the reaction.

The following series of reaction can account for the observed behavior of the cyanogen – active nitrogen reactions.

$$C_2N_2 + N \rightarrow [C_2N_2.N] \rightarrow CN + CN_2 \quad \text{(I)}$$

$$CN_2 + N \rightarrow CN + N_2 \quad \text{(II)}$$

$$2[C_2N_2.N] \rightarrow 2CN + C_2N_2 + N_2 \quad \text{(III)}$$

in competition with the catalytic recombination of nitrogen atoms

$$[C_2N_2.N] + N \rightarrow C_2N_2 + N_2. \quad \text{(IV)}$$

The competition between reactions (I), (II), and (IV) can account for the slow rate at which cyanogen is destroyed by active nitrogen. At high temperatures, the rates of reactions (I) and (II) would be expected to increase, thus using more nitrogen atoms at the expense of reaction (IV), and the concentration of CN radicals would then approach the nitrogen atom concentration.

If only reactions (I), (II), and (IV) are considered, an increase in nitrogen pressure, up to 3.1 mm, would be expected to result in an increase in the rates of all three reactions and no difference should be noted in the rate at which cyanogen was destroyed (Fig. 1). However, it was found that an increase in pressure effected a more rapid rate of destruction of cyanogen and it is then necessary to include reaction (III) which would be expected to occur more readily as the total pressure in the reaction vessel was increased.

It may be noted that the present study does not support the view that the formation of HCN in the reactions of active nitrogen with hydrocarbons involves the initial formation of CN radicals, since such relatively large amounts of hydrogen or hydrocarbon are required to react with one cyanide radical. Furthermore, the results when methane was added indicate that, since hydrocarbon free radicals are presumably formed in the active nitrogen – hydrocarbon reactions, the formation of nitriles would be expected if CN radicals were present in significant amounts, and this behavior is not noted experimentally.

REFERENCES

1. J. H. GREENBLATT and C. A. WINKLER. Can. J. Research, B, **27**, 721 (1949).
2. P. A. GARTAGANIS and C. A. WINKLER. Can. J. Chem. **34**, 1457 (1956).
3. J. VERSTEEG and C. A. WINKLER. Can. J. Chem. **31**, 1 (1953).
4. R. VON NAUMAN. Z. Elektrochem. **16**, 772 (1910).
5. I. M. KOLTHOFF and E. B. SANDELL. Textbook of quantitative inorganic chemistry. Rev. ed. The Macmillan Co., New York. 1948.
6. H. OUILLEMARD. Bull. soc. chim. **1**(4), 196 (1907).
7. T. WALLIS. Ann. **345**, 352 (1906).
8. F. N. RHODES. Ind. Eng. Chem. **4**, 652 (1912).
9. C. HAGGART and C. A. WINKLER. Can. J. Chem. **37**, 1791 (1959).

THE REACTIONS OF ACTIVE NITROGEN WITH HYDROGEN SULPHIDE AND CARBON DISULPHIDE[1]

R. A. WESTBURY[2] AND C. A. WINKLER

ABSTRACT

The destruction of either hydrogen sulphide or carbon disulphide by active nitrogen appears to be minimal at some temperature in the range 200–250° C. Both reactions yield large amounts of polymer.

It is postulated that the main reactions involve destruction of the reactant as it acts as a third body for recombination of nitrogen atoms. As the temperature is increased, dissociation of the nitrogen atom – reactant complex apparently increases. To account for the observed temperature effects, it is assumed that reactions also occur to regenerate reactant.

INTRODUCTION

In his pioneering work with active nitrogen, Strutt (1) found it to react with both hydrogen sulphide and carbon disulphide and suggested that the respective reactions were

$$N + H_2S \rightarrow NS + H_2$$

and

$$N + CS_2 \rightarrow NS + CS$$

with subsequent polymerization of the NS and CS radicals. The N–H_2S reaction yielded a light yellow deposit, which was suggested to consist, "at all events in part", of nitrogen sulphide. Two separate polymers were produced in the N–CS_2 reaction. A blue deposit, which formed on the wall of the reaction vessel, was attributed to polymerized NS radicals. A brown-colored deposit, which appeared on the chilled surface of a liquid-air trap, was thought to be the polymeric carbon monosulphide described previously by Dewar and Jones (2).

The reactions have been studied spectroscopically by Strutt and Fowler (3) and by Fowler and Vaidya (4). A banded deep blue reaction flame was observed in both reactions, and Christy and Naude have shown (5) that this spectrum is derived from an allowed transition of the sulphur molecule, corresponding to the Schumann–Runge bands of oxygen. In the N–CS_2 reaction the only evidence for the presence of carbon was afforded by a weak band of the CN radical at λ 3883 Å.

EXPERIMENTAL

The apparatus used in the present study was of the fast-flow type described previously (6, 7).

Hydrogen sulphide (98.5% pure, Matheson) was twice partially fractionated, the first and last portions being rejected each time. This was followed by three complete cycles of thawing, freezing, and pumping to remove residual air, which was followed in turn by distillation from a bath at −78° C, (acetone – dry ice slurry). The gas finally obtained was sufficiently dry that it gave no indication of reaction with a clean mercury surface, while titration with standard alkali showed that, within experimental error, the gas was free of ammonia.

[1]*Manuscript received November 10, 1959.*
Contribution from the Upper Atmosphere Chemistry Research Group, the Physical Chemistry Laboratory, McGill University, with financial assistance from the National Research Council of Canada, Ottawa.
[2]*Holder of research grants, 1956–58, from the Scientific Research Bureau, Province of Quebec, Quebec.*

Ethylene (99%, Ohio Chemical Co.) was also given two bulb-to-bulb fractionations, followed by distillation from a bath at −78° C.

Carbon disulphide (reagent grade, Merck) was cycled four times through a treatment which consisted of cooling it to −78° C, followed by partial evacuation (10 minutes) and warming (to room temperature) to remove air and other possible volatile impurities. It was then dried by passage as a vapor through a column of activated alumina.

In the temperature range −23° C to +6° C, the purified carbon disulphide had a vapor pressure that agreed, within experimental error, with published data (8). To prevent its attack upon stopcock grease when experiments were not in progress, the purified carbon disulphide was stored at liquid-air temperature.

Unreacted hydrogen sulphide, after being absorbed into 15% NaOH solution, was analyzed by acidifying the solution, adding excess standard iodine solution, and then back-titrating with standard thiosulphate solution (9). Blank experiments showed that this scheme of analysis was quite satisfactory.

Ammonia, produced in the N–H_2S reaction, was absorbed in standard acid, which was then back-titrated with standard alkali after the acid solution had been heated to drive off residual hydrogen sulphide.

Hydrogen cyanide, produced in the high-temperature active nitrogen – ethylene reaction as a measure of nitrogen atom concentration, was titrated according to the Liebig–Dénigès method (10).

Unreacted carbon disulphide was estimated by distillation into a small glass bulb, which could then be weighed on an analytical balance. A graph was established to relate the amount of CS_2 to its pressure in a standard volume at room temperature, in order that reactant flow rates might be calculated from pressure–volume measurements.

RESULTS

The N–H_2S *Reaction*

The only reaction flame observed in the reaction was a deep blue glow that appeared to fill the entire upper half of the reaction vessel. This flame was almost invisible under normal artificial illumination, but could be seen clearly in a darkened room.

In conformity with the early qualitative studies of Strutt, a good deal of dark brown polymer was found to result from this reaction. Much of this polymer deposited on the wall of the reaction vessel when the reaction vessel was not heated externally, although a small amount was carried along in the gas stream, and deposited on the connecting tube to the cold trap. When the reaction vessel was heated externally, polymer was not deposited on the wall but on the cooler connecting tube, which gradually became quite black.

A reaction vessel in which polymer had been deposited at lower temperatures could be cleaned by heating it for 2 to 3 hours at 350° C.

The polymer that deposited on the wall of the reaction vessel was not stable. While it deposited as an unbroken layer, it began to evolve gas almost immediately, and after the polymer had been standing under vacuum for 4–5 days a number of "gas pockets", ranging in size from 5 mm to 20 mm, tended to force the polymer layer off the wall. Several attempts were made to remove the polymer layer intact for analysis, but all were unsuccessful. A dilute solution of ammonia, presumably because of its ability to attack the underlying phosphoric acid wall poison, quickly separated the polymer from the wall, while the solution itself became a deep violet color. However, the brown flakes and shreds almost as quickly hydrolyzed to sulphur.

Several attempts to remove the polymer layer from the reaction vessel by organic solvents, of which CS_2 appeared to be the most promising, gave unsatisfactory results. Only a small amount of material was ever recovered, much less than by using aqueous ammonia solution. The product obtained upon solvent evaporation was usually a reddish-brown sticky substance, which dried to a hard mass. Attempts to fractionate this substance yielded only oils, but qualitative tests showed it to contain both nitrogen and free sulphur.

When present on the wall of the reaction vessel, the polymer markedly affected the decay of the active nitrogen. It appeared to act as a more efficient poison than the 2% metaphosphoric acid normally used, since the nitrogen afterglow was perceptibly brighter after some polymer had been deposited on the wall. It might be noted that Strutt found hydrogen sulphide to be the most effective of a number of substances that he introduced with the nitrogen to poison the walls of the discharge tube and reaction vessel (11).

Special precautions, which need not be detailed here, were taken to ensure that this poisoning effect did not vitiate the experimental results (12).

The amounts of H_2S destroyed at different flow rates, over a range of temperatures,

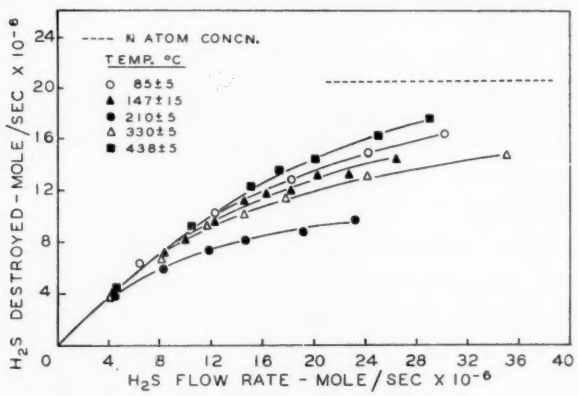

FIG. 1. Relation between H_2S flow rate and amount of H_2S destroyed by active nitrogen at different temperatures.

are shown in Fig. 1. Further experiments using a new discharge tube showed that the reaction was quite reproducible in its behavior with increase in temperature. The amount of ammonia recovered as a product of the reaction was virtually independent of temperature, and accounted for only about 3% of the nitrogen atom concentration, as estimated from the maximum HCN production in the active nitrogen – ethylene reaction.

The N–CS_2 *Reaction*

In this reaction, a pale blue flame was observed to fill the entire reaction vessel at high reactant flow rates, and continue some distance along the connecting tube to the pump. Examination with a small spectroscope (1-in. prism) showed this flame to be a continuum (within the resolution of the instrument) with its limits lying roughly between

λ 4200 Å and λ 6400 Å. At very low flow rates of CS_2, however, this apparent continuum disappeared, to be replaced by what appeared to be the red and violet band systems of the CN radical.

Preliminary work showed that the reaction deposited a good deal of brown polymer on the wall of an unheated reaction vessel. This polymer was similar in appearance to that produced in the N–H_2S reaction, and it, too, slowly evolved gas upon standing. Most, but not all, of this polymer could be removed from the wall of the reaction vessel by heating it strongly. No analysis of the polymer was attempted, owing to the difficulty of removing it and its ease of hydrolysis, in which respects it resembled the polymer from the N–H_2S reaction.

The reaction was complicated by the appearance of a second polymer, of brownish-black color, which spread as a thin dark film on the tube connecting the reaction vessel to the pump, but deposited mainly on the wall of the first trap cooled with liquid air. This second polymer would seem to be the polymeric carbon monosulphide first described by Dewar and Jones (2), since its deposition, if continued long enough (50–100 seconds, depending upon the flow rate of CS_2) almost invariably resulted in an explosion in the trap.

It was quickly realized that the N–CS_2 reaction could be studied successfully only if the explosions could be prevented. This was necessary, since the reaction was followed by recovery and estimation of the unreacted CS_2 at various reactant flow rates, and it was obvious that the explosions might vitiate the results, apart from possible damage to the apparatus. (On several occasions, at the conclusion of an experiment, a vacuum could not be attained prior to distillation of the trapped CS_2, because the explosion had cracked the wall of the trap).

There are a number of references in the literature to this polymerized carbon monosulphide, but no information was available on possible methods of moderating or eliminating the explosions. Experiments showed that coolants at −112° C or −130° C were only partially successful, in that they did not prevent entirely the explosions that occurred in a following trap cooled with liquid air. However, a slurry of isopentane (approximately −160° C) was completely successful in allowing the reaction products to be condensed without subsequent explosion, and as a consequence a slurry of isopentane was usually used to trap excess CS_2 from the flowing gas stream. No explosion was ever observed with such trapping conditions, and blank experiments showed that CS_2 vapor was trapped quantitatively.

The actual character of the explosions is difficult to describe. During an experiment there would be a sudden sharp "click", a flash of light from the tube, and the liquid-air coolant would bubble vigorously for several seconds, indicative of a quite exothermic reaction. On several occasions the discharge faltered for a few tenths of a second, as if there had been a sudden rise of pressure within the discharge tube. Occasionally, the expected explosion did not occur during the deposition of the CS radical, but did take place 1 to 2 minutes after an experiment had been completed, with the discharge shut off, and no gas flowing through the system.

Analysis of the black polymer deposited at −160° C showed it to be a mixture of paracyanogen and $(CS)x$.

In Fig. 2 are shown the relations between the CS_2 flow rates and the amounts of CS_2 destroyed at different temperatures. These data were quite reproducible. The "Prussian blue" test gave no qualitative indication of cyanogen in the condensible products at any of the three reaction temperatures used.

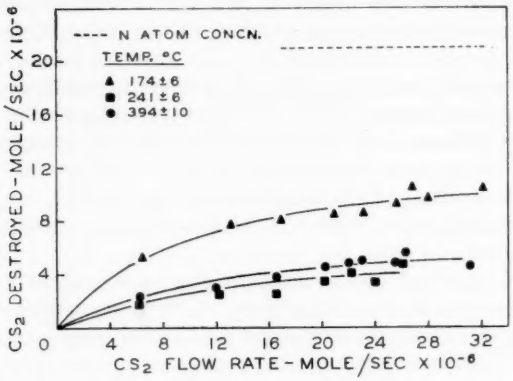

FIG. 2. Relation between CS_2 flow rate and amount of CS_2 destroyed by active nitrogen at different temperatures.

DISCUSSION

It is readily apparent from Figs. 1 and 2 that in both the N–H_2S and N–CS_2 reactions the amount of reactant destroyed passes through a minimum as the temperature is raised. It is tempting to explain this behavior in a similar manner for the two substances, and it will be seen that the proposed mechanisms do have a good deal in common.

The N–H_2S *Reaction*

The initial step involved in this reaction must certainly be the formation of a transition complex

$$N + H_2S \rightarrow N.H_2S. \qquad [1]$$

Decomposition of the complex by the reaction

$$N.H_2S \rightarrow NH + HS \qquad [2]$$

would seem to be improbable, not only because hydrogenation of the imino radical might be expected to yield ammonia in rather larger quantities than those found, but the fast reaction observed does not seem compatible with an activation energy of at least 7 kcal/mole for reaction [2].[3]

The complex might well decompose in the manner suggested by Strutt, i.e.

$$N.H_2S \rightarrow NS(^2\Pi) + H_2 \text{ (see footnote 4)} \qquad [3]$$

since the over-all change represented by reactions [1] and [3] is exothermic to the extent of 44 kcal/mole. However, it does not seem possible to account for the experimental results solely by these reactions.

Decomposition of the $N.H_2S$ complex by reaction [3] involves a change of spin, as well as the splitting of two bonds, and, as such, is likely to require a significant activation energy (13). It is suggested, therefore, that at lower temperatures this complex will have

[3]*Heats of reaction have been calculated on the basis of the following bond energies.* $D(H_2)$, *108.2;* $D(N_2)$, *225.0;* D(NH), *85; (T. L. Cottrell. The strength of chemical bonds. 2nd ed. Butterworth Scientific Publications, London. 1958).* $D(S_2)$, *101.5;* D(NS), *115; (A. G. Gaydon. Dissociation energies and spectra of diatomic molecules. 2nd ed. Chapman & Hall, Ltd., London. 1953).* D(H–SH), *92; (D. P. Stevenson. Trans. Faraday Soc.* **49**, *867 (1953)).* D(S=CS), *90; (L. P. Blanchard and P. LeGoff. Can. J. Chem.* **35**, *89 (1957)).* D(SH), *82;* D(CS), *184; (calculated).*

a lifetime long enough that it might suffer a collision with a second nitrogen atom at low flow rates, or with another $N.H_2S$ complex, at higher flow rates of H_2S, to induce catalytic recombination of nitrogen atoms, with concomitant dissociation of the H_2S molecule. This may be represented at low flow rates of H_2S by

$$N + N.H_2S \rightarrow N_2 + H + HS + 133 \text{ kcal} \quad [4]$$

$$\rightarrow N_2 + 2H + S + 51 \text{ kcal} \quad [5]$$

and at higher flow rates by

$$N.H_2S + N.H_2S \rightarrow N_2 + H_2S + H + HS + 133 \text{ kcal} \quad [6]$$

$$\rightarrow N_2 + H_2S + 2H + S + 51 \text{ kcal} \quad [7]$$

$$\rightarrow N_2 + 2H + 2HS + 41 \text{ kcal.} \quad [8]$$

The hydrogen atoms formed in reactions [4] to [8] should destroy H_2S by the fast reaction

$$H + H_2S \rightarrow H_2 + HS + 11 \text{ kcal} \quad [9]$$

while the HS radicals probably interact by

$$2HS \rightarrow H_2S + S + 10 \text{ kcal} \quad [10]$$

$$\rightarrow H_2 + S_2 + 40 \text{ kcal.} \quad [11]$$

Darwent and Roberts (14) have found, by a steady-state approximation, that at room temperature 87% of the effective collisions of two HS radicals result in reaction [10], and the remaining 13% in reaction [11]. These authors concluded that reactions [10] and [11] occurred rapidly, and without appreciable activation energy. Some, though probably slight, regeneration of H_2S at 35° C might also result from hydrogen atom reaction with sulphur, since experiments showed that hydrogen atoms removed sulphur from the wall of the reaction vessel at room temperature.

The decrease in destruction of H_2S as the temperature is increased to 210° C may now be attributed to the increased recombination of hydrogen atoms at the higher temperature, together with increased regeneration of H_2S from attack of hydrogen atoms on sulphur, perhaps in the gas phase, or as a wall reaction. The apparent increase in destruction of H_2S at still higher temperatures may be explained by assuming that at these higher temperatures, decomposition of the $N.H_2S$ complex by reaction [3] becomes predominant. This follows from the earlier suggestion that this reaction probably has an appreciable activation energy. Decomposition of the $N.H_2S$ complex by reaction [3] would immediately result in a decrease in the production of H atoms and HS radicals, and this in turn should accentuate the decrease in the back reaction [10].

The small amounts of ammonia recovered probably had their origin in the known reaction of nitrogen atoms with hydrogen atoms (15), followed by hydrogenation of the NH radical.

The appearance of polymer is readily understood by polymerization of the NS radical. The monomer might also be produced, particularly at low flow rates of H_2S, by additional reactions such as

$$N + HS \rightarrow NS + H + 33 \text{ kcal,} \quad [12]$$

$$N + S_2 \rightarrow NS + S + 14 \text{ kcal,} \quad [13]$$

[4] *The ground state of the* NS *radical is* $^2\Pi$; *cf. R. F. Barrow, G. Drummond, and P. B. Zeeman. Proc. Phys. Soc. (London), A,* **67**, *365 (1954).*

and

$$N + S + M \rightarrow NS + M + 115 \text{ kcal.} \quad [14]$$

In addition to a number of nitrogen sulphides in various degrees of polymerization, free sulphur might also be expected to deposit, as observed, on the wall of the reaction vessel or on the connecting tubing.

The $N–CS_2$ *Reaction*

As for the $N–H_2S$ reaction, it is suggested that the initial step by which carbon disulphide is destroyed by active nitrogen is formation of a complex

$$N + CS_2 \rightarrow N.CS_2 \quad [15]$$

which might be expected to decompose according to

$$N.CS_2 \rightarrow NS(^2\Pi) + CS. \quad [16]$$

Reactions [15] and [16], considered as a whole, are of course equivalent to the over-all reaction suggested by Strutt,

$$N + CS_2 \rightarrow NS + CS.$$

However, this reaction involves a change of spin if, as seems probable from its relatively long lifetime, the CS radical is formed in the singlet state. This relatively long lifetime is clearly indicated since about 0.3 second was required for the CS radical to pass from the reaction vessel to the trap where explosions occurred. Moreover, Parker has found (16) by flash photolysis of CS_2, that the half life of the reaction

$$n CS \rightarrow (CS)_n \quad [17]$$

was 60 seconds, and he concluded that a half life of this magnitude implied that the CS radical was in the singlet state. Dyne and Ramsay (17) have concluded that, in the gas phase, CS shows the chemical stability of a normal molecule, and this again is consistent only with the singlet state of the radical.

By analogy, then, with H_2S, it is suggested that the destruction of the $N.CS_2$ complex by reaction [16] requires an activation energy, so that, at lower temperatures, the complex may have sufficient lifetime to suffer collision with a further nitrogen atom, at low flow rates of CS_2, or with another complex, at higher reactant flow rates. At low reactant flow rates, the reaction would be

$$N + N.CS_2 \rightarrow N_2 + CS + S + 135 \text{ kcal} \quad [18]$$

while at higher flow rates it would be

$$N.CS_2 + N.CS_2 \rightarrow N_2 + CS_2 + CS + S + 135 \text{ kcal} \quad [19]$$

$$\rightarrow N_2 + 2CS + 2S + 45 \text{ kcal.} \quad [20]$$

It will be noted that the similarity to the mechanism suggested for the $N–H_2S$ reaction is not complete, because there is not enough energy available to break both bonds in the CS_2 molecule.

Again, the results indicate that a reaction to regenerate the parent sulphur compound is an important factor in the mechanism. It might also be inferred from Fig. 2 that this regeneration reaction requires some activation energy, since otherwise more regeneration of CS_2, hence less apparent destruction of it, might have been expected than was actually found at 174° C.

The regeneration step might well be

$$CS + S \rightarrow CS_2^* \rightarrow CS_2 + h\nu \quad [21]$$

in which the collision complex is probably in a triplet state to conserve spin. This is by analogy with the reactions

$$CO + O \rightarrow CO_2^* \rightarrow CO_2 + h\nu \text{ (continuous spectrum)} \quad [22]$$

and

$$CO + O + M \rightarrow CO_2^{**} + M \quad [23]$$

followed by

$$CO_2^{**} \rightarrow CO_2 + h\nu \text{ (band spectrum)} \quad [24]$$

by which the CO flame spectrum may be interpreted (18).

Broida and Gaydon (19) have recently concluded, from studies of the oxygen atom – carbon monoxide reaction, that reaction [22] has an appreciable activation energy, while [23] followed by [24], which occurred rapidly at room temperature, was suggested to require little or no activation energy. It is quite possible that reaction [21] might require rather less activation energy than [22], since the CS radical is probably more reactive than CO.

The analogue of reaction [23] is also possible as a regenerative reaction i.e.

$$CS + S + M \rightarrow CS_2^{**} + M \quad [25]$$

followed of course by

$$CS_2^{**} \rightarrow CS_2 + h\nu \quad [26]$$

and by reasoning similar to the above, reaction [25] should have virtually no activation energy.

Choice between [21] and [25] as the main reaction for regeneration of CS_2 probably can be made only on the basis of spectroscopic data, and a spectroscope of sufficient resolution was not available. As indicated earlier, examination of the N–CS_2 flame with a small glass spectroscope revealed the spectrum to be a continuum, but this is scarcely an adequate basis on which to distinguish between the two reactions.

It is apparent that reactions [18] to [21], the last with a small but significant activation energy, are able to explain both the high rate of destruction of CS_2 by active nitrogen at 174° C, and the apparent decrease in the amount of CS_2 destroyed as the temperature is raised. The increase destruction of CS_2 at 394° C relative to that at 241° C can be explained by assuming that, at the higher temperature, the rate of destruction of CS_2 by reaction [16] becomes important relative to its destruction by reactions [18] to [20] and its regeneration by reaction [21]. This explanation is similar to that suggested for the corresponding behavior of the N–H_2S reaction at high temperatures.

The suggestion that reaction [21] has an activation energy raises a question concerning those sulphur atoms and CS radicals, produced at 174° C, that do not react further by [21]. The fate of these entities must be to deposit eventually on the wall of the reaction vessel, although they may also react by reactions [11] and [12], or by

$$N + CS \rightarrow CN + S + 4 \text{ kcal} \quad [27]$$

followed by

$$2CN + M \rightarrow (CN)_2 + M. \quad [28]$$

Reactions [27] and [28] are consistent both with the small amount of paracyanogen present in the CS matrix, and with the appearance of CN bands in the N–CS_2 reaction flame at very low CS_2 flow rates.

REFERENCES

1. R. J. STRUTT. Proc. Roy. Soc. (London), A, **88**, 539 (1913).
2. SIR JAMES DEWAR and H. O. JONES. Proc. Roy. Soc. (London), A, **85**, 574 (1911).
3. R. J. STRUTT and A. FOWLER. Proc. Roy. Soc. (London), A, **86**, 105 (1912).
4. A. FOWLER and W. H. VAIDYA. Proc. Roy. Soc. (London), A, **132**, 310 (1931).
5. A. CHRISTY and S. M. NAUDE. Phys. Rev. **37**, 490, 903 (1931).
6. J. H. GREENBLATT and C. A. WINKLER. Can. J. Research, B, **27**, 721 (1949).
7. P. GARTAGANIS and C. A. WINKLER. Can. J. Chem. **34**, 1475 (1956).
8. D. R. STULL. Ind. Eng. Chem. **39**, 517 (1947).
9. W. W. SCOTT. Standard methods of chemical analysis. 5th ed. *Edited by* N. H. Furman. D. Van Nostrand, Co., Inc., New York. 1939.
10. I. M. KOLTHOFF and E. B. SANDELL. Textbook of quantitative inorganic analysis. 3rd ed. The Macmillan Co., New York. 1952.
11. R. J. STRUTT. Proc. Roy. Soc. (London), A, **91**, 303 (1915).
12. R. A. WESTBURY. Thesis, McGill University, Montreal, Que. 1959.
13. H. G. V. EVANS and C. A. WINKLER. Can. J. Chem. **34**, 1217 (1956).
14. B. DE B. DARWENT and R. ROBERTS. Proc. Roy. Soc. (London), A, **216** (1953).
15. B. LEWIS. J. Am. Chem. Soc. **50**, 27 (1928).
16. G. PARKER. Proc. Roy. Soc. (London), A, **200**, 284 (1950).
17. P. J. DYNE and D. A. RAMSAY. J. Chem. Phys. **20**, 1055 (1952).
18. A. G. GAYDON. The spectroscopy of flames. Chapman & Hall, Ltd., London. 1957.
19. H. P. BROIDA and A. G. GAYDON. Trans. Faraday Soc. **49**, 1190 (1953).

BACTERIOSTATS

III. OXYAMINES AND THEIR DERIVATIVES[1]

A. F. McKay, D. L. Garmaise, G. Y. Paris, and S. Gelblum

ABSTRACT

A number of benzyloxyamines were prepared for conversion into urea and thiourea derivatives. The benzyloxyamine hydrochlorides on treatment with phosgene gave a mixture of the corresponding benzyl 4-(benzyloxy)-allophanate and benzyloxycarbamyl chloride. Triethylamine converted the benzyloxycarbamyl chlorides into the corresponding 1,3,5-tri-(benzyloxy)-isocyanuric acids. The reactions of the allophanates with amines and sodium hydroxide are described.

A series of oxyamine derivatives has been examined for bacteriostatic activity. These O-substituted oxyamines were prepared by one of the following three routes;

$$RCl + HONHCOOC_2H_5 \xrightarrow{KOH} RONHCOOC_2H_5 \xrightarrow[H_2O]{KOH} RONH_2, \qquad [1]$$

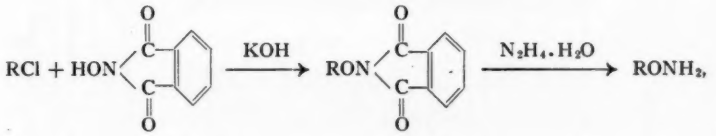

[2]

$$RCl + HON(SO_3K)_2 \xrightarrow{KOH} RON(SO_3K)_2 \xrightarrow[H_2O]{H_2SO_4} RONH_2. \qquad [3]$$

The majority of the urea and thiourea derivatives listed in Table I were obtained by the addition of isocyanates or isothiocyanates to a solution of the oxyamine in an inert solvent such as ether or benzene. 1-(β-Hydroxyethyl)-2-(2,4-dichlorobenzyloxyamino)-2-imidazoline was formed by the reaction of 2,4-dichlorobenzyloxyamine with 1-(β-hydroxyethyl)-2-methylmercapto-2-imidazolinium chloride. β-Aminoethylamine dihydrochloride, γ-aminopropyloxyamine, N-(α-naphthylmethyloxy)-urethane, and N,N′-dicarbethoxy-α,α′-di-(aminoöxy)-p-xylene also were prepared during this investigation.

All of the oxythiourea derivatives were unstable. The white crystalline products, after standing at room temperature for several weeks, changed into a mixture of crystals and red, viscous oil. The product from 1-(3,4-dichlorobenzyloxy)-3-(3,4-dichlorobenzyl)-thiourea was separated into free sulphur, 1,3,5-tri-(3,4-dichlorobenzyl)-isomelamine, and unchanged thiourea. In 1891 Voltmer found that heating 1-ethoxy-3-phenyl-thiourea in solution split it into sulphur, ethanol, and phenylcyanamide according to the following equation

$$C_6H_5NHC(S)NHOCH_3 \rightarrow C_6H_5NHCN + S + C_2H_5OH.$$

The scission of crystalline oxythioureas undoubtedly follows a similar course but in this case the generated 3,4-dichlorobenzylcyanamide trimerized to 1,3,5-tri-(3,4-dichlorobenzyl)-isomelamine (m.p. 171–172° C). N^2,N^4,N^6-Tri-(3,4-dichlorobenzyl)-melamine

[1]*Manuscript received November 10, 1959.*
Contribution No. 25 from the L. G. Ryan Research Laboratories of Monsanto Canada Limited, LaSalle, Que.

Can. J. Chem. Vol. 38 (1960)

TABLE I

R	R′	X	M.p. (°C)	Yield (%)	Formula	C Calc.	C Found	H Calc.	H Found	Cl Calc.	Cl Found	N Calc.	N Found
(*A*) Urea and thiourea derivatives RONHC(X)NHR′													
4-$ClC_6H_4CH_2$	4-ClC_6H_4	O	154–155[a]	74[g]	$C_{14}H_{12}Cl_2N_2O_2$	54.03	54.02	3.89	3.84	22.79	22.97	9.00	9.26
4-$ClC_6H_4CH_2$	4-BrC_6H_4	O	158–159[a]	98[g]	$C_{14}H_{12}BrClN_2O_2$[s]	47.30	47.25	3.40	3.32			7.88	8.32
4-$ClC_6H_4CH_2$	2,5-$Cl_2C_6H_3$	O	135–136[a]	94[g]	$C_{14}H_{11}Cl_3N_2O_2$	48.66	48.84	3.21	3.18	30.78	30.88	8.11	8.50
4-$ClC_6H_4CH_2$	$CH_3(CH_2)_{10}$—	O	81–82[b]	77.5[g]	$C_{19}H_{31}ClN_2O_2$	64.30	64.56	8.81	8.86	9.99	10.02	7.89	7.64
4-$ClC_6H_4CH_2$	CH_2=$CH(CH_2)_8$—	O	70–71[b]	80[g]	$C_{18}H_{27}ClN_2O_2$	63.79	63.72	8.03	7.80	10.46	10.83	8.27	8.40
4-$ClC_6H_4CH_2$	$C_{10}H_7$	O	165–166[c]	86[g]	$C_{18}H_{15}ClN_2O_2$	66.13	66.18	4.63	4.81	10.85	10.74	8.57	8.84
4-$ClC_6H_4CH_2$	4-$ClC_6H_4CH_2$	O	123–124[d]	88.5[h]	$C_{15}H_{14}Cl_2N_2O_2$	55.40	55.43	4.34	4.44	21.81	21.69	8.62	8.61
4-$ClC_6H_4CH_2$	3,4-$Cl_2C_6H_3CH_2$	O	140–141[d]	78[h]	$C_{15}H_{13}Cl_3N_2O_2$	50.09	50.48	3.64	3.63	29.57	29.64	7.79	8.00
4-$ClC_6H_4CH_2$	C_6H_5	S	120–121[d]	100[g]	$C_{14}H_{13}ClN_2OS$[i]	57.42	57.02	4.47	4.44	12.11	12.19	9.57	9.77
4-$ClC_6H_4CH_2$	4-$ClC_6H_4CH_2$	S	115–116[d]	99[g]	$C_{15}H_{14}Cl_2N_2OS$[k]	52.78	53.09	4.13	4.44	20.78	20.46	8.21	8.28
4-$ClC_6H_4CH_2$	3,4-$Cl_2C_6H_3CH_2$	S	116–117[d]	100[g]	$C_{15}H_{13}Cl_3N_2OS$[l]	47.95	47.96	3.49	3.58	28.31	28.51	7.46	7.59
2,4-$Cl_2C_6H_3CH_2$	2,5-$Cl_2C_6H_3$	O	173–174[a]	73.5	$C_{14}H_{10}Cl_4N_2O_2$	44.24	44.20	2.65	2.71	37.32	37.25	7.37	7.49
2,4-$Cl_2C_6H_3CH_2$	4-$ClC_6H_4CH_2$	O	115–116	44[h]	$C_{15}H_{13}Cl_3N_2O_2$	50.09	50.43	3.64	3.53	29.52	29.46	7.78	7.57
2,4-$Cl_2C_6H_3CH_2$	3,4-$Cl_2C_6H_3CH_2$	S	86–87[e]	48.7[g]	$C_{15}H_{12}Cl_4N_2OS$[m]	43.91	44.01	2.95	3.07	34.58	34.30	6.83	6.82
3,4-$Cl_2C_6H_3CH_2$	4-ClC_6H_4	O	141–142[a]	89.5[g]	$C_{14}H_{11}Cl_3N_2O_2$	48.66	48.60	3.21	3.45	30.78	31.01	8.11	8.33
3,4-$Cl_2C_6H_3CH_2$	4-BrC_6H_4	O	148–149[a]	90.8	$C_{14}H_{11}BrCl_2N_2O_2$[n]	43.10	43.13	2.84	2.95			7.18	7.38
3,4-$Cl_2C_6H_3CH_2$	2,5-$Cl_2C_6H_3$	O	153–154[f]	92[g]	$C_{14}H_{10}Cl_4N_2O_2$	44.24	44.37	2.65	2.75	37.32	37.71	7.37	7.60
3,4-$Cl_2C_6H_3CH_2$	4-$ClC_6H_4CH_2$	O	119–120	100[h]	$C_{15}H_{13}Cl_3N_2O_2$	50.09	50.35	3.64	3.64	29.52	29.42	7.78	7.74
3,4-$Cl_2C_6H_3CH_2$	4-$ClC_6H_4CH_2$	S	121–122[d]	96[g]	$C_{15}H_{13}Cl_3N_2OS$[o]	47.95	48.40	3.49	3.50	28.31	28.45	7.46	7.80
3,4-$Cl_2C_6H_3CH_2$	3,4-$Cl_2C_6H_3CH_2$	S	107–108[d]	100[g]	$C_{15}H_{12}Cl_4N_2OS$[p]	43.91	43.93	2.95	2.95	34.58	34.60	6.83	6.75
3,4-$Cl_2C_6H_3CH_2$	CH_3	S	129–130[a]	25[g]	$C_9H_{10}Cl_2N_2OS$[q]	40.77	40.90	3.80	3.91	26.74	26.42	10.52	10.67
4-$NO_2C_6H_4CH_2$	4-$ClC_6H_4CH_2$	O	170–171	50.5[h]	$C_{15}H_{13}ClN_3O_4$	53.66	53.88	4.20	3.90	10.52	10.48	12.53	12.37
(*B*) Diurea derivatives R(NHC(O)NHOR′)$_2$													
$(CH_2)_6$	4-$ClC_6H_4CH_2$		142–143[f]	83.5	$C_{22}H_{28}Cl_2N_4O_2$	54.65	54.62	5.84	5.83	14.67	15.01	11.59	11.54
2,4-Tolyl	4-$ClC_6H_4CH_2$		141–142[r]	81.0	$C_{23}H_{22}Cl_2N_4O_2$	56.44	56.78	4.83	4.65	14.49	14.15	11.45	11.52

[a]Crystallized from ethyl acetate – petroleum ether. [b]From petroleum ether. [c]From acetone–water. [d]From absolute ethanol. [e]From ether – petroleum ether. [f]From ethyl acetate. [g]Prepared from the corresponding isocyanates and isothiocyanates. [h]Prepared from the corresponding allophanates and amines. [i]Halogen: calc., 32.46; found, 32.22. [j]S: calc., 10.95; found, 11.68. [k]S: calc., 9.39; found, 9.01. [l]S: calc., 8.53; found, 8.68. [m]S: calc., 7.82; found, 7.73. [n]Halogen: calc., 38.67; found, 38.53. [o]S: calc., 7.82; found, 7.85. [p]S: calc., 8.53; found, 8.55. [q]S: calc., 12.09; found, 11.78. [r]From ethyl acetate – petroleum ether (1:1) solution.

(m.p. 217–218° C) was prepared from the reaction of cyanuric chloride with 3,4-dichlorobenzylamine for comparison with the isomelamine derivative.

Earlier attempts (2, 3, 4) to prepare esters or salts of the hypothetical acid HONCO have been described in the literature. We also were unsuccessful in preparing the monomeric esters but the corresponding allophanates III and trimers IV were isolated. Phosgene combined with the substituted oxyamines to give the corresponding crude oxycarbamyl chlorides (II).

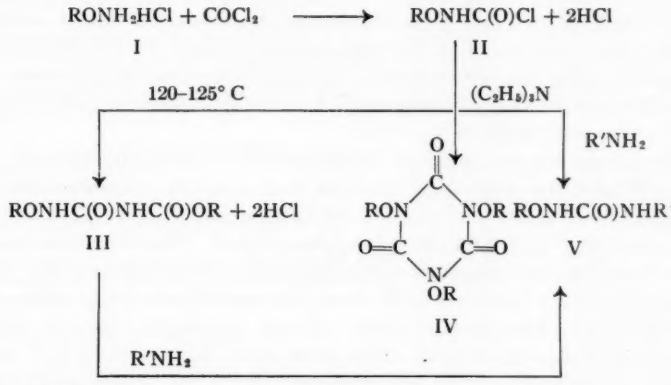

R = $C_6H_5CH_2$; 4-$ClC_6H_4CH_2$; 4-$NO_2C_6H_4CH_2$; 2,4-$Cl_2C_6H_3CH_2$; 3,4-$Cl_2C_6H_3CH_2$.
R′ = 3,4-$Cl_2C_6H_3$; 4-$ClC_6H_4CH_2$.

4-Chlorobenzyloxycarbamyl chloride (II, R = 4-$ClC_6H_4CH_2$—) on treatment with 2 equivalents of 3,4-dichloroaniline gave the calculated yield of 3,4-dichloroaniline hydrochloride and a 51% yield of 1-(4-chlorobenzyloxy)-3-(3,4-dichlorophenyl)-urea (V, R = 4-$ClC_6H_4CH_2$, R′ = 3,4-$Cl_2C_6H_3$). When 4-chlorobenzylamine was added to crude 4-chlorobenzyloxycarbamyl chloride (II, R = 4-$ClC_6H_4CH_2$) in ether, small amounts of 1,5-di-(4-chlorobenzyl)- and 1-(4-chlorobenzyloxy)-5-(4-chlorobenzyl)-biurets were obtained together with the expected 1-(4-chlorobenzyloxy)-3-(4-chlorobenzyl)-urea (V, R and R′ = 4-$ClC_6H_4CH_2$). This indicates that part of the oxycarbamyl chloride and/or the oxyamine hydrochloride is converted into carbamyl chloride and the corresponding benzyl alcohol under the conditions of the phosgene reaction. The benzyl alcohol could be expected to combine with phosgene or carbamyl chloride to yield 4-chlorobenzyl chloroformate or 4-chlorobenzyl carbamate. These products and the unchanged oxycarbamyl chloride supply the components required in the formation of the allophanates (III). The allophanates in turn combine with amines to give derivatives of biuret (5, 6, 7). When non-anhydrous chlorobenzene was used as a solvent in the reaction of phosgene with 4-chlorobenzyloxyamine hydrochloride, a low yield (11.5%) of 4-chlorobenzyl 4-(4-chlorobenzyloxycarbamyl)-allophanate (VI) was

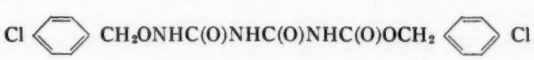

VI

isolated.

If the oxyamine hydrochlorides (I) are heated to 120–125° in anhydrous chlorobenzene

during the reaction with phosgene, they are converted mainly into the corresponding benzyl 4-(benzyloxy)-allophanates (III). When benzyloxyamine hydrochloride was treated with phosgene under these conditions, the benzyl group was chlorinated and 4-chlorobenzyl 4-(4-chlorobenzyloxy)-allophanate (III, R = 4-$ClC_6H_4CH_2$) was obtained. Some unchanged oxycarbamyl chlorides remained in solution after the allophanates were recovered by precipitation with ether. The ether solutions on treatment with triethylamine yielded the corresponding 1,3,5-tribenzyloxy-isocyanuric acids (IV). Several of the oxyurea derivatives (V) described in Table I(*A*) were obtained by heating the aralkyl 4-aralkyloxy-allophanates (III) with amines in chlorobenzene under reflux. The main product from the reaction of 4-chlorobenzylamine with 4-chlorobenzyl 4-(4-chlorobenzyloxy)-allophanate was 1-(4-chlorobenzyloxy)-3-(4-chlorobenzyl)-urea (88% yield) but small quantities of *O*-(4-chlorobenzyl)-4-chlorobenzaldoxime and 1,5-di-(4-chlorobenzyl)-biuret also were isolated.

The products from the treatment of 4-chlorobenzyl 4-(4-chlorobenzyloxy)-allophanate (III, R = 4-$ClC_6H_4CH_2$) with alkali indicate that a rather complex series of reactions occur. The allophanate splits partly into 4-chlorobenzyl alcohol, 4-chlorobenzyloxyamine, 4-chlorobenzaldehyde, and 1-(4-chlorobenzyloxy)-urea. Then 4-chlorobenzyloxyamine condenses with the original allophanate to give 1,5-di-(4-chlorobenzyloxy)-biuret. It also could be considered to combine with 4-chlorobenzaldehyde to produce the isolated *O*-(4-chlorobenzyl)-4-chlorobenzaldoxime. When 3,4-dichlorobenzyl 4-(3,4-dichlorobenzyloxy)-allophanate was treated with methanolic sodium hydroxide solution, 3,4-dichlorobenzaldehyde was isolated from the products as its 2,4-dinitrophenylhydrazone. The other product, which was isolated from this reaction, was 1,5-di-(3,4-dichlorobenzyloxy)-biuret.

Absorption Spectra

The infrared absorption bands associated with the N—H and C=O groups are given in Table II. The infrared absorption bands assigned to the C=O stretching modes in the oxyurea derivatives agree with those assigned in the urea series (8). When an aryl group is attached directly to a nitrogen atom of the urea then the absorption band of the C=O group shifts from 1642–1653 cm^{-1} to 1666–1678 cm^{-1}. In the carbamates, the C=O absorption band occurs between the frequencies associated with the ester and amide C=O group (9). Allophanates display two absorption peaks between 1700 and 1718 cm^{-1} which would be expected from the two C=O groups existing in different environments. The biuret derivatives also give two distinct absorption bands at ca. 1703–1710 cm^{-1} and 1672–1687 cm^{-1}. 4-Chlorobenzyl 4-(4-chlorobenzyloxycarbamyl)-allophanate, which contains three C=O groups, displays three strong absorption peaks at 1788, 1760, and 1735 cm^{-1} and another peak at 1688 cm^{-1} on the shoulder of the 1735 cm^{-1} band. In the cyclic isocyanuric acid derivatives three absorption peaks are also discernible. These absorption bands occur at 1794, 1750, and 1738 cm^{-1} with 1,3,5-tri-(4-chlorobenzyloxy)-isocyanuric acid but in the other isocyanuric acids the latter two bands are not resolved distinctly.

Bacteriostatic Activities

None of the compounds listed in Table I(*A*) nor the allophanates displayed strong bacteriostatic activity. The most active compound of this series, i.e., 1-(3,4-dichlorobenzyloxy)-3-(2,5-dichlorophenyl)-urea, inhibited the growth of the following organisms at the minimal inhibitory concentrations given in parentheses; *M. pyogenes* var. *aureus* (Penicillin sensitive) (1:80,000), *Sarcina lutea* (1:80,000), *Streptococcus faecalis* (1:40,000),

TABLE II

Infrared absorption band (cm^{-1}) assignments

Compound	N—H Stretching modes	C=O Stretching modes	N—H Bending modes
1-(4-Chlorobenzyloxy)-3-(3,4-dichlorobenzyl)-urea	3360, 3240	1650	1540
1-(4-Chlorobenzyloxy)-3-(4-chlorobenzyl)-urea	3300, 3260	1653	1555
1-(3,4-Dichlorobenzyloxy)-3-(4-chlorobenzyl)-urea	3350, 3175	1644	1550
1-(2,4-Dichlorobenzyloxy)-3-(4-chlorobenzyl)-urea	3360, 3160	1642	1544
1-(4-Chlorobenzyloxy)-3-(4-chlorophenyl)-urea	3370, 3170	1673	1539
1-(3,4-Dichlorobenzyloxy)-3-(2,4-dichlorophenyl)-urea	3380, 3135	1686	1527
1-(4-Chlorobenzyloxy)-3-(3,4-dichlorophenyl)-urea	3360, 3170	1672	1526
1-(4-Chlorobenzyloxy)-3-(4-bromophenyl)-urea	3370, 3170	1673	1539
4-Chlorobenzyl carbamate	3440, 3360, 3305, 3212	1695	1622
4-Chlorobenzyl 3,4-dichlorobenzylcarbamate	3305	1691	1539
1,5-Di-(4-chlorobenzyl)-biuret	3320, 3190	1703, 1687	1518
1,5-Di-(4-chlorobenzyloxy)-biuret	3320, 3190	1703, 1687	1518
1,5-Di-(3,4-dichlorobenzyloxy)-biuret	3355, 3150	1712, 1672	1519
4-Nitrobenzyl 4-(4-nitrobenzyloxy)-allophanate	3320	1718, 1700[a,b]	
4-Chlorobenzyl 4-(4-chlorobenzyloxy)-allophanate	3320, 3170	1706[c]	1542
2,4-Dichlorobenzyl 4-(2,4-dichlorobenzyloxy)-allophanate	3320, 3170	1708[c]	1560
3,4-Dichlorobenzyl 4-(3,4-dichlorobenzyloxy)-allophanate	3290, 3190	1718, 1710	1572
4-Chlorobenzyl 4-(4-chlorobenzyloxycarbamyl)-allophanate	3298, 3160	1788, 1760, 1735, 1688	1608, 1503
1,3,5-Tri-(4-chlorobenzyloxy)-isocyanuric acid		1794, 1750, 1738	
1,3,5-Tri-(4-nitrobenzyloxy)-isocyanuric acid		1794(w) 1730[c,d]	
1,3,5-Tri-(benzyloxy)-isocyanuric acid		1796(w), 1730[c]	

(w) indicates weak absorption bands. The remainder are strong absorption bands. [a]NO_2 group asymmetric and symmetric absorption bands at 1520 cm^{-1} and 1348 cm^{-1}. [b]Strong absorption band at 1610 cm^{-1} which could be a combination of N—H bending and aryl absorption bands. [c]Doublets. [d]NO_2 group absorption bands at 1530 cm^{-1} and 1350 cm^{-1}.

E. coli No. 198 (1:20,000), *A. aerogenes* (1:20,000), *S. pullorum* (1:20,000), *P. aeruginosa* (1:40,000), and *P. vulgaris* (1:20,000).

EXPERIMENTAL[2]

Benzyl Isothiocyanates

The preparation and properties of the benzyl isothiocyanates, which were used in the preparation of the thiourea derivatives listed in Table I(*A*), have been described (10).

Hydroxyurethan

Hydroxyurethan was prepared in 77% yield by the method of Fuller and King (11).

N,N′-*Dicarbethoxy-α,α′-di-(aminoöxy)-p-xylene*

α,α′-Dichloro-*p*-xylene (8.75 g, 0.05 mole), hydroxyurethan (21.2 g, 0.2 mole), and 85% potassium hydroxide (8.05 g) in absolute ethanol (300 ml) were refluxed for 4.5 hours. The precipitated potassium chloride was removed by filtration and the clear filtrate was neutralized with concentrated hydrochloric acid. Evaporation of the filtrate gave 24.2 g of residue. This residue on treatment with ether – petroleum ether solution gave 13.7 g (71.5%) of solid melting at 90–94°. Several crystallizations from the same solution raised the melting point to 103–104°. Anal. Calc. for $C_{14}H_{20}N_2O_6$: C, 53.84; H, 6.45; N, 8.97. Found: C, 53.92; H, 6.41; N, 8.73.

[2]*All melting points are uncorrected. Microanalyses were determined by Micro-Tech Laboratories, Skokie, Ill. and Schwarzkopf Microanalytical Laboratory, Woodside, New York.*

α-Chloromethylnaphthalene

α-Chloromethylnaphthalene (n_D^{25} 1.63827) was prepared in 44.5% yield by the method of Cambron (12).

α-Naphthylmethyloxyurethan

An absolute ethanol (100 ml) solution of α-chloromethylnaphthalene (27.7 g, 0.16 mole), hydroxyurethan (10.5 g, 0.1 mole), and potassium hydroxide (6.6 g, 85% pure) was refluxed for 4.5 hours. After removal of the potassium chloride (7.7 g) the filtrate was evaporated to dryness, yield 27.7 g. The residue was dissolved in ether (50 ml) and a solid (m.p. 90–92°) was precipitated by the addition of petroleum ether (50 ml), yield 12.58 g, (51.2%). Crystallization from petroleum ether raised the melting point to 93–94°. Anal. Calc. for $C_{14}H_{15}NO_3$: C, 68.54; H, 6.61; N, 5.71. Found: C, 68.60; H, 5.84; N, 5.83.

2-Bromoethylurethan

2-Bromoethylurethan (b.p. 90°/0.6 mm) was prepared in 80% yield by the method of Katchalski and Ishai (13).

2-(N-Carbethoxyamino)-ethyloxyurethan

A solution of β-bromoethylurethan (9.8 g, 0.05 mole), hydroxyurethan (5.8 g, 0.05 mole), and potassium hydroxide (2.8 g, 0.05 mole) in methanol (50 ml) was refluxed for 15 minutes. The precipitate (5.38 g, 90.4%) of potassium bromide was removed and the filtrate was evaporated to dryness. The residue (9.38 g) was distilled *in vacuo*. The second fraction (b.p. 133°/0.18 mm; n_D^{25} 1.45459, d_4^{26} 1.137) weighed 5.23 g (56.8%). Anal. Calc. for $C_8H_{16}N_2O_5$: C, 43.62; H, 7.33; N, 12.73. Found: C, 43.61; H, 7.20; N, 12.88.

2-Aminoethyloxyamine

2-(N-Carbethoxyamino)-ethyloxyurethan (4.4 g, 0.02 mole) and barium hydroxide (10.29 g, 0.06 mole) in water (250 ml) were heated under reflux for 1 hour. The cooled solution was saturated with carbon dioxide and the precipitated barium carbonate was removed by filtration through Celite. The filtrate was acidified with hydrochloric acid and taken to dryness *in vacuo*. The residue (m.p. 165–169° decomp.) on crystallization from methanol–ether solution gave 1.54 g (51.7%) of crystalline hydrochloride melting at 187° with decomposition.

A large-scale preparation gave a 58.6% yield of the dihydrochloride of 2-aminoethyloxyamine melting at 189° C (decomp.). Anal. Calc. for $C_2H_{10}Cl_2N_2O$: C, 16.11; H, 6.77; Cl, 47.58; N, 18.80. Found: C, 16.38; H, 6.87; Cl, 47.53; N, 18.74.

4-Chlorobenzyloxyurethan

A solution of hydroxyurethan (14.2 g, 0.135 mole) and potassium hydroxide (85% grade) (8.9 g, 0.135 mole) in isopropanol (140 ml) was treated with 4-chlorobenzyl chloride (21.6 g, 0.135 mole) in isopropanol (10 ml). After the solution was refluxed for 4.5 hours, the precipitated potassium chloride was removed by filtration and the filtrate was evaporated to dryness. The yield of crude 4-chlorobenzyloxyurethan (m.p. 73–78°) was 21.6 g (69.7%). Crystallization from petroleum ether (b.p. 65–110°) raised the melting point to 85–86°. Anal. Calc. for $C_{10}H_{12}ClNO_3$: C, 52.27; H, 5.27; Cl, 15.44; N, 6.10. Found: C, 52.46; H, 5.26; Cl, 15.75; N, 6.34.

3,4-Dichlorobenzyloxyurethan

Hydroxyurethan (15.4 g, 0.146 mole), 3,4-dichlorobenzyl chloride (28.7 g, 0.146 mole), and potassium hydroxide (9.6 g) in absolute ethanol (150 ml) were refluxed for 4.5 hours.

The potassium chloride was removed by filtration and the filtrate on evaporation gave 35.5 g (91.5%) of white solid (m.p. 57–62° C). Two crystallizations from petroleum ether (b.p. 65–110° C) raised the melting point to 82–83° C. Anal. Calc. for $C_{10}H_{11}Cl_2NO_3$: C, 45.46; H, 4.20; Cl, 27.85; N, 5.30. Found: C, 45.69; H, 4.21; Cl, 27.67; N, 5.58.

N-Hydroxyphthalimide

N-Hydroxyphthalimide (m.p. 220–225° C) was prepared in 83% yield by the method of Orndorff and Pratt (14). These authors report a melting point of 220–226° C.

3-N-Phthalimidopropyloxy-N-phthalimide

A stirred solution of γ-bromopropylphthalimide (150 g, 0.56 mole), N-hydroxyphthalimide (91.7 g, 0.56 mole), and triethylamine (121 g, 1.2 mole) in dimethylformamide (700 ml) was gradually heated to 90° C over a period of 1 hour and maintained at this temperature for another 30 minutes. The cooled reaction mixture was diluted with water (2 l.) and the precipitate (m.p. 177–179° C) was removed by filtration, yield 176 g (89.3%). Two crystallizations from glacial acetic acid (8 ml/g) raised the melting point to 178–180° C. Anal. Calc. for $C_{19}H_{14}N_2O_5$: C, 65.32; H, 4.03; N, 7.99. Found: C, 64.98; H, 4.20; N, 7.96.

3-Aminopropyloxyamine

Hydrazine hydrate (20 g, 0.4 mole) was added to a solution of 3-N-phthalimidopropyloxy-N-phthalimide (35.0 g, 0.1 mole) in dimethylformamide (200 ml) at 70° C. This solution was allowed to cool over a period of 1 hour after which it was diluted with water (300 ml) and the pH was lowered to 3 with hydrochloric acid. The phthalylhydrazide was removed and the filtrate was evaporated *in vacuo* at 40–50°. The residue was dissolved in methanol (1 l.) and the solution was passed through a column of IRA 400 resin (1 l. in OH form previously treated with methanol). The column was washed with methanol (1.5 l.) and the combined eluates were evaporated. Distillation of the residue gave 3.0 g (45%) of product (b.p. 110–115°/3 mm). Redistillation gave pure material (b.p. 99°/40 mm, n_D^{25} 1.4614; d_4^{25} 0.999), yield 2.06 g. Anal. Calc. for $C_3H_{10}N_2O$: C, 39.97; H, 11.19; N, 31.09; M_R 24.75. Found: C, 39.86; H, 11.11; N, 30.83; M_R 24.58.

A portion (0.32 g) of 3-aminopropyloxyamine in methanol was neutralized with dry hydrogen chloride. Ether was added to the mixture and the precipitated dihydrochloride (m.p. 207–208° decomp.) was recovered by filtration, yield 0.46 g (71.2%). One crystallization from methanol–ether solution raised the melting point to 208–209° with decomposition. Anal. Calc. for $C_3H_{12}Cl_2N_2O$: C, 22.10; H, 7.42; Cl, 43.48; N, 17.19. Found: C, 22.25; H, 7.39; Cl, 43.71; N, 16.85.

The dipicrate (m.p. 208–209° decomp.) was formed in the usual manner from aqueous solution. Anal. Calc. for $C_{15}H_{16}N_8O_{15}\cdot H_2O$: C, 31.79; H, 3.20; N, 19.77. Found: C, 32.00; H, 3.73; N, 20.04.

N-(4-Chlorobenzyloxy)-phthalimide

A methanolic solution of potassium hydroxide (20.2 ml of 4.95 *N* KOH) was added dropwise to a solution of N-hydroxyphthalimide (16.3 g, 0.1 mole) and 4-chlorobenzyl chloride (16.1 g, 0.1 mole) in dimethylformamide (300 ml) at 65° over a period of 1 hour. When the addition was complete, the solution was cooled and diluted with water (1 l.). The precipitate (m.p. 125–130°) was removed by filtration, yield 20.4 g (70.8%). Crystallization from ethanol (60 ml) raised the melting point to 137–138° C. Anal. Calc. for $C_{15}H_{10}ClNO_3$: C, 62.62; H, 3.50; Cl, 12.33; N, 4.87. Found: C, 62.60; H, 3.37; Cl, 12.68; N, 4.76.

N-(3,4-Dichlorobenzyloxy)-phthalimide

N-Hydroxyphthalimide (90.0 g, 0.05 mole) was added portionwise to a stirred solution of 3,4-dichlorobenzyl chloride (108 g, 0.55 mole) and triethylamine (120 g, 1.19 mole) in dimethylformamide (500 ml) at 70° C. When one-half of the N-hydroxyphthalimide was added, a massive precipitate prevented further stirring. The remainder of the phthalimide was added in one portion and the precipitate dissolved while the product separated from solution. The stirring was continued at 70° C for 2 hours. The cooled solution on dilution with water (3 l.) yielded crude N-(3,4-dichlorobenzyloxy)-phthalimide (m.p. 167–171° C), yield 133 g, (74.7%). Recrystallization from methanol raised the melting point to 182–183° C. Anal. Calc. for $C_{15}H_9Cl_2NO_3$: C, 55.92; H, 2.82; Cl, 22.02; N, 4.35. Found: C, 55.97; H, 2.97; Cl, 22.12; N, 4.30.

Dipotassium Hydroxylamine Disulphonate

Solid dipotassium hydroxylamine disulphonate was prepared in 77% yield by the method of Rollefson and Oldershaw (15).

4-Chlorobenzyloxyamine

Method A

A solution of dipotassium hydroxylamine disulphonate (300 g, 0.985 mole) in potassium hydroxide solution (83.7 g, in 560 ml water) was treated with 4-chlorobenzyl chloride (161 g, 1 mole). The stirred mixture was heated on a steam bath for 1.75 hours. After cooling the solid was removed and then refluxed in 1.5 *N* sulphuric acid solution (1000 ml) for 3 hours. The mixture was cooled and made strongly alkaline with 15% sodium hydroxide solution. The mixture was extracted with ether and the dried ethereal extract was taken to dryness. The solid residue (m.p. 35–38°) weighed 80 g (51.5%). Schroeter and Peschkes (16) reported a melting point of 38°. The solid in ether (1 l.) was treated with anhydrous hydrogen chloride and the precipitated 4-chlorobenzyloxyamine hydrochloride (m.p. 243–244° decomp.) was removed by filtration, yield 59 g (60%).

Method B

Potassium hydroxide (10.7 g, 0.19 mole) in water (25 ml) was added to 4-chlorobenzyloxyurethan (10.95 g, 0.098 mole) in isopropanol (60 ml) and this solution was refluxed for 1 hour. Additional water (50 ml) was added and the oily layer was extracted with ether (70 ml). Evaporation of the ether gave 6.5 g (84.2%) of an oil. Fractional distillation *in vacuo* gave 5.53 g (71.6%) of 4-chlorobenzyloxyamine (b.p. 100°/1 mm; m.p. 32–38°) and a second fraction of 1 g (b.p. 150°/1 mm; m.p. 66–71°). The second fraction, after two crystallizations from ethanol (10 ml), melted at 113–114°, yield 0.13 g. The analytical values of this by-product agreed with those calculated for *O*-(4-chlorobenzyl)-4-chlorobenzaldoxime. Anal. Calc. for $C_{14}H_{11}Cl_2NO$: C, 60.00; H, 3.93; Cl, 25.36; N, 5.00. Found: C, 59.81; H, 3.92; Cl, 25.71; N, 5.11. Schroeter and Peschkes (16) reported a melting point of 114° for *O*-(4-chlorobenzyl)-4-chlorobenzaldoxime.

Method C

N-(4-chlorobenzyloxy)-phthalimide (16 g, 0.056 mole) was dissolved in a solution of dimethylformamide (30 ml) in methanol (300 ml). Hydrazine hydrate (6.1 g, 0.123 mole) was added to the solution at 60° and the whole was allowed to stand for 3 hours. The suspension was acidified to pH 2 with 2 *N* hydrochloric acid and the phthalylhydrazide was removed by filtration. The filtrate was taken to dryness and 2 *N* sodium hydroxide solution (75 ml) was added to the residue. This suspension was extracted with ether

(2×40 ml) and the ether extract was distilled to give 3.8 g (57.6%) of 4-chlorobenzyloxyamine (b.p. 95–100°/2 mm; m.p. 38°).

3,4-Dichlorobenzyloxyamine

3,4-Dichlorobenzyloxyamine (b.p. 95–105°/1 mm) was prepared in 88% yield from 3,4-dichlorobenzyloxyurethan by method B described above for the preparation of 4-chlorobenzyloxyamine. A portion (b.p. 121°/3.6 mm; n_D^{25} 1.57140), which had been redistilled in a collar flask, was submitted for analysis. Anal. Calc. for $C_7H_7Cl_2NO$: C, 43.78; H, 3.67; Cl, 36.93; N, 7.29. Found: C, 43.87; H, 3.73; Cl, 36.70; N, 7.55.

A sample of 3,4-dichlorobenzyloxyamine was converted into its picrate in 45.5% yield by treatment with a saturated ether solution of picric acid. Two crystallizations from absolute ethanol – petroleum ether (1:5) solution raised the melting point from 173–175° to 175–176°. Anal. Calc. for $C_{13}H_{10}Cl_2N_4O_8$: C, 37.08; H, 2.39; Cl, 16.84; N, 13.30. Found: C, 37.26; H, 2.48; Cl, 16.96; N, 13.62.

3,4-Dichlorobenzyloxyamine also was prepared in 52% yield from N-(3,4-dichlorobenzyloxy)-phthalimide (method C).

3,4-Dichlorobenzyloxyamine Hydrochloride

3,4-Dichlorobenzyl chloride (190 g, 0.965 mole), dipotassium hydroxylamine disulphonate (303 g, 0.995 mole), and potassium hydroxide (83.7 g) in water (560 ml) were heated on a steam bath for 5 hours. The solid was removed from the cooled solution by filtration, washed with ethanol, and then refluxed in 1.5 *N* sulphuric acid solution (1 l.) for 3 hours. The mixture was made alkaline with 15% sodium hydroxide solution after which it was extracted with ether. Anhydrous hydrogen chloride was bubbled into the dried ether solution and the precipitated 3,4-dichlorobenzyloxyamine hydrochloride was recovered by filtration, yield 58 g (25.4%). Four crystallizations from ethanol raised the melting point from 195–198° C (decomp.) to 200° C (decomp.). Anal. Calc. for $C_7H_8Cl_3NO$: C, 36.78; H, 3.58; Cl, 46.54; N, 6.13. Found: C, 37.00; H, 3.66; Cl, 46.44; N, 6.16.

The hydrochlorides of benzyloxyamine (17), 4-chlorobenzyloxyamine (16), 4-nitrobenzyloxyamine (18), and 2,4-dichlorobenzyloxyamine were prepared similarly in yields of 34.5, 31, 39.5, and 16.5% respectively.

2,4-Dichlorobenzyloxyamine hydrochloride was converted into its free base by treatment with 10% sodium hydroxide. The oil was extracted with ether and distilled *in vacuo* in a collar flask. A sample of the 2,4-dichlorobenzyloxyamine (b.p. 120–121° C/4.6 mm; n_D^{25} 1.57168) was submitted for analysis. Anal. Calc. for $C_7H_7Cl_2NO$: C, 43.78; H, 3.67; Cl, 36.93; N, 7.29. Found: C, 43.91; H, 3.63; Cl, 36.60; N, 7.56.

The picrate formed in 50% yield in the usual manner from ether solution melted at 176–182°. Anal. Calc. for $C_{13}H_{10}Cl_2N_4O_8$: C, 37.08; H, 2.39; Cl, 16.84; N, 13.30. Found: C, 37.10; H, 2.70; Cl, 16.82; N, 13.28.

Reaction of 4-Chlorobenzyloxyamine Hydrochloride with Phosgene

4-Chlorobenzyloxyamine hydrochloride (5.82 g, 0.03 mole) in anhydrous chlorobenzene (60 ml) was saturated with phosgene at room temperature. Phosgene was bubbled through the reaction mixture while the temperature was increased to 95–100° and maintained at this level for 1 hour. Then the excess phosgene was removed by bubbling nitrogen through the reaction mixture and the chlorobenzene was removed *in vacuo*. An oil remained which was considered to be N-(4-chlorobenzyloxy)-carbamyl chloride, yield 6.6 g (100%). Anal. Calc. for $C_8H_7Cl_2NO_2$: N, 6.37; Cl, 32.23. Found: N, 6.98; Cl, 29.87.

The analysis indicated that the oil was not pure. However a part (2.58 g, 0.011 mole) of the oil in ether (100 ml) was treated with 3,4-dichloroaniline (3.80 g, 0.023 mole). The solid 3,4-dichloroaniline hydrochloride was removed by filtration, yield 2.36 g (50% based on added 3,4-dichloroaniline). The filtrate was evaporated to dryness and the residue was crystallized from ethanol, yield 2.07 g (51.2%). One crystallization from ethyl acetate – petroleum ether solution raised the melting point of the 1-(4-chlorobenzyloxy)-3-(3,4-dichlorophenyl)-urea from 135–140° to 150–151°. Anal. Calc. for $C_{14}H_{11}Cl_3N_2O_2$: C, 48.61; H, 3.21; Cl, 30.78; N, 8.11. Found: C, 48.68; H, 3.28; Cl, 30.71; N, 8.48.

4-Chlorobenzyl 4-(4-Chlorobenzyloxy)-allophanate and 1,3,5-Tri-(4-chlorobenzyloxy)-isocyanuric Acid

A suspension of 4-chlorobenzyloxyamine hydrochloride (50 g, 0.257 mole) in chlorobenzene (300 ml) was saturated with phosgene. This reaction mixture was heated at 120–125° for 3.5 hours (until the suspended solid dissolved) while phosgene was bubbled through the reaction mixture. Removal of the chlorobenzene *in vacuo* left a mixed solid and oil residue which was extracted with ether (150 ml). The ether-insoluble 4-chlorobenzyl 4-(4-chlorobenzyloxy)-allophanate (m.p. 147–149° C decomp.) was recovered by filtration, yield 19.55 g (41%). Crystallization from glacial acetic acid raised the melting point to 148–149° with decomposition. Anal. Calc. for $C_{16}H_{14}Cl_2N_2O_4$: C, 52.05; H, 3.82; Cl, 19.21; N, 7.59; mol. wt., 369.20. Found: C, 52.49; H, 3.63; Cl, 19.55; N, 7.90; mol. wt., 398 (Rast).

The ether solution was made alkaline with triethylamine at room temperature. The precipitated solid (m.p. 225–235° decomp.) was removed by filtration and washed with water until the filtrate gave a negative chloride ion test, yield 6 g (12.7%). The melting point of this crude 1,3,5-tri-(4-chlorobenzyloxy)-isocyanuric acid was raised to 248–249° with decomposition by crystallizing from glacial acetic acid. Anal. Calc. for $C_{24}H_{18}Cl_3N_3O_6$: C, 52.34; H, 3.29; Cl, 19.31; N, 7.63; mol. wt., 550.77. Found: C, 52.41; H, 3.22; Cl, 19.20; N, 7.71; mol. wt., 575 (Rast).

When benzyloxyamine hydrochloride was heated with phosgene under the above conditions a 68% yield of 4-chlorobenzyl 4-(4-chlorobenzyloxy)-allophanate (m.p. 148–149° decomp.) and a 4.8% yield of 1,3,5-tri-(4-chlorobenzyloxy)-isocyanuric acid (m.p. 248–249°) were obtained. These compounds were identified by mixed melting point determinations.

In another experiment a suspension of 4-chlorobenzyloxyamine hydrochloride (23.29 g, 0.12 mole) in commercial chlorobenzene (180 ml), which was not dried, was saturated with phosgene at room temperature. Phosgene was bubbled in while the reaction mixture was heated at 95–100° for 1.5 hours and 108–110° for 3 hours. Evaporation of the solution *in vacuo* left a semisolid residue which was triturated with ether (200 ml). The ether-insoluble 4-chlorobenzyl 4-(4-chlorobenzyloxycarbamyl)-allophanate, m.p. 230–260°, was recovered by filtration, yield 2.53 g (11.5% from 2 moles of 4-chlorobenzyloxyamine hydrochloride). Repeated recrystallization from methanol raised the melting point to 271–272°. Anal. Calc. for $C_{17}H_{15}Cl_2N_3O_5$: C, 49.54; H, 3.67; Cl, 17.20; N, 10.20. Found: C, 49.76; H, 3.47; Cl, 17.10; N, 10.50.

Reaction of 4-Chlorobenzylamine with Crude 4-Chlorobenzyloxycarbamyl Chloride

A solution of 4-chlorobenzylamine (11.0 g, 0.078 mole) in ether (50 ml) was added to crude 4-chlorobenzyloxycarbamyl chloride (8.35 g, 0.039 mole) at room temperature. The precipitate of 4-chlorobenzylamine hydrochloride was removed by filtration, yield 5.19 g (75.0%). The filtrate was evaporated and the residue was crystallized from ether, giving

a precipitate of 5.10 g, m.p. 113–115°. Recrystallization from chloroform and from ethanol gave 1-(4-chlorobenzyloxy)-3-(4-chlorobenzyl)-urea, m.p. 123–124°, yield 4.34 g, 24.3%. Elementary analysis of this product is given in Table I(*A*). The mother liquors from this crystallization were evaporated (0.65 g, m.p. 130–140° C) and the residue was recrystallized twice from ethanol, giving 1,5-di-(4-chlorobenzyl)-biuret (m.p. 177–178°), yield 0.043 g (0.3%). Anal. Calc. for $C_{16}H_{15}Cl_2N_3O_2$: C, 54.57; H, 4.29; Cl, 20.14; N, 11.93. Found: C, 54.64; H, 4.54; Cl, 19.91; N, 11.64.

The combined mother liquors were evaporated to dryness and dissolved in ether. Anhydrous hydrogen chloride was passed through the ether solution, causing the separation of additional 4-chlorobenzylamine hydrochloride, yield 2.20 g (31.8%). The total recovery of 4-chlorobenzylamine hydrochloride was 53.4% (based on added 4-chlorobenzylamine).

The filtrate was evaporated to dryness and the residue (5.81 g), in benzene, was chromatographed on alumina (240 g). The fraction eluted by ether (1.79 g) was recrystallized from ethanol – petroleum ether. The crystals melted at 84–85°, yield 0.25 g. The analytical values agree with the calculated for ethyl 4-chlorobenzyloxycarbamate. This apparently arose from presence of ethanol in the ether used as solvent. Anal. Calc. for $C_{10}H_{12}ClNO_3$: C, 52.29; H, 5.27; Cl, 15.44; N, 6.10. Found: C, 52.21; H, 5.02; Cl, 15.34; N, 6.14.

A 2% solution of methanol in absolute ether removed a fraction (1.79 g, m.p. 100–110°) from the column which was recrystallized from ethanol to give additional 1-(4-chlorobenzyloxy)-3-(4-chlorobenzyl)-urea, m.p. 123–124°, yield 0.72 g, 5.7%. The total yield of pure urea was 30.0%.

The fraction eluted by 4% methanol in ether consisted of crude 1-(4-chlorobenzyl)-5-(4-chlorobenzyloxy)-biuret (m.p. 140–145°), yield 0.59 g (0.52%). Crystallization from ethanol raised the melting point to 149–150°. Anal. Calc. for $C_{16}H_{15}Cl_2N_3O_3$: C, 52.20; H, 4.11; Cl, 19.26; N, 11.42. Found: C, 52.14; H, 4.22; Cl, 19.35; N, 11.91.

Reactions of 4-Chlorobenzyl 4-(4-Chlorobenzyloxy)-allophanate

A. Alkaline Hydrolysis

A solution of the allophanate (3.69 g, 0.01 mole) in 1,2-dimethoxyethane (100 ml) was added to sodium hydroxide (0.40 g, 0.01 mole) in water (10 ml). After standing at room temperature for 18 hours, the solution was neutralized with hydrochloric acid and evaporated almost to dryness. The residue was diluted with water (30 ml) and extracted with chloroform (2×100 ml). Evaporation of the dried chloroform extract yielded an oily residue (3.4 g) which on crystallization from chloroform gave 1,5-di-(4-chlorobenzyloxy)-biuret (m.p. 173–175°), yield 0.60 g (31.3%). Crystallizations from chloroform and ethyl acetate raised the melting point to 174.5–175.5°. Anal. Calc. for $C_{16}H_{15}Cl_2N_3O_4$: C, 50.02; H, 3.94; Cl, 18.46; N, 10.94. Found: C, 50.02; H, 4.10; Cl, 18.46; N, 11.04.

Repeated recrystallization of the mother liquors from ether yielded a small quantity (0.07 g) of unchanged allophanate (m.p. 148–149°).

Alumina chromatography of the combined mother liquors gave, in the petroleum ether:benzene (1:1) eluate, *O*-(4-chlorobenzyl)-4-chlorobenzaldoxime (108 mg, 7.8% yield) melting at 113–114°. A mixed melting point determination with a known sample of *O*-(4-chlorobenzyl)-4-chlorobenzaldoxime gave no depression. 4-Chlorobenzyl alcohol, melting point and mixed melting point 71–72°, was isolated from the ether:benzene (1:1) eluate, yield 0.238 g (16.7%).

A 10% methanol in ether solution removed 4-chlorobenzyloxyurea from the column.

This urea melted at 165–166° after recrystallization from ethanol and petroleum ether, yield 0.255 g (12.8%). This product was identified by a mixed melting point determination with a known sample which was prepared as follows: A solution of 4-chlorobenzyloxyamine hydrochloride (1.0 g, 0.0051 mole) and potassium cyanate (0.42 g, 0.0051 mole) in water (25 ml) was refluxed for 5 hours. 4-Chlorobenzyloxyurea (m.p. 163–165°), separated from the cooled solution, yield 0.82 g (86.3%). Crystallization from ethanol – petroleum ether solution raised the melting point to 165–166°. Anal. Calc. for $C_8H_9ClN_2O_2$: C, 47.82; H, 4.52; Cl, 17.65; N, 13.95. Found: C, 47.96; H, 4.52; Cl, 17.93; N, 14.16.

B. Reaction with 4-Chlorobenzylamine

A solution of the allophanate (1.93 g, 0.0052 mole) and 4-chlorobenzylamine (1.47 g, 0.0104 mole) in chlorobenzene (20 ml) was refluxed for 90 minutes. The solution was evaporated to dryness and the residue was crystallized from chloroform, giving 1-(4-chlorobenzyl)-3-(4-chlorobenzyloxy)-urea (m.p. 123–124°), yield 1.51 g, (88.5%). The urea was identified by a mixed melting point determination.

The mother liquors were combined and evaporated to dryness, and the residue on crystallization from petroleum ether weighed 0.55 g (2.1%). It did not depress the melting point of a known sample of 1,5-di-(4-chlorobenzyl)-biuret (m.p. 177–178°).

Chromatography of the remaining mother liquors gave crystals of *O*-(4-chlorobenzyl)-4-chlorobenzaldoxime (m.p. 113–114°), yield 0.073 g (10.0%), and a very small quantity of a substance which sublimed readily to give crystals melting at 90–91°. The aldoxime was identified by a mixed melting point determination.

The other allophanates described in this paper were treated with 4-chlorobenzylamine in the same way. The resulting unsymmetrical ureas are described in Table I(*A*).

4-Chlorobenzyl Chloroformate

4-Chlorobenzyl alcohol (21.4 g, 0.15 mole) and quinoline (19.4 g, 0.15 mole) were added to a stirred solution of phosgene (61 g, 0.165 mole) in toluene (75 ml), and the mixture was allowed to stand for 36 hours. The quinoline hydrochloride was removed by filtration, and the filtrate was evaporated to dryness at 40–45°. An attempt to distill the crude chloroformate resulted in the isolation of 4-chlorobenzyl chloride, b.p. 72–74° (1.4 mm) (hexamethylenetetramine salt, melting point and mixed melting point 200° decomp). The undistilled chloroformate (2.05 g, 0.01 mole) in ether (50 ml) was added to 3,4-dichlorobenzylamine (3.52 g, 0.02 mole) in ether (50 ml) at room temperature. The precipitated 3,4-dichlorobenzylamine hydrochloride (1.10 g, 52%) was filtered, and the filtrate was concentrated to 10 ml. Addition of petroleum ether caused the separation of 4-chlorobenzyl N-3,4-dichlorobenzylcarbamate (m.p. 94–96°), yield 1.55 g, (45%).

Recrystallization from ethanol – petroleum ether raised the melting point to 95–96°. Anal. Calc. for $C_{15}H_{12}Cl_3NO_2$: C, 52.28; H, 3.51; Cl, 30.87; N, 4.06. Found: C, 52.16; H, 3.80; Cl, 30.68; N, 3.95.

The reaction of 4-chlorobenzyl chloroformate with potassium cyanate and potassium thiocyanate did not yield any identifiable products.

1,3-Di-(4-chlorobenzyloxy)-urea

A solution of phosgene (0.2 g, 0.002 mole) in toluene (7.5 ml) was added to a stirred and cooled solution of 4-chlorobenzyloxyamine (1.1 g, 0.007 mole) in benzene (25 ml). The precipitate of 4-chlorobenzyloxyamine hydrochloride was removed by filtration and the filtrate was evaporated to dryness. 1,3-Di-(4-chlorobenzyloxy)-urea (m.p. 116–118°) was

obtained from a solution of the residue in chloroform by addition of petroleum ether, yield 0.418 g (68%). One crystallization from ethanol raised the melting point to 117–118°. Anal. Calc. for $C_{15}H_{14}Cl_2N_2O_3$: C, 52.80; H, 4.14; Cl, 20.78; N, 8.21. Found: C, 52.74; H, 4.11; Cl, 20.68; N, 8.21.

4-Chlorobenzylcarbamate

A mixture of 4-chlorobenzyl alcohol (2.84 g, 0.02 mole), urea (0.60 g, 0.01 mole), and stannic chloride (0.04 g, 0.00015 mole) was stirred at 150° for 8 hours. The cooled reaction mixture was triturated with ether, giving 4-chlorobenzyl carbamate (m.p. 134–137°), yield 1.03 g (55.6%). Crystallization from ethanol raised the melting point to 136.5–137.5°. Anal. Calc. for $C_8H_8ClNO_2$: C, 51.76; H, 4.34; Cl, 19.11; N, 7.55. Found: C, 51.62; H, 4.37; Cl, 19.09; N, 7.25.

3,4-Dichlorobenzyl 4-(3,4-Dichlorobenzyloxy)-allophanate and its Treatment with Methanolic Sodium Hydroxide

3,4-Dichlorobenzyloxyamine hydrochloride was treated with phosgene in anhydrous chlorobenzene at 120–125° as described above in the preparation of 4-chlorobenzyl 4-(4-chlorobenzyloxy)-allophanate. 3,4-Dichlorobenzyl 4-(3,4-dichlorobenzyloxy)-allophanate (m.p. 121–123°) was obtained in 75.5% yield. Crystallization from glacial acetic acid raised the melting point to 125–126° (decomp.). Anal. Calc. for $C_{16}H_{12}Cl_4N_2O_4$: C, 43.87; H, 2.76; Cl, 32.38; N, 6.32; mol. wt., 438.11. Found: C, 44.19; H, 2.61; Cl, 32.67; N, 6.65; mol. wt., 430 (Rast).

A solution of the allophanate (2.19 g, 0.005 mole) and sodium hydroxide (0.2 g, 0.005 mole) in methanol (250 ml) was heated to boiling and then allowed to stand for 3 days. The solution was concentrated almost to dryness and then diluted with water. It gave an oily solid which was filtered and washed with ether. The crystalline residue of 1,5-di-(3,4-dichlorobenzyloxy)-biuret, melted at 156–158°, yield 0.83 g (57%). Crystallization from methanol raised the melting point to 157–158°. Anal. Calc. for $C_{16}H_{12}Cl_4N_3O_4$: C, 42.42; H, 2.89; Cl, 31.31; N, 9.28. Found: C, 42.30; H, 3.09; Cl, 31.36; N, 9.04.

The ether washings were evaporated and the residue was treated with an excess of 2,4-dinitrophenylhydrazine in ethanol. The 2,4-dinitrophenylhydrazone of 3,4-dichlorobenzaldehyde, (m.p. 308–309°) was recovered by filtration, yield 0.45 g (25%). It was identified by a mixed melting point determination with a known sample of the 2,4-dinitrophenylhydrazone of 3,4-dichlorobenzaldehyde.

4-Nitrobenzyl 4-(4-Nitrobenzyloxy)-allophanate and 1,3,5-Tri-(4-nitrobenzyloxy)-isocyanuric Acid

4-Nitrobenzyloxyamine hydrochloride on treatment with phosgene under the conditions described above for 4-chlorobenzyloxyamine hydrochloride gave an 81% yield of 4-nitrobenzyl 4-(4-nitrobenzyloxy)-allophanate (m.p. 183–185° decomp.). Crystallization from glacial acetic acid raised the melting point to 184–185° (decomp.). Anal. Calc. for $C_{16}H_{12}N_4O_8$: C, 49.01; H, 3. 61; N, 14.36; mol. wt., 390.30. Found: C, 49.18; H, 3.62; N, 14.60; mol. wt., 395 (Rast).

Treatment of the ether extract with triethylamine gave a 2.9% yield of 1,3,5-tri-(4-nitrobenzyloxy)-isocyanuric acid (m.p. 183–220° decomp.). The melting point was raised to 251–252° (decomp.) by crystallization from glacial acetic acid, yield 0.8%. Anal. Calc. for $C_{24}H_{18}N_6O_{12}$: C, 49.49; H, 3.12; N, 14.43. Found: C, 49.75; H, 3.04; N, 14.15.

2,4-Dichlorobenzyl 4-(2,4-Dichlorobenzyloxy)-allophanate and 1,3,5-Tri-(2,4-dichlorobenzyloxy)-isocyanuric Acid

When 2,4-dichlorobenzyloxyamine hydrochloride was treated with phosgene under the same conditions, a 34.5% yield of 2,4-dichlorobenzyl 4-(2,4-dichlorobenzyloxy)-allophanate (m.p. 95–98° decomp.) was obtained. Crystallization from glacial acetic acid raised the melting point to 97–98° (decomp.). Anal. Calc. for $C_{16}H_{10}Cl_4N_2O_4$: C, 43.87; H, 2.76; Cl, 32.38; N, 6.32; mol. wt., 438.11. Found: C, 44.28; H, 2.50; Cl, 32.62; N, 6.38; mol. wt., 438 (Rast).

The ether extract on addition of triethylamine gave 0.5% yield of 1,3,5-tri-(2,4-dichlorobenzyloxy)-isocyanuric acid (m.p. 198–200° decomp.). It melted at 201–202° (decomp.) after crystallization from glacial acetic acid. Anal. Calc. for $C_{24}H_{15}Cl_2N_3O_6$: C, 44.07; H, 2.31; Cl, 32.53; N, 6.43. Found: C, 44.25; H, 2.37; Cl, 32.41; N, 6.27.

1,3,5-Tribenzyloxy-isocyanuric Acid

A suspension of benzyloxyamine hydrochloride (9.57 g, 0.060 mole) in chlorobenzene (81 ml) was saturated with phosgene at room temperature. The flow of phosgene was continued while the reaction mixture was heated at 105–110° for 2 hours. The clear solution was evaporated *in vacuo* and the residual oil was dissolved in ether (40 ml). This solution was made basic with triethylamine and the precipitate was filtered and washed with water, yield 4.6 g (51.5%). The melting point was raised from 225–235° (decomp.) to 239–241° (decomp.) by crystallization from glacial acetic acid. Anal. Calc. for $C_{24}H_{21}N_3O_6$: C, 64.29; H, 4.73; N, 9.39; mol. wt., 447.42. Found: C, 64.45; H, 4.61; N, 9.59; mol. wt., 449 (Rast).

Urea and Thiourea Derivatives

The urea and thiourea derivatives prepared by the reaction of isocyanates and isothiocyanates with substituted oxyamines are described in Table I. The following procedure was used in the preparation of all of these derivatives.

4-Chlorobenzyl isothiocyanate (0.82 g, 0.004 mole) in ether (5 ml) was added to 4-chlorobenzyloxyamine (0.71 g, 0.004 mole). The ether on evaporation gave a crystalline residue (m.p. 107–111°), yield 1.51 g (99%). Crystallization from absolute ethanol raised the melting point to 115–116° C.

1-(β-Hydroxyethyl)-2-methylmercapto-2-imidazolinium Chloride

A mixture of 1-(β-hydroxyethyl)-2-imidazolidinethione (19) (612 g, 4.3 moles), methyl chloride (660 g, 13 moles), and isopropanol (1450 ml) was heated at 55–60° C under 30–70 p.s.i. in an autoclave with stirring for 6 hours. A quantitative gravimetric estimation of chloride ion at the end of the reaction period indicated a 92% conversion of the cyclic thiourea to 1-(β-hydroxyethyl)-2-methylmercapto-2-imidazolinium chloride. The autoclave was emptied and washed with isopropanol (2×200 ml). The combined washings and reaction mixture on cooling at 0° C for several hours deposited crystals. These crystals (m.p. 104–106° C) were recovered by filtration, yield 394 g (48%). The remainder of the product was obtained by evaporation of the filtrate *in vacuo*. Crystallization of the crude product from isopropanol raised the melting point to 105–106° C. Anal. Calc. for $C_6H_{13}ClN_2OS$: C, 36.63; H, 6.66; Cl, 18.02; N, 14.24; S, 16.29. Found: C, 37.02; H, 6.95; Cl, 17.92; N, 14.10; S, 15.91.

1-(β-Hydroxyethyl)-2-(2,4-dichlorobenzyloxyamine)-2-imidazoline

1-(β-Hydroxyethyl)-2-methylmercapto-2-imidazolinium chloride (19.67 g, 0.1 mole) and 2,4-dichlorobenzyloxyamine (19.20 g, 0.1 mole) in isopropanol (100 ml) were heated

under reflux for 2 hours. Methyl mercaptan was evolved during the reaction. After the solution stood at 25° C overnight some solid (m.p. 124–125° C), precipitated, yield 2.09 g (11.9%). The melting point was raised to 125–126° C by crystallization from isopropanol. The analyses agree with the calculated values for *O*-(2,4-dichlorobenzyl)-2,4-dichlorobenzaldoxime. Anal. Calc. for $C_{14}H_9Cl_4NO$: C, 48.18; H, 2.60; Cl, 40.64; N, 4.01. Found: C, 48.37; H, 2.61; Cl, 40.46; N, 4.03.

The residue obtained on evaporation of the filtrate to dryness was treated with excess sodium hydroxide solution and the basic solution was extracted with ether. The ether extract was washed with water and dried over anhydrous sodium sulphate. Evaporation of the ether gave a solid melting at 103–105°, yield 18.04 g (59.2%). Crystallization from absolute ethanol – petroleum ether solution raised the melting point to 109–110°. Anal. Calc. for $C_{12}H_{15}Cl_2N_3O_2$: C, 47.37; H, 4.97; Cl, 23.31; N, 13.81. Found: C, 47.67; H, 5.11; Cl, 23.60; N, 14.05.

Isolation of 1,3,5-Tri-(3,4-dichlorobenzyl)-isomelamine

An analytical sample of 1-(3,4-dichlorobenzyloxy)-3-(3,4-dichlorobenzyl)-thiourea (m.p. 107–108°) on standing at room temperature for 2 weeks changed into a mixture of red oil and crystals. A portion (3.95 g) of this mixture was triturated with ether (50 ml) and the insoluble material (m.p. 151–156°) recovered. The solid was taken up in acetone (30 ml) and the insoluble free sulphur (0.11 g, m.p. 116°) was removed by filtration. The filtrate on dilution with water gave 0.72 g of product melting at 168–170°. Two crystallizations from acetone–water solution raised the melting point to 171–172°. Anal. Calc. for $C_{24}H_{18}Cl_6N_6$: C, 47.78; H, 3.01; Cl, 35.27; N, 13.93; mol. wt., 603.18. Found: C, 47.78; H, 3.19; Cl, 35.90; N, 13.82; mol. wt., 580 (Rast).

N^2,N^4,N^6-*Tri-(3,4-dichlorobenzyl)-melamine*

3,4-Dichlorobenzylamine hydrochloride (12.66 g, 0.06 mole) was treated with an excess of 25% sodium hydroxide solution and the free amine was extracted with ether (100 ml). The dried ether solution was treated with cyanuric chloride (1.84 g, 0.01 mole). An exothermic reaction occurred and the ether solution began to reflux. The ether was replaced with *o*-xylene and the mixture was refluxed for 4 hours. The solvent was removed *in vacuo* and the semisolid residue was triturated with acetone (50 ml). The insoluble material (m.p. 210–215°) was removed by filtration, yield 7 g. One crystallization from water raised the melting point to 244°. This solid was identified as 3,4-dichlorobenzylamine hydrochloride by a mixed melting point determination.

The acetone filtrate on dilution with petroleum ether (50 ml) gave crystals which melted at 203–214°, yield 1.84 g (20.9%). Crystallization from absolute ethanol raised the melting point to 217–218°. Anal. Calc. for $C_{24}H_{18}Cl_6N_6$: C, 47.78; H, 3.01; Cl, 35.27; N, 13.93; mol. wt., 603. Found: C, 47.66; H, 3.39; Cl, 35.77; N, 14.11; mol. wt., 643 (Rast).

ACKNOWLEDGMENTS

The bacteriostatic activities reported in this paper were determined by Dr. H. A. Baker of Ayerst, McKenna and Harrison Limited, Montreal, Quebec. The infrared spectra were run by Dr. C. Sandorfy of the University of Montreal, Montreal, Quebec.

REFERENCES

1. L. VOLTMER. Ber. **24**, 378 (1891).
2. J. U. NEF. Ann. **280**, 263 (1894).
3. L. W. JONES. Am. Chem. J. **20**, 1 (1898).
4. L. W. JONES and L. NEUFFER. J. Am. Chem. Soc. **39**, 652 (1917).

5. H. BILTZ and A. JELTSCH. Ber. **56**, 1914 (1923).
6. F. H. S. CURD, D. G. DAVEY, and D. N. RICHARDSON. J. Chem. Soc. 1732 (1949).
7. E. S. GATEWOOD. J. Am. Chem. Soc. **47**, 407 (1925).
8. A. F. MCKAY, G. Y. PARIS, and D. L. GARMAISE. J. Am. Chem. Soc. **80**, 6276 (1958).
9. L. J. BELLAMY. The infrared spectra of complex molecules. 2nd ed. John Wiley & Sons, Inc., New York, N.Y. 1958.
10. A. F. MCKAY, D. L. GARMAISE, R. GAUDRY, H. A. BAKER, G. Y. PARIS, R. W. KAY, G. E. JUST, and R. SCHWARTZ. J. Am. Chem. Soc. **81**, 4328 (1959).
11. A. T. FULLER and H. KING. J. Chem. Soc. 963 (1947).
12. A. CAMBRON. Can. J. Research, B, **17**, 10 (1939).
13. E. KATCHALSKI and D. B. ISHAI. J. Org. Chem. **15**, 1067 (1950).
14. W. R. ORNDORFF and D. S. PRATT. Am. Chem. J. **47**, 89 (1912).
15. G. K. ROLLEFSON and C. F. OLDERSHAW. J. Am. Chem. Soc. **54**, 977 (1932).
16. G. SCHROETER and M. PESCHKES. Ber. **33**, 1975 (1900).
17. A. MICHAELIS and G. SHROETER. Ber. **26**, 2155 (1893).
18. O. L. BRADY and L. KLEIN. J. Chem. Soc. 874 (1927).
19. A. F. MCKAY and G. R. VAVASOUR. Can. J. Chem. **32**, 59 (1954).

PROTON MAGNETIC RESONANCE ABSORPTION IN THE C-FORM OF STEARIC ACID[1]

R. F. GRANT[2] AND B. A. DUNELL

ABSTRACT

The proton magnetic resonance absorption in the C-form of stearic acid has been measured over a temperature range from −78° C to the melting point. The results suggest that the methyl end groups may be free to rotate about their triad axes throughout this temperature range, and that premelting becomes significant above 40° C.

INTRODUCTION

Proton magnetic resonance absorption measurements are sometimes useful for determining the nature and extent of molecular motion in solid organic compounds. This method has been successfully employed in the study of several long chain hydrocarbon compounds. For instance, it has been shown that the methyl groups at the ends of *n*-pentane and *n*-hexane molecules may undergo reorientation about their triad axes at temperatures well below the melting points of these compounds (1). Moreover, considerable reorientation of whole molecules has been reported in the high temperature phases of solid octacosane, *n*-dotriacontane, and lauryl alcohol (2). With the onset of molecular motion, there is a decrease of the proton magnetic resonance line width, if the rate of molecular reorientation is comparable to or greater than the line width expressed in frequency units. The extent of the narrowing will depend upon the rate and nature of the reorientation. Rapid reorientation of the whole molecule about many axes, which may occur in liquids, leads to very narrow line widths.

No extensive motion of stearic acid molecules in the solid has been reported. However, stearic acid exhibits a large, anomalous increase in volume between 60° C and the melting point, 69.6° C (3). Such behavior in long chain hydrocarbon compounds has sometimes been attributed to premelting (4). The following is an investigation of this possibility.

EXPERIMENTAL

The stearic acid used in this investigation was Eastman Kodak white label grade with a freezing point of 68.1° C. The stearic acid was purified by numerous crystallizations at −20° C from freshly distilled acetone, after the method outlined by Brown and Kolb (5). The freezing point of the purified stearic acid was 69.3° C obtained from the plateau of a time – temperature cooling curve run on a 6-g sample of the purified acid using a calibrated thermometer. This value agrees very well with the best setting points (s.p.) obtained by Francis and his co-workers (6, 7), viz., 69.35 and 69.32° C for stearic acid, and indicates that at most a very small amount of impurity was present in our sample. Indeed, Francis, Collins, and Piper found that 1% of palmitic acid impurity added to pure stearic acid (s.p. 69.32° C) lowered the setting point to 69.08° (7).

Narrow proton magnetic resonance line widths from molten stearic acid were recorded with a Varian V-4300 high resolution spectrometer operating at 40 Mc/sec. The broad line widths from solid stearic acid were measured with an oscillating detector spectrometer of conventional design (8), operating at 28 Mc/sec. A Varian electromagnet with

[1]*Manuscript received November 9, 1959.*
Contribution from the Department of Chemistry, University of British Columbia, Vancouver 8, B.C.
[2]*Holder of National Research Council Studentships. Present address: Division of Applied Chemistry, National Research Council of Canada, Ottawa.*

6-in. pole faces and a 1.75-in. gap supplied the magnetic field, which was swept linearly in time and modulated at 27 c/sec.

The samples were placed in 10-mm O.D. Pyrex test tubes. These were maintained at the higher temperatures by arranging the sample container in a glass tube through which hot air was passed from an external heater. Low temperatures were obtained by immersing the sample container in a mixture of dry ice and acetone in a narrow glass dewar. The temperature was measured with a copper–constantan thermocouple placed directly in the sample. The temperature variation during the recording of a magnetic resonance signal was about $\pm 0.5°$ C. The widths of the proton magnetic resonance absorption lines were taken as the separation in gauss of the points of maximum and minimum slope, which are the maximum and minimum of the recorded derivative signal. The second moments of the resonance absorption lines (9) were obtained from the experimental derivative curves by numerical integration (10) and were corrected for the broadening effects of modulation (11).

RESULTS

Although the proton magnetic resonance signal of stearic acid showed no fine structure from $-77°$ C to about room temperature, at about 24° C the derivative absorption line began to show a narrow peak along with the usual broad peak expected for a solid paraffin. Above 24° C this narrow peak became more and more prominent until finally the broad peak almost disappeared. The selection of first derivative lines in Fig. 1 serves to illustrate this behavior. The variation of line width with temperature for the broad peak of the resonance curve from the purified stearic acid is given by Fig. 2. Over the temperature range from $-77°$ C to 66° C, the line width remains approximately constant with values ranging from 14.0 gauss to 14.6 gauss. At 67° C the broad component of the resonance curve is so weak that its width is difficult to measure accurately. A trace of the broad component remains, however, until 69° C.

The true width of the narrow component of the resonance line was not obtained directly. The line width of 0.1 gauss obtained with the broad line spectrometer was

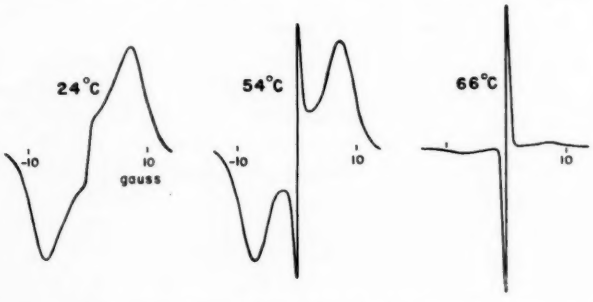

FIG. 1. Examples of derivative absorption curves showing growth of narrow component.

considered to be due to the inhomogeneity of the magnetic field over the sample and to modulation broadening. High resolution spectra from stearic acid were therefore obtained as the molten acid slowly solidified. No proton magnetic resonance absorption could be observed below the freezing point with the high resolution spectrometer, but just before freezing the line width was 0.01 gauss. The true widths of the narrow peaks of the resonance lines are, then, somewhere between 0.1 and 0.01 gauss.

The second moments of the proton magnetic resonance absorption lines decreased as the temperature approached the melting point if one took the second moment of the total curve, including the narrow peak. However, when the narrow peaks on the broad resonance lines were removed by a procedure first employed by Wilson and Pake (12), the second moment values remained almost constant throughout the whole temperature range. These second moment results from stearic acid are given as a function of temperature in Fig. 2.

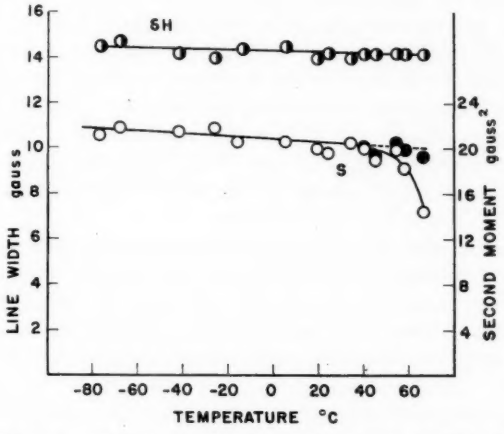

FIG. 2. Line width of broad portion of signal and second moment of stearic acid as functions of temperature. Half-filled circles, line width; open circle, second moment of the entire resonance line; filled circle, second moment calculated after the narrow component of the resonance line has been removed.

DISCUSSION

The second moment of the proton magnetic resonance of stearic acid can be calculated from structural parameters by means of Van Vleck's formula (9). For a polycrystalline sample the second moment, S, of an assembly of protons is

$$S = \frac{716}{N} \sum_{j>k} r_{jk}^{-6}$$

where N is the number of protons whose interactions are considered and r_{jk} is the distance in Å between any two protons j and k (1). We have assumed in using this formula that the crystal lattice is rigid, which in this case means that molecular reorientation occurs at a rate less than about 60 kc/sec, the low temperature experimental line width, expressed as a frequency. We have also assumed that nuclei with non-zero magnetic moments, other than protons, are absent. This is not exactly so, for C^{13} and O^{17} will be present in natural abundance. Their concentrations, however, are too small to have a significant effect on the proton second moment. The calculation of the rigid lattice second moment requires in principle a knowledge of the interproton distances throughout the crystal lattice, but because their contribution to the second moment is very small proton pairs whose separation r_{jk} is greater than 6 Å have been included in the second moment calculation by integration. The distances between pairs can be considered in two categories, namely, the intramolecular and intermolecular distances, which for convenience have been treated separately.

The intramolecular distances have been taken from the model of a long hydrocarbon

chain described by Müller (13). This model represents the molecules as planar zigzag chains of carbon atoms with tetrahedral angles of 109°28′ between the bonds. The C—H bond lengths have been taken as 1.094 Å and the C—C bond distances as 1.54 Å (14). With those parameters, the intramolecular second moment was found to be 18.4 gauss^2. The dimensions of the monoclinic unit cell used to calculate the intermolecular distances in the C-form of stearic acid are from the X-ray diffraction results of Abrahamsson and von Sydow (15). The tilt of the hydrocarbon chains has been assumed to be the same as that of lauric acid, 54°52′ to the basal (001) plane containing the carboxyl groups (16). The packing of the hydrocarbon chains is such that there are two acid dimers per unit cell. The arrangement of these carboxyl dimers has also been assumed to be the same as in lauric acid (16). The O—H bond length of the carboxyl group has been taken as 1.04 Å (17) and hence the interproton distance in the carboxyl dimer as 2.40 Å. The hydrocarbon chains are arranged end-to-end such that the distance between the planes passing through the carbon atoms of opposing methyl end groups is about 2.18 Å. From these data, the intermolecular second moment was found to be 6.0 gauss^2. The total rigid lattice second moment is therefore 24.4 gauss^2.

Since this calculated rigid lattice second moment is 3 gauss^2 larger than the mean experimental value of 21.5 gauss^2 found below −30° C, some molecular motion must be present below −30° C. It has already been mentioned that the methyl end groups might be free to reorient about their triad axes in the solid, even at low temperatures. Moreover, the low moment of inertia of the methyl group makes a tunnelling mechanism quite probable (18). If the methyl end groups reorient freely about their triad axes, the reduction in the theoretical second moment can be calculated following Gutowsky and Pake (19). The intramolecular contribution decreases by 1.92 gauss^2, and if we assume the intermolecular contribution changes proportionately (2), the total decrease is 2.6 gauss^2 and the theoretical second moment of stearic acid with rotating methyl groups is 21.8 gauss^2. This new value agrees within experimental error with the results obtained below −20° C. It is possible, therefore, that the broad portion of the resonance curve represents an almost rigid lattice and that the existing molecular motion probably concerns only the methyl-group ends of the molecules.

On the other hand, there is the possibility that the 3-gauss^2 difference between the experimental second moment below −30° C and the calculated rigid lattice value may be largely due to zero-point vibrational motions of the protons.* A detailed calculation of the importance of this effect would be difficult, but we may obtain an indication of its significance from the following considerations. An analysis of the reduction of the second moment resulting from zero-point motions has been made for ammonium halides and hydrazine fluoride (20–23). Gutowsky, Pake, and Bersohn found that the intramolecular contribution to the second moment of the ammonium ion was reduced by its zero-point torsional oscillations by a factor

$$[1] \qquad 1-\epsilon \cong \left(\left\langle 1-\frac{3}{2}\theta^2 \right\rangle\right)^2$$

where θ is the angle of torsional oscillation (20). If we consider that the significant motions in stearic acid are CH_2 twisting and rocking modes, we might use equations [34] and [35] of Ibers and Stevenson (23) to obtain

$$[2] \qquad \theta^2 = (h/8\pi^2 c)\left(\frac{1}{I_1\nu_1}+\frac{1}{I_2\nu_2}\right)$$

We are indebted to the referee for raising this question.

where ν and I are the torsional frequency and moment of inertia for each mode. Taking $\nu_1 = 720$ cm^{-1} for the rocking mode (24) and I_1 as the moment of inertia of both CH_2 protons about a fixed carbon, and $\nu_2 = 1200$ cm^{-1} for the twisting mode (24) and I_2 as the moment of inertia of both CH_2 protons about the center of the line joining them, one obtains $1-\epsilon = 0.946$ from equations [1] and [2]. This value will apply to the reduction of the second moment contribution of the methylene groups. If we now assume that the whole second moment is reduced by a similar factor we find a reduction of 1.3 gauss^2. The uncertainties involved in this estimation are very large. Ibers and Stevenson (23) suggest that the reduction of the intermolecular contribution may be larger than the reduction of the intramolecular contribution (in this case the CH_2 contribution). On the other hand, we have used the smallest possible values of moments of inertia, and if the methylene carbon is involved in the 720 cm^{-1} rocking mode or the 1180–1350 cm^{-1} band progression assigned to the wagging and twisting modes, the larger moments of inertia which would be appropriate would bring $1-\epsilon$ closer to unity. That these modes do involve the carbon atom is suggested by the fact that the 720 cm^{-1} band appears only in chains $-(CH_2)_n-$ where $n \geqq 4$ (25), and that the 1180 cm^{-1} band progression exists only in the solid state and depends on chain length (26). There is, then, doubt as to whether the end methyl groups rotate. However, lack of an obvious reason for difference between the behavior of the methyl end groups in the fatty acid and in *n*-pentane and *n*-hexane studied by Rushworth (1), together with the uncertainties of the zero-point motional corrections, suggest to us that rotation of the methyl groups is the more probable explanation.

As we have reported above, the narrow component of the proton magnetic resonance line, which exists above about 20° C, does not correspond to a liquid condition, for which a line width of about 10^{-4} gauss might be expected. The observed line width of between 0.1 and 0.01 gauss does suggest, however, rapid molecular motion about several axes. The over-all line shape is similar to the proton magnetic resonance lines obtained from some high polymers for which the narrow component represents an amorphous phase and the broad component a crystalline one (10). In an important respect, however, the comparison with polymer systems breaks down. In polymers, the width of the narrow line is temperature dependent, being comparable to the width of the broad component at low temperatures (12, 27). In stearic acid the width of the narrow line is less than 0.1 gauss regardless of temperature, the change with temperature being in the amplitude of the narrow line. This increasing amplitude suggests that more and more molecules begin to move rapidly as the temperature rises. Since the percentage area under the narrow component corresponds approximately to the percentage of the hydrogen nuclei that are in rapid motion, a comparison of the integrated areas under the broad and narrow components of some of the proton resonance lines has been given in Table I. Although

TABLE I

Fraction of the protons involved in rapid motion

Temp. (° C)	Percentage area of narrow component
40	0.9
45	1.1
54	2.5
58	5.9
66	27.4

parts of molecules rather than entire molecules might be in rapid motion at temperatures above 20° C, it is unlikely that if 27% of each molecule is in rapid motion at 66° C, the remaining portion of each molecule would be rigidly constrained in the lattice as the high second moment of the broad component suggests. It seems more likely that solid stearic acid is present in two phases. One phase, as we have shown, has a rigid, ordered structure, possibly with only end methyl groups rotating and the other has a rather flexible and disordered structure. The amount of disordered phase increases as the temperature rises. This increase in the disordered phase below the melting point could account for the anomalous volume increase in stearic acid between 60° and 69° C (3).

Premelting in some cases has been thought to be due to rotation of molecules below the melting point. It might also be a co-operative increase in the number of holes and interstitial molecules in the solid which leads to the break up of long-range order at the melting point (28). It has been reported that the number of holes in equilibrium with the lattice is abnormally large near the melting points in some long chain hydrocarbons (29). These results suggest that such a process occurs in stearic acid. Lattice defects due to dislocations and impurities in the crystal might allow a few stearic acid molecules to flex and rotate. This could correspond to motion about many axes and lead to the observed narrow component of the proton magnetic resonance line. As the temperature rises these zones of motion and disorder grow in size at the expense of the surrounding ordered structure, until just below the melting point the entire crystal structure is completely disordered or amorphous.

ACKNOWLEDGMENTS

The authors are indebted to Dr. T. M. Connor for the high resolution measurements and to Professor C. A. McDowell for his interest in this problem. We thank the National Research Council for a studentship awarded to one of us (R.F.G.) and for a grant-in-aid of the research.

REFERENCES

1. F. A. Rushworth. Proc. Roy. Soc. (London), A, **222**, 526 (1954).
2. E. R. Andrew. J. Chem. Phys. **18**, 607 (1950).
3. W. S. Singleton, T. L. Ward, and F. G. Dollear. J. Am. Oil Chemists' Soc. **27**, 143 (1950).
4. A. R. Ubbelohde. Trans. Faraday Soc. **34**, 282 (1938).
5. J. B. Brown and D. K. Kolb. Progress in the chemistry of fats and other lipids. The Pergamon Press, Ltd., London. Vol. 3. 1955. p. 58.
6. F. Francis and F. J. E. Collins. J. Chem. Soc. 137 (1936).
7. F. Francis, F. J. E. Collins, and S. H. Piper. Proc. Roy. Soc. (London), A, **158**, 691 (1937).
8. H. S. Gutowsky, L. H. Meyer, and R. E. McClure. Rev. Sci. Instr. **24**, 644 (1953).
9. J. H. Van Vleck. Phys. Rev. **74**, 1168 (1948).
10. G. E. Pake and E. M. Purcell. Phys. Rev. **74**, 1184 (1948).
11. E. R. Andrew. Phys. Rev. **91**, 425 (1953).
12. C. W. Wilson and G. E. Pake. J. Chem. Phys. **27**, 115 (1957).
13. A. Müller. Proc. Roy. Soc. (London), A, **154**, 624 (1936).
14. L. Pauling. The nature of the chemical bond. Cornell Univ. Press, Ithaca, N.Y. 1948. p. 161.
15. S. Abrahamsson and E. von Sydow. Acta Cryst. **7**, 591 (1954).
16. V. Vand, W. M. Morley, and T. R. Lomer. Acta Cryst. **4**, 324 (1951).
17. M. M. Davies and G. B. B. M. Sutherland. J. Chem. Phys. **6**, 755 (1938).
18. T. P. Das. J. Chem. Phys. **27**, 763 (1957).
19. H. S. Gutowsky and G. E. Pake. J. Chem. Phys. **18**, 162 (1950).
20. H. S. Gutowsky, G. E. Pake, and R. Bersohn. J. Chem. Phys. **22**, 643 (1954).
21. L. E. Drain. Discussions Faraday Soc. **19**, 200 (1955).
22. C. M. Deeley and R. E. Richards. Trans. Faraday Soc. **50**, 560 (1954).
23. J. A. Ibers and D. P. Stevenson. J. Chem. Phys. **28**, 929 (1958).
24. R. G. Sinclair, A. F. McKay, and R. N. Jones. J. Am. Chem. Soc. **74**, 2570 (1952).
25. L. J. Bellamy. The infrared spectra of complex molecules. Methuen & Co., Ltd., London. 1954. p. 26.
26. R. N. Jones, A. F. McKay, and R. G. Sinclair. J. Am. Chem. Soc. **74**, 2575 (1952).
27. D. W. McCall and W. P. Slichter. J. Polymer Sci. **27**, 171 (1957).
28. J. E. Lennard-Jones and A. F. Devonshire. Proc. Roy. Soc. (London), A, **170**, 464 (1939).
29. J. W. H. Oldham and A. R. Ubbelohde. Trans. Faraday Soc. **35**, 328 (1939); Proc. Roy. Soc. (London), A, **176**, 50 (1940).

ELECTRONIC POTENTIAL SURFACES OF ACETYLENE IN LCAO/MO APPROXIMATION[1]

G. W. KING

ABSTRACT

A digital computer has been programmed to carry out 6-electron LCAO/ASMO calculations for linear and *trans*-bent acetylene, with the following input variables; coefficients of the LCAO/MOs, carbon–carbon bond length, and effective nuclear charge on the carbon atoms. The effect of varying these parameters upon the calculated electronic energy levels is discussed, and approximations to "best" MOs are obtained for various states of the molecule, leading to values of hybridization parameters for the carbon atoms. Certain assumptions enable the electronic energies to be related to the C—C—H bending angle; from this it is concluded the ground state is linear and the lowest A_u excited state is bent, in accordance with experiment. Values are given for electronic transition energies and hydrogen-bending force constants.

INTRODUCTION

In the LCAO/MO method for calculating the electronic energies of molecules, an orthogonal set of single-electron molecular orbitals[2] ϕ_i are formed by linear combination of n atomic orbitals χ_n:

$$[1] \qquad \phi_i = \sum_n c_{in}\,\chi_n.$$

These are combined in determinantal form to give ASMO wave functions:

$$[2] \qquad \Phi_p = (N!)^{-\frac{1}{2}}|\phi_0(q_0)\ \phi_1(q_1)\ \ldots\ldots\ \phi_N(q_N)|.$$

In general, the eigenvalues of the system have the expectation value

$$[3] \qquad \int \Psi_k{}^{S*}\, H\, \Psi_k{}^{S}\, d\tau$$

where the $\Psi_k{}^S$ are linear combinations of the ASMO functions:

$$[4] \qquad \Psi_k{}^{S} = \sum_p d_{kp}\,\Phi_p.$$

If a large number of suitable Φ_p are taken in each such linear combination [4] (i.e., allowed to interact configurationally), and the stationary states of the system are found by solving the corresponding secular determinantal equations of high order, then the forms of the ϕ_i in [1] are of secondary importance. But if only a few Φ_p are taken in [4], it is necessary that the ϕ_i resemble the "best" MOs for a given electronic state as closely as possible, that is, the eigenfunctions of the Hartree–Fock operator for that state. The variational way to achieve this is an iterative one that becomes extremely complex for configurations comprising partly filled molecular orbitals, in which Ψ_k must be constructed from at least two suitably chosen Φ_p in order to be in accord with the Pauli principle.

For simple and highly symmetric molecules, the ϕ_i in [1] are usually chosen to transform like irreducible representations of the appropriate symmetry point group. This

[1]*Manuscript received November 9, 1959.*
Contribution from the Burke Chemical Laboratories, Hamilton College, McMaster University, Hamilton, Ontario.

[2]*The notation follows that of Howard and King, reference 1.*

often fixes values for certain of the c_{in}, and some of the remaining coefficients in [1] may be interrelated by orthogonality requirements between the MOs, leaving only a small number of coefficients c_j as independent parameters defining the whole set. Instead of attempting to find the best values of these by a cyclic self-consistent procedure, a more direct approach is used here in evaluating [3] for a wide range of values of the parameters c_j and locating the position of minimum energy for a given electronic state graphically, by plotting electronic energy [3] as a function of these parameters. This method is well suited to computer calculation, since a basic program can be written to evaluate concurrently the energies of different electronic states, with the c_j as the variable input parameters. Furthermore, it can be applied to configurations with partly filled orbitals.

It must be noted, however, that the various configurational wave functions for states of the same symmetry class are not necessarily orthogonal in the approximation used below. The only orthogonality present is due to differences in symmetry class, and a configuration interaction treatment would improve the values obtained for the energies.

APPLICATION TO ACETYLENE

The electronic states of *trans*-acetylene are considered here as a 6-electron problem, in LCAO/MO approximation. This example has certain disadvantages owing to the approximations it is necessary to make, especially those concerning the carbon–hydrogen bonds. On the other hand, there is considerable spectroscopic data available for the linear ground Σ_g^+ state (2) and for the lowest excited A_u *trans*-bent state (3, 4), which differ widely in geometry. LCAO/MO/CI calculations have been carried out by Ross (5) for the linear states with $r_{CC} = 1.203$ Å, corresponding to the observed ground state value, and by Howard and King (1) for bent states with $r_{CC} = 1.383$ Å and $\angle CCH = 120°$, corresponding to the observed values for the A_u state. The computer program closely followed the procedures used by Howard and King to obtain the diagonal elements E' of their equation [7], except that the coefficients listed in their paper[3] for the hybrid AOs χ_1–χ_8 were replaced by the general forms given below. Orthogonality was maintained between MOs of the same symmetry class.[4]

Let Cartesian axes be attached to each carbon atom with the z-axes pointing towards each other and with parallel y-axes in the molecular plane. Then the hybrid AOs on the carbon nuclei a and b may be written:

$$\chi_1 = t^{-1}(\lambda \cos\theta . a_s + r . a_z) \qquad \chi_2 = t^{-1}(\lambda \cos\theta . b_s + r . b_z)$$
$$\chi_3 = a_x \qquad \chi_4 = b_x$$
$$\chi_5 = t^{-1}(r\lambda \sin\theta . a_s - 2^{-1}\lambda^2 \sin 2\theta . a_z + t^2 . a_y)$$
$$\chi_6 = t^{-1}(r\lambda \sin\theta . b_s - 2^{-1}\lambda^2 \sin 2\theta . b_z - t^2 . b_y)$$
$$\chi_7 = r . a_s - \lambda \cos\theta . a_z - \lambda \sin\theta . a_y \qquad \chi_8 = r . b_s - \lambda \cos\theta . b_z + \lambda \sin\theta . b_y$$

where $t = (1-\lambda^2 \sin^2\theta)^{\frac{1}{2}}$ and $r = (1-\lambda^2)^{\frac{1}{2}}$, $0 < \theta < 90°$.

All the coefficients are expressed here in terms of two independent parameters, θ and λ. θ is the acute angle between the orbitals χ_7 or χ_8 and a line through the carbon nuclei,

[3]*See ref. 1, p. 703.*

[4]*Strictly, the electronic energies would be independent of the actual forms chosen for such* MOs *only if they were exact solutions of the Hartree–Fock equations. We note that in the calculations both of Ross and of Howard and King, the introduction of* CI *had only a small effect on the energies of many of the electronic states, indicating that the* MOs *they used were reasonably good approximations for these states.*

and λ is the amount of p character in each of these orbitals when they are written in the vectorial form

$$\chi_{7,8} = \eta s + \lambda p, \qquad 0 < \lambda < 1.$$

In previous calculations (1, 5), the hydrogen atoms were formally attached to χ_7 and χ_8 respectively, making θ the complement of the C—C—H bond angle. The validity of this assumption is discussed in a later section. Inserting $\theta = 60°$ and $\lambda = (2/3)^{\frac{1}{2}}$, we obtain the AOs used by Howard and King in which three equivalent sp^2 hybrids are centered on each carbon atom; $\theta = 0$ and $\lambda = 2^{-\frac{1}{2}}$ gives the sp hybrid AOs used by Ross for the linear molecule. Situations such as $\theta = 0$, $\lambda = 0$, for example, in which the H atoms are bound by pure $2s$ carbon orbitals are highly improbable, and the calculations show that very high energies are associated with such states. In general, one would not expect the C—H bond to have less p character than it does in the linear state, and it will be seen that the minima of potential surfaces fall within the anticipated range of values for λ.

χ_3 and χ_4 are pure p orbitals above and below the molecular plane, and remain unchanged as θ is varied. This is similar to the qualitative approach used by Walsh (6).

A Bendix D-15G computer, using the "Intercom 1000 Double Precision" interpretative subroutine was programmed to calculate energies of all the low-lying electronic states of *trans*-acetylene over all permissible (θ,λ) values at intervals of $(10°, 0.1)$. The E' for each (θ,λ) value was computed in 12 minutes. These are simply the values of the diagonal elements of the secular determinants: limitations in the storage capacity of the computer prevented evaluation of the off-diagonal elements and the calculation of configuration interaction between states of the same symmetry. However, the program included interpolation in the tables of molecular integrals of Kotani (7), enabling the effective nuclear charge for $n = 2$ and also the separation of the carbon atoms to be included as additional variable parameters. The effective nuclear charge for $1s$ carbon atomic orbitals, to which the $2s$ orbitals were made orthogonal, was kept at 5.70.

The program was readily checked by comparison at different stages with results obtained by Ross and by Howard and King, using the appropriate (θ,λ) values. Excellent agreement was obtained.

Once a potential minimum for a given state had been located approximately, its position was accurately fixed by a "fine" scan over the region at $(1°, 0.01)$ intervals.

RESULTS

Figure 1 shows energy contours, relative to the minimum value, for the lowest A_g state of acetylene, with $r_{CC} = 1.203$ Å. The contours were obtained by graphical interpolation of the computer results. This A_g state correlates with the ground Σ_g^+ state of the linear molecule. The potential minimum occurs at $(0°, 0.643)$, λ having a slightly lower value than that of 0.707 for simple sp-type hybridization. Thus the C—H bond has slightly more, and the C—C bond slightly less, $2s$ character than is commonly supposed. Moffitt (8), on the basis of fairly general arguments, has predicted slight effects in the opposite direction.

Figure 2 is a similar diagram for the lowest A_u state, calculated for $r_{CC} = 1.383$ Å. This is the spectroscopically observed state. The potential minimum, indicated by a cross, is at the point $(44°, 0.81)$. λ is fairly close to the value for ordinary sp^2-type

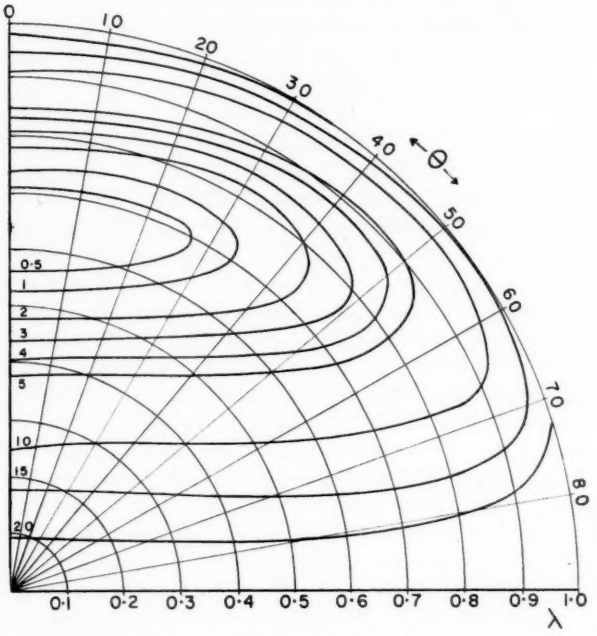

FIG. 1. Energy contours in ev for ground A_g (Σ_g^+) electronic state of *trans*-acetylene. r_{CC} = 1.203 Å, Z_{eff} = 3.18.

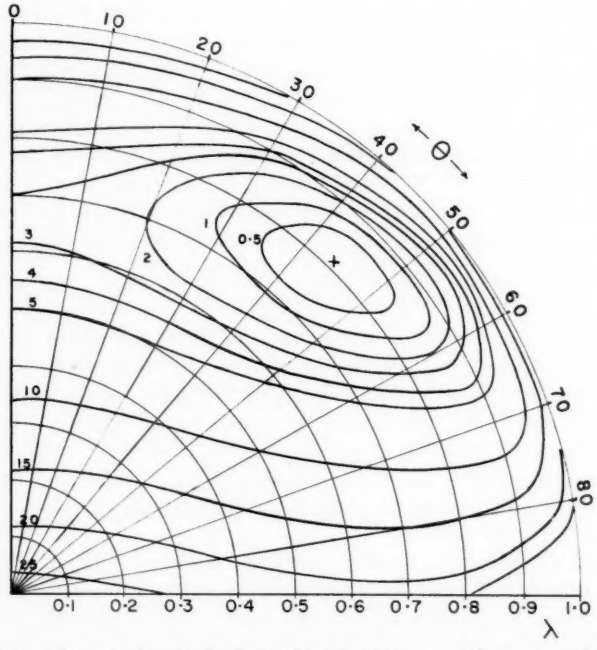

FIG. 2. Energy contours in ev for lowest A_u electronic state of *trans*-acetylene. r_{CC} = 1.383 Å, Z_{eff} = 3.18.

hybridization; this agrees with the observation (3) that the molecule in this state resembles ethylene with two *trans*-hydrogen atoms missing.

In these two figures, the effective nuclear charge Z_{ett} on the carbon atoms for $n = 2$ in the Slater AOs, is 3.18. In Fig. 3, the calculations of Fig. 2 have been repeated with

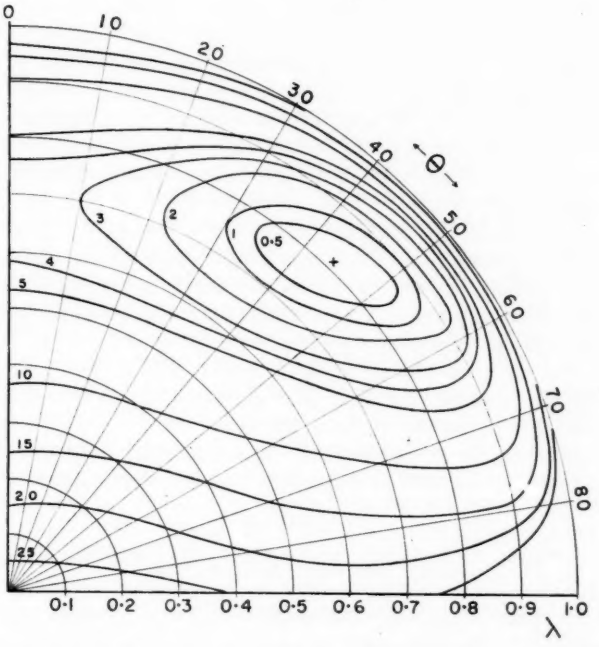

FIG. 3. Energy contours in ev for lowest A_u electronic state of *trans*-acetylene. $r_{CC} = 1.383$ Å, $Z_{ett} = 3.50$.

$Z_{ett} = 3.50$. Only small differences in the position of the energy minimum (44°, 0.82) and in the shapes of the energy contours are observed. This was found to be true generally for similar calculations with Z_{ett} ranging down to a 2.80. The relative energy levels for a given (θ,λ) in the region of minimum energy only changed slightly on varying Z_{ett}. Shull and Ellison (9) found this to hold also for benzene. Consequently, in subsequent calculations reported here, Z_{ett} was fixed at the free atom value of 3.18. Minimization of all potential energies with respect to Z_{ett} would have represented an unjustifiably large increase in the amount of computation.

TABLE I

Positions of electronic energy minima for the lowest A_u state for various C—C distances to nearest (1°, 0.01) intervals of (θ,λ)

r_{CC} (Å)	1.34	1.36	1.383	1.40	1.42
θ	44	44	44	45	45
λ	0.81	0.81	0.81	0.82	0.82

TABLE II

Positions of electronic energy minima for the ground Σ_g^+ state for various C—C distances, to nearest 0.001 intervals of λ, $\theta = 0°$

r_{CC} (Å)	1.18	1.203	1.22
λ	0.638	0.643	0.647

Tables I and II show the positions of potential minima for the A_u and A_g states respectively for different values of r_{CC}. Very little change occurs in each case. Table II indicates a slight increase in p character of the σ-type C—C bond as r_{CC} decreases.

In order to minimize the energy with respect to r_{CC}, and also to calculate the energy of the A_u–Σ_g^+ transition, it is necessary to evaluate energies of repulsion between the carbon nuclei. These have a magnitude of several hundred ev, and are very sensitive to small changes in the value for the nuclear charge, which depends on the extent of electron screening. In addition, variation of r_{CC} will affect electrostatic contributions to the energy due to any polarity in the C—H bonds, which is an unknown factor. In the circumstances, we merely report the value of 2.5 ev for transition between the potential minima of the two states, assuming a carbon nuclear charge of +4. The experimental value is 5.24 ev. The agreement is not as good as that obtained by Howard and King. It must, however, be remembered that the calculated figure is a difference between two quantities each of magnitude of some 250 ev.

The positions of minimum energy for the lowest states of the four symmetry classes of point group C_{2h} are summarized in Table III. These are all values for $r_{CC} = 1.383$ Å.

TABLE III

Electronic configurations and positions of minimum energy for lowest states of each symmetry class

State	Configuration	(θ,λ)
A_g	$(a_g\sigma_g2sp^2)^2(a_u\pi_u2p)^2(b_u2sp^2)^2$	(0, 0.67)
A_u	$(a_g\sigma_g2sp^2)^2(a_u\pi_u2p)(b_u2sp^2)^2(a_g2sp^2)$	(44, 0.81)
B_g	$(a_g\sigma_g2sp^2)^2(a_u\pi_u2p)(b_u2sp^2)(a_g2sp^2)^2$	(50, 0.8)
B_u	$(a_g\sigma_g2sp^2)^2(a_u\pi_u2p)^2(b_u2sp^2)(a_g2sp^2)$	(0, 0.65)

The B_g state has $\theta > 0$. The B_u state is apparently linear, but this conclusion is invalid for the following reason. Certain of the lower excited states of bent acetylene correlate with degenerate species of the linear molecule; thus, $A_u + B_u \rightarrow \Delta_u$ (see ref. 3, Part III, Table 7). However, the calculated energies of such states do not converge in pairs upon the corresponding degenerate linear states as $\theta \rightarrow 0$; on the contrary, for example, the lowest pair of A_u states converge on each other, as do the lowest pair of B_u states, and each species would require a proper CI treatment to sort them in accordance with correlation relationships. Thus energy values for $\theta = 0$ for such states as calculated here are in error, which decreases as θ increases and states of the same symmetry move apart in energy. This does not apply to the lowest A_g state, which correlates with a single Σ_g^+ state; the next A_g state lies some 18 ev higher in the linear molecule for $\lambda = 0.643$, but this separation does decrease somewhat as θ increases to 90°.

THE CARBON–HYDROGEN BONDS

Two assumptions are made here: that the potentials of the hydrogen atoms can be neglected, and that they can be regarded as attached to orbitals χ_7 and χ_8 respectively,

with complete localization of the C—H bond electrons. A refined calculation would include these in MOs extending over all four atoms of the molecule; and the coefficients of the carbon AOs in the "best" MOs, in the Hartree–Fock sense, need not bear a simple relationship to the C—C—H bond angles (although a suitable unitary transformation could be made to localize charge in the C—H bond directions).

On the other hand, it may be argued that for linear and moderately bent models, there is quite a small overlap between symmetry MOs formed purely from the well-separated C—H bond orbitals and the MOs of the C—C bond, and hence little interaction between them. There will also be a very small charge concentration of C—C bond electrons in the neighborhood of the hydrogen nuclei. The overlap would be greater if the C—H symmetry MOs contained several modes, but states in which such MOs are occupied will be high in energy and unlikely to affect the energies of low-lying electronic states. Hence in a first approximation θ can be correlated with the C—C—H angle; this becomes increasingly in error both as $\theta \rightarrow 90°$ and as $\lambda \rightarrow 0$, as interactions between C—C and C—H bond electrons increase. Since in general such interactions will lower the energies of our electronic states, it follows that the values calculated here are too high for small λ and large θ values; the necessary correction would shift the positions of the potential minima for bent states in the direction of these, and thus, for example, improve agreement with the observed 120° bending angle in the A_u state.

Ellison and Shull (10) have obtained SCF/MOs for the water molecule at different bond angles, and converted these by unitary transformations into equivalent orbitals directed towards the hydrogen atoms. They found that localization of electrons in O—H bond equivalent orbitals was not a justifiable assumption, as had been supposed by Pople (11) in his original treatment. Similar conclusions follow from the calculations of Higuchi (12) on the NH_2 radical. In these molecules, however, one would expect large interactions between electrons in any orbital representations directed along the X—H axes, owing to their proximity. This is not the case in acetylene.

If θ is identified with the acute C—C—H angle, some interesting conclusions emerge. The A_g (Σ_g^+) state in Fig. 1 is predicted to be linear and the A_u state in Fig. 2 to be *trans*-bent, in accordance with observation. The lowest B_u state is also expected to be bent.

Bending force constants can be derived for the C—H bonds. The two hydrogen atoms are approximated by a point executing small harmonic oscillations about the potential minimum at constant λ. This gives a bending constant of 0.24×10^{-11} erg/radian^2 for the A_g state, identical with the value derived from the known vibrational frequencies (13). The value for the A_u state is 4×10^{-11} erg/radian^2, which is much larger than would be expected; for example, the force constant for the comparable hydrogen-bending motion in benzene (3) is 0.8×10^{-11} erg/radian^2. The potential well for the A_u state is, however, very anharmonic, and the assumption of constant λ for this motion is somewhat provisional.

It would be helpful if λ could be related to r_{CH} and some estimate obtained for C—H stretching force constants. Various empirical expressions for the dependence of r_{CH} on degree of hybridization at a carbon atom are to be found in the literature (14, 15, 16). It was found that stretching constants several hundred times too large were obtained if any of these were used. Apart from the fact that none of them provides a good fit to experimental data, and that those methods based on addition of covalent bond radii are open to criticism (17), such expressions are derived using series of molecules in which both θ and λ vary with carbon atom hybridization, and cannot be readily employed here.

In conclusion, a 6-electron, two-center approximation seems to give a better picture of the linear ground state of acetylene than of the bent excited states. The assumptions inherent in the treatment give only a qualitative significance to the results, but nevertheless avoid the troublesome calculation of three- and four-center integrals that would be entailed in more precise calculations.

ACKNOWLEDGMENT

Financial support for this work was provided by the National Research Council.

REFERENCES

1. H. HOWARD and G. W. KING. Can. J. Chem. **37**, 700 (1959).
2. B. D. SAKSENA. J. Chem. Phys. **20**. 95 (1952).
3. C. K. INGOLD and G. W. KING. J. Chem. Soc. 2702 (1953).
4. K. K. INNES. J. Chem. Phys. **22**, 863 (1954).
5. I. G. ROSS. Trans. Faraday Soc. **48**, 973 (1952).
6. A. D. WALSH. J. Chem. Soc. 2288 (1953).
7. M. KOTANI, A. AYAO, I. EIICHI, and K. TOSAKU. Tables of molecular integrals. Maruzen Co., Ltd., Tokyo. 1955.
8. W. MOFFITT. Proc. Roy. Soc. (London), A, **202**, 548 (1950).
9. H. SHULL and F. O. ELLISON. J. Chem. Phys. **19**, 1595 (1951).
10. F. O. ELLISON and H. SHULL. J. Chem. Phys. **23**, 2348 (1955).
11. J. A. POPLE. Proc. Roy. Soc. (London), A, **202**, 323 (1950).
12. J. HIGUCHI. J. Chem. Phys. **24**, 535 (1956).
13. J. W. LINNETT, D. F. HEATH, and P. J. WHEATLEY. Trans. Faraday Soc. **45**, 832 (1949).
14. L. PAULING, H. D. SPRINGALL, and K. J. PALMER. J. Am. Chem. Soc. **61**, 927 (1939).
15. M. G. BROWN. Trans. Faraday Soc. **55**, 694 (1959).
16. H. J. BERNSTEIN. J. Phys. Chem. **63**, 567 (1959).
17. M. J. S. DEWAR and H. N. SCHWEISING. Tetrahedron, **5**, 166 (1959).

TRITIUM EXCHANGE BETWEEN CELLULOSE AND WATER: ACCESSIBILITY MEASUREMENTS AND EFFECTS OF CYCLIC DRYING[1]

A. R. G. LANG[2] AND S. G. MASON

ABSTRACT

Tritium exchange between cellulose and water vapor was used to measure the accessibilities of amylopectin, amylose, regenerated cellulose, wood pulp, bacterial and Valonia cellulose, and cellulose trinitrate using both gas counting and solid counting techniques. The results compare satisfactorily with other accessibility and crystallinity measurements.

The incomplete reversibility of the exchange reaction was used to study directly changes in the accessibility of regenerated cellulose which occurred during repeated wetting and drying from water. The results indicated that a partial interchange of accessible and inaccessible regions occurs during wetting and drying.

INTRODUCTION

This paper describes preliminary experiments which use the exchange reaction of tritium between cellulose and water to study the "accessibility" of cellulose to water vapor, and to measure directly the formation of new inaccessible regions in cellulose during successive wetting and drying cycles.

Deuterium has been used extensively as a tracer in the exchange of hydrogen isotopes between cellulose and water (1–11), but only the more recent studies of Frilette, Hanle, and Mark (3), Almin (5), and Mann and Marrinan (8–11) are of value in accessibility studies. The exchange reaction, which was almost complete in 1 hour, was attributed to exchange with the hydroxyl hydrogens of the cellulose units in the amorphous regions and on the faces of the crystallites. The ratio of the cellulose participating in the reaction to the total, calculated by assuming that 3 hydroxyl groups reacted per anhydroglucose unit, was taken as a quantitative measure of the accessibility. These accessibilities were in good agreement with other accessibility and crystallinity measurements.

In the present work tritium (H^3), which, being radioactive, has the advantage that it may be easily, accurately, and sensitively determined, was introduced as a tracer in the exchange reaction

$$R.OH + HTO \rightleftharpoons R.OT + H_2O \qquad [1]$$

where R.OH is a carbohydrate containing accessible hydroxyls. The extent of this reaction was used to determine the accessibility of the carbohydrate. Measurements were made on a variety of samples in two ways.

1. By a gas counting technique in which cellulose and tritiated water vapor were reacted together, and the adsorbed and vapor-phase water removed and analyzed by gas counting. The extent of the reaction was calculated from the stoichiometry of the system and the dilution of the tritium in the water.

2. A radioactivity counting method for solid samples was used in which cellulose was exchanged with tritiated water vapor, the water removed, and the tritium in the cellulose measured by counting the solid sample. This method required a special apparatus, the Vacuum Transfer Counter (VTC), described elsewhere (12).

The gas counting method was used chiefly for calibration and corroboration of the solid counting method.

[1]*Manuscript received October 29, 1959.*

Contribution from Physical Chemistry Division, Pulp and Paper Research Institute of Canada, and Department of Chemistry, McGill University, Montreal, Que.

[2]*Holder, Frank J. Sensenbrenner Fellowship 1956–57, and National Research Council of Canada Studentships 1957–58 and 1958–59.*

Confirming the observations of Mann and Marrinan (9) with deuterated water, it was found that the exchange of the accessible regions was not completely reversible; cellulose dried from tritiated water contained some tritium which could not be removed by soaking in water, i.e. some of the cellulose was rendered inaccessible by the wetting and drying. This newly formed inaccessibility is believed to be due to the formation of new interchain bonds during drying.

A number of additional experiments were conducted in which this newly created inaccessibility was used to study changes in cellulose caused by alternate wetting and drying. Two quantities were measured.

1. The amount of inaccessible material, $\delta\omega_n$, formed during the nth cycle, was determined by alternately wetting and drying the cellulose from ordinary water $(n-1)$ times, followed by a single wetting and drying from tritiated water for the nth cycle. The labile tritium was removed by soaking in ordinary water, and the amount of inaccessible cellulose formed in the nth cycle determined by counting the solid cellulose sample in the VTC. This quantity is analogous to the "resistant OD groups" of Mann and Marrinan (9).

2. The net inaccessible cellulose, W_n, formed during n cycles was determined by wetting and drying cellulose from tritiated water (n) times. The labile tritium was removed and the sample counted as before.

Both $\delta\omega_n$ and W_n were expressed as percentages of the total cellulose.

EXPERIMENTAL PART

Samples

(*a*) Amylopectin (Ramelin-G from Stein Hall and Co., Inc.) was dissolved in cold water and evaporated on a mercury surface to form a film with a superficial density of about 3 mg per sq. cm.

(*b*) Amylose (Superlose from Stein Hall) was dissolved in water at 160° C. A film (about 3 mg per sq. cm) was formed by evaporation of the solution on a mirror-finished stainless steel plate.

(*c*) Air-dried cellulose film (Dupont of Canada Ltd.) made from viscose was used, having a superficial density of 3.0 mg per sq. cm (about 23 μ thick). It had been neither plasticized nor coated.

(*d*) Acetate-grade softwood dissolving pulp having an α-cellulose (Tappi method) content of 96% was formed into sheets of superficial density 7.8 and 3 mg per sq. cm on a British sheet machine, pressed, and air-dried against a glazing plate.

(*e*) Bacterial cellulose grown from *Acetobacter xylinum* (kindly supplied by Dr. J. R. Colvin, National Research Council) was made into a sheet of superficial density 3 mg per sq. cm on a British sheet machine, pressed, and air-dried against a glazing plate.

(*f*) Valonia cellulose, obtained in a water–formaldehyde mixture from the General Biological Supply House, was purified by the method of Ranby (13), i.e. refluxed in 1.0% sodium hydroxide for 6 hours with a solvent change after 3 hours, then washed in dilute acetic acid and water.

(*g*) Ramie cellulose trinitrate (N content 13.80% corresponding to 97.7% complete nitration) was cast into a film (3 mg per sq. cm) from ethyl acetate on a mirror-finished stainless steel sheet.

Accessibility by Gas Counting

A dry sample containing exchangeable hydrogens was reacted with tritiated water and

then all the water was recovered by distillation. The accessibility of the sample was calculated from the resultant dilution of the radioactivity in the water and the stoichiometry of the system.

The apparatus used is shown in Fig. 1. The reaction vessel (C), which has a removable top (B) sealed with an O-ring, was fitted with a Pirani gauge (Edwards MA-5) (A), a

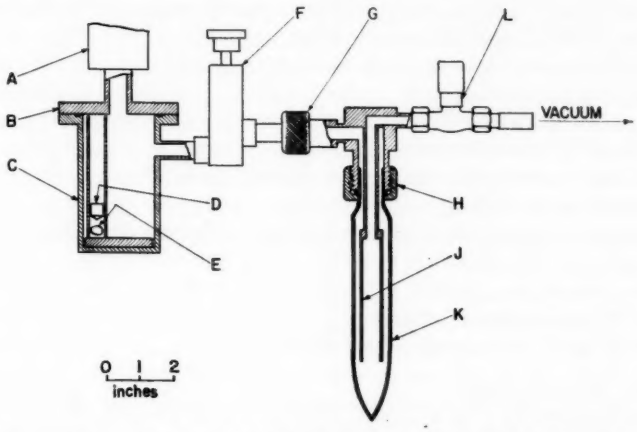

FIG. 1. Gas counting method apparatus. A, Pirani gauge; B, reaction vessel top; C, reaction vessel; D, ampoule breaker; E, ampoule; F, vacuum valve; G and H, vacuum couplings; J, trap inner tube; K, trap jacket; L, vacuum valve.

special ampoule breaker (D), and a Veeco high vacuum valve (L38S) (F). It could either be joined directly to the high vacuum system consisting of a liquid air trap, a two-stage oil diffusion pump, and a mechanical pump, or to the trap (K) by a Veeco quick coupling (G). The trap, which accommodated a special syringe (not shown) within the inner tube (J), could be dismantled by loosening another quick coupling (H) and was connected through a Hoke bellows seal-valve (L) to the vacuum system. The apparatus was, except for the Pyrex glass jacket of the trap (K), made of copper and brass, with connections either soldered or sealed with rubber O-rings. The metal and glass syringe with Teflon gaskets was made as described by Robinson (14).

About 0.4 ml of tritiated water with an activity of 0.5 microcurie (μc) per g was syringed into a weighed, thin-walled, Pyrex ampoule; freed of air by freezing, evacuating, and melting several times; then sealed and reweighed. Cellulose samples *a*, *c*, and *d* were used, of superficial densities 3, 3, and 7.8 mg per sq. cm, respectively. The ampoule, and a 2-g sample cut into strips about 7.5 cm wide and folded to expose as much surface as possible, were placed into the reaction vessel (C). This was sealed, and then evacuated for at least 11 hours at 70° C or for 43 hours at room temperature, and then isolated by closing valve F. The reaction was started by shaking until the ampoule was broken by the plunger (D) and continued at room temperature for an arbitrary period of 7 hours for amylopectin, and 1 hour for all other samples since this period was found adequate by other workers (3, 9).

Meanwhile the trap was assembled with the syringe, set to contain 0.2 ml, inside the central tube (J) so that the needle rested in the bottom of the jacket (K), and the isolated

reaction vessel was coupled to the trap, which was then evacuated. After the reaction the water was recovered by cooling the trap with liquid air, closing valve L and opening valve F during the first rapid distillation, then opening valve L to the vacuum and heating the reaction vessel to 70° C for 4 to 46 hours. Valves F and L were closed, the water in the trap was melted and collected in the bottom of the jacket (K); then air, let in through valve L, forced the water into the still-evacuated syringe. This procedure prevented dilution of the radioactivity in the water by exposure to the water vapor in the atmosphere. Table I lists the experimental details.

The water in the syringe was analyzed for tritium by the method of Robinson (15), i.e. by reacting it with methyl grignard in butyl ether to form radioactive methane under carefully controlled conditions, fractionating the methane, metering it into a gas counting tube, and measuring the radioactivity with a suitable scaler. Several improvements or modifications were made to the apparatus described by Robinson.

1. A Kjeldahl flask was used for the reaction.
2. The burner heating the water bath was replaced by an annular electrical heater to ensure temperature uniformity.
3. Commercial glass, gas counting tubes patterned on those of Bernstein and Ballentine (16) replaced the metal gas counters.

The method of assay was found to be very satisfactory.

Accessibility by Solid Counting

A variety of samples (*b*, *c*, *d*, *e*, *f*, and *g*) were measured using the Vacuum Transfer Counter (VTC) and following procedures described earlier (12). Briefly stated, the sample was mounted on a suitable holder, evacuated in the VTC, treated with tritiated water vapor at a relative humidity of 79 to 97% at about 25° C for 1 hour, evacuated again, transferred while under vacuum to a counter, and the radioactivity of the sample measured. Corrections were made for contamination of the counter and absorption of radiation by the counter window.

It was shown (12) that a 1-hour reaction was sufficient for replication of results, and that the time for completion of the reaction probably depended upon the establishment of isotopic equilibrium throughout the apparatus after the dilution of activity by the cellulose; therefore, the mass of sample was kept constant by using a superficial density of 3 mg per sq. cm. The only exception was Valonia (1.1 mg per sq. cm) since there was insufficient material.

All samples were "infinitely" thick; i.e. their thicknesses exceeded the range of tritium β-particles (1 mg per sq. cm) (17, 18).

Amylopectin films could not be measured because they buckled and broke when exposed to the water vapor.

Cyclic Drying Experiments

Gel cellulose of the same stock as sample *c*, but which had never been dried, was used in all of these experiments.

(*i*) *Determination of* $\delta\omega$

Samples were placed in a vacuum desiccator containing anhydrous magnesium perchlorate or deaerated saturated sodium chloride solution to provide relative humidities of 0 and 75% respectively, evacuated for about 10 minutes, then isolated. After the 23 hours required for moisture equilibrium (19), the desiccator was opened and a sample removed. The remainder was soaked for 1 hour in distilled water at about 25° C, then

replaced in the desiccator. Each drying and wetting cycle was repeated to 30 and 56 times for the 0 and 75% r.h. experiments respectively, with periodic removal of samples. The dried samples together with a piece of the original undried sample were mixed for 7 hours in a 50-ml flask with at least 1 ml tritiated water (about 8 μc per mg) per 80 mg of sample. Then the water was poured into a trap and the remaining water removed by vacuum distillation and collected in the same trap cooled with liquid air. Samples cycled at 0% r.h. were dried as quickly as possible with the flask surrounded by a water bath at 25° C; the 75% r.h. samples were distilled at a vapor pressure equivalent to 75% r.h. as measured with a mercury manometer, by throttling the vapor flow to the trap. Distillations at 0% r.h. were made in 3 batches and at 75% in 2 batches. The water removed from the samples was assayed for tritium by the gas counting method already described.

Labile tritium was removed from the cellulose by soaking in distilled water for at least 2 days with four changes of water. The wet sample was mounted on a holder (ref. 12, Fig. 4) dried in the air for 1 hour, evacuated in the VTC for 1 hour, then counted. The background determined immediately before counting was subtracted directly from the observed count rate, which was then corrected for window absorption (12).

(*ii*) *Determination of W*

An inverted U-tube of 15-mm o.d. Pyrex glass tubing with sealed arms 20 cm and 14 cm long was used in each experiment. One milliliter of tritiated water (about 8 μc per mg) was added to a sheet of undried gel cellulose (2.5×5 cm) held in the 20-cm arm by glass fingers. The tube, after being evacuated through a 5-mm o.d. side arm for 15 seconds so that water vapor purged the air from the apparatus, was sealed off with a torch. The sample and liquid water were mixed by shaking the tube and equilibrated for 7 hours, then the free water was poured from the sample into the 14-cm arm. The arm containing the cellulose was put in a water bath at 25.0±0.1° C and the other arm either in dry ice – acetone mixture or a water bath at 20.0±0.2° C for distillations at 0 and 75% r.h. respectively. After 23 hours the U-tube was removed from the baths, and the water poured back onto the cellulose for 1 hour, then the drying cycle repeated. The number of cycles was varied up to 28 corresponding to 0% r.h. and 57 to 75% r.h. Finally the U-tube was broken open, the water assayed for tritium, the labile tritium was removed from the sample by soaking in water, and the sample counted as before.

(*iii*) *Control Experiments*

Gel cellulose samples were soaked in tritiated water (6.5 μc per mg) for 1 hour, 12 hours, and 31 days, then, without drying, soaked in distilled water to remove the labile tritium and counted as before.

RESULTS AND DISCUSSION

Accessibility by Gas Counting

The results are summarized in Table I.

The per cent accessibility, A'_g, was calculated from the relation

$$[2] \qquad A'_g = 600 \frac{m}{M} \left(\frac{N_0}{N_r} - 1 \right)$$

where m is the mass of water in the ampoule (g), M is the mass of the sample on an over-dry (105° C) basis (g), N_0 and N_r are the original and final activities in the water in the same units; the factor 600 converts the masses m and M to molecular equivalents and the results to a percentage. This expression assumes that:

TABLE I

Accessibility by the gas counting method

Expt.	Sample	Evacuation: Time (hours)	Evacuation: Temp. (° C)	Water recovery (hours)	m/M	Accessibility (%): A'_g	Accessibility (%): A_g corrected for isotope effects
1	Cellulose film	11	70	9	0.192	89	
2	Cellulose film	11	70	11	0.192	87	
3	Cellulose film	44	25	46	0.192	89	
4	Cellulose film	43	25	25	0.196	85	
					Mean	87.5	71
5	Wood pulp	12	70	15	0.185	69	
6	Wood pulp	13	70	11	0.195	66	
7	Wood pulp	12	70	12	0.179	62	
					Mean	66	54
8	Amylopectin	20	70	4	0.207	129	
9	Amylopectin	37	70	5	0.197	117	
					Mean	123	100

NOTE: Pressure after water recovery was $< 0.1\ \mu$ Hg except for expts. 8 and 9 which were 5 and 3 μ respectively.

$$\frac{m}{M} = \frac{\text{mass of water in ampoule}}{\text{mass of dry cellulose}}.$$

1. There are three exchangeable hydrogens per anhydroglucose unit.

2. There is no adsorbed water on the cellulose prior to the reaction. Work described elsewhere (20) showed that under the conditions of the experiment the residual adsorbed water was generally zero and always less than 4 mg per g, corresponding to an apparent accessibility of 2.4%.

3. There is no isotope effect in eq. [1]; i.e.

$$[3] \qquad k_1 = \frac{\text{T/H in accessible part of carbohydrate}}{\text{T/H in adsorbed water}} = 1.$$

4. There is no change in the tritium concentration in the carbohydrate during the recovery of adsorbed water.

Equation [2] is equally applicable to linear and branched chain molecules of anhydroglucose units, provided that the D.P. is sufficiently high that the additional exchangeable end group per molecule may be neglected, since with branched chains the loss of one hydroxyl at the branch is exactly balanced by the gain in the additional end unit.

Since amylopectin, the highly branched fraction of starch, has been shown (21) to have a completely amorphous X-ray diffraction pattern (an observation which we have confirmed) all its hydroxyl hydrogens should be accessible to exchange with water. However, A'_g (expts. 8 and 9, Table I) exceeded the expected value of 100%. This suggested that some of the C—H linked hydrogens in addition to the hydroxyls were participating in the exchange. However, infrared measurements on cellulose (8) and the accessibility measurements on cellulose nitrate described later showed that no exchange occurred between hydrocarbon hydrogens of cellulose and water. It was concluded that the abnor-

mally high A'_g was due to two isotope effects, one in the exchange reaction (eq. [1]) and the other in the recovery of tritiated water.

The reported values of the isotope distribution factor k_1 (eq. [3]) for the exchange equilibria between alcohols and deuterated water vary from 0.96 to 1.25 (22–28); of these the value of Hobden *et al.* (27) of 1.09 is probably the best. Although no data are available it is probable that similar effects exist for alcohols and tritiated water.

An isotope effect probably occurred in the recovery of the tritiated water from the sample because the equilibrium vapor pressure of HTO is lower than H_2O. From direct measurements of liquid/vapor equilibria, Price (29) has reported ratios of the vapor pressures of HTO and H_2O which may be expressed by the separation factor

$$\alpha = \frac{\text{T/H in liquid}}{\text{T/H in vapor}}. \qquad [4]$$

At 26° C, $\alpha = 1.29$. Therefore during a simple distillation, the distillate is deficient in HTO, while the water being distilled is correspondingly enriched. When all the water is distilled it has, of course, the same average composition as the original liquid; all distillations were, therefore, taken to completion. However, a complication probably occurred during the distillations from solids containing exchangeable hydrogens: as the tritium concentration in the adsorbed water increased, the equilibrium in eq. [1] was probably driven to the right, so that more tritium became attached to the hydroxyl oxygens to cause an additional decrease of tritium in the distillate. This would cause the accessibility calculated by eq. [2] to be high.

The possible magnitude of such an effect is indicated by first considering the equilibrium distillation of a mixture of H_2O and HTO. At low concentrations of tritium the molecular species T_2O may be neglected, so that the problem becomes the simple distillation of a mixture of two volatile components HTO and H_2O, and the expression

$$\log_e \frac{L_1}{L_2} = \frac{1}{k-1} \log_e \frac{x_1}{x_2} \qquad [5]$$

derived by Perry (30) is applicable, where L_1 is the number of moles of original water, L_2 is moles of residual water, x_1 and x_2 are the mole fractions of HTO in the original water and the residual water respectively, and

$$k = \frac{\text{mole fraction HTO in vapor}}{\text{mole fraction HTO in liquid}} \text{ at equilibrium.}$$

Note that the original derivation was made in terms of the more volatile component, but eq. [5] is equally applicable to the less volatile component, i.e., HTO.

When the concentration of $T \ll H$, as in the conditions studied,

$$k \simeq \frac{\text{HTO/H}_2\text{O in vapor}}{\text{HTO/H}_2\text{O in liquid}} \simeq \frac{1}{\alpha} \qquad [6]$$

and

$$\frac{x_1}{x_2} \simeq \frac{\text{T/H in original water}}{\text{T/H in residual water}} = \frac{t_0}{t} \qquad [7]$$

i.e., replacing the mole fraction of HTO by the atom fraction of T. Using eqs. [6] and [7], the approximate value of $\alpha = 1.3$, and putting $L_1/L_2 = 1/m$, where m is the fraction of original liquid which has not been distilled, eq. [5] becomes

[8] $$\log_e m = \frac{1.3}{0.3} \log_e \frac{t_0}{t}.$$

This expression gives the ratio of the atom fractions of tritium in the original to the residual water at any stage during the distillation.

By making a material balance this can be re-expressed to give the ratio F of the atom fraction in the original liquid to the average atom fraction in the distillate at any stage

[9] $$F = (1-m^{1/1.3})/(1-m).$$

If equilibrium is maintained between amylopectin and tritiated water at all times, the complete distillation of water from amylopectin may be considered as a partial liquid distillation in which the amylopectin corresponds to the residual liquid. Thus assuming that $k_1 = 1$ (eq. [3]), the value of m corresponding to 2 g amylopectin and 0.4 g water is 0.453, and by substitution in eq. [8], $F = 0.834$. If the correction for such a fractionation were neglected the accessibility, A'_g, calculated from eq. [2] would be 142%. While this value represents an upper limit, it serves to show the importance of this isotope effect.

The isotope effects in this exchange reaction are of some interest and will be discussed in a subsequent paper. For the present work the values in Table I were used as reference values for the accessibility of cellulose films which were subsequently measured in the solid counter (VTC). The measured accessibility values, A'_g, in Table I were corrected by multiplying by the factor 100/123 on the assumptions that amylopectin was 100% accessible and the correction for the isotope effect was given by a single factor which was the same for all samples, and hence cancelled out of the calculations.

Table II shows that this method of obtaining the corrected values, A_g, gave good agreement with comparable values obtained by other methods (3, 9–11, 31, 32).

TABLE II

Accessibility of samples by solid counting and comparison of data

	Accessibility (%)						
	Liquid D_2O		D_2O vapor, Mann and Marrinan	HTO vapor		Amorphous cellulose (%)†	
Sample	Frilette *et al.*	Mann and Marrinan		Gas counting (A_g)	Solid counting* (A_s)	By X-ray diffraction	By density measurements
Amylopectin				100			
Amylose					100±3 (2)		
Cellulose film	81	83	75	71	71±5 (4)	60	60
Cellulose film dried at 75% r.h. 56 times					73±1.5 (2)		
Wood pulp	54–68			54	60±0.3 (2)	35	50
Bacterial cellulose		39	30		42±2.5 (2)	60	
Valonia purified					27 (1)	30–35	29
Cellulose trinitrate					0±3 (2)		—

*Number of replicates given in parentheses and range by limits.
†Values of Hermans (31) except for underlined value (32).

The advantages of the gas counting method are good reproducibility, relatively simple apparatus, and the fact that the surface roughness of the sample does not affect the results. The principal disadvantage is the uncertain magnitude of the isotope effects; these must be known in order to yield absolute values of the accessibilities.

Accessibility by Solid Counting

Table II contains a summary of the results obtained in the VTC. The percentage accessibility, A_s, of a sample was calculated from the relation

$$[10] \qquad A_s = \frac{\text{count rate of sample}}{\text{count rate of cellulose film}} \times 71$$

where 71 is the accessibility (A_g) of the cellulose film determined by the gas counting method. As in the gas counting method it is probable that isotope effects occurred in the exchange reaction and during the removal of water. It is assumed that the correction for the isotope effects was given by a single factor, which was the same for all the samples and hence cancelled out of eq. [10].

In this calculation no consideration has been given to differences in relative humidity during the reactions in the gas counting and solid counting methods. In the gas counting method the relative humidity for sample *c* was estimated from the sorption isotherm for viscose rayon given in the literature (33) as about 80%, while the measured relative humidity for the solid counting method ranged from 79 to 97%. The effect of relative humidity on the accessibility has not been studied, but it is believed that at high relative humidities it is not great.

Since radioactive water remaining adsorbed on the cellulose would contribute to the count rate, it was necessary to estimate the amount adsorbed under the experimental conditions. Separate experiments using oxygen isotope exchange between water vapor and cellulose sample *c*, which are described elsewhere (20), showed that the adsorbed water remaining on cellulose under the conditions of the present experiment, i.e. after 23 hours evacuation, was 6.5 mg per g, equivalent to an accessibility of 4%. Although a different apparatus was used, the value should be approximately the same for the VTC. However, the amount of adsorbed water in the other samples was roughly proportional to the accessibility (34), so that the total activity from the sample, arising from exchanged hydroxyls in the accessible regions and the small contribution from adsorbed water, remained proportional to the accessibility of the sample. Since only relative total activities are used to calculate A_s, the actual error introduced by the adsorbed water was less than 4%.

The amount of water which passed from the sample in the VTC into the vapor phase between isolation of the sample and the completion of counting (30 minutes) was calculated to be 0.016 μg from the pressure rise in separate adsorption experiments (20), and by making allowance for the much smaller sample in the VTC. This amount of water corresponded to 44 counts per minute which was negligible. Therefore, any errors caused by extraneous water were well within the experimental accuracy and may be neglected.

Table II shows that the accessibility values agreed reasonably with the D_2O vapor accessibilities of Mann and Marrinan (9–11). Although accessibilities and amorphous cellulose determined by X-ray diffraction and density methods measured different quantities, both methods graded the samples in the same order, except for bacterial cellulose. The X-ray values for bacterial cellulose were respectively twice and one and one-half times as high as the accessibility values of Mann and Marrinan and those of the present work. In making the comparisons the difference in the samples as well as the experimental methods should be borne in mind.

Amylose sheets have given an indication of an oriented X-ray diffraction pattern (35); however, the 100% accessibility of amylose (Table II) showed that the crystalline fraction was very small, or that the crystallites were unstable in the presence of water vapor. The

$100 \pm 2\%$ value also gave excellent confirmation of the self-consistency of the solid counting method. The 98% nitrated cellulose had the expected accessibility of zero since practically all its hydroxyl groups were replaced, and showed convincingly that only hydroxyl hydrogens take part in the exchange.

Because of the short range of tritium β-particles (about 6 μ in cellulose) and the difficulty of preparing reproducible samples (18, 36), it was expected that surface roughness might have a large effect on the accuracy of the measurements with the VTC, and so normally only smooth-surfaced samples were used. However, a sheet of acetate grade dissolving pulp having a fluffy surface, gave an accessibility only 6% higher than the value by the gas counting method, which is independent of surface roughness. This indicated that the VTC may also be used to compare paper samples with similar surfaces.

These results show that the solid counting method, once calibrated, provides reliable accessibilities for starch and cellulosic samples. It is believed that the simplicity of the method will make it useful for characterizing various kinds of cellulose and other substances.

Cyclic Drying Experiments

The results of these experiments are plotted in Figs. 2 and 3. The percentage of in-

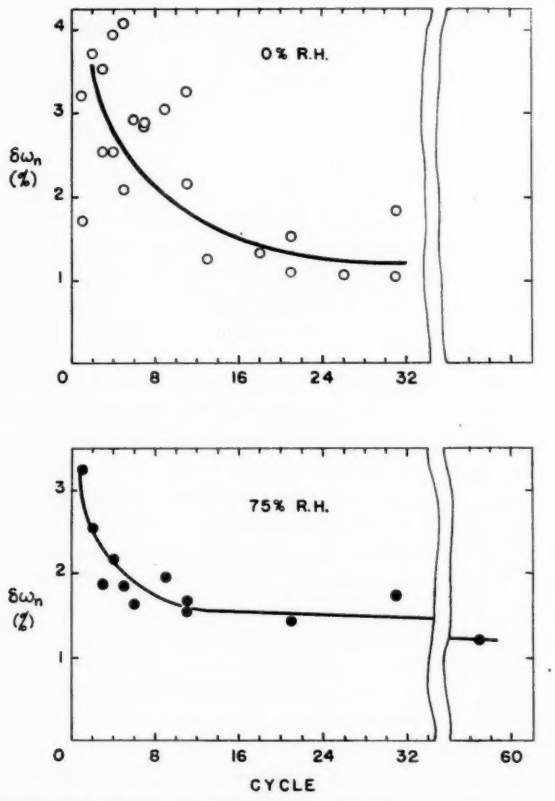

FIG. 2. Inaccessible cellulose formed during each wetting and drying cycle ($\delta\omega_n$). Top graph, 0% relative humidity. Bottom graph, 75% relative humidity.

accessible cellulose, $\delta\omega_n$ or W_n, formed by drying tritiated water was calculated from the equation

$$[11] \qquad \delta\omega_n \quad \text{or} \quad W_n = \frac{N}{13{,}200} \times \frac{1.20}{S} \times 100$$

where N is the corrected counts per minute from the cycled sample, 13,200 the counts per minute for a completely exchanged sample calculated from the observed count rate of cellulose film (9400 per minute) and its known accessibility (71%), and 1.20 and S are the specific activities in μc per mg of the tritiated water used in the accessibility measurements and the cyclic experiments respectively. Each point on Fig. 2 was obtained from a separate piece of cellulose, but some of the pieces had common distillation steps from tritiated water. Because of the possibility of irregular temperature variations from one distillation to another, particularly at 0% r.h., the experimental points cannot strictly be considered as representing completely separate experiments. On the other hand, each point on Fig. 3 was obtained from a completely independent experiment. The newly formed inaccessibilities of the control samples soaked in tritiated water, but not dried, were only 0.2, 0, and 2.3% for the 1-hour, 12-hour, and 31-day soakings respectively, showing that only changes occurring during the wetting and drying need be considered for the interpretation of the values of $\delta\omega_n$ or W_n.

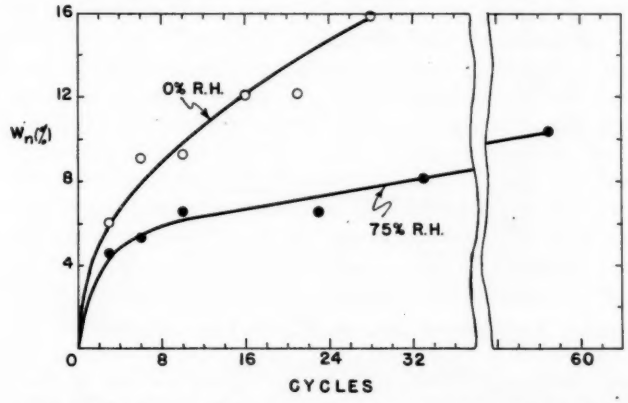

FIG. 3. Net inaccessibility formed during a number of wetting and drying cycles (W_n). At 0% and 75% relative humidity.

The values of $\delta\omega_n$ at both 0% and 75% r.h. decreased to a limiting value of 1.3% with increasing number of cycles. The corresponding W_n (Fig. 3) showed an initial rapid increase followed by a slower rise, but there was no indication of a limiting value at either 0% or 75% r.h. up to 28 and 57 cycles respectively. Somewhat unexpectedly the values of W_n for 0% r.h. were always greater than those at 75% r.h., since previous values of the liquid water permeability (19) and dimensional swelling (37) of cellulose cyclically dried at different relative humidities were interpreted to mean that more cross-linking occurred on drying at higher humidities. However, in the present experiments at 0% r.h. the temperature decreased during the rapid removal of water from the cellulose, and the influence of temperature on the processes is at present unknown. No difference was definable for the values of $\delta\omega_n$ at 0% and 75% r.h., possibly because of the scatter of the 0% r.h. results.

The value of $\delta\omega_n$ is the inaccessibility to liquid water caused by the nth cycle alone, and that of W_n the net inaccessibility resulting from n cycles. Therefore, if the inaccessible material is formed irreversibly it follows that

$$[12] \qquad \sum_{1}^{n} \delta\omega_n = W_n.$$

Figure 4 shows that this is not so, but that $\sum\delta\omega_n$ at 75% r.h. increasingly exceeded W_n. Some of the newly formed inaccessible cellulose represented by $\delta\omega_n$ must therefore have become accessible during subsequent wettings and dryings. Furthermore, W_n at 10 and 28 cycles at 0% r.h. and 10 and 33 cycles at 75% r.h. decreased by 1.6, 4.5, 2.2, and 1.6 respectively when the samples were cycled four more times using ordinary water and drying at the relative humidity of their preparation.

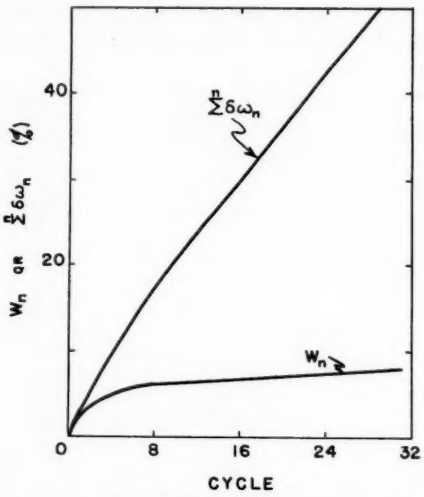

FIG. 4. Comparison of $\Sigma\delta\omega_n$ and W_n at 75% relative humidity.

It is believed that these experiments give the first direct evidence of the conversion of inaccessible to accessible cellulose by wetting and drying. In view of this it should be noted that all measurements were made after the samples had an additional wetting and drying cycle using ordinary water to remove labile tritium and to mount the sample on the holder. It is interesting to note that decreases of 0.5 to 1 in $\delta\omega_n$ and W_n occurred immediately after removal from the VTC, presumably by exchange between the atmospheric water and the inaccessible cellulose rendered accessible by the drying in the VTC. However, since exactly the same techniques of soaking, mounting, and drying were carefully followed in the measurements of $\delta\omega_n$ and W_n, the preceding observation does not affect the comparison made in Fig. 4.

After the initial small loss of activity immediately after removal from the VTC, the sample was stable for weeks, showing that the anhydroglucose units in the inaccessible part of the dried cellulose did not become accessible; otherwise the tritium would have exchanged with the atmospheric water (5).

The results discussed so far have shown that part of the newly formed inaccessible cellulose becomes once again accessible after further wetting and drying, but they give

no direct information about the stability of the inaccessible cellulose present in the original wet sample either while standing in water or on wetting and drying. However, the small inaccessibilities formed in the control experiments mentioned previously showed quantitatively that in the swollen state any formation of inaccessible cellulose was very slow. Nevertheless the 2.3% value showed that, in time, changes do occur which may be caused by (*a*) an increase in the total accessibility (which is, however, unlikely since the accessibility probably reached a constant value during the 6 months of soaking which preceded the experiment), (*b*) by penetration of tritiated water into the crystallites, or (*c*) by a slow process of interconversion of accessible and inaccessible regions. Thus there is the possibility that the inaccessible regions in the original undried gel may not be stable to prolonged soaking in water.

If the original inaccessible cellulose becomes accessible during the cyclic treatment then W_n should be greater than the decrease in accessibility caused by the corresponding number of cycles. The increase of W_n during 28 cycles at 0% r.h. and 57 cycles at 75% r.h. was not reflected by a decrease in the accessibility, A_s, between 1 and 56 cycles at 75% r.h. (Table II). However Mann and Marrinan (10, 11) reported a decrease of 3% and 5% in accessibility during the second wetting and drying of viscose film. D_2O accessibility measurements by Brickman *et al.* (6) of cyclically dried samples gave erratic results.

A net decrease in accessibility of cellulose on wetting and drying is consistent with many of the published experimental values which are believed to be related to the extent of the cross-bonding in cellulose. Thus irreversible decreases occurred in the dimensional swelling (37), permeability of water (19), moisture regain (6, 31), and heat of wetting (6). On the other hand, the X-ray crystallinity of cellulose was almost constant during drying from the gel state (38) and on cyclically drying (39). However, the experimental difficulties of the X-ray measurements and the relative small changes occurring in the cyclic experiments may account for these conflicting results. Under some experimental conditions the accessibility of cellulose to nitration (6, 40) and hydrolysis (41) showed a small but definite increase with successive wetting and drying; this appears to be at variance with the notion of lower accessibility after wetting and drying. It was not possible to decide definitely from this partly conflicting data whether or not inaccessible regions in the original cellulose are rendered accessible by wetting and drying.

CONCLUDING REMARKS

The unexpected difference between $\sum\delta\omega_n$ and W_n may be explained by the following hypothesis.

1. Cellulose chain molecules are continually moving, particularly when wet, and undergo segmental jumping, as shown by dielectric measurements (42). Thus an arrangement of chains, once formed, does not necessarily remain unchanged. The stability of a particular molecular configuration depends upon the attraction between chains resulting from van der Waals' forces and, more important, hydrogen bonding. For example in a crystalline configuration, which requires the greatest energies to separate the chains and is thus the most stable, there are one or two interchain hydrogen bonds per anhydroglucose unit (43, 44). Less regular arrangements having fewer interchain bonds are less stable, so that a spectrum of stabilities exists.

2. A configuration may be disrupted by (*i*) the formation of hydrogen bonds between cellulose and water at the expense of cellulose–cellulose interchain bonds, (*ii*) mechanical stresses resulting from the effort of neighboring molecules to arrange themselves into more stable configurations, and (*iii*) segmental thermal motion. In a very stable arrangement

of cellulose chains such as in the crystalline regions, weakening of interchain bonds by water molecules alone is energetically unfavorable: the water molecule forms hydrogen bonds with the cellulose which may be equal in energy to those which are replaced; but the chains have to separate to accommodate the water molecule which stretches and weakens the neighboring interchain bonds, so that an increase in energy is required. However a stable configuration may be rendered less stable if the competition of water molecules for interchain hydrogen bond positions occurs simultaneously with the disruptive action of a number of mechanical stresses which act by chance in co-operation.

3. When cellulose is very wet, the water forms hydrogen bonds with all hydroxyl groups attached to *mobile* chains and the formation of new more stable configurations from these mobile chains is almost completely prevented. Furthermore, under these conditions no mechanical stresses arise to disrupt existing stable configurations. At the other extreme, in dry cellulose the mobility of the chains is decreased by the greater number of interchain bonds, so that rearrangement into new stabler configurations almost ceases. Therefore, new stable configurations do not form in very wet or very dry cellulose, but only at some intermediate, possibly narrow, range of moisture content. At this critical moisture content some of the stable regions are being continually disrupted while new stable configurations are being formed.

4. From simple statistical considerations, the rate of formation of the stabler configurations will decrease, and the rate of destruction increase, as the quantity of cellulose in stable configurations becomes larger. Thus, at the critical moisture content, the amount of cellulose in the stable configurations slowly increases with time until an equilibrium value is reached.

The mechanical stresses mentioned above are believed to be identical with those which cause cellulose to shrink when it is dried.

The hypothesis is now considered in terms of wetting and drying. Stable configurations which form and are not broken by the next wetting and drying cycle are measured as newly formed inaccessible regions by the cyclic drying experiments. Note that the critical moisture content which is favorable to the formation of stable configurations is traversed once on wetting and once on drying, so that inaccessible regions should form twice during a cycle but not necessarily in identical amounts.

The only reliable data which do not appear to be consistent with this hypothesis are the nitration of cyclically dried cellulose (6, 40), and the hydrolysis of dried cellulose (41). No reasons can be cited, but it may be significant that the hydrolysis measurements were made on samples dried from ethanol instead of water.

The hypothesis also explains the formation of "resistant OD groups" in the experiments of Mann and Marrinan (9), which are closely analogous to the $\delta\omega$ values. A careful study of their results showed that a necessary, and, except for one experiment involving a rapid treatment of a cyclically dried sample, a sufficient condition for the formation of resistant OD groups is that the cellulose be passed through the intermediate moisture range in the presence of D_2O, either by being wet or dried. Similarly their "deuteration of crystalline regions" (11), in which a higher accessibility was found with liquid D_2O than with the vapor, can be attributed to the deuteration by the liquid of cellulose which was accessible at any stage during the wetting and drying cycle, i.e. the cellulose originally available to the vapor, as well as the inaccessible cellulose which was rendered accessible during the wetting and drying processes. It follows also that the difference between this quantity (8% of the total viscose film) and the decrease in accessibility (3%) measured by their D_2O vapor method (11) after wetting and drying should be comparable with $\delta\omega_n$ for the

second cycle. The actual difference of about 5% is, considering the differences in technique, in very good agreement with the direct measurement of 2.5% in the present experiments.

The new feature of this hypothesis is the reversible interconversion of accessible (and possibly amorphous) and inaccessible (and possibly crystalline) regions on repeated wetting and drying. Thus it may be possible to completely deuterate the hydroxyl groups of cellulose by using a sufficient number of wetting and drying cycles with liquid D_2O.

It is proposed to continue these experiments.

REFERENCES

1. K. F. Bonhoeffer. Z. Elektrochem. **40**, 469 (1934).
2. G. Champetier and E. Viallard. Bull. soc. chim. France, Ser. 5, **5**, 1042 (1938).
3. V. J. Frilette, J. Hanle, and H. Mark. J. Am. Chem. Soc. **70**, 1107 (1948).
4. J. W. Rowen and E. K. Plyler. J. Research Natl. Bur. Standards, **44**, 313 (1950).
5. K. E. Almin. Svensk Papperstidn. **55**, 767 (1952).
6. W. J. Brickman, H. B. Dunford, E. M. Tory, J. L. Morrison, and R. K. Brown. Can. J. Chem. **31**, 550 (1953).
7. H. Corte and H. Schaschek. Das Papier, **9**(21/22), 519 (1955).
8. H. J. Marrinan and J. Mann. J. Appl. Chem. **4**, 204 (1954).
9. J. Mann and H. J. Marrinan. Trans. Faraday Soc. **52**, 481 (1956).
10. J. Mann and H. J. Marrinan. Trans. Faraday Soc. **52**, 487 (1956).
11. J. Mann and H. J. Marrinan. Trans. Faraday Soc. **52**, 492 (1956).
12. A. R. G. Lang and S. G. Mason. Intern. J. Appl. Radiation and Isotopes. In press. 1960.
13. B. G. Ranby. Inaugural dissertation, University of Uppsala. 1952.
14. C. V. Robinson. Anal. Chem. **26**, 1100 (1954).
15. C. V. Robinson. Nucleonics, **13** (11), 90 (1955).
16. W. Bernstein and R. Ballentine. Rev. Sci. Instr. **21**, 158 (1950).
17. W. F. Libby. Anal. Chem. **19**, 2 (1947).
18. M. L. Eidinoff and J. E. Knoll. Science, **112**, 250 (1950).
19. J. M. Kuzmak. Ph.D. thesis, McGill University, Montreal. 1953.
20. A. R. G. Lang and S. G. Mason. Can. J. Chem. **37**, 1829 (1959).
21. F. L. Bates, D. French, and R. E. Rundle. J. Am. Chem. Soc. **65**, 142 (1943).
22. W. J. C. Orr. Trans. Faraday Soc. **23**, 1033 (1936).
23. M. Harada and T. Titani. Bull. Chem. Soc. Japan, **11**, 465 (1936).
24. M. Koizumi and T. Titani. Bull. Chem. Soc. Japan, **13**, 427 (1938).
25. C. K. Ingold and C. L. Wilson. Z. Elektrochem. **44**, 62 (1938).
26. J. O. Halford and B. Pecherer. J. Chem. Phys. **6**, 571 (1938).
27. F. W. Hobden, E. F. Johnston, L. H. P. Weldon, and C. L. Wilson. J. Chem. Soc. 61 (1939).
28. J. Hine and C. H. Thomas. J. Am. Chem. Soc. **75**, 739 (1953).
29. A. H. Price. Nature, **181**, 262 (1958).
30. J. H. Perry. Chemical engineers' handbook. 3rd ed. McGraw-Hill Book Co., Inc., New York. 1950. p. 580.
31. P. H. Hermans. Physics and chemistry of cellulose fibres. Elsevier Pub. Co. Inc., Amsterdam. 1949.
32. R. D. Preston, E. Nicolai, R. Reed, and A. Millard. Nature, **162**, 665 (1948).
33. E. Ott and H. M. Spurlin. Cellulose and cellulose derivatives. Part I. 2nd ed. Interscience Publishers, Inc., New York. 1954. p. 420.
34. L. Valentine. Chem. & Ind. **43**, 1279 (1956).
35. R. E. Rundle, L. Daasch, and D. French. J. Am. Chem. Soc. **66**, 130 (1944).
36. F. L. Jackson and H. W. Lampe. Anal. Chem. **28**, 1735 (1956).
37. E. Hubert, A. Matthes, and K. Weisbrod. Kolloid-Z. **98**, 173 (1942).
38. P. H. Hermans and A. Weidinger. Makromol. Chem. **18/19**, 75 (1956).
39. M. Kouris, H. Ruck, and S. G. Mason. Can. J. Chem. **36**, 931 (1958).
40. T. P. Yin and R. K. Brown. Can. J. Chem. **37**, 444 (1959).
41. B. G. Ranby. *In* Fundamentals of papermaking fibres. The British Paper and Board Makers Association, Inc. Technical Section. 1958. p. 52.
42. R. Seidman and S. G. Mason. Can. J. Chem. **32**, 744 (1954).
43. J. Mann and H. J. Marrinan. J. Polymer Sci. **32**, 357 (1958).
44. D. W. Jones. J. Polymer Sci. **32**, 371 (1958).

SEPARATION OF CARBOHYDRATE DERIVATIVES BY GAS–LIQUID PARTITION CHROMATOGRAPHY[1]

C. T. Bishop and F. P. Cooper

ABSTRACT

Gas–liquid partition chromatography has been used to separate all of the possible tetra- and tri-*O*-methyl ethers of methyl α- and β-D-glucopyranoside. Anomeric methyl glycosides of each isomer were well separated except those of 3,4,6-tri-*O*-methyl-D-glucose. The six di-*O*-methyl-D-glucopyranoses were partially resolved as their methyl glycosides. The four possible mono-*O*-methyl-D-glucopyranoses were completely resolved after conversion to the corresponding mono-*O*-methyl-penta-*O*-acetyl-D-glucitols, a series of compounds which, except for the 6-*O*-methyl isomer, have not been reported previously. Quantitative estimations of mixtures containing varying amounts of methyl-2,3,4-tri-*O*-methyl-β-D-xylopyranoside and methyl-2,3,4,6-tetra-*O*-methyl-α-D-glucopyranoside showed that molar ratios of components in a mixture could be determined with a mean deviation of ±0.5 in 100.

Since its development by James and Martin (1) in 1952, gas–liquid partition chromatography has been used to separate a wide variety of volatile organic compounds. The first report of its application to carbohydrates dealt with the separation of fully methylated methyl glycosides of some monosaccharides (2). Good separations were obtained and it was also established that the compounds were stable under the conditions used because they could be recovered unchanged from the effluent gas stream. These results encouraged further investigation to see if gas–liquid partition chromatography could be extended to more general use in carbohydrate chemistry. This paper describes the separation of methyl ethers of glucose and also deals with the accuracy of gas–liquid partition chromatography in quantitative estimations of carbohydrate derivatives.

All separations shown in the figures were obtained on an apparatus employing an ionization detector (3). The high sensitivity of this detector permitted the use of small samples (2–4 γ) and this resulted in a considerable increase in resolution of components over that obtained in the apparatus previously described (2), which contained a thermal conductivity cell as a detector. However, the latter apparatus was used when it was necessary to collect samples from the effluent gas stream.

Retention volumes of the compounds used were dependent on the composition of the stationary liquid phase. It was advantageous to use two columns, one containing a polar liquid phase, the other a non-polar, because separations of some isomeric methyl ethers could be obtained on one and not on the other. Butanediol succinate polyester and Apiezon M were used as the polar and non-polar stationary liquid phases respectively. A number of other liquid phases were tried in preliminary work including Dow Corning silicone grease, carbowax 4000, zinc stearate, D-mannitol, partially benzylated raffinose, methyl cellulose (methoxyl, 27.9%), and mannitol hexastearate. The silicone gave separations comparable with those obtained on Apiezon M but was less convenient to use because a solvent extraction was required to remove low molecular weight material from the liquid phase. Most separations on carbowax were similar to those obtained on butanediol succinate polyester but the carbowax was not as suitable for general use. Mannitol, mannitol hexastearate, and zinc stearate gave columns having poor resolving power. The benzylated raffinose was unstable and the columns bled excessively at operating tempera-

[1]*Manuscript received November 30, 1959.*
Contribution from the Division of Applied Biology, National Research Council of Canada. Presented at the 136th meeting of the American Chemical Society, Atlantic City, N.J., September 1959.
Issued as N.R.C. No. 5522.

tures of 150–200° C; the methyl cellulose was not liquid at these temperatures. The carbohydrate derivatives mentioned were tested as liquid phases because their structural similarities to the components to be separated might be expected to give enhanced separations. Although none of the carbohydrate derivatives tested here were useful as liquid phases, Kircher (4) has reported recently the separation of fully methylated methyl glycosides of monosaccharides by gas–liquid partition chromatography using fully methylated hydroxyethyl cellulose as the liquid phase.

Alkali-washed Celite 545 was chosen as the inert support for the liquid phase because the alkali washing decreased the tendency of those compounds which passed easily through the column to give asymmetrical peaks (due to adsorption). However, the number of derivatives that could be eluted from the columns was reduced considerably by the use of alkali-washed Celite because of increased adsorption of sugars in which the anomeric hydroxyl group was free or substituted by an acetyl group and in which there were a large number of free hydroxyls. These derivatives which were adsorbed by alkali-washed Celite could be eluted, but with poor resolution, from columns in which the inert support was acid-washed Celite, firebrick, powdered glass, or sodium chloride. The alkali-washed Celite was sieved to give narrow screen fractions which facilitated even packing of the columns but the particle size appeared to have little effect on resolving power.

Because 1-*O*-acetyl- and free reducing sugars were adsorbed by alkali-washed Celite it was necessary to block the reducing group by formation of methyl glycosides. The diethyl mercaptals and *N*-phenyl glycosylamines were also tested but these derivatives, even when formed from fully methylated sugars, were not sufficiently volatile. The first publication (2) concerning this work reported that the anomeric methyl glycosides of 2,3,4-tri-*O*-methyl-L-arabinose and of 2,3,4,6-tetra-*O*-methyl-D-galactose were not separated under the conditions used. However, this was either a property of the particular conformations of these sugars or was caused by the lower resolving power of the instrument used in that work because it has now been found that anomeric methyl glycosides of methyl ethers of glucose can be separated.

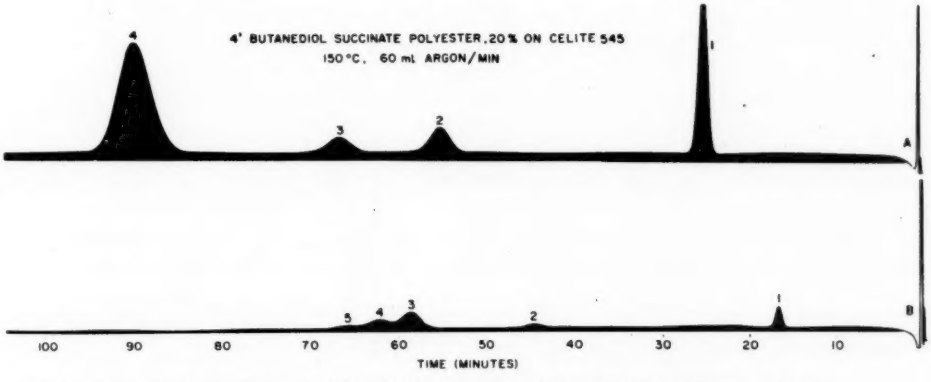

FIG. 1. Separation of tetra- and tri-*O*-methyl ethers of methyl α- and β-D-glucopyranosides.

(A) α-Methyl glycosides of:
(1) 2,3,4,6-Tetra-*O*-methyl-D-glucose.
(2) 2,3,4-Tri-*O*-methyl-D-glucose.
(3) 3,4,6-Tri-*O*-methyl-D-glucose.
(4) 2,3,6- and 2,4,6-Tri-*O*-methyl-D-glucose.

(B) β-Methyl glycosides of:
(1) 2,3,4,6-Tetra-*O*-methyl-D-glucose.
(2) 2,3,4-Tri-*O*-methyl-D-glucose.
(3) 2,4,6-Tri-*O*-methyl-D-glucose.
(4) 2,3,6-Tri-*O*-methyl-D-glucose.
(5) 3,4,6-Tri-*O*-methyl-D-glucose.

The largest number of possible methyl ethers of glucose was best obtained by partial methylation and, because anomers were separable, methyl-α-D-glucopyranoside and methyl-β-D-glucopyranoside were partially methylated separately. Figure 1 shows the separation of the tetra- and tri-*O*-methyl ethers that resulted from these partial methylations. Identities were assigned to these peaks as described in the experimental section. All of the anomeric methyl-D-glucopyranosides were separated except those of 3,4,6-tri-*O*-methyl-D-glucose; isomers within an anomeric series were clearly distinguishable except for the methyl 2,3,6- and 2,4,6-tri-*O*-methyl-α-D-glucopyranosides which were both under peak 4, line A, in Fig. 1. This peak was collected from the effluent gas stream and rechromatographed on the non-polar Apiezon M column. As shown by Fig. 2 the two components were separated completely and it was possible therefore, by using the polar and non-polar liquid phases, to separate all of the isomeric tri-*O*-methyl-D-glucopyrano-

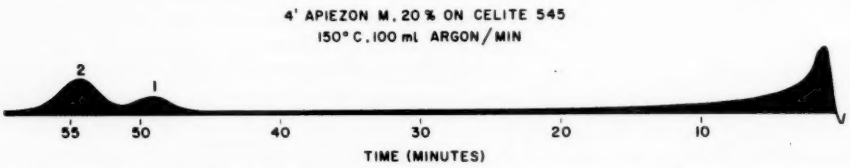

FIG. 2. Separation of methyl 2,3,6- and 2,4,6-tri-*O*-methyl-α-D-glucopyranosides. α-Methyl glycosides of: (1) 2,3,6-Tri-*O*-methyl-D-glucose. (2) 2,4,6-Tri-*O*-methyl-D-glucose.

sides. Table I gives the retention volumes of each of these components relative to that of methyl-2,3,4,6-tetra-*O*-methyl-α-D-glucopyranoside as a standard. An empirical observation based on these results is that in the glucose series the α-methyl glycosides, in which the anomeric methoxyl occupies the axial position, always had higher retention volumes than the corresponding β-methyl glycosides where the anomeric methoxyl is equatorial; this indicated a greater solubility of the axially oriented anomers in both the polar and

TABLE I

Retention volumes of methyl ethers of methyl α- and β-D-glucopyranoside relative to methyl-2,3,4,6-tetra-*O*-methyl-α-D-glucopyranoside

On butanediol succinate polyester		On Apiezon M
β-2,3,4,6	0.67	0.82
α-2,3,4,6	1.000 (standard)	1.000 (standard)
β-2,3,4	1.78	0.98
α-2,3,4	2.19	1.12
β-2,4,6	2.34	1.09
β-2,3,6	2.48	1.12
β-3,4,6	2.62	1.13
α-3,4,6	2.65	1.13
α-2,3,6	3.56	1.26
α-2,4,6	3.56	1.38

Conditions: 20% liquid phase on alkali-washed Celite 545; 4-ft column, 150° C, 60 ml argon/min.

non-polar phases. These relative retention volumes are much more reproducible than *R* values in paper chromatography and, although not obviating the necessity for preparing crystalline derivatives, constitute a much more sensitive and reliable criterion of purity and identification than any other chromatographic method.

The di-*O*-methyl ethers of glucose were not resolved as well as the tri-*O*-methyl ethers. Figure 3 shows a separation of the products from partial methylation of methyl-β-D-glucopyranoside and presumably all six of the di-*O*-methyl isomers should be present. Crystalline methyl-2,4-di-*O*-methyl-β-D-glucopyranoside was isolated from peak 4 but a

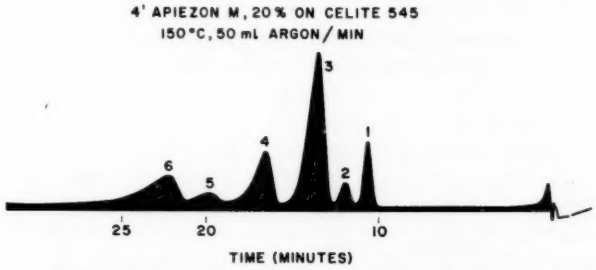

FIG. 3. Separation showing methyl di-*O*-methyl-β-D-glucopyranosides. β-Methyl glycosides of: (1) 2,3,4,6-Tetra-*O*-methyl-D-glucose. (2) 2,3,4-Tri-*O*-methyl-D-glucose. (3) Tri-*O*-methyl-D-glucoses (mainly 2,4,6-). (4), (5), and (6) Di-*O*-methyl-D-glucoses.

lack of standards has prevented assignments to the other peaks. Under the conditions used in this work it was found that skewed peaks invariably indicated heterogeneity and it is therefore almost certain that peaks 4, 5, and 6 in Fig. 3 each represent more than one component. This separation was done on Apiezon M in which the methyl-di-*O*-methyl α- and β-D-glucopyranosides moved quite rapidly but were not resolved sufficiently. On the butanediol succinate polyester column these compounds were retarded considerably because of the extra polar hydroxyl group and a useful separation was not feasible. A more selective liquid phase, or possibly one that is intermediate in polarity between those used here, is obviously needed to achieve a complete separation of all the possible methyl-di-*O*-methyl α- and β-glucopyranosides. However, Fig. 3 shows that the methyl glycosides of di-*O*-methyl hexoses are sufficiently volatile to be analyzed by gas–liquid partition chromatography. It should be mentioned that on freshly prepared columns, using alkali-washed Celite 545, the first few samples of methyl-di-*O*-methyl hexosides were irreversibly adsorbed. The columns were conditioned by running a few samples which presumably covered the active sites and no further adsorption of these compounds was encountered. There was no evidence of exchange or displacement of the samples used to condition the columns. Practically, the lack of complete separation of as complex a mixture of di-*O*-methyl hexoses as just described is not too serious because methanolysis of a methylated polysaccharide seldom yields more than three di-*O*-methyl hexoses. Work to be published on application of this technique to the structural investigation of polysaccharides has shown that the di-*O*-methyl hexoses in these less complex mixtures can be separated and identified easily (5).

The methyl mono-*O*-methyl-D-glucopyranosides were not sufficiently volatile to be separated by gas–liquid partition chromatography. Methyl mono-*O*-methyl hexopyranosides, and indeed methyl hexopyranosides, passed through columns that were conditioned as described for the methyl-di-*O*-methyl glucopyranosides. However, their retention volumes were so great that resolution of a mixture was not possible. The following sequence of reactions was therefore applied to the mono-*O*-methyl-D-glucose to give derivatives that were sufficiently volatile to be separated by gas–liquid partition chromatography. The mono-*O*-methyl-D-glucoses were reduced to the corresponding mono-*O*-methyl-D-

glucitols which were then acetylated. The resolution of these mono-*O*-methyl-penta-*O*-acetyl-D-glucitols is shown in Fig. 4. It appears that the only one of these isomeric compounds to be reported previously was the 1,2,3,4,5-penta-*O*-acetyl-6-*O*-methyl-D-glucitol (6). Because anomeric methyl glycosides were separable by gas–liquid partition chromatography it appeared that this procedure of reduction and acetylation was a good way to

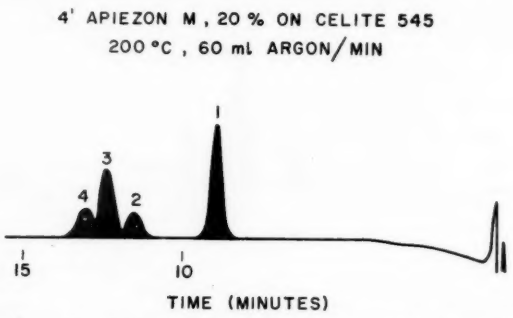

FIG. 4. Separation of mono-*O*-methyl-penta-*O*-acetyl-D-glucitols. (1) 6-*O*-methyl-D-sorbitol pentaacetate. (2) 2-*O*-Methyl-D-sorbitol pentaacetate. (3) 3-*O*-Methyl-D-sorbitol pentaacetate. (4) 4-*O*-Methyl-D-sorbitol pentaacetate.

avoid the complex mixture of anomers that might be expected in the methanolysis products from a methylated polysaccharide. However, there could be difficulty in deciding on the location of a methyl group in the original sugar when the resulting sugar alcohol was symmetrical and, in practice, it was found that methanolysis of methylated polysaccharides did not yield as complex mixtures as had been anticipated.

Gas–liquid partition chromatography affords a quick and accurate means of estimating the relative amounts of individual components in a mixture of methylated sugars. Table II gives the results from estimations of various molar ratios of two components and the mean deviation in the estimation was ±0.5 in 100. The argon ionization detector used in the

TABLE II

Molar ratios of two methylated monosaccharides as determined by gas–liquid partition chromatography

Calculated		Found	
A	*B*	*A*	*B*
60.7	39.3	60.5	39.5
50.6	49.4	50.0	50.0
33.8	66.2	33.1	66.9
20.3	79.7	20.6	79.4
0.9	99.1	1.3	98.7
		Mean deviation = ±0.5	

A, methyl-2,3,4-tri-*O*-methyl-β-D-xyloside. B, methyl-2,3,4,6-tetra-*O*-methyl-α-D-glucoside.

present work was developed by Lovelock (3) and shown to respond on a molar basis. It was therefore possible to obtain a molar ratio of components in a mixture directly from the separation curve simply by measuring the areas under the peaks. The method can also be used for measuring absolute quantities provided that a known percentage of an internal standard can be added to the mixture. The technique has proved extremely

useful in examining the methanolysis products of methylated polysaccharides. Although methyl mono-*O*-methyl hexosides and methyl hexosides are not sufficiently volatile to permit the separation of individual isomers, it is possible to obtain an estimate of these components, as one peak, relative to the more highly methylated products. Ratios of isomers within that one peak can then be determined by the procedure described for the mono-*O*-methyl glucoses. Other methods for estimating relative amounts of methylated sugars in a mixture depend on separation of the components by paper chromatography, elution from the paper, and estimation of the individual components by stoichiometric reaction of the reducing groups (e.g., 7) or spectrophotometric measurement of the color produced with specific reagents (e.g., 8, 9). Accuracies in these methods ranged from $\pm 0.8\%$ to $\pm 10\%$ and are, of course, influenced by impurities eluted from the paper; spectrophotometric methods require standard absorption curves for each component. Gas–liquid partition chromatography is therefore at least as accurate, much faster, and more convenient than any of those methods for estimating methylated sugars in a mixture. Each separation of the two components given in Table II required about 10 minutes and for quantitative estimation the peaks were simply cut from the chart and weighed.

EXPERIMENTAL

Apparatus

The apparatus with ionization detector was a "Pye Argon Chromatograph"* and some of its pertinent characteristics are listed below.

Column size, 4 ft, 5 mm I.D.
Detector, ionization (80 μc radium D).
Carrier gas, argon.
Sample size, 2–4 γ.
Resolution, up to 1000 theoretical plates/ft.
Limit of detection, 0.01 γ.
Temperatures used, 150° C and 200° C.

Column Packing

Celite 545 was screened to remove fines and material retained on the 100-mesh sieve was stirred with 5% methanolic potassium hydroxide for 2 hours. The solid was filtered and dried, first by air sucked through the filter and finally in an oven at 100° C. This dried material was used to prepare the columns described below.

Apiezon M vacuum grease (2 g/8 g Celite) was dissolved in petroleum ether (30–60° C) and added to the Celite in an open beaker. Sufficient solvent was used to give a mobile slurry, which was stirred during evaporation of the solvent at room temperature by a stream of air. Last traces of solvent were removed in an oven at 100° C, the mixture being stirred intermittently during this process. The dried material was then used to pack the columns and any traces of volatile material remaining were removed by equilibration of the column under operating conditions for 6–7 hours.

The butanediol succinate polyester was prepared (10) from succinic acid (50 g) and 1,4-butanediol (50 g) using zinc chloride (0.1 g) as catalyst. The mixture was stirred and heated for 3 hours at 160° C then for 2 hours at 190° C. The water formed during esterification was removed through an air condenser by a stream of nitrogen. Heating was continued for another 2 hours during which 1,4-butanediol was removed *in vacuo*. The mixture was then cooled to room temperature to give a white, crystalline solid which softened at 90° C and was completely melted at 96° C. To remove catalyst the mixture

Obtained from Technical Service Laboratories, Toronto, Ont.

was dissolved in chloroform and poured through a short column of Amberlite IR-120 ion exchange resin. Columns containing this liquid phase were prepared as described for those containing Apiezon M, except that chloroform was used as solvent instead of petroleum ether.

Partial Methylation

Methyl-α-D-glucopyranoside and methyl-β-D-glucopyranoside were methylated separately with 30% sodium hydroxide and dimethyl sulphate using one-third of the amount of dimethyl sulphate theoretically required for complete methylation. The reactions were stirred for 6 hours after the dropwise addition of dimethyl sulphate had been completed and the products were then isolated by extraction with chloroform.

Identification of Components

To assign identities to the peaks on the separation curves authentic samples of the various glucose methyl ethers were converted individually into glucosides by refluxing with 2% methanolic hydrogen chloride. These derivatives were then separated by gas chromatography each one giving two peaks, one of which coincided with the peak of that particular isomer in the α-series, the other with a peak in the β-series. It was not possible to establish the separations reported in this paper by using only authentic samples of glucose methyl ethers because, after methyl glycoside formation, each sample gave two peaks and it could not be proved which one was the α-anomer and which the β-. This could only be done by preparing the methyl ethers of each anomeric methyl glycoside as just described.

Mono-O-methyl-penta-O-acetyl-D-glucitols

Authentic samples of 2-, 3-, 4-, and 6-*O*-methyl-D-glucose were reduced separately with an equal weight of potassium borohydride in aqueous solutions. To assure complete reduction the reactions were allowed to stand at room temperature for 24 hours. Amberlite IR-120 ion exchange resin was then added until gas evolution ceased. The resin was then filtered, washed with methanol, and the combined filtrates and washings were evaporated under diminished pressure at 35° C. Repeated evaporation from methanol removed borate and the sirupy mono-*O*-methyl-D-glucitols were acetylated with acetic anhydride and sulphuric acid. The acetylation reactions were added directly to silica gel columns and the products were eluted with chloroform. Evaporation of the chloroform eluates left the isomeric mono-*O*-methyl-penta-*O*-acetyl-D-glucitols; the 6-*O*-methyl isomer crystallized on evaporation of the solvent and the 2-*O*-methyl isomer crystallized after being stored for 1 week in an evacuated desiccator over sodium hydroxide. The 3- and 4-*O*-methyl isomers have not crystallized. Anal. Calc. for $C_{17}H_{28}O_{11}$: C, 50.24%; H, 6.45%; acetyl, 52.9%. Found:

(*a*) 2-*O*-methyl-1,3,4,5,6-penta-*O*-acetyl-D-glucitol; m.p. 53–54° C (recrystallized from ether:hexane), $[\alpha]_D^{24} = +24° \pm 1°$ (*c*, 1.6% in chloroform). C, 50.15%; H, 6.64%; acetyl, 52.8%.

(*b*) 3-*O*-methyl-1,2,4,5,6-penta-*O*-acetyl-D-glucitol; $[\alpha]_D^{24} = +3° \pm 1°$ (*c*, 1.85% in chloroform). C, 50.52%; H, 6.75%; acetyl, 53.04%.

(*c*) 4-*O*-methyl-1,2,3,5,6-penta-*O*-acetyl-D-glucitol; $[\alpha]_D^{24} = +5° \pm 1°$ (*c*, 1.5% in chloroform). C, 49.92%; H, 6.71%; acetyl, 52.5%.

(*d*) 6-*O*-methyl-1,2,3,4,5-penta-*O*-acetyl-D-glucitol; m.p. 109–110° C (recrystallized from methanol:water), $[\alpha]_D^{24} = +6° \pm 1°$ (*c*, 1.71% in chloroform). C, 50.21%; H, 6.49%; acetyl, 53.07%. Vargha and Puskas (6) reported m.p. 105° C and $[\alpha]_D^{20} = +7.6°$ (*c*, 2.624% in chloroform) for this compound.

Quantitative Estimations

Solutions of known concentration were made up in methanol of methyl-2,3,4-tri-*O*-methyl-β-D-xylopyranoside and methyl-2,3,4,6-tetra-*O*-methyl-α-D-glucopyranoside. Samples were pipetted accurately from these standard solutions and mixed to give the molar mixtures listed in Table II. Aliquots from these mixtures were then analyzed by gas–liquid partition chromatography and the peaks on the separation curve were cut out and weighed giving the results shown in Table II.

ACKNOWLEDGMENTS

The authors wish to thank Mr. A. G. McInnes for many valuable discussions about this work. We would also like to thank Dr. B. M. Craig for making available detailed directions for preparing the butanediol succinate polyester prior to publication. A generous donation of many of the authentic samples of glucose methyl ethers by Dr. T. E. Timell is gratefully acknowledged, and our thanks are due to Dr. A. Wickstrom for a sample of 3,4,6-tri-*O*-methyl-D-glucose. Microanalyses were done by Mr. A. E. Castagne.

REFERENCES

1. A. T. JAMES and A. J. P. MARTIN. Biochem. J. **50**, 679 (1952).
2. A. G. MCINNES, D. H. BALL, F. P. COOPER, and C. T. BISHOP. J. Chromatog. **1**, 556 (1958).
3. J. E. LOVELOCK. J. Chromatog. **1**, 35 (1958).
4. H. W. KIRCHER. Am. Chem. Soc., 136th meeting. Atlantic City. 1959. Abstr. p. 18D.
5. C. T. BISHOP and F. P. COOPER. Unpublished results.
6. L. VARGHA and T. PUSKAS. Chem. Ber. **76**, 859 (1943).
7. E. L. HIRST, L. HOUGH, and J. K. N. JONES. J. Chem. Soc. 928 (1949).
8. J. K. N. JONES and J. B. PRIDHAM. Biochem. J. **58**, 288 (1954).
9. T. A TIMELL, C. P. J. GLAUDEMENS, and A. L. CURRIE. Anal. Chem. **28**, 1916 (1956).
10. B. M. CRAIG and N. L. MURTY. J. Am. Oil Chemists' Soc. **36**, 549 (1959).

THE BIOGENESIS OF ALKALOIDS

XXV. THE ROLE OF HYGRIC ACID IN THE BIOGENESIS OF STACHYDRINE[1]

A. V. ROBERTSON[2] AND LÉO MARION

ABSTRACT

In alfalfa 2–3 weeks old neither labelled ornithine nor labelled proline act as precursors of stachydrine. It has been shown, however, that the methyl group of methionine becomes incorporated into the alkaloid so that the biogenesis appears to occur at that time of growth. It is now shown that hygric acid (N-methylproline) is a precursor of stachydrine. The implications of the results obtained are discussed.

It has been shown previously that in alfalfa seedlings, the activity of administered proline labelled with ^{14}C in the carboxyl group or at position 2 is not incorporated in the stachydrine subsequently isolated (1–4). Nevertheless, radioactive stachydrine is produced at the same plant age by feeding Me-^{14}C-methionine (4). The implications of these results have been discussed and several alternatives were suggested to circumvent the most obvious conclusion that proline is not a precursor of stachydrine (4). One of these hypotheses was that only processes involving the formation of the second N-methyl group of stachydrine were taking place in alfalfa 2–3 weeks old, the heterocyclic ring having been formed from proline at some other time. For example, the final step in the biosynthesis of stachydrine might be a methylation of already preformed hygric acid (N-methylproline). Possibly one of the methyl groups of stachydrine is dynamically involved in alfalfa transmethylation reactions, in which case the methylation of hygric acid to stachydrine would be reversible. Leete and Bell (5) have shown that the methyl group of nicotine is in equilibrium with methyl acceptors in tobacco plants.

Information has now been obtained about the role of hygric acid in stachydrine biosynthesis from experiments in which carboxyl-^{14}C-hygric acid was fed to alfalfa seedlings 17 days old. The plants were harvested 4 days later at which time most of the radioactivity in the nutrient solution had disappeared. The alkaloids were isolated by established methods (6), and the crystalline mixture of pure stachydrine and homostachydrine hydrochlorides obtained was highly radioactive. Paper chromatographic assay showed that there was no contamination due to hygric acid, and that all of the activity was present in the stachydrine. Although homostachydrine has been obtained pure from the mixture of betaine hydrochlorides (7), it has not yet proved possible to separate pure stachydrine on a preparative scale. Decarboxylation to isolate the radioactive carbon as barium carbonate was therefore performed on the mixture. Appropriate corrections were made for the relative proportions of the compounds in the mixture, and for the yields of barium carbonate obtained from either component in separate experiments with inactive material. Within the limits of experimental error, all of the activity in the stachydrine was present in the carboxyl group. Therefore hygric acid serves as an efficient precursor for the heterocyclic ring of this alkaloid.

All attempts so far to show the role of ornithine or proline in the biogenesis of stachydrine have failed (1–4), and the only definite precursor of the alkaloid that has been found is hygric acid. It is conceivable that the formation of proline and its conversion to hygric acid take place at an earlier stage of growth of the plant, but since some of the

[1]*Manuscript received November 9, 1959.*
Contribution from the Division of Pure Chemistry, National Research Council, Ottawa, Canada.
Issued as N.R.C. No. 5532.
[2]*National Research Council of Canada Postdoctoral Fellow, 1957–59.*

experiments previously reported were done after only 12 days of growth this does not seem too probable. Further, since ornithine can be converted to proline in the plant in the presence of pyridoxal (2), it also seems improbable that the failure of proline to give rise to stachydrine at the same period of growth could be attributable to the possibility that the proline might not get to the site of synthesis. The observation of Abelson and Vogel (8) concerning the difference in behavior between exogenous and endogenous ornithine in *Neurospora crassa*, however, supports such a possibility. If hygric acid were formed from proline one would have to conclude that proline was synthesized in two different sites, and that neither the ornithine nor proline from one site could find its way to the other site. The concept of multiple sites is not in itself reluctant, but it is difficult to accept that the required precursors existing in one part of the plant could not be translocated to the site where they are needed when hygric acid is. Although the suggestion is made with hesitancy, the results obtained so far could best be explained if hygric acid were synthesized not from proline, but directly from smaller fragments. Further work will be necessary to prove or disprove such a suggestion, but it becomes impossible to ignore the repeated failures to implicate ornithine or proline in the pathway to stachydrine.

EXPERIMENTAL

Synthesis of Carboxyl-^{14}C-DL-hygric Acid

Carboxyl-^{14}C-DL-proline (0.1 mc, sp. act. 2.7 mc/mmole) was diluted with DL-proline (44 mg) and monomethylated by the method of Ingram (9) (see also Bowman and Stroud (10)). The product was sublimed at 140°/1 mm giving a quantitative yield of pure hygric acid.

Feeding Experiment and Extraction of Alkaloids

Alfalfa seed (240 g) was grown in 8 trays as previously described (6) and on the 18th day, carboxyl-^{14}C-DL-hygric acid (54 mg, total activity 1.8×10^8 d.p.m.) in water (80 ml) was divided evenly among the trays. The radioactivity in the nutrient solution decreased as follows: 9% remained after 1 day, 4% after 2 days, 3% after 3 days, less than 2% after 4 days. The plants were harvested on the 22nd day and the alkaloids were isolated by the usual extraction procedure (6). In this experiment the crude betaine hydrochlorides obtained by ion exchange of the reineckates were discolored and oily. The oil was removed by ether extraction of an aqueous acid solution of the hydrochlorides before purification through the mercuric chloride complex. The crystalline mixture of pure homostachydrine and stachydrine hydrochlorides had an activity of 2.82×10^3 d.p.m./mg. Paper chromatography in 95% ethanol – concentrated aqueous ammonia (95:5) showed that all of the activity was confined to the stachydrine spot, R_F 0.45, and that homostachydrine, R_F 0.54, was the only other component. Hygric acid had R_F 0.51 on the same paper. Hygric acid does not give a satisfactory reaction with Dragendorff's reagent or iodine vapor, so the orcinol – sulphuric acid method of Ingram (9) was used. The betaines are also developed by this reagent. The mixture was estimated by the intensity of spots on paper chromatograms (developed with Dragendorff's reagent) to contain 60±5% (w/w) of stachydrine hydrochloride. The activity of the stachydrine hydrochloride is therefore 4.7×10^3 d.p.m./mg and sp. act. 8.4×10^5 d.p.m./mmole.

Degradation to Isolate Radioactivity

Fifty milligrams of the mixture of betaine hydrochlorides in quinoline (2 ml) was heated with copper powder (100 mg) and the temperature was gradually raised from 210–250° (1 hour). A slow stream of purified nitrogen was passed through the reaction

flask and the nitrogen and evolved gases were bubbled through barium hydroxide solution. The precipitated barium carbonate (42 mg) had an activity of 2.70×10^3 d.p.m./mg. In separate experiments with inactive stachydrine hydrochloride, homostachydrine hydrochloride, and mixtures of the two compounds, the weight of barium carbonate obtained under the above conditions was $86\pm2\%$ of the weight of starting material. Hence the ratio of the weights of barium carbonate arising from stachydrine to that from homostachydrine is equal (within $\pm2\%$) to the ratio of stachydrine to homostachydrine (w/w) in the mixture which was decarboxylated. The weight of barium carbonate arising from stachydrine is thus 60% of the total weight of the radioactive barium carbonate sample. Therefore barium carbonate formed by decarboxylation of radioactive stachydrine has an activity of 4.5×10^3 d.p.m./mg and sp. act. 8.9×10^5 d.p.m./mmole.

REFERENCES

1. E. LEETE, L. MARION, and I. D. SPENSER. J. Biol. Chem. **214**, 71 (1955).
2. A. MORGAN and L. MARION. Can. J. Chem. **34**, 1704 (1956).
3. G. WIEHLER and L. MARION. J. Biol. Chem. **231**, 799 (1958).
4. A. V. ROBERTSON and L. MARION. Can. J. Chem. **37**, 1197 (1959).
5. E. LEETE and V. M. BELL. J. Am. Chem. Soc. **81**, 4358 (1959).
6. A. V. ROBERTSON and L. MARION. Can. J. Chem. **37**, 1043 (1959).
7. G. WIEHLER and L. MARION. Can. J. Chem. **36**, 339 (1958).
8. P. H. ABELSON and H. J. VOGEL. J. Biol. Chem. **213**, 355 (1955).
9. V. M. INGRAM. J. Biol. Chem. **202**, 193 (1953).
10. R. E. BOWMAN and H. H. STROUD. J. Chem. Soc. 1342 (1950).

THE ACIDITY OF SOME AROMATIC FLUORO ALCOHOLS AND KETONES[1]

ROSS STEWART AND R. VAN DER LINDEN[2]

ABSTRACT

A series of five trifluoroacetophenones and five phenyl trifluoromethyl carbinols have been synthesized and their ionization constants in water measured. They are the unsubstituted, *p*-methoxy, *p*-methyl, *m*-bromo, and *m*-nitro compounds. The ketones exist as hydrates in aqueous solution and each is about two pK units stronger than the corresponding alcohol. The acidities of both series are correlated by the Hammett relation with ρ values of 1.11 and 1.01 for the ketone hydrates and alcohols respectively. The acid strengths vary from a pK_a of 9.18 for *m*-nitro-α,α,α-trifluoroacetophenone to 12.24 for *p*-methoxyphenyl trifluoromethyl carbinol.

In connection with an investigation of the mechanism of the permanganate oxidation of alcohols (1) we have examined a series of trifluoromethyl carbinols (2). These were chosen because their enhanced acidity permitted measurements to be made of the concentration of the alkoxide ion believed to be the intermediate in the oxidation mechanism. The trifluoromethyl carbinols and the ketones from which they are prepared are interesting compounds in their own right because of their acidities, the hydrates of the latter being of similar strength to phenols. We would like to report herein the synthesis of a series of substituted phenyl trifluoromethyl alcohols and ketones and the determination of their acidities.

EXPERIMENTAL

Reagents

α,α,α-Trifluoroacetophenone was obtained from Columbia Organic Chemicals and was fractionally distilled before use. All other reagents used were of reagent grade.

p-Methyl-α,α,α-trifluoroacetophenone

p-Tolylmagnesium bromide was prepared in the usual way from *p*-bromotoluene (34.7 g, 0.203 mole) and an equivalent amount of magnesium. Trifluoroacetic acid (7.5 g, 0.066 mole) dissolved in ether was added dropwise with vigorous stirring over a period of 2 hours at room temperature. After refluxing for 1 hour the reaction mixture was poured onto a 10% sulphuric acid – ice mixture and extracted several times with ether. The ether extracts were dried and distilled and a clear fraction boiling at 69° at 13 mm was obtained; yield, 30–50%, $n_D^{25} = 1.4710$ (lit., $n_D^{20} = 1.4693$ (3)); 2,4-dinitrophenylhydrazone, m.p. 133–136°. Calc. for $C_9H_7OF_3$: C, 57.4; H, 3.7; F, 30.3. Found: C, 57.8; H, 3.9; F, 26.8. This compound has been synthesized previously using a different procedure (3).

m-Bromo-α,α,α-trifluoroacetophenone

To a Carius tube of approximately 100 ml volume was added α,α,α-trifluoroacetophenone (20 g, 0.115 mole), anhydrous ferric chloride (0.1 g), and bromine (9 ml, 0.168 mole). The mixture was cooled in liquid nitrogen, the tube was sealed and then heated in a furnace for 6 days at 130°.

After reaction the liquid was extracted with aqueous sodium bromide and then fractionally distilled giving a small amount of unreacted ketone, a solid residue, and a clear liquid, b.p. 83.5° at 12 mm, $n_D^{24} = 1.5030$; yield, 50%. Calc. for $C_8H_4OF_3Br$: C, 38.0; H, 1.5; F, 22.5. Found: C, 38.2; H, 1.6; F, 20.6. 2,4-Dinitrophenylhydrazone, m.p.

[1]*Manuscript received November 18, 1959.*
Contribution from the Department of Chemistry, University of British Columbia, Vancouver, B.C.
[2]*Present address: Imperial Oil Limited, Sarnia, Ontario.*

121.5–123°. Calc. for $C_{14}H_8O_4N_4F_3Br$: C, 38.6; H, 1.9; N, 12.9; F, 13.2. Found: C, 38.8; H, 2.5; N, 12.0; F, 12.0.

As a check on the identity of this compound a sample was hydrolyzed with aqueous base and gave *m*-bromobenzoic acid, identical with an authentic sample.

m-Nitro-α,α,α-trifluoroacetophenone

Sixty milliliters of concentrated sulphuric acid was added slowly with stirring to trifluoroacetophenone (27.2 ml, 0.2 mole) with the temperature kept at 0° or below. A nitrating mixture (made up from 12 ml concentrated nitric acid, 4 ml fuming nitric acid, and 24 ml concentrated sulphuric acid) was added dropwise with cooling to keep the temperature from rising above 0°. A yellow solid began to precipitate after part of the nitrating mixture had been added. The mixture was poured onto crushed ice and extracted with ether. The latter was dried and on removal of the ether gave a yellow oil which on fractional distillation gave a pale yellow, low melting solid, b.p. 113° at 12 mm; yield, 75%. Calc. for $C_8H_4O_3F_3N$: C, 43.8; H, 1.8; F, 26.0; N, 6.4. Found: C, 43.4; H, 1.9; F, 24.3; N, 6.6. 2,4-Dinitrophenylhydrazone, m.p. 128–132°. Calc. for $C_{14}H_8O_5N_5F_3$: C, 42.2; H, 2.0; N, 17.6; F, 14.3. Found: C, 43.1; H, 2.8; N, 17.0; F, 13.4.

Alkaline hydrolysis of the ketone gave *m*-nitrobenzoic acid, identical with an authentic sample.

p-Methoxy-α,α,α-trifluoroacetophenone

This compound was prepared by the Grignard procedure essentially as described for *p*-methyl-α,α,α-trifluoroacetophenone. B.p. 64° at 0.5 mm; $n_D^{23} = 1.5051$. Calc. for $C_9H_7F_3O_2$: C, 52.9; H, 3.5. Found: C, 51.9; H, 3.6. 2,4-Dinitrophenylhydrazone, m.p. 104–105° (decomp.).

Phenyl Trifluoromethyl Carbinols

The unsubstituted, *m*-bromo, and *p*-methyl compounds were prepared by a lithium aluminum hydride reduction of the corresponding ketones by a standard method. Data are listed in Table I. The yields of crude product before purification were of the order of 80–90%.

TABLE I

Physical properties and analytical data for the fluoro alcohols

$YC_6H_4CHOHCF_3$	B.p.	Refractive index	Phenylurethan m.p.	Analysis*	
				Calculated	Found
H	82° (13 mm)	$1.4590^{28°}$	103–104°	C, 61.0; H, 4.1; F, 19.3	C, 61.2; H, 4.2; F, 19.0
p-CH_3O	80° (0.5 mm)	$1.4780^{23°}$		C, 52.4; H, 4.4	C, 52.2; H, 4.6
p-CH_3	94.5° (12 mm)	$1.4650^{24°}$	104–105°	C, 56.9; H, 4.7; F, 30.0	C, 57.1; H, 5.0; F, 26.6
				C, 62.1; H, 4.5; F, 18.4; N, 4.5	C, 62.1; H, 4.5; F, 16.7; N, 5.1
m-Br	115° (12 mm)	$1.5005^{27°}$		C, 37.1; H, 2.4; F, 22.4; Br, 31.4	C, 38.0; H, 2.5; F, 20.0; Br, 31.6
m-NO_2	106° (2 mm) (m.p. = 47–48°)			C, 43.5; H, 2.7; F, 25.8; N, 6.3	C, 43.7; H, 3.1; F, 23.7; N, 6.4
			102–103°	C, 53.0; H, 3.2; F, 16.8; N, 8.2	C, 53.1; H, 3.6; F, 16.3; N, 8.3

*Analysis by A. Bernhardt, Mulheim, West Germany.

m-Nitrophenyl Trifluoromethyl Carbinol

m-Nitro-α,α,α-trifluoroacetophenone (10 g, 0.045 mole) and aluminum isopropoxide

(8.2 g, 0.04 mole) dissolved in 40 ml of dry isopropyl alcohol were distilled slowly for 2 hours with the alcohol being replaced as it distilled. The mixture was poured onto a 3 *M* HCl–ice mixture and extracted with ether. Distillation yielded a viscous oil, b.p. 106° at 2 mm, which crystallized on standing. Recrystallization from benzene – petroleum ether gave pale yellow needles, m.p. 47–48°.

p-Methoxyphenyl Trifluoromethyl Carbinol

This compound was prepared by essentially the method described for *m*-nitrophenyl trifluoromethyl carbinol. See Table I for physical constants.

pK_a *Measurements*

Stock solutions of the alcohols and ketones of appropriate concentration were prepared by weighing out the pure liquids (purified in most cases by gas chromatography), and dissolving them with shaking in distilled water. Usually 10 ml of these solutions and 10 ml of phosphate buffer were added to a 25-ml volumetric flask which was then made up to volume with distilled water. The buffer consisted of 0.02 *M* Na_2HPO_4 solution to which 1 *N* NaOH or 1 *N* H_2SO_4 was added to produce approximately the desired pH. Solutions more basic than pH 13 were obtained by using NaOH directly rather than the buffer. The pH of these solutions was obtained directly from the concentration of NaOH present. The optical density of a few milliliters of the buffered ketone or alcohol solution was then measured using a Beckman DU spectrophotometer at a suitable wavelength. The latter was located by measuring the entire spectrum of the ketone or alcohol in neutral and basic solution (usually pH 4.0 and 13.6) using a Cary model 14 recording spectrophotometer. The absorption maxima are listed in Tables I and II. The cell compartment of the DU spectrophotometer was kept at 25° by means of thermospacers.

TABLE II

Ultraviolet spectral data for trifluoroacetophenone and derivatives

Trifluoro-acetophenone	Neutral aqueous solution		Basic aqueous solution		Cyclohexane solution	
	λ_{max}	ϵ	λ_{max}	ϵ	λ_{max}	ϵ
Unsubstituted	267	350	266	144	253	13,300
	260	474	260	237	288	1000
	255	427	256	278		
	250	345	250	247		
m-Br	274.5	342	273.5	213	254	10,500
	267.5	451	267	306	302	1520
	261.5	358	261	258		
	255 (sh)	250	255 (sh)	200		
m-NO_2	263	14,000	269	13,600	233	20,800
					302	900
					292	1050
p-CH_3	265	590	294	73	264	15,700
	259	607	260	356		
			253	390		
			243	410		
p-CH_3O	300	1360	276	980	289	15,900
	277	1530	270	1080	231	9300
	270	1390			225	11,000

After the optical density readings were made the pH of the remainder of the solution was measured using a Beckman model G pH meter which was standardized against

buffer at pH 7.00 and 10.00. It has been reported (4) that trifluoroacetophenones are decomposed by alkali to CHF_3 and the corresponding benzoic acid. The alkaline solutions we used were stable during the time of the measurements but it was noted that decomposition was occurring in some cases after a few hours.

Calculations

For all the compounds studied a plot of optical density against pH gave a typical titration curve. The ionization constants were calculated using the equation,

$$pK_a = pH \pm \log [(D - D_{A^-})/(D_{HA} - D)]$$

where D is the optical density of the solution at the selected wavelength, D_{A^-} that at complete ionization obtained by measuring the optical density of a 0.6 N NaOH solution of the compound (corrected in the case of the alcohols for incomplete ionization), and D_{HA} that of the completely unionized form obtained by a measurement at pH 4. A minimum of three values in the vicinity of half ionization was obtained for each compound and these values averaged to obtain the values listed in Table III. The probable error varies from compound to compound because of the differences in spectra but is generally of the order of ± 0.06 pK units.

The wavelengths in millimicrons used for the pK measurements were as follows, with the alcohol listed first and the ketone second: H (260, 260); *p*-CH_3O (280, 276); *p*-CH_3 (269, 260); *m*-Br (274, 274.5 and 267.5); *m*-NO_2 (330, 320).

TABLE III

Ultraviolet spectral data for phenyl trifluoromethyl carbinol and derivatives

Phenyl trifluoromethyl carbinol	Neutral aqueous solution		Basic aqueous solution	
	λ_{max}	ϵ	λ_{max}	ϵ
Unsubstituted	266	140	262	149
	260	210	257	200
	256	224	251	165
	250	163	247	130
m-Br	274	254	274	162
	267	340	267	244
	261	286		
m-NO_2	264	7600	270	7000
p-CH_3	265	156	271	192
	260	225	262	275
	254	194	256	230
p-CH_3O	278	1130	277	1080
	272	1320	271	1240

RESULTS

Polyfluorinated ketones exist in the hydrated form in aqueous solution (5, 6) presumably because of the strongly electron-withdrawing group which raises the energy of the dipolar canonical structure and shifts the following equilibrium to the right.

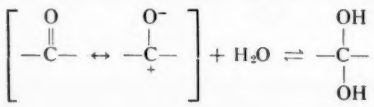

The trifluoroacetophenones reported herein are all hydrated in aqueous solution as can be seen from an examination of their ultraviolet spectra. Table II which lists the absorption maxima of the ketones in cyclohexane and in water and Fig. 1 which shows the spectrum of *m*-bromo-α,α,α-trifluoroacetophenone in water reveal the absence of the usual phenyl ketone absorption in aqueous solution. The latter spectrum appears when these compounds are dissolved in cyclohexane. (The absorption of the *p*-methoxy ketone

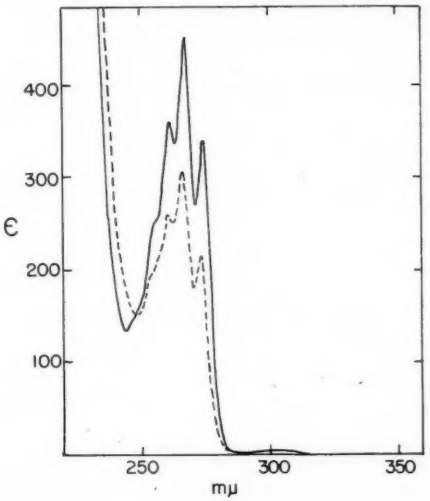

FIG. 1. The ultraviolet spectrum of *m*-bromo-α,α,α-trifluoroacetophenone in water: solid line, pH 4; broken line, pH 13.

at 300 mμ is probably due to the presence of some unhydrated ketone since this ketone is the one expected to be least hydrated in water.) When trifluoroacetophenone is dissolved in ethanol the characteristic phenyl ketone absorption at 253 mμ rapidly decays until the spectrum resembles that in aqueous solution.

The ultraviolet spectrum of the hydrate of trifluoroacetophenone is essentially a benzene spectrum modified by the side chain. When one of the hydroxyls in the side chain is ionized in basic solution the spectrum is sufficiently altered to enable measurements of the concentrations of the two forms to be made (Fig. 1).

The same applies to the alcohols, and in fact the spectra of the ketone hydrates and their anions were found to be very similar to those of the corresponding alcohols and their anions. Tables II and III reveal the close similarity in the wavelength maxima in the two series. The extinction coefficients are, however, somewhat larger for the ketone hydrates than for the alcohols.

Comparison of Acidities in the Two Series

The ionization constants of the alcohols and ketone hydrates are listed in Table IV; Fig. 2 shows the pK values plotted against σ, the Hammett substituent constant (7, 8). A satisfactory linear relation is obtained for both series. It can be seen that the ketone hydrates are about 2 pK units more acidic than the alcohols. This 100-fold increase in

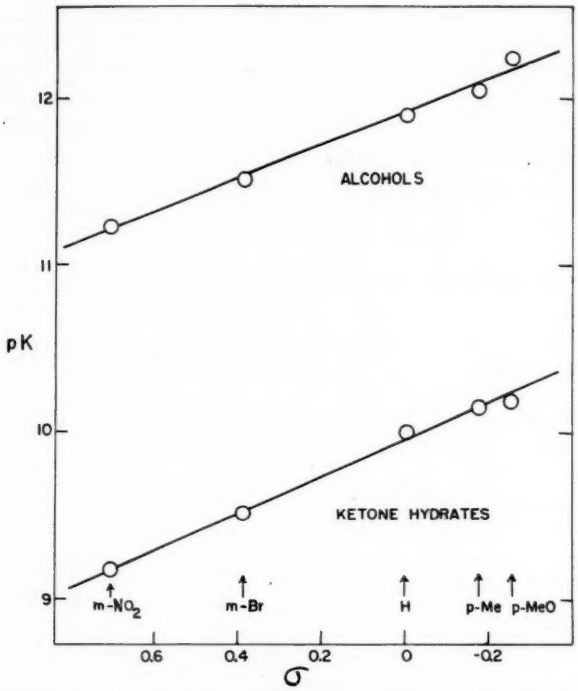

FIG. 2. Hammett plots for the ionization of phenyl trifluoromethyl carbinols (alcohols) and ketones.

TABLE IV

Acidities of substituted phenyl trifluoromethyl carbinols and ketone hydrates

Substituent	Carbinol (pK)	Ketone hydrate (pK)
H	11.90	10.00
p-CH_3O	12.24	10.18
p-CH_3	12.04	10.15
m-Br	11.50	9.51
m-NO_2	11.23	9.18

ionization constant (50-fold if a statistical correction is made for the extra ionizable proton in the ketone hydrate) is due entirely to the electronegative nature of the additional oxygen atom in the former.

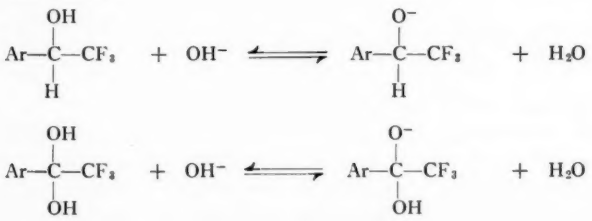

In these two systems resonance effects on the ionization are completely absent and it is worth comparing the effect of the additional oxygen atom on the acidity of the hydroxyl group with that in analogous cases. Table V shows that the addition of an oxygen atom

TABLE V
Effect of oxidation on acidities

Acid	K_I	Acid	K_{II}	K_{II}/K_I	Reference
$C_6H_5C(OH)HCF_3$	1.2×10^{-12}	$C_6H_5C(OH)_2CF_3$	1.0×10^{-10}	80	Herein
$HCOOH$	1.8×10^{-4}	HO_2COH	2×10^{-4}*	~1	(9)
$HP(O)(OH)_2$	1×10^{-2}	$HOP(O)(OH)_2$	1.6×10^{-2}	1.6	(10)
$C_6H_5CH(OH)_2$	1.2×10^{7}	$C_6H_5C(OH)_3$	1.8×10^{7}	1.5†	(11, 12)

*Corrected for incomplete hydration of CO_2.

†This ratio varies with the substituent in the ring. The *p*-CH_3O substituent reduces the importance of resonance *within* the carbonyl group and raises this ratio to a value of 13.

to formic acid, hypophosphorous acid, and benzaldehyde conjugate acid produces much smaller charges in acidity than the addition of an oxygen atom to phenyl trifluoromethyl carbinol. In the former cases the electron-withdrawing inductive effect of oxygen is largely cancelled by its electron-donating resonance effect, assuming in the case of phosphorous acid that resonance occurs with the expanded valence shell of phosphorus. Resonance involving the oxygen atoms is not possible in the case of the ketone hydrates.

The Reaction Constant

The values of the reaction constant, ρ (the slopes in Fig. 2) (7, 8), are 1.01 for the alcohols and 1.11 for the ketone hydrates. Values close to 1.0 are expected for ionizations in which the proton is removed from the second atom of the side chain (13) as in both the present cases.*

Rate of Ionization of the Fluoroketones

When the fluoroketones reported herein are dissolved in water they react rapidly to form the hydrates since the spectrum taken immediately after solution is effected is identical with that taken after long standing. The ionization of these weak acids is essentially instantaneous as expected for hydroxylic compounds. This rather obvious point is referred to here because certain fluorinated ketone hydrates have been shown to ionize only slowly with base. Thus hexafluoroacetylacetone which exists in solution as

*NOTE ADDED IN PROOF: *Since there is no conjugation between the sidechain and the substituents in these series one should obtain a better correlation with the recently derived σ^0 values (R. W. Taft, Jr., S. Ehrenson, I. C. Lewis, and R. Glick. J. Am. Chem. Soc.* **81**, *5352 (1959)) than with the standard sigma values. Even though σ and σ^0 are not greatly different for the substituents studied in this work it does appear that the correlation is slightly better for σ^0 than for σ.*

the dihydrate, I,

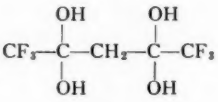

I

although a much stronger acid ($pK = 4.35$) than trifluoroacetophenone hydrate ($pK = 10.0$) ionizes at a relatively slow rate requiring over 3 hours for neutralization with 1 *M* NaOH (14, 15). A similar situation exists with thenoyltrifluoroacetone (14). The reason for the apparent discrepancy is the following. The stable anion of I is undoubtedly not ion II, but ion III.

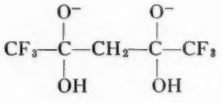

II

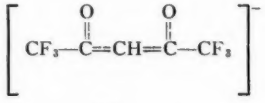

III

The slow neutralization by base is due to ion II, which is almost certainly formed immediately by the action of strong base, having to revert to the unhydrated form and then eliminate a proton from the central carbon to form the more stable ion III. Such an enolate anion is, of course, not possible with aromatic ketones so that the further, slow, ionization does not take place.

ACKNOWLEDGMENT

The financial support of the National Research Council is gratefully acknowledged.

REFERENCES

1. R. STEWART. J. Am. Chem. Soc. **79**, 3057 (1957).
2. R. STEWART and R. VAN DER LINDEN. To be published.
3. J. D. PARK, H. A. BROWN, and J. R. LACKER. J. Am. Chem. Soc. **73**, 709 (1951).
4. J. H. SIMONS and E. O. RAMLER. J. Am. Chem. Soc. **65**, 389 (1943).
5. A. L. HERNE, J. W. SHEPHARD, and E. J. YOUNG. J. Am. Chem. Soc. **72**, 3577 (1950).
6. E. H. COOK and R. W. TAFT, JR. J. Am. Chem. Soc. **74**, 6103 (1952).
7. L. P. HAMMETT. Physical organic chemistry. McGraw-Hill Book Co., Inc., New York. 1940. Chap. VII.
8. H. H. JAFFÉ. Chem. Revs. **53**, 191 (1953).
9. W. W. LATIMER and J. H. HILDEBRAND. Reference book of inorganic chemistry. Macmillan Co., New York. 1951. p. 282, 285.
10. W. W. LATIMER and J. H. HILDEBRAND. Reference book of inorganic chemistry. Macmillan Co., New York. 1951. p. 229.
11. K. YATES and R. STEWART. Can. J. Chem. **37**, 664 (1959).
12. K. YATES. Ph.D. Thesis, The University of British Columbia, Vancouver, B.C.
13. R. W. TAFT, JR. and I. C. LEWIS. J. Am. Chem. Soc. **80**, 2436 (1958).
14. R. W. TAFT, JR. and E. H. COOK. J. Am. Chem. Soc. **81**, 46 (1959).
15. L. G. VAN UITART. M.Sc. Thesis. The Pennsylvania State College. 1951. Referred to in ref. 14.

THE IONIZATION AND DISSOCIATION OF SOME HALOGEN MOLECULES BY ELECTRON IMPACT[1]

D. C. Frost and C. A. McDowell

ABSTRACT

The ionization and dissociation of chlorine, bromine, iodine, iodine monochloride, and iodine monobromide by electron impact have been studied in a mass spectrometer which uses a monoenergetic electron source. Many ionization potentials have been observed for these molecules which, of course, refer to the formation of the parent molecular ions in different excited states. These experimental results are discussed in terms of simple molecular orbital theories of the electronic structures of the different halogen molecules.

Electron-induced dissociative ionization processes for the different substances have also been studied. Where possible, appearance potentials of both the positive and negative ions have been determined. These results have been used to construct potential energy diagrams illustrating the origin of some of the negative ion and dissociation processes observed.

INTRODUCTION

Modern electron impact methods (1, 2, 5, 6) which use monoenergetic electron sources can provide much information concerning the excited states of molecular ions. The data so obtained are of importance in understanding the electronic structure of the molecules studied. They also can be used to provide means of assessing quantum mechanical calculations. Frequently these data are the only source of information about the energy levels and excited states of the molecular ions of quite common molecules. This is so because in many cases little or nothing is known about the spectra of the molecular ions concerned.

In this paper we present the results of a detailed study of the ionization and dissociation of some halogen molecules. We have used the retarding potential difference (R.P.D.) method to obtain essentially monoenergetic electrons. The molecules studied are chlorine, bromine, iodine, iodine monochloride, and iodine monobromide.

EXPERIMENTAL

The mass spectrometer used was that described in our earlier publications (2, 3). Krypton was used as a calibrating gas for the measurements on positive ions; its ionization potential is 112,914.5 cm^{-1} (7) or 13.997 ev. For negative ions, the appearance potential of SF_6^- from sulphur hexafluoride at 0.03 ev (9) and the appearance potentials of O^- from oxygen at 4.53 ev (4) and 17.26 ev (8) were taken as standards.

In the sections dealing with resonance capture processes allowance has been made for the electron energy distribution (see reference 10) in the quoted capture energies.

Where ICl and IBr are concerned, we present results on the parent ions only, since the dissociative ionization was complicated through large contributions to the fragment ion currents from I_2 and Cl_2 or Br_2 impurities which could not be completely eliminated. Owing to the corrosive nature of the vapors studied, it was frequently necessary to remove the ion source for cleaning to retain an electron energy bandwidth of less than 0.2 ev.

[1]*Manuscript received October 30, 1959.*
Contribution from the Department of Chemistry, University of British Columbia, Vancouver 8, B.C., Canada.

Can. J. Chem. Vol. 38 (1960)

RESULTS AND DISCUSSION

(A) The Ionization of Chlorine, Bromine, and Iodine

(i) Chlorine

The electronic structure of Cl_2, Br_2, and I_2 may be represented (11) by the formula:

[1] $$----- (\sigma_g ns)^2(\sigma_u ns)^2(\sigma_g np)^2(\pi_u np)^4(\pi_g np)^4, \ ^1\Sigma_g^+$$

where $n = 3$, 4, or 5 for Cl_2, Br_2, and I_2 respectively. The inner electrons are omitted and the orbitals are written in order of decreasing binding energy.

The outer $(\pi_g np)^4$ and $(\pi_u np)^4$ orbitals are mainly atomic in character, and the energies necessary to remove an electron from either of them would not be expected to be too different. The ion formed by the removal of an electron from one of these π orbitals would be expected to have the configuration $-----(\pi_u)^4(\pi_g)^3$, $^2\Pi_g$, or at a higher energy, $----- (\pi_u)^3(\pi_g)^4$, $^2\Pi_u$, and each of these $^2\Pi$ states would be a doublet ($^2\Pi_{3/2}$, $^2\Pi_{1/2}$) with an energy separation somewhat less than that existing in the relevant halogen atom ion ground state. The energy separations for the doublet ground states of the halogen atoms are 0.11 ev for Cl, 0.46 ev for Br, and about 0.7 ev for I. The actual energy difference between the $^2\Pi_u$ and $^2\Pi_g$ states will depend on the overlap between the wave functions for the $(np\pi)^4$ and $(np\pi)^3$ atomic groups. Mulliken (11) predicted that the overlap should be quite small, perhaps small enough to give the order of ionic electronic states as:

$$^2\Pi_{3/2,\,g};\ ^2\Pi_{3/2,\,u};\ ^2\Pi_{1/2,\,g};\ ^2\Pi_{1/2,\,u}.$$

We will now consider the case of chlorine. Watanabe (12), using a photoionization technique, measured the first Cl_2 ionization potential to be 11.48 ± 0.01 ev. Morrison and Nicholson (13) and Thorburn (14) found a value of 11.8 ev by electron impact. The value obtained in our work is 11.63 ± 0.04 (standard deviation) ev. It will be noted that the electron impact figures are considerably higher than Watanabe's, and this is no doubt due to a low ionization cross section at the threshold. The Cl_2^+ ground state potential energy curve will be displaced in equilibrium internuclear distance from the $Cl_2(^1\Sigma^+)$ since primary ionization involves the removal of an antibonding electron.

The only spectroscopic observations on the chlorine molecular ion Cl_2^+ have been of the high frequency emission spectrum. This consists of ultraviolet continua and red-degraded bands from 3400 to at least 5500 Å. Ota and Uchida (15) arranged these bands into three systems, and later Elliott and Cameron (16) remeasured them and were unable to accept the former workers' analysis. Elliott and Cameron in 1938 (17) further analyzed the rotational structure of 18 bands and concluded that they belonged to $^2\Pi$–$^2\Pi$ transitions with system origins at approximately 20,800 and 20,600 cm^{-1}. This placed the $^2\Pi$ states about 2.55 ev apart.

Howell (18) disagreed with Elliott and Cameron's interpretation of their analysis, and put forward strong arguments in favor of assigning the bands to transitions with a common lower state deriving from $^2\Pi$, and the upper state from separate $^2\Sigma$ type levels. It will be shown later that this most recent interpretation fits in with our new electron impact data.

In the present work, there appear to be several ionic energy levels within about 0.6 ev of the ionization threshold (Fig. 1), and it seems very probable that within this energy range the Cl_2^+ ion is being formed in its $^2\Pi_g$ and $^2\Pi_u$ electronic states, each with an expected doublet separation of about 0.1 ev. This would explain the inability of the instrument to resolve any breaks in this neighborhood. Furthermore, since the curvature extends over

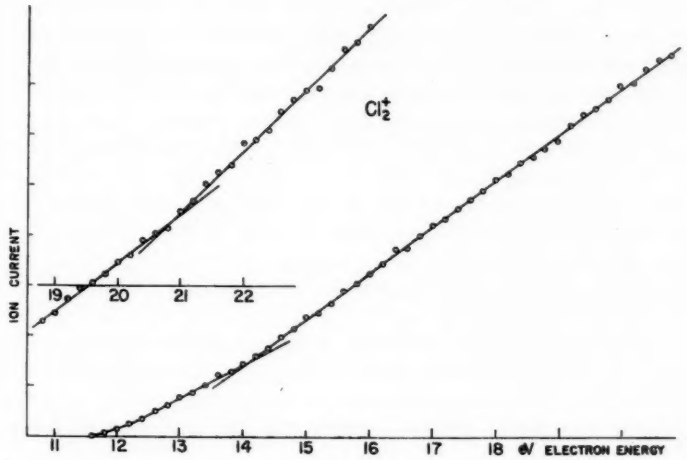

FIG. 1. The ionization efficiency curve for the formation of Cl_2^+ from chlorine by electron impact.

as great an energy as 0.6 ev, it appears probable that the $^2\Pi$ doublets do not overlap. The order of the $^2\Pi$ states would then be

$$^2\Pi_{3/2,\,g};\ ^2\Pi_{1/2,\,g};\ ^2\Pi_{3/2,\,u};\ ^2\Pi_{1/2,\,u}$$

in order of increasing energy. If the $^2\Pi_{3/2,\,u}$ did overlap the $^2\Pi_{1/2,\,g}$ level then the curvature in the ionization efficiency curve tail would be unlikely to spread over more than 0.3 or 0.4 ev.

The next inner ionization potential would be expected to refer to the removal of an electron from the strongly bonding $(\sigma_g 3p)^2$ orbital to leave the ion with the configuration;

[2] $$KKLL\ (\sigma_g 3s)^2(\sigma_u 3s)^2(\sigma_g 3p)(\pi_u 3p)^4(\pi_g 3p)^4,\ ^2\Sigma_g^+.$$

The $^2\Sigma_g^+$ ion formed by this process would therefore be expected to have a dissociation energy much less and an equilibrium internuclear distance greater than the Cl_2 molecule in the ground state.

The lowest Cl_2^+ dissociation limit, at 15.434 ev where $Cl^+(^3P)$ and $Cl(^2P)$ are the products, correlates with the molecular states Σ^+, Σ^- (2), Π (2), and Δ as doublets and quartets. These include the observed $^2\Pi_u$ and $^2\Pi_g$ and also a $^2\Sigma^+$. The next highest dissociation limit for Cl_2^+ occurs at 24.35 ev (giving at infinite separation $Cl^+(^4P) + Cl(^2P)$) and it is most unlikely that this limit is a sociated with the $^2\Sigma_g^+$ state of expression [2] since the corresponding ionization potential would be of the order of 22 ev. The energy required for the removal of a $Cl_2(\sigma_g 3p)$ electron would be expected to be much less than this.

It is fairly certain, then, that the Cl_2^+ ion represented by configuration [2] will have 15.434 ev as the dissociation limit; and for the following reasons it is proposed to assign the electron impact ionization potential at 14.09 ev to the process giving rise to this ion species. First, having assumed that ionization from the chlorine $(\pi_u)^4$ and $(\pi_g)^4$ orbitals takes place near the threshold, one would expect from expression [2] the first break in the curve (above the commencement of linearity) to refer to the removal of a $(\sigma_g 3p)$ electron. Secondly, Howell's (18) interpretation of the available spectroscopic data places

the $^2\Sigma_g^+$ state 2.55 ev above the $^2\Pi$, and this is in good agreement with the electron impact separation of 2.46 ev between the first ionization potential at 11.63 ev and the one at 14.09 ev. Thirdly, the vertical ionization potential at 14.09 ev infers that the ionic state has a dissociation energy of about 1 ev less than that for $Cl_2(^1\Sigma_g^+)$ (2.475 ev). This means the ionic state arises through the removal of a bonding electron. Lastly, Cl^+ fragment ions are observed to be formed at 15.51 ev (see below), this is strong evidence that at this energy vertical transitions are taking place to an upper stable state of Cl_2^+, having an internuclear distance r_e greater than that for $Cl_2(^1\Sigma_g^+)$, and to a region on the ionic potential energy curve opposite to the dissociation limit of 15.434 ev. It is fairly reasonable then to conclude that the electron impact ionization potential at 14.09 ev refers to the removal of a $(\sigma_g 3p)$ bonding electron to leave the ion with the configuration [2].

The next inner ionization potential would be expected to refer to the removal of a $(\sigma_u 3s)$ electron. This orbital is likely to have a somewhat antibonding nature, and so the energy necessary to remove an electron from it would be less than 24.46 ev, the binding energy of a Cl 3*s* electron. It seems reasonable to assign the electron impact ionization potential at 20.51 ev to a process which leaves the Cl_2^+ ion with the configuration

[3] $$KKLL\ (\sigma_g 3s)^2(\sigma_u 3s)(\sigma_g 3p)^2(\pi_u 3p)^4(\pi_g 3p)^4,\ ^2\Sigma_g^+.$$

(ii) Iodine

For iodine, five distinct processes leading to ion formation were observed, and they were found to occur at 9.35±0.03 ev, 9.97±0.02 ev, 10.91±0.04 ev, 11.72±0.04 ev, and 13.64±0.06 ev, quoted with standard deviations. Watanabe found the first ionization potential to be 9.28 ev (12).

A typical ion efficiency curve for the I_2^+ ion is shown in Fig. 2. The electronic structure of the iodine molecule may be written in a similar way to that for chlorine:

[4] $$KKLLMM(N)(N)(\sigma_g 5s)^2(\sigma_u 5s)^2(\sigma_g 5p)^2(\pi_u 5p)^4(\pi_g 5p)^4,\ ^1\Sigma_g^+.$$

The outer two π orbitals will be largely atomic iodine 5*p*, and the main bonding orbital is the $(\sigma_g 5p)^2$. As with chlorine, each of the ionic states formed when an electron is removed from either of the two outer orbitals will be split into two owing to spin–orbit interaction.

The magnitude of the splitting is expected to be somewhat less than 0.7 ev. That is just what is found in our work. The first two ionization potentials at 9.35 and 9.97 ev are 0.62 ev apart, and the second two at 10.91 and 11.72 ev are 0.81 ev apart.

The ionization potentials at 9.35 and 9.97 ev therefore refer to the removal of an electron from the outer $(\pi_g 5p)^4$ orbital to form the I_2^+ ion with the electronic configuration

[5] $$\text{-----}\ (\sigma_g 5p)^2(\pi_u 5p)^4(\pi_g 5p)^3,\ ^2\Pi_{g;\ 3/2,\ 1/2}$$

and the third and fourth ionization potentials will refer to ionization from the $(\pi_u 5p)^4$ orbital to form the I_2^+ ion in the $^2\Pi_{u,\ 3/2}$ and $^2\Pi_{u,\ 1/2}$ states.

A fifth ionization potential is observed at 13.64 ev, and from the molecular orbital formula for I_2 this should be the energy necessary to ionize from the bonding $(\sigma_g 5p)^2$ orbital to leave the I_2^+ ion in the $^2\Sigma_g^+$ electronic state. It would be expected that the $(\sigma_g 5p)^2$ iodine ionization potential is less than that of the chlorine $(\sigma_g 3p)^2$, previously found to be 14.09±0.03 ev, since $D(I_2) < D(Cl_2)$. It is therefore reasonable to assume that the 13.64 ev ionization potential arises through the removal of a $(\sigma_g 5p)$ electron to leave the ionic configuration:

[6] $$\text{-----}\ (\sigma_g 5p)(\pi_u 5p)^4(\pi_g 5p)^4,\ ^2\Sigma_g^+.$$

(iii) Bromine

In the case of bromine we find that there are five distinct processes giving rise to ion formation within the energy range used. They occur at 10.69±0.03, 11.05±0.05, 11.97±0.03, 12.36±0.04, and 13.72±0.04 ev. An ion efficiency curve for the Br_2^+ ion is shown in Fig. 3.

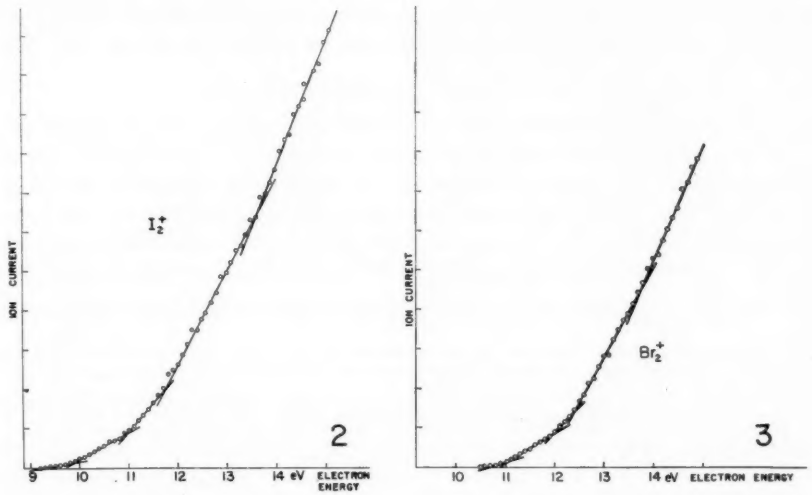

FIG. 2. The ionization efficiency curve for the formation of I_2^+ from iodine by electron impact.
FIG. 3. The ionization efficiency curve for the formation of Br_2^+ from bromine by electron impact.

Previous determinations of the first ionization potential of Br_2 have been made by Watanabe (12) (10.55 ev) and Morrison and Nicholson (13) (10.92 ev). The figure of 10.69 ev we obtain may be due to a low ionization cross section near the threshold as with chlorine.

As with iodine and chlorine, we expect four ionization potentials to lie near the ionization threshold, but here the separation of the components of each set of two is expected to be somewhat less than 0.45 ev. The first four experimental ionization potentials for bromine, quoted above, bear out this expectation. The components of each set are about 0.4 ev apart, and so we infer that at the energies of the first four processes Br_2^+ are being formed in the $^2\Pi_{g,\,3/2}$, $^2\Pi_{g,\,1/2}$, $^2\Pi_{u,\,3/2}$, and $^2\Pi_{u,\,1/2}$ electronic states. From expression [1], the next inner ionization potential would be expected to arise through the removal of one of the main bonding ($\sigma_g 4p$) electrons. It has been shown above that similar processes in Cl_2 and I_2 require 14.09 and 13.64 ev respectively. Since $D(I_2) < D(Br_2) < D(Cl_2)$, the bromine ($\sigma_g$) ionization potential should lie between the chlorine and iodine (σ_g) values, i.e. 14.09 and 13.64 ev. The next innermost bromine ionization potential does lie between these values, at 13.72 ev, and will therefore refer to the formation of Br_2^+ with the structure

$$[7] \qquad \text{-----}(\sigma_g 4p)(\pi_u 4p)^4(\pi_g 4p)^4,\ ^2\Sigma_g^+.$$

(B) The Ionization of Iodine Monochloride and Monobromide

Figures 4 and 5 show the ion efficiency curves for ICl^+ and IBr^+ respectively, and

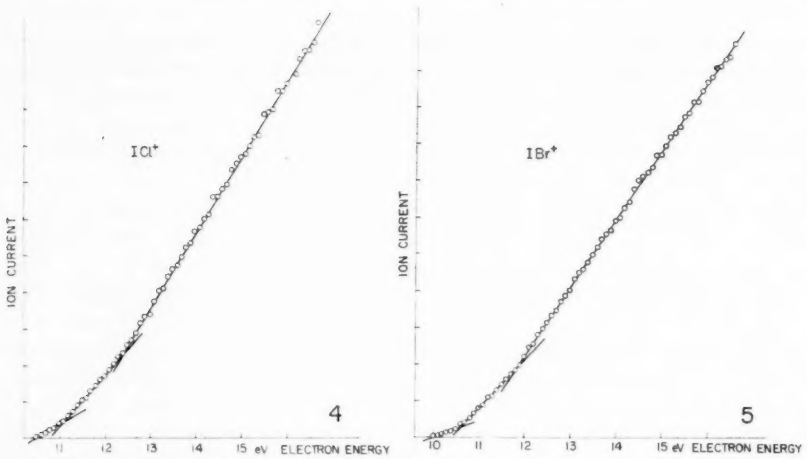

FIG. 4. The ionization efficiency curve for the formation of ICl^+ from iodine monochloride by electron impact.
FIG. 5. The ionization efficiency curve for the formation of IBr^+ from iodine monobromide by electron impact.

clearly they both exhibit three ionization processes. They occur, for ICl at 10.31 ± 0.02, 10.79 ± 0.03, and 12.13 ± 0.04 ev and for IBr at 9.98 ± 0.03, 10.49 ± 0.03, and 11.59 ± 0.05 ev.

The electronic configuration of ICl and IBr may be written, in order of decreasing binding energy (see reference 11)

[8] $$\text{-----}\,(np\sigma_X+5p\sigma_I,\,\sigma)^2(np\pi_X)^4(5p\pi_I)4,\ {}^1\Sigma^+$$

where X refers to either Cl or Br. The outer two orbitals are mainly atomic X (X = Cl, or Br) and I π-type, whilst the $(\sigma+\sigma,\,\sigma)$ is mainly bonding. The first ionization potential should therefore correspond to the removal of a $(5p\pi_I)$ electron leaving the ionic structure

[9] $$\text{-----}\,(np\sigma_X+5p\sigma_I,\,\sigma)^2(np\pi_X)^4(5p\pi_I)^3,\ {}^2\Pi_{3/2,\,1/2}.$$

The $^2\Pi$ states should be inverted, with a doublet separation mainly determined by the $(5p\pi_I)^3$ group and therefore similar to the spin–orbit splitting of the I^+ ground state. This splitting is about 0.7 ev, however the $^2\Pi$ splitting in ICl^+ and IBr^+ is expected to be less than this. The difference will depend on the degree of mixing of the outer (π_X) and (π_I) orbitals, and how much of the initial ionization occurs at the expense of the X atom. The evidence of this work is that for both ICl and IBr the splitting is less than the estimated value by about 0.2 ev (see Table I).

TABLE I
Electron impact ionization potentials of Cl_2, Br_2, I_2, ICl, and IBr

Proposed electronic state of ion	Ionization potentials, ev				
	Cl_2	Br_2	I_2	ICl	IBr
$^2\Pi_{g,\,3/2}$	$11.48\pm.01$	$10.69\pm.03$	$9.35\pm.03$	$10.31\pm.02$	$9.98\pm.03$
$^2\Pi_{g,\,1/2}$	~11.6	$11.05\pm.05$	$9.97\pm.02$	$10.79\pm.03$	$10.49\pm.03$
$^2\Pi_{u,\,3/2}$	~11.8	$11.97\pm.03$	$10.91\pm.04$	$12.13\pm.04$	$11.59\pm.05$
$^2\Pi_{u,\,1/2}$	~11.9	$12.36\pm.04$	$11.72\pm.04$	~12.2	~11.7
$^2\Sigma_g^+$	$14.09\pm.03$	$13.72\pm.04$	$13.64\pm.06$	—	—
$^2\Sigma_u^+$	$20.61\pm.06$	—	—	—	—

The first ionization potential of iodine monochloride is found to be 10.31 ev, and the second at 10.79 ev. Since these are 0.48 ev apart, i.e. less than 0.7 ev, we can reasonably assume that they refer to the formation of ICl^+ in the $^2\Pi_{3/2}$ and $^2\Pi_{1/2}$ states respectively.

Similar processes would seem to be responsible for the first two IBr ionization potentials we observe at 9.98 and 10.49 ev. The splitting here is 0.51 ev. We observe one additional increase in ion efficiency for each species, at 12.13 ev for ICl and at 11.59 ev for IBr. From expression [8] we would expect these ionization potentials to refer to the removal of, in each case, an $(np\pi_X)$ electron to leave the electronic configuration

[10] $$\text{-----}\ (np\sigma_X+5p\sigma_I,\ \sigma)^2(np\pi_X)^3(5p\pi_I)^4,\ ^2\Pi_{3/2,\ 1/2}.$$

The $^2\Pi$ splitting is expected to be 0.08 ev for ICl or 0.35 ev for IBr. It is clear, however, from Figs. 4 and 5 that we have been unable to resolve these doublets.

No further breaks are observed in the ion efficiency curves up to an electron energy of 18 ev, which infers that the cross sections for formation of ICl^+ and IBr^+ in their $^2\Sigma^+$ states through ionization from the σ bond are too small to be detected here. Probably the ion with the structure $\text{-----}\ (\sigma+\sigma,\ \sigma)(\pi)^4(\pi)^4$ immediately dissociates.

(C) The Dissociative Ionization of Chlorine, Bromine, and Iodine

(i) Chlorine

The Cl^- resonance capture peak is observed to have an onset energy of 1.60 ± 0.05 ev, a peak maximum at 2.4 ± 0.1 ev, and an over-all width of 1.6 ± 0.2 ev. It is most probable that the Cl^- ions are being produced by transitions to a repulsive Cl_2^- state, of dissociation limit equal to $D(Cl_2)-EA(Cl)$, or -1.055 ev with respect to the Cl_2 ground state. The process occurring is clearly

[11] $$Cl_2+e \rightarrow Cl^-+Cl+K+E$$

where K and E are respectively the total kinetic and excitation energies of the fragments.

The potential energy diagram illustrating the formation of Cl^- by process [11] is sketched in Fig. 7, and a typical Cl^- capture peak with a SF_6^- calibration peak is shown in Fig. 6.

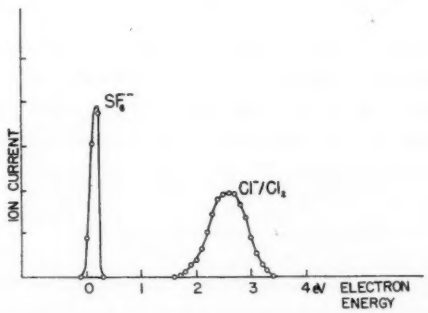

FIG. 6. The resonance capture peak for the formation of Cl^- from chlorine by electron impact.

Figure 8 shows the ion efficiency curve for Cl^+ from Cl_2. There are clearly only two processes here, and their onset energies are 11.86 ± 0.04 ev and 15.51 ± 0.03 ev. The former is identified with an ion pair process since Cl^- is observed to appear at the similar energy of 11.93 ± 0.06 ev (Fig. 9).

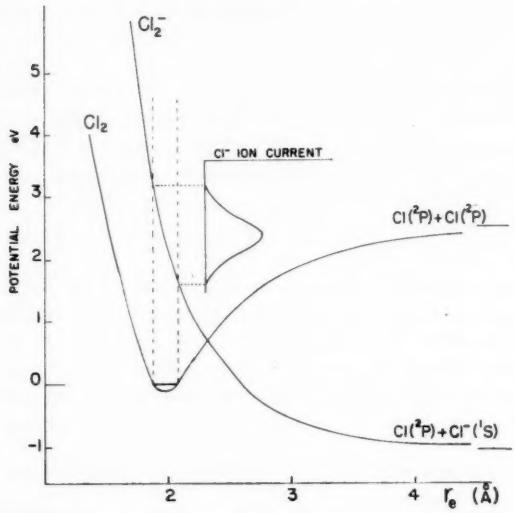

FIG. 7. Potential energy diagram to illustrate the formation of Cl^- from chlorine by a resonance capture process.

The lowest dissociation limit involving a Cl^+ and Cl^- ion pair is at 11.96 ev, assuming $EA(Cl) = 3.53$ ev (19), $D(Cl_2) = 2.48$ ev (20), and $I(Cl) = 13.01$ ev (21). The observed appearance potentials are very close to this limit, and so it is most probable that transitions are occurring from $Cl_2(^1\Sigma_g^+)$ to a stable excited state of Cl_2 having its dissociation limit at 11.96 ev.

The only other Cl^+ appearance potential detected below 23 ev is at 15.51 ev, and this clearly refers to vertical transitions from $Cl_2(^1\Sigma_g^+)$ to $Cl_2^+(^2\Sigma_g^+)$. Transitions to the ionic state will be likely to occur near the energy of the dissociation limit since the internuclear distance, r_e, for the $^2\Sigma_g^+$ is expected to be appreciably greater than r_e for the Cl_2 ground state.

These results on Cl^+ and Cl^- are in good agreement with Thorburn's (14) except that we do not detect the process producing Cl^- ions which he observed to occur at 4.4 ev.

(ii) Bromine

At low electron energies Br^- is observed to be formed with maximum probability at 0.03 ± 0.03 ev, and the ion current rapidly decreases to zero at 0.72 ± 0.05 ev. The process occurring is obviously

$$[12] \qquad Br_2+e \rightarrow Br^-+Br+K+E.$$

Assuming the fragments to be formed in their ground states, Fig. 10 shows the form of the potential energy curves involved here. The Br^- and SF_6^- resonance capture peaks are shown in Fig. 11.

Figure 12 shows an ion efficiency curve for Br^+ formation from Br_2. Several of the breaks are shallow, but repeated observations indicate that processes occur at energies of 10.38 ± 0.05, 12.30 ± 0.06, 14.31 ± 0.03, 15.88 ± 0.04, 17.06 ± 0.04, 17.97 ± 0.06, and 19.98 ± 0.06 ev.

Figure 13 concerns Br^- formation through processes other than resonance capture.

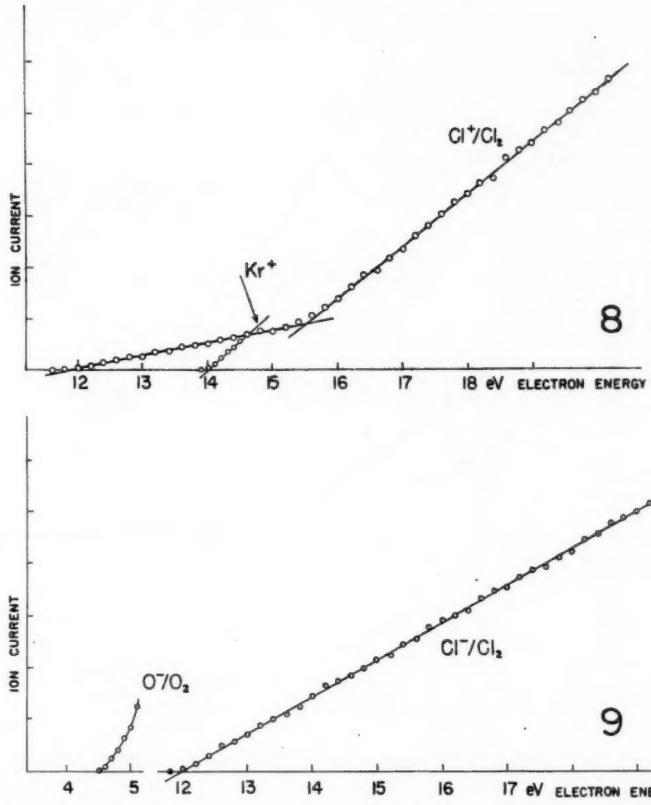

FIG. 8. The ionization efficiency curve for the formation of Cl^+ from chlorine by electron impact.
FIG. 9. The ionization efficiency curve for the formation of Cl^- from chlorine by an ion pair process as the result of electron impact.

There are two, and they occur at 10.34 ± 0.04 and 12.27 ± 0.05 ev. The first two appearance potentials for Br^- agree closely with the first two for Br^+, and so it is probable that these result from ion pair processes:

$$[13] \qquad Br_2+e \rightarrow Br^+ + Br^- + K + E + e.$$

The average observed Br^+ and Br^- appearance potentials are 10.36 and 12.28 ev. Assuming $EA(Br) = 3.49$ ev (21), $D(Br_2) = 1.97$ ev (20), and $I(Br) = 11.80$ ev (21), the energy necessary to form Br^+ and Br^- in their ground states from $Br_2(^1\Sigma^+)$ is 10.28 ev. The ion pair process at 10.36 ev would therefore seem to be occurring through transitions to the potential curve of an excited Br_2 state at points opposite to the dissociation limit to give $Br^+(^2P_{3/2})+Br^-(^1S)$. A repulsive Br_2 excited state is unlikely to be involved here as the observed appearance potential is very close to the dissociation limit energy.

The first excited state of the Br atom is the $^2P_{1/2}$ state, 0.457 ev above the ground $^2P_{3/2}$ state, and there is the possibility of a dissociation limit 10.74 ev above the ground $Br_2(^1\Sigma^+)$ state. The second ion pair process at 12.28 ev could therefore be occurring

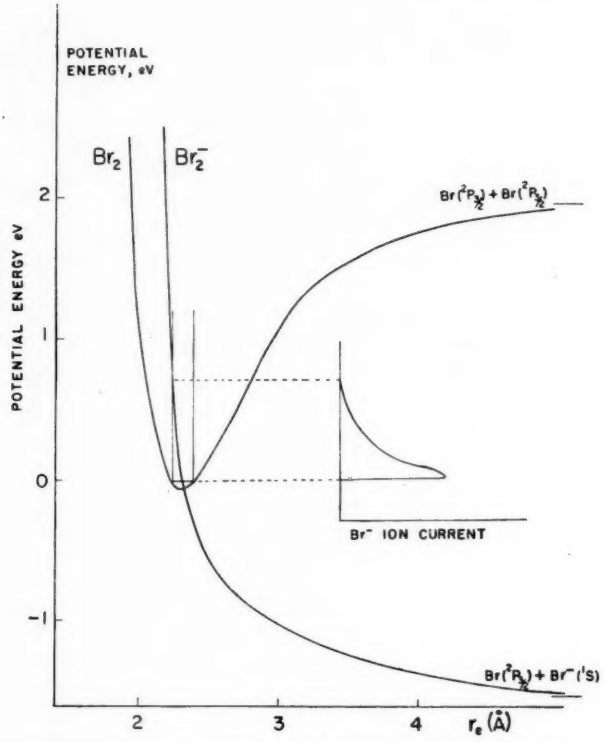

FIG. 10. Potential energy diagram to illustrate the formation of Br^- from bromine by a resonance capture process.

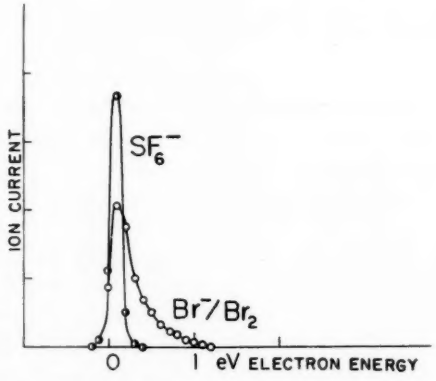

FIG. 11. The resonance capture peak for the formation of Br^- from bromine by electron impact.

through transitions to an excited unstable Br_2 state having a dissociation limit at 10.28 ev or at 10.74 ev. No further breaks in the Br^- ion efficiency curve were observed up to 18 ev.

The Br^+ ion is next formed at 14.31 ev, and from Fig. 12 it is evident that this process is easily the most important for Br^+ production. There are dissociation limits for Br_2^+ at

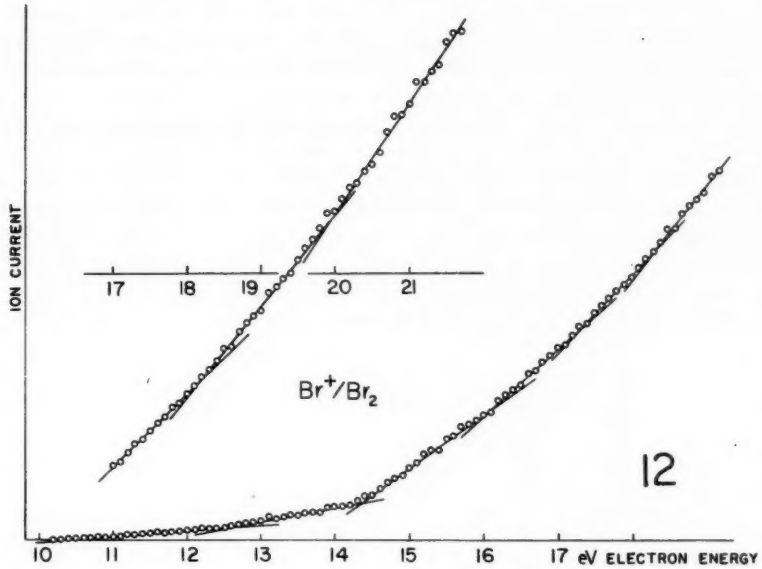

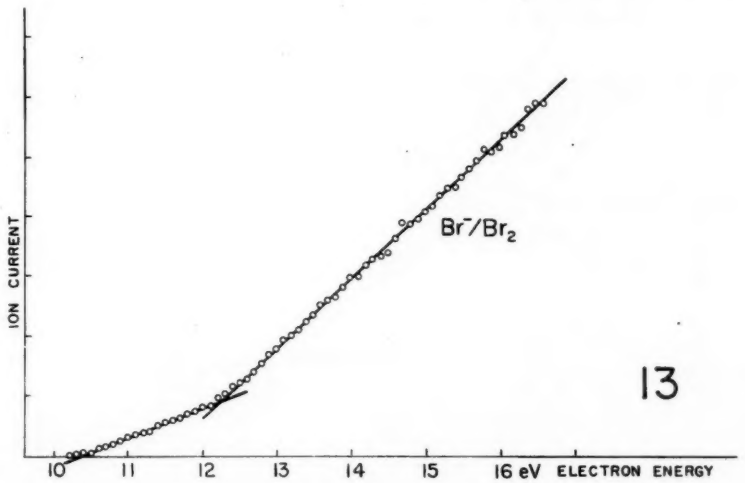

FIG. 12. The ionization efficiency curve for the formation of Br^+ from bromine by electron impact.
FIG. 13. The ionization efficiency curve for the formation of Br^- from bromine by ion pair processes as the result of electron impact.

13.77 and 14.23 ev, and we have observed a stable state (probably $^2\Sigma^+$) of Br_2^+ at 13.72 ev which probably dissociates into normal fragments at 13.77 ev. The $^2\Sigma^+$ state could, however, dissociate to $Br^+(^5S)+Br(^2P_{1/2})$ at 14.23 ev, and if this is so then the Br^+ ion group at 14.31 ev could be formed by transitions to the $^2\Sigma_g^+$ state just above the dissociation limit—a possibility since the internuclear distance, r_e, for this state is likely to be appreciably greater than that for $Br_2(^1\Sigma_g^+)$. Otherwise, the Br^+ ion formation here must result from transitions to a repulsive Br_2^+ state associated with the 13.77 ev dissociation limit.

Br^+ ions are next observed to appear at 15.88 ev, and must be formed through transitions to a repulsive Br_2^+ state associated with the fragments $Br^+(^5S)+Br(^2P_{3/2})$ or $+Br(^2P_{1/2})$ mentioned above, or with a $Br(^2P)+Br^+(^5D)$ limit a few hundredths of a volt above the $Br^+(^5S)$ one.

At 17.06, 17.97, and 19.98 ev Br^+ ions are formed, and it is possible to write down the many possible processes in each case. However, little is to be gained by this since the kinetic energy with which the fragments are endowed upon formation is unknown and therefore it is not possible to make other than tentative suggestions regarding the processes occurring.

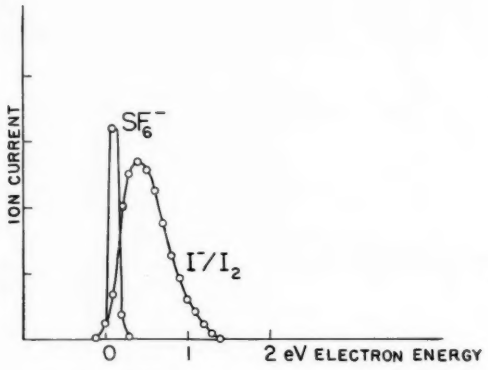

FIG. 14. The resonance capture peak for the formation of I^- from iodine by electron impact.

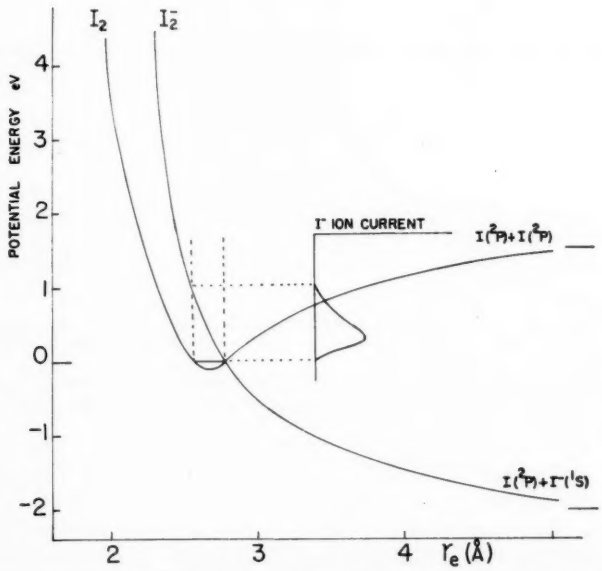

FIG. 15. Potential energy diagram to illustrate the formation of I^- from iodine by a resonance capture process.

(iii) Iodine

We find the I^- resonance capture process onset energy to be 0.03 ± 0.03 ev, the upper energy limit to be 1.08 ± 0.04 ev, and the energy for maximum capture cross section to be 0.34 ± 0.07 ev. A typical I^- capture peak, with the one for SF_6^-, is shown in Fig. 14.

The process responsible for I^- formation here will be

$$I_2+e \rightarrow I^-+I+K+E \qquad [14]$$

and is illustrated in Fig. 15 where the relevant potential curves are sketched. We have described the formation of I^- from I_2 by resonance capture in more detail elsewhere (10).

Figure 16 shows the ion efficiency curve for I^+ from I_2 at electron energies between 8 and 17 ev. There are clearly four different processes possible for I^+ formation that have been resolved, and these are found to occur at 8.62 ± 0.06, 12.02 ± 0.04, 12.72 ± 0.04, and

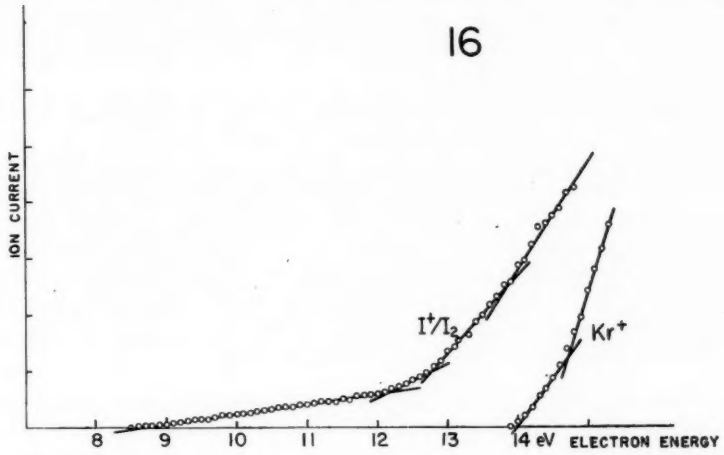

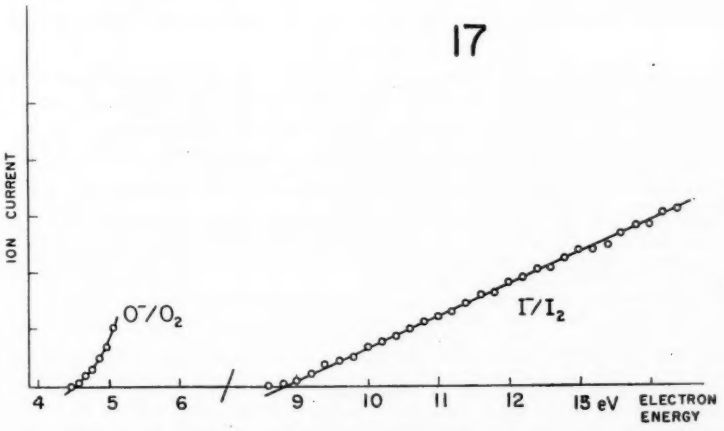

FIG. 16. The ionization efficiency curve for the formation of I^+ from iodine by electron impact.
FIG. 17. The ionization efficiency curve for the formation of I^- from iodine by ion pair processes as the result of electron impact.

13.71±0.06 ev. A typical ion efficiency curve for I^- is shown in Fig. 17, and there is evidence for only one process—found to occur at 8.68±0.07 ev.

The first appearance potentials for I^+ and I^- are very close together and we assume that the ion pair process

[15] $$I_2+e \rightarrow I^+(^3P_2)+I^-(^1S)+K+E+e$$

is responsible for their formation. Assuming no kinetic energy to be involved the minimum appearance potential for the pair would be 8.84 ev, since $EA(I) = 3.14$ ev (22), $I(I) = 10.44$ ev (21), and $D(I_2) = 1.542$ ev (20).

The excited I_2 upper state involved here must be stable because if it were not then the I^+ and I^- appearance potentials would be expected to considerably exceed the minimum energy required for their formation.

The second I^+ appearance potential occurs at 12.02 ev, and the upper state involved is almost certainly the $I_2^+(^2\Pi_u)$—of r_e greater than r_e of $I_2(^1\Sigma_g^+)$ and shown above to have components at 10.91 and 11.72 ev above the $I_2(^1\Sigma_g^+)$. This $^2\Pi_u$ state should dissociate to normal $I^+(^3P_2)+I(^2P_{3/2})$ at 11.98 ev.

I^+ ions are next formed at 12.72 ev, probably through transitions to a repulsive I_2^+ state associated with the dissociation limit just mentioned at 11.98 ev.

At 13.71 ev a further process giving rise to I^+ ions occurs, and it is probable that the $I_2^+(^2\Sigma_g^+)$ state is concerned here. We have deduced this state to lie 13.64 ev above the I_2 ground state, and it is likely to have an internuclear distance r_e much greater than r_e of the $I_2(^1\Sigma_g^+)$ since it arises through the removal of a strongly bonding σ electron. The I_2^+ ion in the $^2\Sigma_g^+$ state will therefore have a much lower dissociation energy than $I_2(^1\Sigma_g^+)$, and could dissociate to $I^+(^1D_2)+I(^2P_{3/2})$ at 13.68 ev. In this case, vertical transitions to $I_2^+(^2\Sigma_g^+)$ would be expected to produce not only I_2^+ but also I^+ ions, and this process is suggested to account for the I^+ observed to occur at 13.71 ev.

This work was supported in part by the Geophysical Research Directorate of the United States Air Force Cambridge Research Centre, Air Research and Development Command, under Contract No. AF19-(604)-2275, and by grants from the National Research Council of Canada.

REFERENCES

1. R. E. Fox, W. M. Hickam, T. Kjeldaas, Jr., and D. J. Grove. Phys. Rev. **84**, 859 (1951).
2. D. C. Frost and C. A. McDowell. Proc. Roy. Soc. A, **232**, 227 (1955).
3. D. C. Frost and C. A. McDowell. Proc. Roy. Soc. A, **236**, 278 (1956).
4. D. C. Frost and C. A. McDowell. J. Am. Chem. Soc. **80**, 6183 (1958).
5. D. C. Frost and C. A. McDowell. J. Chem. Phys. **29**, 503 (1958).
6. D. C. Frost and C. A. McDowell. Can. J. Chem. **36**, 39 (1958).
7. R. F. Becker and S. Goudsmit. Atomic energy states. McGraw-Hill Book Co., Inc., New York.
8. L. M. Branscomb. J. Chem. Phys. **29**, 452 (1958).
9. W. M. Hickam and R. E. Fox. J. Chem. Phys. **25**, 642 (1956).
10. D. C. Frost and C. A. McDowell. J. Chem. Phys. **29**, 964 (1958).
11. R. S. Mulliken. Phys. Rev. **46**, 549 (1934).
12. K. Watanabe. J. Chem. Phys. **26**, 542 (1957).
13. J. D. Morrison and A. J. Nicholson. J. Chem. Phys. **20**, 1021 (1952).
14. R. Thorburn. Proc. Phys. Soc. **123**, 122 (1959).
15. Y. Ota and Y. Uchida. Japan. J. Phys. **5**, 53 (1928).
16. A. Elliott and W. H. B. Cameron. Proc. Roy. Soc. A, **158**, 681 (1937).
17. A. Elliott and W. H. B. Cameron. Proc. Roy. Soc. A, **164**, 531 (1938).
18. H. G. Howell. Proc. Phys. Soc. A, **66**, 759 (1953).
19. H. O. Pritchard and H. A. Skinner. Chem. Revs. **55**, 745 (1955).
20. G. Herzberg. Spectra of diatomic molecules. D. Van Nostrand Co., Inc., New York. 1950.
21. G. Herzberg. Atomic spectra and atomic structure. Dover Publications, New York. 1944.
22. P. P. Sutton and J. E. Meyer. J. Chem. Phys. **3**, 20 (1935).

ABSOLUTE THERMAL NEUTRON FISSION YIELDS OF U^{233} [1]

D. C. SANTRY[2] AND L. YAFFE

ABSTRACT

The absolute fission yields of 22 nuclides formed in the thermal neutron fission of U^{233} have been measured radiochemically. Disintegration rates were measured by 4π β-proportional counting techniques. The identity of each nuclide was established by chemical separations and decay characteristics as determined by 4π β-counting and γ-ray scintillation spectrometry. The reaction $Co^{59}(n,\gamma)Co^{60}$ was used as a neutron flux monitor. Yields were calculated on the basis of $\sigma_f^{U^{233}}/\sigma_c^{Co^{59}} = 524/36.3$.

INTRODUCTION

Although the thermal neutron fission yields for U^{235} have been investigated extensively, yields reported for the fission products of U^{233} are few and inconsistent. Relative radiochemical yields for U^{233} fission have been measured by Grummitt and Wilkinson (1), and Steinberg *et al.* (2, 3). The yields given by the latter groups were determined relative to their absolute yield value of 6.0% for Ba^{140} which had been measured by direct fission counting (2). The uncertainty in the application of correction factors to observed counting rates of fission products in order to obtain disintegration rates accounted for most of the large errors (10% to 20%) associated with radiochemical yields.

In applying the mass-spectrometric method to isotope abundance measurements of U^{233} fission products, Steinberg *et al.* (4), Fleming *et al.* (5), and Melaika *et al.* (6) were able to measure relative yields believed reliable to 3% to 5%. These relative yields were often normalized with the aid of radiochemical yields (7, 8). Such mass-spectrometric data were then no more accurate on an absolute basis than the yields to which they were normalized.

Isotope dilution techniques have more recently been used in mass spectrometry by Anikina *et al.* (9), Kukavadze *et al.* (10), and Ivanov *et al.* (11) to measure the absolute yields of some stable and long-lived fission products in U^{233} fission. These investigators determined the number of fission events which occurred by measuring the depletion of U^{233} in a heavily irradiated sample. The errors associated with these measurements range from 2% to 15%.

Thus all fission yields for the thermal neutron fission of U^{233} previously measured possess rather large experimental errors. Such errors obscure the presence or absence of fine structure in the fission product, mass distribution curve.

The purpose of this work was to establish, radiochemically, accurate yields for various nuclides along the yield–mass curve. It was felt that by using 4π β-counting techniques, and by determining absolute rather than relative yields, the errors associated with radiochemical yields could be greatly reduced.

The $Co^{59}(n,\gamma)Co^{60}$ reaction was used to measure the neutron flux. Absolute yields could then be expressed in terms of the known values for the thermal neutron capture and fission cross sections for Co^{59} and U^{233} respectively.

It can be shown that, if U_0 atoms of U^{233} were irradiated in a thermal flux I of a nuclear

[1]*Manuscript received in original form April 27, 1959, and, as revised, December 9, 1959.*
Contribution from the Radiochemistry Laboratory, Department of Chemistry, McGill University, Montreal, Que., with financial assistance from the National Research Council of Canada, Atomic Energy Control Board, and the Defence Research Board.

[2]*Holder of a National Research Council Studentship, 1956–57. Present address: Chemistry Branch, Atomic Energy of Canada Limited, Chalk River, Ontario.*

reactor for a time T, then at some time t, after removal from the reactor, the following equation would apply:

$$[1] \qquad N\lambda = U_0 I\sigma_t Y_t(1-e^{-\lambda T})e^{-\lambda t}.$$

In the above equation λ is the disintegration constant of the fission product being studied and N is the number of atoms of that nuclide present at time t. Thus $N\lambda$ is the disintegration rate. The fission cross section of U^{233} is represented by σ_t, and Y_t is the probability of formation, or the fission yield of the nuclide under study.

If some cobalt were irradiated simultaneously with and under the same conditions as the U^{233}, then the following equation would obtain:

$$[2] \qquad N_1\lambda_1 = N_{Co} I\sigma_c(1-e^{-\lambda_1 T})e^{-\lambda_1 t}.$$

As before, $N_1\lambda_1$ would be the disintegration rate of Co^{60}, N_{Co} the number of cobalt atoms placed in the reactor, and σ_c the thermal neutron cross section for the reaction $Co^{59}(n,\gamma)Co^{60}$.

If equations [1] and [2] are now divided, the term I cancels, all other quantities are easily measurable, and Y_t, the fission yield, can be determined in terms of σ_t/σ_c.

EXPERIMENTAL AND RESULTS

(a) Irradiation

Accurately weighed amounts (2.30 to 6.18 mg) of uranium oxide (U_3O_8) were sealed into thin quartz tubes. Isotopic analysis of the uranium used indicated 97.746% U^{233},* the remainder being U^{238}. A spectrographic analysis showed that the level of impurities was too low to form any of the fission products by (n,γ) reactions. Into similar tubes were sealed weighed amounts (1.00 to 1.50 mg) of "spec-pure" cobalt wire (0.005-in. diameter). The tubes containing the fissile uranium and the cobalt wire were irradiated together in a "self-serve" position of the NRX reactor at Chalk River for a period of 24 hours. The position chosen was one where the neutron spectrum was predominantly thermal.

(b) Disintegration Rate Determinations

All disintegration rates were determined with good precision, using the 4π β-counters described by Pate and Yaffe (12–16). Sources were deposited on calibrated gold-plated VYNS films (10–19 $\mu g/cm^2$). Pretreatment of the films with a 5% insulin solution ensured an even deposition of the source over a known area. Sources were dried under infrared radiation.

Corrections for loss of the radiation in the exceedingly thin source-mount were obtained from the data of Pate and Yaffe (14) and were very small. Self-absorption losses were determined by combining the results of Pate and Yaffe (15) with those of Fishman and Yaffe (17) into a plot of self-absorption as a function of β-end-point energy and source thickness. The sources were all of high specific activity, so that the correction factors were usually small and accurately known.

(c) Treatment of Flux Monitor

The irradiated cobalt wire was removed from its quartz capsule, dissolved in nitric acid, and made up to a known volume. The fraction of Co^{60} activity lost by recoil into the quartz vial was measured on a γ-ray scintillation counter and found to be 0.31%.

Aliquots of the master solution were removed for disintegration rate determination.

*We wish to acknowledge with thanks the fact that this material was obtained on loan from A.E.C.L., Chalk River, Ontario.

The source superficial density was always less than 10 $\mu g/cm^2$. The self-absorption correction was 0.6% while that for source-mount absorption was 0.1%.

The neutron attenuation in the sample was calculated, using the formula

$$I = I_0 e^{-N\sigma\rho d/A}$$

where I and I_0 are the final and initial fluxes, N is Avogadro's number, σ is the total cross section of the sample for neutrons, ρ is the density of the sample, A the atomic weight, and d the thickness.

The attenuation factor was found to be 0.979* for a wire of 0.0064-cm radius.

The cobalt thermal neutron capture cross section and the half-life used were 36.3 barns (18, 19) and 5.24 years (20) respectively.

The epi-thermal contribution in the irradiation position used was determined by shielding the cobalt wire during one irradiation with $\frac{1}{2}$-mm cadmium. The epi-cadmium contribution was determined to be 1.76%.

(d) Treatment of U^{233}

The fissile sample was dissolved by crushing the irradiated vial under a warm nitric acid solution. To reduce the loss of activities by adsorption effects, 1 mg each of appropriate inactive ions (Cs^+, Ba^{++}, La^{+++}, and I^-) had been added to the nitric acid solution as "carriers". The dissolved uranium and fission products were transferred to a volumetric flask. The finely crushed remains of the vial were washed several times with small portions of nitric acid to recover fission products imbedded in the quartz. Measured aliquots of the fission product stock solution were removed and added to known amounts (10 to 20 mg) of inactive carriers of the elements to be separated. Standard methods (21, 22, 23) were used for the separation of fission product elements. In many cases slight modifications to reported procedures were used to ensure radiochemical purity. After decontamination, the element of interest was precipitated in a suitable chemical form, dissolved, and made up to a known volume. Aliquots of the solution were removed periodically for activity measurements and later for the determination of chemical recovery, using standard analytical techniques.

After the chemical separation, the radiochemical purity and identity of each nuclide was confirmed by the presence or absence of γ-radiation. A sodium iodide crystal spectrometer was used to measure gamma energies and half-lives.

The very high stability of the 4π β-counting equipment enabled the accurate measurement of both half-lives and disintegration rates.

The amount of Ba^{140} and Sr^{89} formed in cadmium-covered and -uncovered samples, irradiated under otherwise identical conditions, was measured. The epi-cadmium contribution was found to be 2.10%.

The neutron attenuation in the uranium oxide was calculated for all samples. The values ranged from 0.975 for the heaviest sample to 0.997 for the lightest.

Data given for the various nuclides include the half-life and other factors involving time. This was done so that corrections could be made later by others should more accurate nuclear constants be obtained.

(e) Individual Elements

(1) Bromine

The method of Glendenin *et al.* (24) was used to separate bromine. The activity of the

**This is in excellent agreement with that determined experimentally by Dr. R. E. Jervis, A.E.C.L., Chalk River, and we are grateful to him for making available to us the results of his determination.*

sample was measured for 100 hours and showed a pure 34.5-hour half-life corresponding to Br^{82}. Since the extraction was carried out 40 hours after the end of the irradiation, one would not expect to find any 2.3-hour Br^{83}.

Br^{82} is a shielded nuclide produced only by direct formation, so that measurement of its fission yield constitutes an independent yield determination. The relevant data are given in Table I.

TABLE I

Fission yield data for 36-hour Br^{82}

Time in reactor	24 hours
Time after irradiation	40.6 hours
Activity at saturation	1.694×10^{5} disintegrations/sec
Fission rate	2.270×10^{10} fissions/sec
Fission yield	$(7.46\pm0.17)\times10^{-4}\%$

(2) Strontium

A slight modification to the method of Glendenin (25) was used for this separation. Strontium and barium carriers were added and precipitated with fuming nitric acid. Further purifications were effected by scavenging with ferric hydroxide. Barium was removed by a chromate precipitation in a buffered solution. Strontium was precipitated as the oxalate, dissolved in nitric acid, and reprecipitated with fuming nitric. The nitrate precipitate was washed with ethanol before being dissolved in water and made up to volume.

Isotopes of strontium likely to be detected in this work are Sr^{89}, Sr^{90}, and Sr^{91}.

Each strontium separation showed the presence of a 50.0- to 50.5-day activity corresponding to Sr^{89} and a long-lived component. One separation performed shortly after the end of the irradiation exhibited the 9.7-hour Sr^{91} activity in addition to these. No γ-photopeaks were observed on the scintillation spectrometer except when the 9.7-hour activity was present. A plot of γ-counting rate vs. time showed that the 750- and 1020-kev peaks decayed with a 9.7-hour half-life. The initial growth and decay of the 550-kev peak indicated the formation of the 51-minute Y^{91m} daughter of Sr^{91}. The apparent purity of the sample was indicated by the absence of other γ-rays and the consistent half-lives obtained from the β- and γ-ray measurements allowed the assignment of the long-lived component to Sr^{90} (27.7 years).

When in equilibrium, the disintegration rates of Sr^{90} and Y^{90} are equal. Therefore one-half of the observed residual counting rate, after applying absorption corrections, could be attributed to the Sr^{90}. On this basis, the fission yield of Sr^{90} was calculated. As a further check on this yield, a separated strontium sample was allowed to decay and the yttrium which formed was separated and counted. The fission yield of Sr^{90}, calculated in this way from the Y^{90} daughter, agreed well with that in which the Sr^{90} was counted directly.

The counting rate of 50-day Sr^{89} was determined in the usual way by subtracting the amount of long-lived activity observed.

It is not possible to obtain the amount of Sr^{91} activity by direct analysis of the gross decay curve owing to the formation of Y^{91}. However, from the following considerations, it is possible to determine the amount of Sr^{89} and Sr^{91} present. At the end of the strontium separation there is no yttrium, therefore the total observed activity (N_T^0) is

$$N_T^0 = Sr^{89^0}+Sr^{91^0}+Sr^{90}.$$

At a time later when the Sr^{91} has completely decayed to form Y^{91}, the total observed counting rate (N_T^1) is

$$N_T^1 = Sr^{89^0}\exp(-\lambda_1 T)+\frac{\lambda_3}{\lambda_2-\lambda_3}Sr^{91^0}\exp(-\lambda_3 t)+(Sr^{90}+Y^{90^1})$$

where λ_1, λ_2, and λ_3 are the decay constants for Sr^{89}, Sr^{91}, and Y^{91} respectively, and t is the time from the end of separation until the time when N_T^1 is measured. Since N_T^0, N_T^1, $(Sr^{90}+Y^{90^1})$ can be measured, it is possible to solve for Sr^{89^0} and Sr^{91^0}. Since the decay of Sr^{91} involves delayed γ-emission, i.e. γ-emission from the Y^{91m} state, it is necessary to know the efficiency of the counting unit for the detection of Y^{91m} disintegrations. The important factors involved are: (*i*) the γ-detection efficiency, (*ii*) the amount of internal conversion, and (*iii*) the efficiency for detection of internal conversion electrons. By means of growth and decay equations and starting with pure Sr^{91}, the relative counting rates for Sr^{91}, Y^{91}, and Y^{91m} were calculated for various decay times. The calculated rates were then compared to the observed relative counting rates at the same decay times. The observed relative counting rates were obtained by dividing the observed counting rate at time t by the counting rate obtained by extrapolating the initial portion of the strontium decay curve to the time at which the separation had ended. This extrapolation procedure is justified if counting had begun soon after the separation, before Y^{91m} reached equilibrium with Sr^{91}. The observed relative counting rate agreed very well with that calculated for Sr^{91} plus Y^{91}, indicating that the efficiency for counting Y^{91m} in the 4π-proportional counter is very low.

The relevant data for the fission yields of the strontium isotopes are given in Tables II, III, and IV.

TABLE II

Fission yield data for 50.4-day Sr^{89}

Irradiation No.	A 1	A 2	B 1	C 1	D_a 1	D_a 2	D_b 1	D_b 2	E	F
Time in reactor (hours)	24	24	24	24	18.5	18.5	18.5	18.5	23.83	24.17
Time after irradiation (days)	17.35	29.10	9.90	3.75	15.44	95.44	73.25	115.41	27.0	1.5
Activity at saturation (d/s)	6.279×10^8	6.010×10^8	1.199×10^9	1.637×10^9	7.936×10^8	7.904×10^8	4.079×10^8	4.091×10^8	1.295×10^7	1.406×10^9
Fission rate (f/s)			2.270×10^{10}	2.885×10^{10}	1.464×10^{10}	1.464×10^{10}	7.225×10^9	7.225×10^9	Fast fission	2.587×10^{10}
Fission yield (%)	*	*	5.28 ± 0.14	5.67 ± 0.07	5.42 ± 0.18	5.40 ± 0.08	5.65 ± 0.06	5.66 ± 0.06	—	5.43 ± 0.08

*All fission yields calculated for irradiation A were determined relative to Sr^{89} since no cobalt monitor was bombarded. The value for the fission yield of Sr^{89}, which will be discussed later, was taken as 5.56% for that irradiation.

TABLE III

Fission yield data for 27.7-year Sr^{90}

Irradiation No.	A 1	D_a 2*	D_b 2*
Time in reactor (hours)	24	18.5	18.5
Time after irradiation (days)	17.35	106	115.41
Activity at saturation (d/s)	6.867×10^8	9.025×10^8	4.481×10^8
Fission rate (f/s)	(Relative yield)	1.464×10^{10}	7.225×10^9
Fission yield (%)	6.16 ± 0.12	6.16 ± 0.07	6.20 ± 0.09

*Determined by counting 64.3-hour Y^{90}.

TABLE IV

Fission yield data for 9.7-hour Sr^{91}

Irradiation No.	F 1
Time in reactor	24.16 hours
Time after irradiation	36.0 hours
Activity at saturation	1.246×10^{9} d/s
Fission rate	2.587×10^{10} f/s
Fission yield	$(4.82\pm0.25)\%$

(3) Yttrium

The yttrium was separated by the method given by Ballou (26). Sufficient time was allowed to elapse after the strontium was separated, so that the 65-hour Y^{90} had decayed. The yttrium fraction was followed for a period of 400 days and decayed cleanly with a half-life of 59 days, corresponding to Y^{91}. The data are presented in Table V.

TABLE V

Fission yield data for 59-day Y^{91}

Irradiation No.	B 1	C 1
Time in reactor	24 hours	24 hours
Time after irradiation	158 days	137.64 days
Activity at saturation	7.897×10^{8} d/s	1.039×10^{9} d/s
Fission rate	2.269×10^{10} f/s	2.885×10^{10} f/s
Fission yield	$(3.48\pm0.18)\%$	$(3.60\pm0.11)\%$

(4) Zirconium

The separation used was essentially a combination of procedures given by Hume (27) and Moore (23). The zirconium was extracted with 2-thenoyl-trifluoroacetone (TTA) and back-extracted from the organic phase with a nitric – hydrofluoric acid mixture. The zirconium was precipitated as barium zirconyl fluoride, dissolved in a boric acid – nitric acid mixture and passed through a Dowex-1 anion exchanger to remove borate and fluoride ions. The zirconium was precipitated with ammonia, dissolved in nitric acid, and made to volume.

The measurements in the 4π β-proportional counter indicated an initial growth and subsequent decay with a 65-day half-life. A 740-kev γ-photopeak, observed on the scintillation spectrometer, was a combination of the 722- and 754-kev γ-rays emitted by Zr^{95}. This peak also showed an initial increase and tailed off with a half-life of 65 days. The growth of this peak was due to the formation of the 770-kev γ-emitter Nb^{95} which is a daughter of Zr^{95}.

The counting rate for Zr^{95} was obtained by measuring sources immediately after the separation and by making a short extrapolation back to the end of separation where no niobium activity was present. A correct counting rate for Zr^{95} in the presence of niobium activities was not obtained due to incomplete knowledge of the decay schemes involved and the detection efficiency of radiations emitted. The fission yield data for Zr^{95} are given in Table VI.

TABLE VI

Fission yield data for 65-day Zr^{95}

Irradiation No.	A 1	B 1
Time in reactor	24 hours	24 hours
Time after irradiation	13.1 days	28.63 days
Activity at saturation	5.365×10^{8} d/s	1.309×10^{8} d/s
Fission rate	Relative yield	2.270×10^{10} f/s
Fission yield	$(4.82\pm0.50)\%$	$(5.77\pm1.44)\%$

(5) Niobium

The separation of niobium from other fission products was based on the specific precipitation of Nb_2O_5 from an oxalate solution with chloric acid (28).

Sources of the niobium activity were counted in the 4π-proportional counter. All sources which had been separated at least 33 days after the end of the irradiation were followed for at least 200 days and decayed with a half-life of 35 days. A sample of the niobium when analyzed on the scintillation spectrometer indicated the presence of a nuclide emitting a 770-kev γ-ray with a half-life of about 35 days. No 90-hour Nb^{95m} could be detected, indicating that the amount of this isomer formed from the decay of Zr^{95} must indeed be small as is indicated by the decay scheme.

The β-end-point energy for Nb^{95} is 0.160 Mev. The calculation of a disintegration rate for this nuclide involves rather large self-absorption corrections ($\sim$25%). To keep the niobium in solution, it was necessary to add an excess of oxalic acid which increased the superficial density of the source. The total source thickness was determined by weighing an aliquot of the sample which had been evaporated on a known area.

The data for the fission yield of Nb^{95} are given in Table VII.

TABLE VII

Fission yield data for 35-day Nb^{95}

Irradiation No.	F 1	F 2
Time in reactor	24.17 hours	24.17 hours
Time after irradiation	87.1 days	114.25 days
Activity at saturation	1.281×10^{9} d/s	1.561×10^{9} d/s
Fission rate	2.587×10^{10} f/s	2.587×10^{10} f/s
Fission yield	(4.94 ± 0.29)%	(6.03 ± 0.99)%

(6) Ruthenium

Carriers of ruthenium (Ru^{+3}), iodide, and bromide were added to an aliquot of the fission product stock solution. After an oxidation with sodium bismuthate and perchloric acid, ruthenium was separated from the other fission products by distilling the volatile RuO_4 into a sodium hydroxide solution (29). Ruthenium oxide was precipitated several times in the presence of sodium hydroxide by reduction with ethanol. The final oxide separated was dissolved in 6 *M* hydrochloric acid, and made up to volume.

The decay of ruthenium was measured in the 4π-proportional counter. A drop of dilute lithium hydroxide was added to the active sources on VYNS films to aid in drying. A 40-day activity and a longer-lived component ($\sim$1 year) were observed. A γ-spectrum was obtained showing the presence of a 500-kev γ-ray which decayed with a half-life of 40 days. The 40-day activity could then be conclusively attributed to Ru^{103}.

The residual activity with a half-life of about 1 year was assigned to Ru^{106}, a known fission product with a half-life of 1.02 years (30) and a β-end-point energy of 39.2 kev (31).

The measurement of a disintegration rate for both Ru^{103} and Ru^{106} is difficult due to the low energy of the radiation and the presence of short-lived daughter activities.

For Ru^{103} it was necessary to consider the effects of the delayed γ-emitter Rh^{103m}. The total internal conversion coefficient (α_T) for the 40.2-kev γ-ray is about 484 (32). From this value can be calculated N_{e^-}, the number of conversion electrons emitted.

$$N_{e^-} = \alpha_T/(1+\alpha_T) = 0.998.$$

Therefore, 99.8% of Rh^{103m} disintegrations involve conversion electron emission. The

energies of these electrons are low enough so that only 5% are not absorbed in the source and source-mount and are detected by the counter.

The observed 1-year activity represents an equilibrium counting rate for Ru^{106} and Rh^{106}. Absorption losses are to be expected for the Ru^{106} radiation but not for Rh^{106} since the latter has maximum β-energies of 3.5 (82%) and 2.3 (18%) Mev (33).

Fission yield data are presented for Ru^{103} and Ru^{106} in Tables VIII and IX respectively.

TABLE VIII

Fission yield data for 40-day Ru^{103}

Irradiation No.	B 1
Time in reactor	24 hours
Time after irradiation	22.53 days
Activity at saturation	4.581×10^{8} d/s
Fission rate	2.269×10^{10} f/s
Fission yield	(2.02 ± 0.08)%

TABLE IX

Fission yield data for 1.02-year Ru^{106}

Irradiation No.	B 1
Time in reactor	24 hours
Time after irradiation	22.53 days
Activity at saturation	5.881×10^{7} d/s
Fission rate	2.269×10^{10} f/s
Fission yield	(0.259 ± 0.03)%

(7) Rhodium

The separation of rhodium was based on its extraction into pyridine from a strongly alkaline solution (34).

Sources, when counted in the 4π-proportional counter, were observed to give a 36-hour decay curve, and the presence of a 320-kev photopeak in the γ-spectrum for this activity helped establish its identity as Rh^{105}.

The fission yield data for Rh^{105} are given in Table X.

TABLE X

Fission yield data for 36.5-hour Rh^{105}

Irradiation No.	F 1
Time in reactor	24.16 hours
Time after irradiation	144.6 hours
Activity at saturation	3.770×10^{7} d/s
Fission rate	2.587×10^{10} f/s
Fission yield	(0.146 ± 0.037)%

(8) Silver

Silver was separated from other fission products by precipitating silver chloride. Additional decontamination was achieved, as suggested by Glendenin (35), by alternative ferric hydroxide scavengings and silver sulphide precipitations from an ammoniacal solution.

The silver decay curves were obtained with the 4π β-proportional counter. The length of time from the end of the irradiation to the silver separation was such that any Ag^{112}

present had been formed from the decay of the parent Pd^{112}. Because of this, the Ag^{112} data have been presented in Table XIII with the fission yield data for Pd^{112}. The fission yield calculated for Ag^{111} is given in Table XI.

TABLE XI

Fission yield data for 7.6-day Ag^{111}

Irradiation No.	B 1	D 1
Time in reactor	24 hours	18.5 hours
Time after irradiation	1.91 days	2.5 days
Activity at saturation	4.28×10^{6} d/s	2.701×10^{6} d/s
Fission rate	2.270×10^{10} f/s	1.464×10^{10} f/s
Fission yield	$(0.0188\pm0.0003)\%$	$(0.0185\pm0.0007)\%$

(9) Palladium

The separation of palladium from other fission products was accomplished by the precipitation of palladium dimethylglyoxime from an acid solution. Scavenging with ferric hydroxide and silver iodide was performed for additional purification. Palladium was finally precipitated with dimethylglyoxime, dissolved in hot concentrated nitric acid and made up to volume.

The decay curves for palladium were measured on the 4π-proportional counter. They were found to contain a 65-day (probably Zr^{95}) and a 9-day impurity. A 21-hour activity was resolved by analyzing the initial portion of the gross decay curve. This activity was taken as Pd^{112} (36) and a fission yield was calculated (Table XII). The peaks observed on the scintillation spectrometer were not sufficiently resolved to permit an identification of nuclides present. If the 65-day activity represented Zr^{95}, then 17-hour Zr^{97} might also be present and add to the counting rate of Pd^{112}. As a further check on the Pd^{112} yield, the daughter activity Ag^{112} was counted and from its measurements the yield for Pd^{112} was indirectly determined (Table XIII). The values obtained for the yield of Pd^{112} by both methods agreed favorably.

TABLE XII

Fission yield data for 21-hour Pd^{112}

Irradiation No.	B 1	F 1
Time in reactor	24 hours	24 hours
Time after irradiation	69.5 hours	76.2 hours
Activity at saturation	2.776×10^{6} d/s	3.180×10^{6} d/s
Fission rate	2.270×10^{10} f/s	2.587×10^{10} f/s
Fission yield	$(0.0122\pm0.0001)\%$	$(0.0123\pm0.0001)\%$

TABLE XIII

Fission yield data for 21-hour Pd^{112}*

Irradiation No.	B 1	D 1
Time in reactor	24 hours	18.5 hours
Time after irradiation	44.8 hours	58.7 hours
Activity at saturation	2.938×10^{6} d/s	1.729×10^{6} d/s
Fission rate	2.270×10^{10} f/s	1.464×10^{10} f/s
Fission yield	$(0.0129\pm0.0001)\%$	$(0.0118\pm0.0005)\%$

*Determined from the daughter 3.2-hour Ag^{112}.

(10) Antimony

The method of Boldridge and Hume (37) was used to separate antimony from other fission products. The decay of antimony activities, as measured by the 4π-proportional counter, yielded half-lives of 3.79 days and 75 days. An intense 245-kev γ-photopeak was observed on the scintillation spectrometer which also decayed with a 3.6-day half-life. Two less-defined γ-peaks were observed at 740 and 480 kev. These peaks appeared to be associated with the 75-day activity. The shorter-lived activity was assigned to Sb^{127}. Half-lives reported recently for this nuclide are 88 hours (38) and 93 hours (39). The value used in this work was the observed 91 hours. The γ-peaks at 480 and 740 kev appeared to correspond to the reported 463- and 772-kev energies of Sb^{127} but decayed with a 75-day half-life. No observed 75-day antimony activity has been reported in fission. The only antimony nuclide positively identified in this work is that of mass number 127 and the data for this are given in Table XIV. A fission yield was calculated for the observed longer-lived antimony activity, using a half-life of 75 days, and the data are shown in Table XV.

TABLE XIV

Fission yield data for 91-hour Sb^{127}

Irradiation No.	B 1	D 1
Time in reactor	24 hours	18.5 hours
Time after irradiation	14.82 days	3.23 days
Activity at saturation	1.524×10^{8} d/s	7.511×10^{7} d/s
Fission rate	2.270×10^{10} f/s	1.464×10^{10} f/s
Fission yield	$(0.67\pm0.13)\%$	$(0.51\pm0.12)\%$

TABLE XV

Fission yield data for "75-day Sb"

Irradiation No.	B 1
Time in reactor	24 hours
Time after irradiation	14.82 days
Activity at saturation	1.121×10^{8} d/s
Fission rate	2.270×10^{10} f/s
Fission yield	$(0.53\pm0.14)\%$

(11) Tellurium

A direct separation of radiochemically pure tellurium was obtained by using a method reported by Glendenin (40).

The decay of tellurium was measured in the 4π-proportional counter. The curve could be resolved into activities with half-lives of 3.2 days, 37 days, and 105 days corresponding to Te^{132}, Te^{129m}, and Te^{127m} respectively. A freshly separated tellurium sample analyzed on the scintillation spectrometer at first showed only a 220-kev γ-photopeak corresponding to Te^{132}. Then the 670- and 780-kev γ-peaks of the I^{132} daughter grew in and later decayed. In equilibrium, all three peaks decayed with a half-life of 3.2 days.

The data involved in the calculation of a fission yield for Te^{132} are given in Table XVI. An additional yield measurement for Te^{132} was obtained by separating and measuring 2.3-hour I^{132}. Data for the latter measurements are listed in Table XVII.

(12) Iodine

A rapid solvent extraction method for the separation of iodine has been reported by Glendenin and Metcalf (41) and has been used in this work. To the final iodine, separated

TABLE XVI

Fission yield data for 77-hour Te^{132}

Irradiation No.	A 1	C 1
Time in reactor	24 hours	24 hours
Time after irradiation	28.65 days	16.84 days
Activity at saturation	5.227×10^{8} d/s	1.215×10^{8} d/s
Fission rate	Relative yield	2.885×10^{9} f/s
Fission yield	$(4.70\pm0.94)\%$	$(4.21\pm0.63)\%$

TABLE XVII

Fission yield data for 77-hour Te^{132}*

Irradiation No.	A 3	B 1	C 1	F 1
Time in reactor (hours)	24	24	24	24.16
Time after irradiation (hours)	15.76	87.01	301.9	433.4
Activity at saturation (d/s)	5.266×10^{8}	9.56×10^{8}	1.320×10^{9}	1.073×10^{8}
Fission rate (f/s)	Relative yield	2.270×10^{10}	2.885×10^{10}	2.587×10^{10}
Fission yield (%)	4.71 ± 0.14	4.21 ± 0.13	4.57 ± 0.16	4.15 ± 0.05

*Determined from the daughter 2.3-hour I^{132}.

in the form of iodide, was added a small amount of lithium hydroxide and the solution was diluted to volume.

The method used for source preparation was that suggested by Bartholomew *et al.* (42), in which the iodide solution was added to a drop of very dilute silver nitrate already present on the prepared VYNS film. The purpose of the silver is to prevent the oxidation and subsequent volatilization of iodine. Prior to each measurement, each iodine source was heated for 15 minutes under an infrared lamp. This technique was used to remove xenon decay products formed from iodine. The half-lives observed by 4π-counting were 2.3-hour I^{132}, 20.9-hour I^{133}, and 8.0-day I^{131}. All γ-photopeaks observed on the scintillation spectrometer decayed with similar half-lives. Peaks at 670, 780, 980, and 1400 kev decayed with a half-life of 2.2 hours. The 520-kev peak decayed with a half-life of 20.3 hours and the 360- and 640-kev peaks with a half-life of 8.4 days. No attempt was made to remove xenon decay products from the sources used on the scintillation spectrometer.

Iodine separations were performed at a time after the irradiation when any independently formed I^{132} had completely decayed. The observed I^{132} activity resulted from the decay of Te^{132} and consequently its disintegration rate was used to calculate the yield of Te^{132} (Table XVII). The fission yields of I^{131} and I^{132} are given in Tables XVIII and XIX.

TABLE XVIII

Fission yield data for 8.05-day I^{131}

Irradiation No.	A 3	B 1	C 1
Time in reactor	24 hours	24 hours	24 hours
Time after irradiation	15.81 days	88 hours	12.6 days
Activity at saturation	3.420×10^{8} d/s	6.866×10^{8} d/s	8.833×10^{8} d/s
Fission rate	Relative yield	2.270×10^{10} f/s	2.885×10^{10} f/s
Fission yield	$(3.06\pm0.10)\%$	$(3.02\pm0.09)\%$	$(3.06\pm0.09)\%$

(13) Cesium

The procedure used for the isolation of cesium activity from other fission products was that given by Glendenin and Nelson (43).

TABLE XIX

Fission yield data for 20.9-hour I^{133}

Irradiation No.	B 1	D 1
Time in reactor	24 hours	18.5 hours
Time after irradiation	87.01 hours	62.6 hours
Activity at saturation	8.31×10^{8} d/s	4.504×10^{8} d/s
Fission rate	2.270×10^{10} f/s	1.464×10^{10} f/s
Fission yield	$(3.66\pm0.10)\%$	$(3.08\pm0.10)\%$

An activity of 13 days was found attributable to Cs^{136}. This is a shielded nuclide and is therefore produced directly in fission as a primary fragment. After 80 days of counting, the cesium activity remained constant at a value well above the background counting rate for the counter due to the presence of long-lived Cs^{137}. The data for the independent fission yield of Cs^{136} are given in Table XX. By assuming that the residual cesium activity was due to Cs^{137}, calculations were made for the fission yield of this nuclide.

In the decay, 95% of the transitions go to the 2.6-minute Ba^{137m} state. Corrections for the contribution to the 4π β-counting rate were made, using the following data:

$$\alpha_K = 0.097$$

$$K/L = 4.9.$$

Therefore

$$\alpha_L = .02.$$

Assume

$$\alpha_M+\alpha_N+\ldots = 0.004.$$

Therefore

$$\alpha_T = .121.$$

The efficiency of the 661-kev γ-ray in our counter has been found to be 0.45%.

The total number of conversion electrons

$$N_e = \alpha_T/(1+\alpha_T) \text{ (total } \gamma\text{-transitions)}.$$

The number of unconverted γ's

$$N = 1/(1+\alpha_T) \text{ (total } \gamma\text{-transitions)}.$$

Therefore counts registered equal

$$\frac{\alpha_T}{1+\alpha_T}(0.95)n+0.0045\frac{1}{1+\alpha_T}(0.95)n+n$$

where n = true disintegration rate. Therefore counts registered = $1.106\,n$. The counting rate registered was divided by this number.

The half-life of Cs^{137} has recently been reported as 30.0 years (44) and 26.6 years (45). The fission yield for Cs^{137} is given in Table XXI using both half-lives.

(14) Barium

After the separation of barium from the strontium by a chromate precipitation, as described previously, the barium was dissolved and reprecipitated twice by means of a

TABLE XX

Fission yield data for 12.9-day Cs^{136}

Irradiation No.	D 1
Time in reactor	18.5 hours
Time after irradiation	31.3 days
Activity at saturation	1.244×10^{7} d/s
Fission rate	1.464×10^{10} f/s
Fission yield	$(0.0849\pm0.0022)\%$

TABLE XXI

Fission yield data for Cs^{137}

Irradiation No.	D 1	
Reported half-life	30.0 years	26.6 years
Time in reactor	18.5 hours	18.5 hours
Time after irradiation	31.3 days	31.3 days
Activity at saturation	7.887×10^{8} d/s	7.100×10^{8} d/s
Fission rate	1.464×10^{10} f/s	1.464×10^{10} f/s
Fission yield	$(5.39\pm0.11)\%$	$(4.85\pm0.10)\%$

cold hydrochloric acid – ether mixture. The final barium chloride precipitate was dissolved in water and made to volume.

Barium sources were mounted and counted as soon after the end of a separation as possible. The counting rate, as measured by the 4π-proportional counter, increased with time reaching a maximum value at about 4 days, and then decreased with a half-life of 12.8 days. For the first few hours after a barium separation the growth of La^{140} is linear with respect to time. Therefore a plot of the total counting rate vs. time can be accurately extrapolated back to the time at which barium was separated. By using growth and decay equations, it is also possible to calculate the amount of Ba present initially from a measured Ba plus La counting rate at a known time after the separation. The calculated values agreed with those obtained by back-extrapolating the initial portions of the growth and decay curves.

Barium sources counted were about 30 $\mu g/cm^2$ thick. A decrease in the thickness by a factor of 100 showed no change in the source specific activity. This observation, together with the agreement between calculated and observed growth and decay curves, indicated that absorption effects, as described by Grummitt *et al.* (46), were not significant in this work.

Each barium separation was analyzed on the scintillation spectrometer. No extraneous γ-peaks were observed. A plot of peak heights against time produced a curve similar to the net growth and decay as obtained in the 4π β-counter. The fission yield data for Ba^{140} are given in Table XXII.

TABLE XXII

Fission yield data for 12.8-day Ba^{140}

Irradiation No.	A 1	A 2	B 1	B 2	C 1	C 2	D_a 1	D_a 2	E 2	F 1
Time in reactor (hours)	24	24	24	24	24	24	18.5	18.5	23.8	24.16
Time after irradiation (days)	17.0	23.83	4.69	10.69	3.56	56.71	16.01	67.06	5.0	13.08
Activity at saturation (d/s)	5.300×10^{8}	5.913×10^{8}	1.214×10^{9}	1.121×10^{9}	1.548×10^{9}	1.567×10^{9}	7.247×10^{8}	7.552×10^{8}	1.217×10^{7}	1.318×10^{9}
Fission rate (f/s)	Relative yield		2.269×10^{10}	2.269×10^{10}	2.885×10^{10}	2.885×10^{10}	1.464×10^{10}	1.464×10^{10}	Fast fission	2.587×10^{10}
Fission yield (%)	4.76 ± 0.66	5.31 ± 0.13	5.35 ± 0.23	4.94 ± 0.16	5.37 ± 0.16	5.43 ± 0.22	4.95 ± 0.05	5.16 ± 0.11		5.09 ± 0.05

(15) Cerium

Two procedures were used for the separation of cerium activity. The first was similar to that used for the separation of yttrium (26). After Ce, Y, and the rare earths were isolated from other fission products, cerium was oxidized and precipitated twice as the iodate. The precipitate was dissolved in a nitric acid – hydrogen peroxide mixture and further purified by zirconium iodate scavenging. Precipitations of ceric hydroxide, cerous hydroxide, and cerous oxalate produced radiochemically pure cerium. The final precipitate was washed with water, dissolved in a minimum of nitric acid, and made up to a known volume.

The second method used for the separation of cerium was described by Glendenin *et al.* (22). Cerium carrier and sodium bromate were added to an aliquot of the fission product stock solution. Cerium was extracted into methylisobutyl ketone. The organic layer was separated and washed with dilute nitric acid containing sodium bromate. Cerium was back-extracted into water containing a little 30% hydrogen peroxide. An oxalate precipitation was used to recover cerium from the aqueous layer. The cerium was then dissolved in dilute nitric acid, diluted, and reprecipitated with oxalic acid. The final oxalate precipitate was dissolved and made up to volume.

Cerium activities detected in this work were 33-day Ce^{141}, 33-hour Ce^{143}, and 285-day Ce^{144}. A 290-kev photopeak, attributed to Ce^{145}, was observed on the scintillation spectrometer to decay with a 33-hour half-life.

The data, for which the fission yields for Ce^{141}, Ce^{143}, and Ce^{144} were calculated, are given in Tables XXIII, XXIV, and XXV respectively.

TABLE XXIII

Fission yield data for 33-day Ce^{141}

Irradiation No.	A 1	B 2	C 1	C 2
Time in reactor (hours)	24	24	24	24
Time after irradiation (days)	61.0	35.51	5.0	124.1
Activity at saturation (d/s)	2.966×10^{8}	1.236×10^{9}	1.553×10^{9}	1.555×10^{9}
Fission rate (f/s)	Relative yield	2.270×10^{10}	2.885×10^{10}	2.885×10^{10}
Fission yield (%)	5.22±0.04	5.44±0.16	5.38±0.23	5.39±0.48

TABLE XXIV

Fission yield data for 33-hour Ce^{143}

Irradiation No.	C 1
Time in reactor	24 hours
Time after irradiation	5.0 days
Activity at saturation	2.018×10^{8} d/s
Fission rate	2.885×10^{10} f/s
Fission yield	(6.99±0.35)%

TABLE XXV

Fission yield data for 285-day Ce^{144}

Irradiation No.	B 2	C 1
Time in reactor	24 hours	24 hours
Time after irradiation	35.51 days	5.0 days
Activity at saturation	8.724×10^{9} d/s	9.999×10^{8} d/s
Fission rate	2.269×10^{10} f/s	2.885×10^{10} f/s
Fission yield	(3.84±0.11)%	(3.47±0.15)%

The errors in these experiments are as follows:

(*a*) Systematic errors. These, such as weighing, dilutions, pipetting, were less than 0.5% due to the use of a sensitive microbalance, calibrated glassware, etc. The major error lies in the chemical yield determinations. In order to minimize source self-absorption corrections, minimal amounts of carriers were used. This made chemical yield determinations difficult, and this is reflected in the limits placed on the determinations.

(*b*) The fast fission correction was small ($\sim$2%) and the error in correcting for this is $\pm$0.2%.

(*c*) Loss of activity by fission recoil $\pm$0.2%.

(*d*) Source-mount absorption $\pm$0.2%.

(*e*) Self-absorption in the sample, 0.1 $\rightarrow$ 2%, depending on the energy of the β-emitter and sample thickness.

(*f*) Saturation activity calculations. The pile power was constant during all but one irradiation. In this latter irradiation, the saturation factor was obtained by use of an analogue computer.*

(*g*) External errors. Errors in reported decay schemes and decay constants may greatly influence the results. Each fission yield is given in terms of the half-life as observed and the decay schemes as discussed.

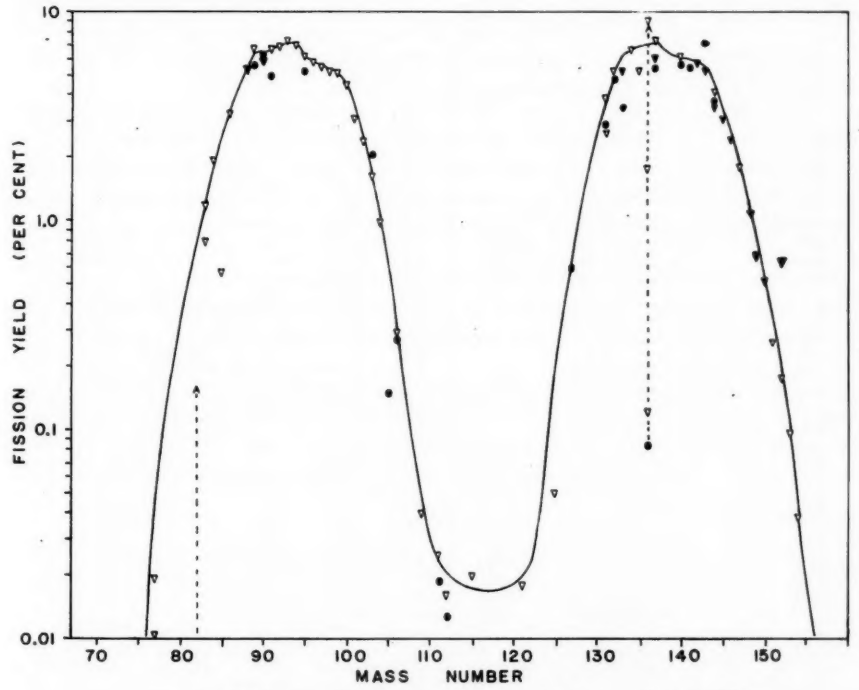

FIG. 1. Yield–mass distribution in the thermal neutron fission of U^{233}.
▽ Relative yields } previously reported.
▼ Absolute yields }
● Absolute yields, this work.
Broken line represents the correction for chain yield.

We are grateful to Dr. J. G. Bayly, Reactor Physics Branch, A.E.C.L., for performing these calculations.

All yields were calculated relative to σ_t/σ_{Co} and can be renormalized should the necessity arise.

When several determinations were made for one nuclide, an average fission yield was calculated by weighing each individual value according to the reciprocal of its own experimental error. The error quoted finally is the root-mean-square deviation.

DISCUSSION

The absolute yields obtained are presented in Table XXVI. Included in this table are values measured by other investigators. Those listed in column 3 do not necessarily represent total chain yields, but merely refer to the cumulative yield for the nuclide given. No attempt was made to correct any of the values for delayed neutron emission, and no corrections were required for loss or gain due to neutron capture among the

TABLE XXVI

Thermal neutron fission yields for U^{233}

			This work					This work	
	Nuclide	Literature values (%)	Absolute yield of nuclide (%)	Estimated isobaric yield (%)		Nuclide	Literature values (%)	Absolute yield of nuclide (%)	Estimated isobaric yield (%)
12-*h*	Ge^{77}	0.010			Mass	115	0.020		
39-*h*	As^{77}	0.019			27.5-*h*	Sn^{121}	0.018		
36-*h*	Br^{82}		0.000746±0.000017	0.158	9.6-*d*	Sn^{126}	0.05		
2.4-*h*	Br^{83}	0.79			91-*h*	Sb^{127}		0.59±0.08	0.59
Stable	Kr^{83}	1.14			8.05-*d*	I^{131}	2.7	2.84±0.20	2.84
Stable	Kr^{84}	1.90			Stable	Xe^{131}	3.74		
10.3-*y*	Kr^{85}	0.56			77-*h*	Te^{132}		4.32±0.25	4.64
Stable	Kr^{86}	3.18			Stable	Xe^{132}	5.10		
Stable	Sr^{88}	5.3*			20.9-*h*	I^{133}		3.37±0.29	3.40
50.4-*d*	Sr^{89}	6.5	5.56±0.15	5.56	Stable	Cs^{133}	5.20†		
27.7-*y*	Sr^{90}	5.8*	6.19±0.03	6.19	Stable	Xe^{134}	6.54		
9.7-*h*	Sr^{91}		4.82±0.25	4.82	6.7-*h*	I^{135}	5.1		
59-*d*	Y^{91}		3.55±0.06	3.55	3×10^6-*y*	Cs^{135}	4.9		
Stable	Zr^{91}	6.53			12.9-*d*	Cs^{136}	0.12	0.0849±0.0022	8.5
Stable	Zr^{92}	6.70			86-*s*	I^{136}	1.7		
10^6-*y*	Zr^{93}	7.10			Stable	Xe^{136}	8.9		
Stable	Zr^{94}	6.82			30-*y*	Cs^{137}	7.16	5.39±0.11	5.39
65-*d*	Zr^{95}	5.9	5.01±0.56	5.01			5.80†		
35-*d*	Nb^{95}		5.16±0.64	5.16	12.8-*d*	Ba^{140}	6.0	5.21±0.27	5.48
Stable	Mo^{95}	6.1			Stable	Ce^{140}	5.45†		
Stable	Zr^{96}	5.6			33-*d*	Ce^{141}		5.30±0.10	5.30
Stable	Mo^{97}	5.35			Stable	Ce^{142}	5.50†		
Stable	Mo^{98}	5.18			33-*h*	Ce^{143}		6.99±0.35	6.99
67-*h*	Mo^{99}	4.8			Stable	Nd^{143}	5.00†		
Stable	Mo^{100}	4.40			285-*d*	Ce^{144}	4.1	3.69±0.18	3.69
Stable	Ru^{101}	3.00			Stable	Nd^{144}	3.80†		
Stable	Ru^{102}	2.37			Stable	Nd^{145}	2.82†		
40-*d*	Ru^{103}	1.6	2.02±0.08	2.02	Stable	Nd^{146}	2.20†		
Stable	Ru^{104}	0.96			Stable	Sm^{147}	1.71		
36.5-*h*	Rh^{105}		0.146×0.037	0.146	Stable	Nd^{148}	1.03†		
1.02-*y*	Ru^{106}	0.28	0.259±0.030	0.264	Stable	Sm^{149}	0.66†		
13.4-*h*	Pd^{109}	0.040			Stable	Nd^{150}	0.51†		
7.6-*d*	Ag^{111}	0.025	0.0187±0.0002	0.0187	80-*y*	Sm^{151}	0.26		
21-*h*	Pd^{112}	0.016	0.0125±0.0004	0.0128	Stable	Sm^{152}	0.60†		
43-*d*	Cd^{115m}	0.001			47-*h*	Sm^{153}	0.095		
53-*h*	Cd^{115}	0.019			Stable	Sm^{154}	0.037		

*Most recent values by Anikina *et al.* (48) published after this work was complete.

†Most recent values by Ivanov *et al.* (49) published after this work was complete.

All other values are as listed by Katcoff (7).

The relative yields of Bartholomew *et al.* (50) were published after this paper had been compiled. A renormalization of their yields to our value of 5.21% for Ba^{140} gives Sr^{89} = 5.46, Sr^{91} = 5.22, Ba^{139} = 5.20, and La^{141} = 5.74%.

fission products themselves. The same fast fission factor has been applied to all values determined. This correction will certainly apply to values on or near the peaks of the yield–mass curve. The effect on the mass distribution of increasing the neutron energy above the thermal region is to increase the probability of symmetric fission. For this reason the yields of nuclides in the trough of the curve (Ag^{111} and Pd^{112}) are to be considered maximum values. However, the position of the sample inside the reactor was such that the epi-cadmium neutrons detected could not have possessed high energy. Recent investigations on the fission of U^{235} with energies as high as 9.5 ev show no significant change in the trough yields from that produced by thermal neutrons (47), so that little change in the trough yields is to be expected.

In the last column are estimated mass yields for the chains studied. These were calculated by determining the most probable nuclear charge of a particular mass number from the curves given by Katcoff (51). A chain correction factor is then obtained for a value of the displacement from the most probable charge. The cumulative yield can then be estimated from the product of the actual measured fission yield and its cumulative fractional chain yield.

The agreement between yields measured in this work and other absolute yields determined mass spectrometrically is good. However, yields which were determined earlier either radiochemically or normalized to radiochemical values are generally higher.

There appears to be a discrepancy between the observed yields of 4.82% for Sr^{91} and 3.55% for Y^{91}. A decrease in cumulative yield along a chain is not to be expected. Such a difference might well be due to an incomplete knowledge of the mass 91 chain. Other investigators have also reported irregularities in this chain (52, 53). The low yield of I^{133} obtained appeared real since I^{131} and Te^{132} yields, calculated on the same samples, gave normal results. The high yield at mass 143 was based on one measurement and has not been confirmed. The absolute yield measured mass spectrometrically does not agree with this value. However, the mass 141 yield, determined on the same sample, seems to give a reasonable result.

Absolute yields for Sr^{90} on the light mass peak and Ce^{140} on the heavy mass peak, which were reported by Anikina and Ershler (9) and Kukavadze *et al.* (10), respectively, were not dependent on cross-section values. The agreement with this work indicated that the value of σ_t/σ_c used appears correct.

The yield values in Table XXVI are plotted in Fig. 1. The curve drawn is that suggested by Katcoff (7) for the thermal neutron fission of U^{233} and is such that the sum of the yields is the required 200%. The measured independent yields of Br^{82} and Cs^{136} have been corrected to chain yields as indicated by the broken arrows.

REFERENCES

1. W. E. Grummitt and G. Wilkinson. Nature, **161**, 520 (1948).
2. E. P. Steinberg, J. A. Seiler, A. Goldstein, and L. Dudley. U.S. Atomic Energy Rept. MDDC-1632 1948.
3. L. E. Glendenin and E. P. Steinberg. Intern. Conf. on the Peaceful Uses of Atomic Energy, **7**, 3 (1956).
4. E. P. Steinberg, L. E. Glendenin, M. G. Inghram, and R. J. Hayden. Phys. Rev. **95**, 867 (1954).
5. W. F. Fleming, R. H. Tomlinson, and H. G. Thode. Can. J. Phys. **32**, 522 (1954).
6. E. A. Melaika, M. J. Parker, J. A. Petruska, and R. H. Tomlinson. Can. J. Chem. **33**, 830 (1955).
7. S. Katcoff. Nucleonics, **16**, 78 (1958).
8. S. Peterson. U.S. Atomic Energy Comm. ORNL Rept. 55-6-144. 1955.
9. M. P. Anikina and B. V. Ershler. J. Nuclear Energy, **6**, 169 (1957).
10. G. M. Kukavadze, M. P. Anikina, L. L. Goldin, and B. V. Ershler. Conf. Acad. Sci. S.S.S.R. on Peaceful Uses of Atomic Energy, 125 (1955).
11. R. N. Ivanov, V. K. Gorshkov, M. P. Anikina, G. M. Kukavadze, and B. V. Ershler. Atomnaya Energ. **3**, 546 (1957).

12. B. D. PATE and L. YAFFE. Can. J. Chem. **33**, 15 (1955).
13. B. D. PATE and L. YAFFE. Can. J. Chem. **33**, 610 (1955).
14. B. D. PATE and L. YAFFE. Can. J. Chem. **33**, 929 (1955).
15. B. D. PATE and L. YAFFE. Can. J. Chem. **33**, 1656 (1955).
16. B. D. PATE and L. YAFFE. Can. J. Chem. **34**, 265 (1956).
17. J. B. FISHMAN and L. YAFFE. Unpublished data.
18. R. S. CARTER, H. PALEVSKY, V. W. MYERS, and D. J. HUGHES. Phys. Rev. **92**, 716 (1953).
19. L. YAFFE, R. C. HAWKINGS, W. F. MERRITT, and J. H. CRAVEN. Phys. Rev. **82**, 553 (1951).
20. K. W. GEIGER. Phys. Rev. **105**, 1539 (1957).
21. C. D. CORYELL and N. SUGARMAN. (*Editors*). Radiochemical studies: The fission products. National nuclear energy series. Div. IV. McGraw-Hill Book Co., Inc., New York. 1951. Paper 9.
22. L. E. GLENDENIN, K. F. FLYNN, R. F. BUCHANAN, and E. P. STEINBERG. Anal. Chem. **27**, 59 (1955).
23. F. L. MOORE. Anal. Chem. **28**, 997 (1956).
24. L. E. GLENDENIN, R. R. EDWARDS, and H. GEST. *In* Radiochemical studies: The fission products. *Edited by* C. D. Coryell and N. Sugarman. National nuclear energy series. Div. IV. McGraw-Hill Book Co., Inc., New York. 1951. Paper 232.
25. L. E. GLENDENIN. *In* Radiochemical studies: The fission products. *Edited by* C. D. Coryell and N. Sugarman. National nuclear energy series. Div. IV. McGraw-Hill Book Co., Inc., New York. 1951. Paper 236.
26. N. E. BALLOU. *In* Radiochemical studies: The fission products. *Edited by* C. D. Coryell and N. Sugarman. National nuclear energy series. Div. IV. McGraw-Hill Book Co., Inc., New York. 1951. Paper 292.
27. D. N. HUME. *In* Radiochemical studies: The fission products. *Edited by* C. D. Coryell and N. Sugarman. National nuclear energy series. Div. IV. McGraw-Hill Book Co., Inc., New York. 1951. Paper 245.
28. L. E. GLENDENIN. *In* Radiochemical studies: The fission products. *Edited by* C. D. Coryell and N. Sugarman. National nuclear energy series. Div. IV. McGraw-Hill Book Co., Inc., New York. 1951. Paper 253.
29. L. E. GLENDENIN. *In* Radiochemical studies: The fission products. *Edited by* C. D. Coryell and N. Sugarman. National nuclear energy series. Div. IV. McGraw-Hill Book Co., Inc., New York. 1951. Paper 260.
30. W. F. MERRITT, P. J. CAMPION, and R. C. HAWKINGS. Can. J. Phys. **35**, 16 (1957).
31. H. M. AGNEW. Phys. Rev. **77**, 655 (1950).
32. P. AVIGNON, A. MICHALOWICZ, and R. BOUCHEZ. J. phys. radium, **16**, 404 (1955).
33. W. C. PEACOCK. Phys. Rev. **72**, 1049 (1947).
34. N. E. BALLOU. *In* Radiochemical studies: The fission products. *Edited by* C. D. Coryell and N. Sugarman. National nuclear energy series. Div. IV. McGraw-Hill Book Co., Inc., New York. 1951. Paper 263.
35. L. E. GLENDENIN. *In* Radiochemical studies: The fission products. *Edited by* C. D. Coryell and N. Sugarman. National nuclear energy series. Div. IV. McGraw-Hill Book Co., Inc., New York. 1951. Paper 267.
36. J. A. SEILER. *In* Radiochemical studies: The fission products. *Edited by* C. D. Coryell and N. Sugarman. National nuclear energy series. Div. IV. McGraw-Hill Book Co., Inc., New York. 1951. Paper 119.
37. W. F. BOLDRIDGE and D. N. HUME. *In* Radiochemical studies: The fission products. *Edited by* C. D. Coryell and N. Sugarman. National nuclear energy series. Div. IV. McGraw-Hill Book Co., Inc., New York. 1951. Paper 272.
38. H. BOSCH and H. MUNCZEK. Phys. Rev. **106**, 983 (1957).
39. M. C. DAY and A. F. VOIGT. Phys. Rev. **101**, 1784 (1956).
40. L. E. GLENDENIN. *In* Radiochemical studies: The fission products. *Edited by* C. D. Coryell and N. Sugarman. National nuclear energy series. Div. IV. McGraw-Hill Book Co., Inc., New York. 1951. Paper 274.
41. L. E. GLENDENIN and R. P. METCALF. *In* Radiochemical studies: The fission products. *Edited by* C. D. Coryell and N. Sugarman. National nuclear energy series. Div. IV. McGraw-Hill Book Co., Inc., New York. 1951. Paper 278.
42. R. M. BARTHOLOMEW, F. BROWN, R. C. HAWKINGS, and L. YAFFE. Can. J. Chem. **31**, 120 (1953).
43. L. E. GLENDENIN and C. M. NELSON. *In* Radiochemical studies: The fission products. *Edited by* C. D. Coryell and N. Sugarman. National nuclear energy series. Div. IV. McGraw-Hill Book Co., Inc., New York. 1951. Paper 283.
44. F. BROWN, G. R. HALL, and A. J. WALTERS. J. Inorg. & Nuclear Chem. **1**, 241 (1955).
45. D. M. WILES and R. H. TOMLINSON. Phys. Rev. **99**, 188 (1955).
46. W. E. GRUMMITT, J. GUERON, G. WILKINSON, and L. YAFFE. Can. J. Research, B, **25**, 357 (1947).
47. R. NASUHOGLU, S. RABOY, G. R. RINGO, L. E. GLENDENIN, and E. P. STEINBERG. Phys. Rev. **108**, 1522 (1957).
48. M. P. ANIKINA, R. N. IVANOV, G. M. KUKAVADZE, and B. V. ERSHLER. J. Nuclear Energy, **9**, 167 (1959).
49. R. N. IVANOV, V. K. GORSHKOV, M. P. ANIKINA, G. M. KUKAVADZE, and B. V. ERSHLER. J. Nuclear Energy, **9**, 46 (1959).
50. R. M. BARTHOLOMEW, J. S. MARTIN, and A. P. BAERG. Can. J. Chem. **37**, 660 (1959).
51. S. KATCOFF. Low-energy induced fission. Handbook of nuclear engineering. Addison-Wesley Pub. Co., Inc., Cambridge, Mass. 1956.
52. W. E. GRUMMITT and G. M. MILTON. J. Inorg. & Nuclear Chem. **5**, 93 (1957).
53. A. P. BAERG and R. M. BARTHOLOMEW. Can. J. Chem. **35**, 980 (1957).

PERFLUOROALKYL ARSENICALS

PART I. THE PREPARATION OF ALKYL PERFLUOROALKYL ARSENICALS[1]

W. R. CULLEN

ABSTRACT

The reaction of tetramethyldiarsine with trifluoroiodomethane gives dimethyltrifluoromethylarsine. Trifluoroiodomethane and iodomethane similarly react with the compounds $(CF_3)_2M—M(CF_3)_2$ to give the compounds $(CF_3)_2M$ and $(CF_3)_2MCH_3$ respectively (M = As or P). Trifluoroiodomethane reacts with iododimethylarsine and diiodomethylarsine in the presence of mercury to give dimethyltrifluoromethylarsine and methylbistrifluoromethylarsine respectively. Heptafluoropropyldimethylarsine can be isolated from a similar reaction using heptafluoroiodopropane.

INTRODUCTION

Trifluoromethyl derivatives of phosphorus and arsenic are prepared by the action of trifluoroiodomethane on the elements, a mixture of products being obtained (1, 2).

$$M + CF_3I \rightarrow (CF_3)_3M + (CF_3)_2MI + CF_3MI_2 + MI_3 \qquad (M = As \text{ or } P)$$

Alkyl-trifluoromethyl-arsines and -phosphines can be obtained from Grignard reactions using trifluoromethyl-iodo-arsines (3, 4) and from exchange reactions using the compounds $(CF_3)_3M$ and $(CH_3)_3M$ (4, 5, 6).

$$(CF_3)_3M + CH_3I \rightarrow (CH_3)_2MCH_3 + CF_3I$$

$$2(CH_3)_3M + CF_3I \rightarrow (CH_3)_2MCF_3 + (CH_3)_4MI$$

In this paper new methods of preparing alkyl-perfluoroalkyl-arsines and -phosphines are described.

DISCUSSION AND RESULTS

Organometallic compounds containing metal—metal bonds are known to be highly reactive. Tetramethyldiarsine spontaneously inflames in air and the As—As bond is readily split by halogens (7) or alkyl halides (8). The tin—tin bond is similarly reactive (9) and hexamethylditin has been recently found to react at 80° with trifluoroiodomethane to give trimethyltrifluoromethyltin (10).

$$(CH_3)_3Sn—Sn(CH_3)_3 + CF_3I \rightarrow (CH_3)_3SnCF_3 + (CH_3)_3SnI$$

It has now been found that tetramethyldiarsine reacts at room temperature with trifluoroiodomethane to give dimethyltrifluoromethylarsine.

$$(CH_3)_2As—As(CH_3)_2 + CF_3I \rightarrow (CH_3)_2AsCF_3 + (CH_3)_2AsI$$

When excess trifluoroiodomethane is used the reaction appears to be complete. Trifluoroiodomethane reacts less readily with tetrakistrifluoromethyldiarsine to give tristrifluoromethylarsine and iodobistrifluoromethylarsine.

$$(CF_3)_2As—As(CF_3)_2 + CF_3I \rightarrow (CF_3)_3As + (CF_3)_2AsI$$

At 75° with excess trifluoroiodomethane the reaction is 60% complete after 14 hours and could probably be brought to completion if the conditions were adjusted appropriately. Tetrakistrifluoromethyldiarsine reacts also with iodomethane to give methylbistrifluoromethylarsine and iodobistrifluoromethylarsine.

$$(CF_3)_2As—As(CF_3)_2 + CH_3I \rightarrow (CF_3)_2AsCH_3 + (CF_3)_2AsI$$

[1]*Manuscript received October 5, 1959.*
Contribution from the Chemistry Department, University of British Columbia, Vancouver, B.C.

The reaction in this case seems to be slower, as at 75° with excess diarsine very little reaction takes place and even after 14 hours at 105° the reaction is only 10% complete.

Tetrakistrifluoromethyldiphosphine reacts similarly with both trifluoroiodomethane and iodomethane. After 20 hours at 70° the reaction with excess trifluoroiodomethane is 60% complete. However the diphosphine, like the diarsine, reacts more slowly with iodomethane and after 20 hours at 70°, using excess diphosphine, only a trace of methylbistrifluoromethylphosphine is formed, and at 105° there is little reaction after 18 hours. At 150° the reaction goes further, resulting in the conversion of up to 76% of the iodomethane after 48 hours.

It has also been found that perfluoroalkyl iodides will react at room temperature with a mixture of alkyl-iodo-arsines and mercury to give perfluoroalkyl-alkyl-arsines. Thus dimethyltrifluoromethylarsine and heptafluoropropyldimethylarsine are obtained from iododimethylarsine, and methylbistrifluoromethylarsine is obtained from diiodomethylarsine.

$$(CH_3)_2AsI + Hg + IR \rightarrow (CH_3)_2AsR + HgI_2 \qquad (R = CF_3 \text{ or } C_3F_7)$$

$$CH_3AsI_2 + 2Hg + 2CF_3I \rightarrow CH_3As(CF_3)_2 + 2HgI_2$$

The reaction of iododimethylarsine with trifluoroiodomethane is much faster than the reaction of the arsine with heptafluoroiodopropane Similarly the reaction of trifluoroiodomethane with iododimethylarsine is much faster than with the diiodo-arsine. The reaction of trifluoroiodomethane with chlorodimethylarsine in the presence of mercury is very slow.

Further work is in progress in an attempt to elucidate the exact nature of these reactions in view of their great synthetic potential.

Heptafluoropropyldimethylarsine is the first compound to be isolated with the As—C_3F_7 link. The reaction of heptafluoroiodopropane with arsenic appears to produce heptafluoropropyl arsenicals but these cannot be separated from by-products (11). As would be expected this new arsenical is similar to dimethyltrifluoromethylarsine in being unattacked by water and in being difficult to hydrolyze with base (5, 6). It is only 26% hydrolyzed by 10% sodium hydroxide solution after 3 days at 100°. Methylbistrifluoromethylarsine is only 9% hydrolyzed by 20% aqueous sodium hydroxide after 3 days at room temperature, whereas tristrifluoromethylarsine is completely hydrolyzed in less than 24 hours under the same conditions (6).

EXPERIMENTAL

Apparatus and Technique

Conventional vacuum techniques were used for the manipulation of reactants and products out of contact with moisture and oxygen. Molecular weights were determined by Regnault's method. Reactions were carried out in sealed Pyrex tubes in the absence of air and light. The infrared spectra of the trifluoromethyl derivatives of phosphorus and arsenic were used extensively for the identification of pure compounds and the constituents of mixtures impossible to separate by trap-to-trap distillation. These spectra have been reported previously (1, 3, 4, 12) and the very strong C—F stretching bands in the region 1050–1250 cm^{-1} together with the C—F deformation bands at ca. 700 cm^{-1} enabled ready characterization. The spectra were measured in the gas phase on a Perkin–Elmer Model 21 double-beam instrument with rock-salt optics.

Reaction of Tetramethyldiarsine with Trifluoroiodomethane

Tetramethyldiarsine was prepared by the reaction of chlorodimethylarsine with zinc

dust at 100° (13). The diarsine (1.627 g) and trifluoroiodomethane (5.359 g) were mixed in a sealed tube (100 ml). A yellow solid was produced which was soluble in the trifluoroiodomethane giving a green solution. The tube was opened after 28 days at room temperature. All the products were volatile and trap-to-trap distillation gave unchanged trifluoroiodomethane (3.866 g) identified spectroscopically and by its molecular weight (mol. wt.: found 197, calc. 196), a fraction condensing at −98° (1.198 g, 88%) identified spectroscopically as dimethyltrifluoromethylarsine, and a fraction condensing at −64° (1.435 g). This fraction was a relatively involatile red liquid which did not react with excess iodomethane at room temperature indicating that no unreacted diarsine was present (8). With iodomethane at 105° for 1 hour in a sealed tube (5 ml) crystals of tetramethylarsonium triiodide were obtained (m.p.: found 133°, lit. value 133° (8)). This identified the fraction as iododimethylarsine (8) (80% yield).

Reaction of Tetrakistrifluoromethyldiarsine with Trifluoroiodomethane

Tetrakistrifluoromethyldiarsine was obtained from the reaction of iodobistrifluoromethylarsine with mercury (4). The diarsine (1.125 g) and trifluoroiodomethane (1.991 g) in a sealed tube (30 ml) were heated to 75° for 14 hours. All the products were volatile and trap-to-trap distillation gave unreacted trifluoroiodomethane (1.681 g; mol. wt.: found 197, calc. 196), a fraction condensing at −98° which was identified spectroscopically and by molecular weight determination as nearly pure tristrifluoromethylarsine (0.475 g; mol. wt.: found 284, calc. 282; 61% yield based on the diarsine), and a fraction condensing at −64° (0.950 g). This fraction was shown by spectroscopic examination to be a mixture of iodobistrifluoromethylarsine and tetrakistrifluoromethyldiarsine. After the fraction was shaken with mercury at room temperature for 24 hours in a sealed tube (20 ml) spectroscopic examination showed it then contained only tetrakistrifluoromethyldiarsine. The loss of weight was 0.212 g corresponding to the formation of iodobistrifluoromethylarsine in 63% yield (based on the diarsine).

Reaction of Tetrakistrifluoromethyldiarsine with Iodomethane

The diarsine (0.975 g) and iodomethane (0.280 g) in a sealed tube (20 ml) were heated to 75° for 24 hours after which spectroscopic examination of the contents of the tube showed that only a very small amount of methylbistrifluoromethylarsine had been produced. The reaction mixture was then heated in a sealed tube (20 ml) for 14 hours at 105°. Trap-to-trap distillation and spectroscopic examination of the fractions showed that only a little more methylbistrifluoromethylarsine had been produced. All the fractions were combined and shaken with excess mercury in a sealed tube (20 ml) for 24 hours at room temperature to convert the iodobistrifluoromethylarsine to tetrakistrifluoromethyldiarsine. The loss of weight was 0.026 g corresponding to reaction of 10% of the iodomethane.

Reaction of Tetrakistrifluoromethyldiphosphine with Trifluoroiodomethane

Tetrakistrifluoromethyldiphosphine was prepared by the reaction of iodobistrifluoromethylphosphine with mercury (1). The diphosphine (0.848 g) and trifluoroiodomethane (3.072 g) in a sealed tube (20 ml) were heated to 70° for 20 hours. All the products were volatile and trap-to-trap distillation gave unreacted trifluoroiodomethane (2.800 g; mol. wt.: found 195, calc. 196), a fraction condensing at −112° which was identified spectroscopically and by molecular weight determination as nearly pure tristrifluoromethylphosphine (0.363 g; mol. wt.: found 236, calc. 238; 61% yield based on the diphosphine), and a fraction condensing at −78° (0.761 g). This fraction was shaken with

excess mercury in a sealed tube (20 ml) at room temperature for 3 days, to convert the iodobistrifluoromethylphosphine to tetrakistrifluoromethyldiphosphine. The loss of weight was 0.217 g corresponding to the formation of the iodo-phosphine in 58% yield (based on the diphosphine).

Reaction of Tetrakistrifluoromethyldiphosphine with Iodomethane

The diphosphine (1.516 g) and iodomethane (0.452 g) in a sealed tube (30 ml) were heated to 70° for 20 hours after which spectroscopic examination of the contents of the tube showed that only a trace of methylbistrifluoromethylphosphine had been produced. The reaction mixture was next heated to 105° for 18 hours. Spectroscopic examination then showed that more methylbistrifluorophosphine had been formed; iodobistrifluoromethylphosphine was also present. The reaction mixture was shaken with mercury for 3 days in a sealed tube (30 ml) to convert the iodobistrifluoromethylphosphine to the diphosphine. The loss of weight was 0.084 g corresponding to reaction of not more than 2% of the iodomethane. The recovered reactants and products were finally heated to 150° for 48 hours. All the products were volatile and trap-to-trap distillation combined with spectroscopic examination of the fractions showed that a considerable quantity of methylbistrifluoromethylphosphine was present; tristrifluoromethylphosphine was also found but only a trace of unreacted iodomethane remained. The loss of weight on shaking the combined fractions with excess mercury for 3 days at room temperature was 0.308 g corresponding to an over-all reaction up to 76% of the iodomethane.

There is much uncertainty in estimating the extent of the reactions of the diphosphine, especially at higher temperatures, owing to the tendency of the iodo-phosphines to disproportionate (1).

$$2(CF_3)_2PI \leftrightarrow (CF_3)_3P + CF_3PI_2$$

Reactions of this kind would then increase the expected yield of tristrifluoromethylphosphine. The presence of tristrifluoromethylphosphine in the products of the reaction of the diphosphine with iodomethane indicates such disproportionation has taken place as it is unlikely that methylbistrifluoromethylphosphine would disproportionate within the temperature range used for the reactions (6). Similarly estimating the extent of the reactions by loss of weight of iodine can at best be only approximate as the reaction of iodobistrifluoromethylphosphine with mercury is not quantitative (1), and the reaction of diiodotrifluoromethylphosphine with mercury gives involatile polymers, $(CF_3P)_x$, as well as mercuric iodide (14) resulting in a greater loss of weight than would occur if only the mercuric iodide remained in the reaction tube.

Reaction of Iododimethylarsine with Trifluoroiodomethane in the Presence of Mercury

Iododimethylarsine was prepared by the reduction of a solution of cacodylic acid in hydrochloric acid with sulphur dioxide, in the presence of potassium iodide (15). The iodo-arsine (15 g), trifluoroiodomethane (37.99 g), and mercury (200 g) in a sealed tube (150 ml) were shaken for 3 days at room temperature. Trap-to-trap distillation of the volatile contents of the tube gave unreacted trifluoroiodomethane (28.35 g) and a fraction condensing at −98°. This fraction was distilled in a nitrogen atmosphere at 760 mm in a low temperature still to give dimethyltrifluoromethylarsine (4.52 g, 40%; b.p.: found 58°, lit. value 58° (5)).

Reaction of Diiodomethylarsine with Trifluoroiodomethane in the Presence of Mercury

Diiodomethylarsine was prepared by the reduction of a solution of methylarsonic acid

in hydrochloric acid with sulphur dioxide, in the presence of potassium iodide (16). The iodo-arsine (38.9 g), trifluoroiodomethane (81.7 g), and mercury (300 g) in a sealed tube (150 ml) were shaken for 1 week at room temperature. Trap-to-trap distillation of the volatile products gave methylbistrifluoromethylarsine (3.689 g, 14%) which was identified spectroscopically and by molecular weight determination (mol. wt.: found 224, calc. 228).

Reaction of Chlorodimethylarsine with Trifluoroiodomethane in the Presence of Mercury

Chlorodimethylarsine was prepared by the reduction of a solution of cacodylic acid in hydrochloric acid with hypophosphorous acid (17). The arsine (7.2 g), trifluoroiodomethane (23.32 g), and mercury (150 g) in a sealed tube (150 ml) were shaken for 3 days at room temperature. Spectroscopic examination of the various fractions isolated by trap-to-trap distillation showed that only a trace of dimethyltrifluoromethylarsine had been produced. The recovery of trifluoroiodomethane was almost quantitative (23.19 g).

Reaction of Iododimethylarsine with Heptafluoroiodopropane in the Presence of Mercury

The iodo-arsine (8.2 g), heptafluoroiodopropane (33.5 g), and mercury (250 g) in a sealed tube (150 ml) were shaken at room temperature for 5 days. Fractionation of the volatile products gave unreacted heptafluoroiodopropane (19.9 g) and a fraction condensing at −64°. This fraction was distilled in a nitrogen atmosphere to give a further 11.1 g of heptafluoroiodopropane (b.p. 42°) and heptafluoropropyldimethylarsine (b.p. 93°) (1.6 g, 16%). Anal. calc. for $C_5H_6AsF_7$: C, 21.9; H, 2.19; As, 27.4; F, 48.5%; mol. wt., 274. Found: C, 22.2; H, 2.42; As, 27.5; F, 47.2%; mol. wt., 271.

The infrared spectrum showed the following absorption bands: vapor phase: 3010(vw), 2930(w), 2830(vw), 1427(w), 1345(vs), 1232(vs), 1224(vs), 1180(vs), 1157(s), 1129(vs), 1114(vs), 1070(m), 1042(s), 905(m), 882(m), 855(s), 822(s), 737(vs), 670(s).

Hydrolysis of Heptafluoropropyldimethylarsine

The arsine (0.168 g) and water (10 ml) were immiscible in a sealed tube (40 ml). Fractionation of the contents of the tube after 11 days at room temperature showed that no heptafluoropropane had been produced. The arsine (0.246 g) and 10% sodium hydroxide solution (10 ml) in a sealed tube (40 ml) were heated to 100° for 3 days. Fractionation of the contents of the tube gave heptafluoropropane (0.040 g, 26%) which was identified spectroscopically.

ACKNOWLEDGMENTS

The author wishes to acknowledge financial assistance from the National Research Council of Canada. He is also indebted to Drs. H. C. Clark and C. J. Willis for helpful discussions. Microanalyses for C, H, As, and F were carried out by Dr. Alfred Bernhardt.

REFERENCES

1. F. W. Bennett, H. J. Emeléus, and R. N. Haszeldine. J. Chem. Soc. 1565 (1953).
2. G. R. A. Brandt, H. J. Emeléus, and R. N. Haszeldine. J. Chem. Soc. 2552 (1952).
3. H. J. Emeléus, R. N. Haszeldine, and R. C. Paul. J. Chem. Soc. 881 (1954).
4. H. J. Emeléus, R. N. Haszeldine, and E. G. Walachewski. J. Chem. Soc. 1552 (1953).
5. R. N. Haszeldine and B. O. West. J. Chem. Soc. 3631 (1956).
6. R. N. Haszeldine and B. O. West. J. Chem. Soc. 3880 (1957).
7. A. Cahours. Ann. **122**, 192 (1862). C. J. Mortimer and H. A. Skinner. J. Chem. Soc. 4331 (1952).
8. W. Steinkopf and G. Schwenn. Ber. **54**, 1437 (1921).
9. C. A. Kraus and W. V. Sessions. J. Am. Chem. Soc. **47**, 2361 (1925). G. Gruttner. Ber. **50**, 1808 (1917).
10. H. C. Clark and C. J. Willis. J. Am. Chem. Soc. In press.
11. H. J. Emeléus and J. D. Smith. J. Chem. Soc. 375 (1959).

12. B. O. WEST. Ph.D. Thesis, Cambridge. 1954.
13. R. W. BUNSEN. Ann. **42**, 14 (1842).
14. W. MAHLER and A. B. BURG. J. Am. Chem. Soc. **80**, 6161 (1958).
15. G. J. BURROWS and E. E. TURNER. J. Chem. Soc. 1373 (1920).
16. G. J. BURROWS and E. E. TURNER. J. Chem. Soc. 426 (1921).
17. W. STEINKOPF and W. MIEG. Ber. **53**, 1013 (1920).

PERFLUOROALKYL ARSENICALS

PART II. THE PREPARATION AND PROPERTIES OF ARYL PERFLUOROALKYL ARSENICALS[1]

W. R. CULLEN

ABSTRACT

The reaction of iododiphenylarsine with trifluoroiodomethane in the presence of mercury produces diphenyltrifluoromethylarsine. Phenylbistrifluoromethylarsine and methylphenyltrifluoromethylarsine are prepared from similar reactions using diiodophenylarsine and iodomethylphenylarsine respectively. The properties of these new trifluoromethyl arsenicals are compared with those of related compounds.

DISCUSSION AND RESULTS

Although alkyl-trifluoromethyl-arsines have been known for some time (1, 2) no method of preparing aryl-trifluoromethyl-arsines was available. The reaction of trifluoroiodomethane with methyl-iodo-arsines in the presence of mercury has been recently found to yield methyl-trifluoromethyl-arsines (3) and by extending this reaction it has now been found that aryl-trifluoromethyl-arsines can be similarly prepared from aryl-iodo-arsines. Thus diphenyltrifluoromethylarsine is prepared by the reaction of trifluoroiodomethane with iododimethylarsine in the presence of mercury, phenylbistrifluoromethylarsine is prepared from diiodophenylarsine, and methylphenyltrifluoromethylarsine from iodomethylphenylarsine.

$$(C_6H_5)RAsI + Hg + ICF_3 \rightarrow (C_6H_5)RAsCF_3 + HgI_2 \qquad R = C_6H_5 \text{ or } CH_3$$

$$C_6H_5AsI_2 + 2Hg + 2ICF_3 \rightarrow C_6H_5As(CF_3)_2 + 2HgI_2.$$

The aryl-trifluoromethyl-arsines are involatile, colorless liquids of faint odor; they are stable to oxygen and moisture at ordinary temperatures. Table I gives their boiling points and those of related compounds, and it is apparent that the usual increase in volatility found on replacing all the hydrogens of methyl groups by fluorine is shown by these new compounds.

TABLE I

Compound	B.p.	Compound	B.p.
$(C_6H_5)_3As$	>360°	$C_6H_5As(CH_3)_2$	193–200°
$(C_6H_5)_2AsCH_3$	100–101 (10^{-3} mm)	$C_6H_5As(CF_3)_2$	160
$(C_6H_5)_2AsCF_3$	86–88 (10^{-3} mm)	$C_6H_5(CH_3)AsCF_3$	186

Diphenyltrifluoromethylarsine is less stable thermally than triphenylarsine, being decomposed slowly at 250° and at a much faster rate at 300°. The main volatile decomposition products are fluoroform and benzene. Triphenylarsine is stable above 360° and tristrifluoromethylarsine is unstable at 350° (4).

Diphenyltrifluoromethylarsine is stable to concentrated hydrochloric acid at 85° and is only slowly hydrolyzed to fluoroform by 10% aqueous sodium hydroxide at the same temperature. It is, however, unstable to alcoholic potassium hydroxide at 85°. The rate of hydrolysis of the aryl-trifluoromethyl-arsines increases as the number of trifluoromethyl groups is increased. A similar trend is shown by the rates of hydrolysis of the compounds $(CF_3)_nM(CH_3)_{3-n}$ (M = P, As, or Sb) (2). Methylphenyltrifluoromethylarsine is

[1]*Manuscript received November 23, 1959.*
Contribution from the Chemistry Department, University of British Columbia, Vancouver, B.C.

hydrolyzed much faster than is diphenyltrifluoromethylarsine indicating that alkyl-trifluoromethyl-arsines would be hydrolyzed more easily than the aryl-trifluoromethyl-arsines. When liquid ammonia is the solvolytic agent both diphenyltrifluoromethyl- and methylphenyltrifluoromethyl-arsine are only slowly attacked. The ammonolysis of phenylbistrifluoromethylarsine is faster as would be expected since ammonolysis of trifluoromethyl compounds parallels hydrolysis (5).

Diphenyltrifluoromethylarsine reacts with bromine in carbon tetrachloride solution to give diphenyltrifluoromethylarsenic dibromide. This compound, m.p. 110° (decomp.), is unstable to moisture and is easily hydrolyzed by aqueous sodium hydroxide to fluoroform (cf. the stability of diphenyltrifluoromethylarsine). In this case the fluoroform could easily be produced by elimination from an initially formed hydroxybromide. At 120° it decomposes to bromotrifluoromethane and bromodiphenylarsine. Bromination of methylphenyltrifluoromethylarsine under similar conditions appears to produce the pentavalent dibromide but this is unstable and decomposes to give mainly bromomethane, together with bromotrifluoromethane.The involatile liquid produced by the reaction is probably mainly bromophenyltrifluoromethylarsine. Although phenylbistrifluoromethyl-arsine was decomposed by bromine no evidence was obtained for the intermediate formation of a pentavalent dibromide; at 20° no decolorization of the bromine solution took place on addition to a solution of the arsine and no solid was obtained from the reaction. Tristrifluoromethylarsine is also decomposed by bromine without the formation of a pentavalent compound (6). Tertiary arsine dihalides containing both aromatic and alkyl groups decompose on heating to an alkyl halide and a secondary halogenated arsine (7).

$$RR_2'AsX_2 \rightarrow R_2'AsX + RX \qquad R = \text{alkyl group}$$

$$R_2R'AsX_2 \rightarrow RR'AsX + RX \qquad R' = \text{aryl group}$$

Thus the ease of loss of groups from the pentavalent dibromides seems to be in the order $C_6H_5 < CF_3 < CH_3$.

The aryl-trifluoromethyl-arsines do not easily form -onium compounds with iodomethane. No reaction occurs when ether solutions of the arsines and iodomethane are mixed and the reaction of diphenyltrifluoromethylarsine with excess iodomethane at 150° produces trifluoroiodomethane and fluoroform. Both tristrifluoromethylarsine and methyl-bistrifluoromethylarsine behave similarly (6, 2), but dimethyltrifluoromethylarsine reacts directly with iodomethane to give trimethyltrifluoromethylarsonium iodide (1). Dimethyl-trifluoromethylarsine is also the only arsine containing trifluoromethyl groups which is known to form a complex with mercuric chloride (8) since the aryl-trifluoromethyl-arsines failed to react on mixing solutions of mercuric chloride with solutions of the arsines.

The infrared spectra of the aryl trifluoromethyl arsenicals show the usual strong C—F stretching bands in the region 1050–1250 cm^{-1}. The compounds with only one trifluoromethyl group in the molecule show only two bands in this region, a feature which has been observed for other trifluoromethyl compounds (9, 10). The bands associated with the phenyl groups show little variation in intensity or position from compound to compound. The ultraviolet spectra of these and related compounds have been studied and the results will be published later.

Radical exchange reactions have previously been used to prepare alkyl-trifluoromethyl-arsines, as follows (1, 2, 6):

$$2(CH_3)_3As + CF_3I \rightarrow (CH_3)_2AsCF_3 + (CH_3)_4AsI,$$

$$(CF_3)_2As + CH_3I \rightarrow (CF_3)_2AsCH_3 + CF_3I.$$

In the present work it was found that analogous reactions do not produce aryl-trifluoromethyl-arsines. There is no reaction between tristrifluoromethylarsine and iodobenzene at 240°, and the reaction of trifluoroiodomethane with triphenylarsine at 210° gives a mixture of products including fluoroform, benzotrifluoride, benzene, and arsenic triodide. Neither phenylbistrifluoromethyl- nor diphenyltrifluoromethyl-arsine is produced.

EXPERIMENTAL

Apparatus and Technique

Conventional vacuum techniques were used for the manipulation of volatile reactants and products out of contact with moisture and oxygen. Reactions were carried out in sealed Pyrex tubes in the absence of air and light. Gas phase molecular weights were determined by Regnault's method. Infrared spectra were measured on a Perkin–Elmer Model 21 double-beam instrument with rock-salt optics.

Reaction of Iododiphenylarsine with Trifluoroiodomethane in the Presence of Mercury

Iododiphenylarsine was prepared by the action of hydriodic acid on bis-diphenylarsenic oxide (11). The oxide was prepared from phenylmagnesium bromide and arsenious oxide (12). The iodo-arsine (19.5 g), trifluoroiodomethane (41.2 g), and mercury (200 g) in a sealed tube (150 ml) were shaken at 20° for 3 days. Trap-to-trap distillation of the volatile contents of the tube gave only trifluoroiodomethane (30.6 g). The remaining contents of the tube were extracted with benzene which was then removed by distillation at 760 mm in a nitrogen atmosphere leaving a colorless involatile liquid. The liquid was distilled at 10^{-3} mm and the fraction boiling at 86–88° collected. This fraction (12.4 g) was identified as *diphenyltrifluoromethylarsine* (76% yield). Anal. calc. for $C_{12}H_{10}AsF_3$: C, 52.4; H, 3.4; As, 25.2; F, 19.1%; mol. wt., 298. Found: C, 52.3; H, 3.5; As, 25.4; F, 19.4%; mol. wt., 286. The infrared spectrum showed the following absorption bands: liquid film: 3075(m), 2220(w), 1963(w), 1882(w), 1813(w), 1755(w), 1650(w), 1584(w), 1490(m), 1443(m), 1387(w), 1340(w), 1311(w), 1272(w), 1257(w), 1190(w), 1137(vs), 1105(vs), 1028(m), 1003(m), 974(w), 916(w), 848(w), 738(s), 726(m), 696(s) cm^{-1}.

Reaction of Diiodophenylarsine with Trifluoroiodomethane in the Presence of Mercury

Diiodophenylarsine was prepared from phenylarsineoxide and hydriodic acid (13). The iodo-arsine (41.7 g) trifluoroiodomethane (80 g), and mercury (350 g) in a sealed tube (150 ml) were shaken for 7 days at 20°. The excess trifluoroiodomethane was removed by trap-to-trap distillation and the remaining contents of the tube were extracted with benzene. Distillation of the benzene extracts at 760 mm in an atmosphere of nitrogen gave *phenylbistrifluoromethylarsine*, b.p. 160° (2.9 g, 10% yield). Anal. calc. for $C_8H_5AsF_6$: C, 33.1; H, 1.7; As, 25.8; F, 39.3%; mol. wt., 290. Found: C, 33.2; H, 1.7; As, 26.3; F, 39.0%; mol. wt., 276. A small amount of an unidentified substance which boiled at 90–95° (10^{-3} mm) was also isolated. Qualitative tests showed that this substance did not contain any As—I bonds. The infrared spectrum of phenylbistrifluoromethylarsine showed the following absorption bands: liquid film: 3085(w), 2220(w), 1970(w), 1908(w), 1889(w), 1833(w), 1815(w), 1759(w), 1658(w), 1584(w), 1492(m), 1447(m), 1390(w), 1342(w), 1264(w), 1168(vs), 1126(vs), 1100(vs), 1064(m), 1051(m), 1030(m), 1005(m), 975(w), 922(w), 850(w), 828(w), 792(m), 765(m), 742(s), 733(s), 695(s).

Reaction of Iodomethylphenylarsine with Trifluoroiodomethane in the Presence of Mercury

Iodomethylphenylarsine was prepared by the reduction of a hydrochloric acid solution of methylphenylarsinic acid with sulphur dioxide in the presence of potassium iodide. The

arsinic acid was prepared from iodomethane and phenylarsenoxide (14). The iodo-arsine (11 g), trifluoroiodomethane (40 g), and mercury (200 g) in a sealed tube (150 ml) were shaken for 5 days at 20°. The contents of the tube were worked up in the same manner as described for the preparation of phenylbistrifluoromethylarsine and *methylphenyltrifluoromethylarsine*, b.p. 186° (760 mm), was isolated in 67% yield. Anal. calc. for $C_8H_8AsF_3$: C, 40.7; H, 3.4; F, 24.2%; mol. wt., 236. Found: C, 41.0; H, 3.6; F, 24.5%; mol. wt., 235. The infrared spectrum showed the following absorption bands: liquid film: 3080(w), 3025(w), 2925(w), 2240(w), 1985(w), 1965(w), 1900(w), 1879(w), 1810(w), 1753(w), 1648(w), 1585(w), 1490(m), 1443(m), 1423(m), 1388(w), 1337(w), 1309(w), 1264(w), 1252(w), 1189(w), 1141(vs), 1098(vs), 1073(s), 1027(m), 1003(m), 971(w), 913(w), 891(w), 852(m), 815(w), 740(s), 725(m), 696(s).

Solvolysis of the Aryl Trifluoromethyl Arsenicals

The results of a number of solvolysis experiments which were carried out in sealed tubes (40 ml) are given below. The identity and purity of the fluoroform isolated by trap-to-trap distillation from these reactions was checked spectroscopically and, where possible, by molecular weight measurement. Fluoride ion was not detected as a product from any of the reactions.

TABLE II

Compound	mmoles	Solvolysis reagent	Time	Temp.	Yield of fluoroform
$(C_6H_5)_2AsCF_3$	1.12	10% aqueous NaOH (5 ml)	5 days	85°	11.5%
$(C_6H_5)_2AsCF_3$	1.37	Liquid NH_3 (3.59 g)	5 days	20°	Trace[a]
$(C_6H_5)_2AsCF_3$	1.03	Conc. HCl (10 ml)	2 days	85°	None
$(C_6H_5)_2AsCF_3$	1.52	10% ethanolic KOH (5 ml)	3 hours	85°	94.5%
$C_6H_5As(CF_3)_2$	0.641	10% aqueous NaOH (5 ml)	5 days	85°	98%
$C_6H_5As(CF_3)_2$	0.934	Liquid NH_3 (3.51 g)	10 days	20°	56.5%[b]
$C_6H_5As(CF_3)CH_3$	0.779	10% aqueous NaOH (5 ml)	5 days	85°	60%
$C_6H_5As(CF_3)CH_3$	0.943	Liquid NH_3 (3.96 g)	10 days	20°	Trace[c]
$(C_6H_5)_2CF_3AsBr_2$	0.146	10% aqueous NaOH (5 ml)	4 days	20°	94%

[a]Recovered 1.36 mmoles of $(C_6H_5)_2AsCF_3$.

[b]A white hygroscopic crystalline solid, soluble in ammonia but insoluble in ether was left in the tube after the volatile contents had been removed. The solubility in ether precludes the possibility that the compound was $C_6H_5As{=}NH$ (15). The infrared spectrum of the solid suggested that it was $(C_6H_5AsCF_3)_2NH$ since only one N—H stretching band and only two C—F stretching bands were present (9, 10).

[c]No solid was produced and the involatile liquid remaining in the reaction tube after removal of the more volatile NH_3 and CF_3H was identified spectroscopically as unchanged $(C_6H_5)CH_3AsCF_3$.

Reactions of Diphenyltrifluoromethylarsine

(a) Preparation of Diphenyltrifluoromethylarsenic Dibromide

A solution of bromine (1 g, 6.24 mmoles) in carbon tetrachloride (5 ml) was slowly added to a solution of diphenyltrifluoromethylarsine (1.174 g, 3.94 mmoles) in the same solvent (5 ml). The bromine was decolorized until excess was present. The solvent and excess bromine were removed *in vacuo* at 20° to give a pale yellow solid (1.836 g), the increase in weight corresponding to the addition of bromine to the arsine in the mole ratio of 1.05 to 1. The solid was recrystallized from ether to give colorless, hygroscopic rhombohedrons which melted at 110° with decomposition. Analysis identified the solid as *diphenyltrifluoromethylarsenic dibromide*. Anal. calc. for $C_{13}H_{10}AsBr_2F_3$: Br, 34.9%. Found: Br, 35.1%. The infrared spectrum showed the following absorption bands: Nujol mull and KBr disk: 3395(w), 2330(w), 1570(w), 1559(w), 1480(m), 1460(w), 1442(m), 1380(w), 1330(w), 1304(w), 1273(w), 1187(s), 1171(s), 1158(s), 1082(s), 1019(w), 966(w), 828(w),

744(s), 736(s), 681(s). The dibromide (0.065 g) in a sealed tube (5 ml) was heated to 120° for 18 hours. Trap-to-trap distillation of the volatile products together with spectroscopic examination and molecular weight determination showed that only bromotrifluoromethane had been produced (0.0204 g, 97%; mol. wt.: found 153, calc. 149). A white solid which remained in the tube was identified as impure bromodiphenylarsine (m.p.: found 48–50°, lit. value 54–56° (11)).

(b) Thermal Decomposition of Diphenyltrifluoromethylarsine

The arsine (0.121 g) in a sealed tube (5 ml) was heated to 247° for 20 hours. Trap-to-trap distillation and spectroscopic examination of the very small amount of volatile product (1 mg) showed that this was mainly fluoroform. The liquid which remained in the reaction tube when examined spectroscopically was found to be mainly unchanged arsine. The arsine (0.113 g) in a sealed tube (5 ml) was heated to 302° for 48 hours. A black solid was deposited on the tube walls and no liquid remained. Trap-to-trap distillation of the volatile products gave a fraction which condensed at −196° (0.026 g) which was identified spectroscopically as a mixture of fluoroform, silicon tetrafluoride, and carbon dioxide, and a fraction which condensed at −98° (0.035 g) which was identified spectroscopically as benzene.

(c) Reaction with Methyl Iodide

The arsine (0.229 g) in ether solution (3 ml) was mixed with a solution of methyl iodide (1 g) in ether (5 ml). No precipitate was formed and after removal of the volatile materials the arsine (0.229 g) was recovered. The arsine (0.276 g) and methyl iodide (2.27 g) in a sealed tube (10 ml) were heated to 112° for 12 days; a very small amount of solid was formed. The tube was then left at 150° for a further 10 days. Trap-to-trap distillation of the volatile products gave a fraction condensing at −196° (0.019 g) which was identified spectroscopically as a mixture of fluoroform and trifluoroiodomethane, and a fraction condensing at −132° (0.099 g) which was shown spectroscopically and by molecular weight measurement to be slightly impure trifluoroiodomethane (mol. wt.: found 190, calc. 196). The remaining volatile fractions and the tarry material remaining in the reaction tube were not further investigated.

(d) Reaction with Mercuric Chloride and Cadmium Chloride

The arsine failed to give a complex with mercuric chloride when alcohol or ether solutions of the two reactants were mixed. Similarly, no complex was obtained from alcohol or ether solutions of the arsine and cadmium chloride.

Reaction of Methylphenyltrifluoromethylarsine with Bromine

A solution of bromine (1 g) in carbon tetrachloride (5 ml) was added to a solution of the arsine (0.721 g) in the same solvent (3 ml). The bromine was decolorized until excess was present. The volatile materials were removed *in vacuo* at 20° and a pale yellow solid remained which on standing for 2 hours at 20° decomposed to a colorless liquid (0.240 g). Spectroscopic examination of this liquid showed that trifluoromethyl and phenyl groups were still present and that no bromobenzene had been produced. The volatile products of the reaction were shaken with mercury in a sealed tube to remove the excess bromine. Trap-to-trap distillation of the contents of the tube gave a fraction (0.377 g), which had a molecular weight of 107, and which was found spectroscopically to be a mixture of bromomethane and bromotrifluoromethane. On the basis of the molecular weight this corresponds to loss of up to 100% of the methyl groups and loss of ca. 19% of the trifluoromethyl groups from the starting material. Thus the liquid formed in the initial reaction was probably mainly bromophenyltrifluoromethylarsine.

Reactions of Phenylbistrifluoromethylarsine

(a) Reaction with Bromine

A solution of bromine (0.7 g) in carbon tetrachloride (25 ml) was added to a solution of the arsine (0.652 g) in the same solvent; the bromine was not decolorized. The reaction mixture was left for 30 minutes at 20° after which the volatile materials were removed *in vacuo* at 20°. No solid was formed and an involatile liquid (0.374 g) was left in the reaction vessel. Qualitative tests showed that the liquid contained bromine and spectroscopic examination showed that the material contained no bromobenzene and was probably mainly bromophenyltrifluoromethylarsine.

(b) Reactions with Iodomethane and Mercuric Chloride

When ether solutions of iodomethane and the arsine were mixed no precipitate was obtained and after removal of the volatile materials the arsine was recovered. No precipitate was obtained on mixing ethanol solutions of the arsine and mercuric chloride.

Reaction of Tristrifluoromethylarsine with Iodobenzene

Tristrifluoromethylarsine was obtained from the reaction of trifluoroiodomethane with arsenic (6). The arsine (0.989 g) and iodobenzene (2.654 g) in a sealed tube (20 ml) were heated to 220° for 36 hours. Spectroscopic examination of the products of the reaction showed that no fluoroform or trifluoroiodomethane had been formed. The tristrifluoromethylarsine was recovered quantitatively (0.982 g; mol. wt: found 281, calc. 282).

Reaction of Triphenylarsine with Trifluoroiodomethane

The arsine (3.81 g) and trifluoroiodomethane (26.02 g) in a sealed tube (100 ml) were left at 20°. The arsine was completely soluble and there was no sign of reaction. After 7 days trifluoroiodomethane (25.89 g) was recovered unchanged. Similarly, there was no reaction between the arsine (2.05 g) and trifluoroiodomethane (4.932 g) after 4 days at 85°. The arsine (4.5 g) and trifluoroiodomethane (10.15 g) in a sealed tube (150 ml) were heated to 210° for 12 hours. Trap-to-trap distillation of the volatile products gave impure trifluoroiodomethane (4.62 g) which spectroscopic examination showed to contain fluoroform and a fraction condensing at −98° (2.69 g) which was identified spectroscopically as a mixture of benzene and benzotrifluoride. A yellow involatile liquid and a yellow solid remained in the tube. The liquid was extracted from the tube with ether which was then removed by distillation in a nitrogen atmosphere. Spectroscopic examination of the involatile residue showed the absence of either phenylbistrifluoromethylarsine or diphenyltrifluoromethylarsine. The solid (1.7 g) was identified as arsenic triiodide (m.p.: found 145°, lit. value 146°).

ACKNOWLEDGMENTS

The author wishes to acknowledge financial assistance from the National Research Council of Canada. He is also indebted to Dr. C. J. Willis for helpful discussions. Microanalyses for C, H, As, F and determinations of molecular weight were carried out by Dr. Alfred Bernhardt.

REFERENCES

1. R. N. Haszeldine and B. O. West. J. Chem. Soc. 3631 (1956).
2. R. N. Haszeldine and B. O. West. J. Chem. Soc. 3880 (1957).
3. W. R. Cullen. Can. J. Chem. **38**, 439 (1960).
4. P. B. Ayscough and H. J. Emeléus. J. Chem. Soc. 3381 (1954).
5. W. R. Cullen and H. J. Emeléus. J. Chem. Soc. 372 (1959).
6. H. J. Emeléus, R. N. Haszeldine, and E. G. Walachewski. J. Chem. Soc. 1552 (1953).

7. C. W. RAIZISS and J. L. GAVRON. Organic arsenical compounds. The Chemical Catalog Co., Inc., New York. 1923.
8. H. J. EMELÉUS, R. N. HASZELDINE, and R. C. PAUL. J. Chem. Soc. 881 (1954).
9. F. W. BENNETT, H. J. EMELÉUS, and R. N. HASZELDINE. J. Chem. Soc. 1565 (1953).
10. W. MAHLER and A. B. BURG. J. Am. Chem. Soc. **80**, 6161 (1958).
11. W. J. POPE and E. E. TURNER. J. Chem. Soc. 1447 (1920).
12. F. F. BLICKE and F. D. SMITH. J. Am. Chem. Soc. **51**, 1558 (1929).
13. A. MICHAELIS and C. SCHULTE. Ber. **14**, 912 (1881).
14. G. J. BURROWS and E. E. TURNER. J. Chem. Soc. 426 (1921).
15. A. MICHAELIS. Ann. **320**, 271 (1902).

STEROIDS AND RELATED PRODUCTS

XIII. THE SYNTHESIS OF 6α-FLUORO-17α-BROMOPROGESTERONE[1, 2]

CH. R. ENGEL AND R. DEGHENGHI

ABSTRACT

The synthesis of 6α-fluoro-17α-bromoprogesterone, a new potent gestogen, from pregnenolone acetate, is reported.

In a previous publication of this series (2) our group reported the synthesis and marked progestational activity of 17α-bromoprogesterone. Revesz *et al.* (3) further investigated the biological properties of this compound and established *inter alia* that unlike progesterone, 11-dehydroprogesterone, and 17α-methylprogesterone, it exhibited oral luteoid activity and that it showed no oestrogenic or androgenic side effects. Recently, a number of laboratories reported that certain substitutions in position 6α of the steroid nucleus markedly increased the progestational effect, especially the oral activity, of the parent compound (4–14, compare also 15). Among the biologically most interesting substances of this kind were 6α-halogenated steroids (compare 9, 10, 14, and 15).

It seemed attractive to combine the work in these two fields by preparing 6-substituted 17-halogenated progesterone derivatives, since, in addition to producing compounds of potential biological interest, this would allow us to broaden our investigation of the influence of 17-substituents, especially of a large size, on the progestational activity. It was hoped that this study would ultimately lead to a better understanding of the mechanism by which such groups exert their activity-enhancing action.

In the present paper we report the synthesis of 6α-fluoro-17α-bromoprogesterone (IV), the first 6,17-dihalogenated progesterone derivative.

Pregnenolone acetate (I) served as starting material. We transformed it, according to the procedure of Bowers and Ringold (16) [compare also the article by Henbest and Wrigley (17)], via the 5α,6α-epoxide, to 6β-fluoro-3β-acetoxy-5α-hydroxy-20-oxopregnane (II) which, upon treatment with N-bromosuccinimide under illumination (compare 18), gave in 80–85% yield the corresponding 17α-bromide III. The assignment of location of the bromine substituent to position 17α is in accord with analogous brominations (1, 18, 19) and was confirmed by the conversion of the derivative IV to the 16-unsaturated diketone VIII (*vide infra*). The typical levorotatory shift produced by bromination of 20-ketones in 17α (1, 2, 21) was observed.

Hydrolysis with perchloric acid in methanol (2, 20) gave in high yield the 3-hydroxy derivative VI which was oxidized with chromic acid and sulphuric acid in acetone (compare 16, 22, 23) to 6β-fluoro-17α-bromo-5α-hydroxy-3,20-dioxopregnane (V) in 60–70% yield. Dehydration with concomitant epimerization in 6 by treatment with hydrogen chloride in acetic acid (compare 16) gave the desired 6α-fluoro-17α-bromoprogesterone (IV) in approximately 70% yield.

The configuration of the 6-fluoro substituent was ascertained by the comparison of its molecular rotation (+50°) with the calculated value. Indeed, if, in accordance with the results in the 6-unsubstituted series (2), one assumes that the decrement of molecular rotation upon bromination in position 17α is −560°, one obtains from the rotations of the

[1]*Manuscript received November 19, 1959.*
Contribution from the Department of Chemistry, Laval University, Quebec, Que.
[2]*For Paper XII of this series see reference 1.*

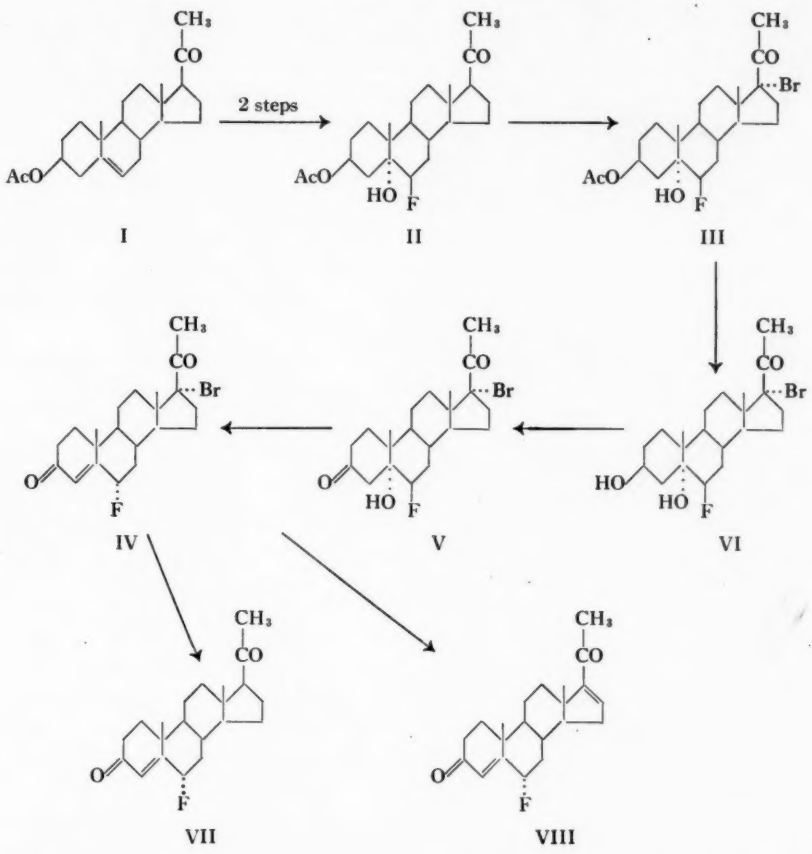

6α- and 6β-fluoroprogesterones reported in the literature (10, 16) the values for the 6α- and 6β-fluoro-17α-bromoprogesterones, given in Table I. It can be clearly seen that the configuration of the 6-substituent of our 6,17-dihalogenated progesterone must be α. Comparable results are obtained when the decrements of molecular rotation, obtained upon bromination in 17α, are chosen from other series of experiments (compare i.e. 1, 21).

TABLE I

Molecular rotations of 6α- and 6β-fluoro-17α-bromoprogesterones[a]

Compound	$[M]_D$ calc.	$[M]_D$ found
6α-Fluoro-17α-bromoprogesterone	+35°[b] +75°[c]	+50°
6β-Fluoro-17α-bromoprogesterone	−290°[b] −215°[c]	

[a]The molecular rotations were calculated to the nearest 5°.
[b]Calculated from the values of the 17-unsubstituted products reported by Hogg *et al.* (10).
[c]Calculated from the values of the 17-unsubstituted products reported by Bowers and Ringold (16).

The structure of the new progesterone derivative IV was confirmed both by reduction with hydriodic acid (under the reaction conditions described by Zimmerman and Wen-Hsuan Cheng (24)), to 6α-fluoroprogesterone (VII) (10, 16) and by elimination of hydrogen bromide with dimethylformamide and lithium chloride (compare 25), leading to 16-dehydro-6α-fluoroprogesterone (VIII), which showed the typical spectral characteristics of the Δ^4-3-keto and Δ^{16}-20-keto moieties.

According to preliminary biological assays, for which we are indebted to Drs. M. Eisler and P. Perlman, 6α-fluoro-17α-bromoprogesterone (IV) exhibits marked progestational activity. A detailed account of the biological results will be published elsewhere.*

EXPERIMENTAL[3, 4, 5]

6β-Fluoro-17α-bromo-3β-acetoxy-5α-hydroxy-20-oxopregnane (III)

Following the procedure of Bowers and Ringold (16), pregnenolone acetate (I) was converted, via the 5α,6α-epoxide, to *6β-fluoro-3β-acetoxy-5α-hydroxy-20-oxopregnane* (II). The product crystallized from acetone–hexane in two modifications, one in leaflets melting at 186.5–187°, the other in prisms melting at 214–216°;[6] $[\alpha]_D^{22}$ +36° (*c*, 1.17 in $CHCl_3$); ν_{max}^{KBr} 1255 and 1730 cm^{-1} (acetate), 1692 cm^{-1} (20-ketone), 3360 cm^{-1} (hydroxy). Anal. Calc. for $C_{23}H_{35}O_4F$: C, 70.02; H, 8.94; F, 4.82. Found: C, 70.10; H, 9.00; F, 5.00.

To a solution of 1.082 g of 6β-fluoro-3β-acetoxy-5α-hydroxy-20-oxopregnane (II), m.p. 210–214°, in 18 cc of dichloromethane, 620 mg of N-bromosuccinimide and, subsequently, 36 cc of carbon tetrachloride were added. The solution was refluxed over a photoflood lamp for 10 minutes, cooled to room temperature, diluted with further quantities of dichloromethane, and washed with a cold 10% sodium bisulphite solution. The solution was dried with sodium sulphate, the solvent was removed *in vacuo*, and the residue (1.549 g) was crystallized from acetone to give 680 mg of bromoketone III, m.p. 159–160° decomp. The mother liquors were chromatographed on 30 g of silica gel. Benzene, containing 4% of ethyl acetate, eluted 401 mg of pure III, m.p. 168° decomp. (total yield 83%). A sample was recrystallized from methylene chloride – ether for analysis; colorless needles, m.p. 165° decomp., $[\alpha]_D^{24}$ −60.2° (*c*, 0.85 in $CHCl_3$); ν_{max}^{KBr} 1250 and 1720 cm^{-1} (acetate), 1692 cm^{-1} (20-ketone), 3400 cm^{-1} (5α-hydroxy). Anal. Calc. for $C_{23}H_{34}O_4FBr$: C, 58.35; H, 7.24; F, 3.92; Br, 16.88. Found: C, 58.06; H, 7.15; F, 4.22; Br, 16.79.

6β-Fluoro-17α-bromo-3β,5α-dihydroxy-20-oxopregnane (VI)

To a solution of 680 mg of 6β-fluoro-17α-bromo-3β-acetoxy-5α-hydroxy-20-oxopregnane (III), m.p. 159–160° decomp., in 90 cc of methanol was added, at room temperature, 4.5 cc of 70% aqueous perchloric acid. The solution was stored for 22 hours at 25° and was subsequently poured into iced dilute sodium bicarbonate solution. The precipitate was extracted with dichloromethane and the organic solution was washed with water, and was dried over sodium sulphate. Evaporation of the solvent *in vacuo* gave 670 mg of a foamy residue which, upon crystallization from acetone–hexane, afforded 530 mg (85% yield) of

[3]*The melting points were taken in evacuated capillaries and the temperatures were corrected.*

[4]*The microanalyses were performed by Dr. O. Schwarzkopf and his associates, New York, N.Y., to whom we express our sincere appreciation.*

[5]*For chromatography, Davison's silica gel No. 923 and non-alkaline aluminum oxide Woelm, activity II–III, were used.*

[6]*Bowers and Ringold (16) reported only the higher melting modification.*

*NOTE ADDED IN PROOF. — *Dr. R. Gaudry, Ayerst, McKenna & Harrison, Ltd., Montreal, informed us that his group also synthesized 6α-fluoro-17α-bromoprogesterone and that he intends to publish the results of his team shortly.*

crystalline hydroxy ketone VI, m.p. 156–158° decomp. A sample was recrystallized from acetone–hexane for analysis; needles, m.p. 165° decomp., $[\alpha]_D^{26}$ −66.6° (*c*, 1.05 in $CHCl_3$); ν_{max}^{KBr} 1695 cm^{-1} (20-ketone), 3380 cm^{-1} (5α-hydroxy), 3500 cm^{-1} (3β-hydroxy). Anal. Calc. for $C_{21}H_{32}O_3FBr$: C, 58.47; H, 7.47; F, 4.41; Br, 18.52. Found: C, 58.57; H, 7.25; F, 3.91; Br, 18.42.

6β-Fluoro-17α-bromo-5α-hydroxy-3,20-dioxopregnane (V)

To a solution of 608 mg of 6β-fluoro-17α-bromo-3β,5α-dihydroxy-20-oxopregnane (VI), m.p. 156–158° decomp., in 50 cc of absolute acetone, was added dropwise and with stirring, at 0–5°, 1 cc of an 8 *N* solution of chromic acid. The stirring was continued for 2.5 minutes and subsequently the mixture was poured into ice water and the colorless precipitate was filtered, washed to neutral, and dried. There was obtained 590 mg of a white solid which, upon crystallization from acetone–ether, gave 400 mg (65% yield) of V, m.p. 171° decomp. A sample was recrystallized from acetone–ether for analysis; prisms, m.p. 160° decomp., $[\alpha]_D^{24}$ −34.4° (*c*, 0.758 in $CHCl_3$); ν_{max}^{KBr} 1690 cm^{-1} (20-ketone), 1705 cm^{-1} (3-ketone), 3380 cm^{-1} (5α-hydroxy). Anal. Calc. for $C_{21}H_{30}O_3BrF$: C, 58.74; H, 7.04; F, 4.42; Br, 18.61. Found: C, 58.48; H, 7.10; F, 4.24; Br, 18.80.

Δ^4-6α-Fluoro-17α-bromo-3,20-dioxopregnene (6α-Fluoro-17α-bromopregesterone) (IV)

At 10°, a stream of dry hydrogen chloride was passed for a period of 2 hours through a stirred solution of 470 mg of 6β-fluoro-17α-bromo-5α-hydroxy-3,20-dioxopregnane (V), in 47 cc of acetic acid. The solution was kept for 19 hours at 5–10° and was subsequently poured into ice water. The precipitate was filtered, washed to neutral, and dried. The resulting product (406 mg) was chromatographed on 45 g of silica gel. Benzene – ethyl acetate (97:3) eluted 312 mg (69% yield) of crystalline Δ^4-6α-fluoro-17α-bromo-3,20-dioxopregnene (6α-fluoro-17α-bromoprogesterone) (IV), m.p. 157° decomp. A sample was recrystallized from acetone–hexane for analysis; fine needles, m.p. 169–170° decomp., $[\alpha]_D^{24}$ +12.1° (*c*, 2.46 in $CHCl_3$); λ_{max}^{EtOH} 236–237 mμ (log ε 4.2), ν_{max}^{KBr} 1621 and 1680 cm^{-1} (Δ^4-3-ketone doublet), 1704 cm^{-1} (20-ketone). Anal. Calc. for $C_{21}H_{28}O_2FBr$: C, 61.31; H, 6.86; F, 4.62; Br, 19.43. Found: C, 61.33; H, 6.98; F, 4.40; Br, 19.63.

Reduction [6α-Fluoroprogesterone (VII)]

To a solution of 200 mg of 6α-fluoro-17α-bromoprogesterone (IV), m.p. 169–170° decomp., in 8 cc of absolute acetone was added, dropwise and with stirring, within 1.5 minutes, a solution of 1 cc of 55% hydriodic acid in 5 cc of absolute acetone. The mixture was poured into iced dilute sodium bisulphite solution, and the precipitate was extracted with dichloromethane. The organic solution was washed with dilute sodium bicarbonate solution and with water and was dried over sodium sulphate. Upon removal of the solvent there was obtained 150 mg of an oil, which crystallized from acetone–hexane to give colorless needles, m.p. 135–139°. A sample was recrystallized twice for analysis; long, silky needles, m.p. 143°, $[\alpha]_D^{26}$ +175° (*c*, 0.8 in $CHCl_3$); ν_{max}^{KBr} 1620 and 1680 cm^{-1} (Δ^4-3-keto doublet), 1701 cm^{-1} (20-ketone); λ_{max}^{EtOH} 236 mμ (log ε 4.1). Anal. Calc. for $C_{21}H_{29}O_2F$: C, 75.87; H, 8.79; F, 5.71. Found: C, 76.16; H, 8.91; F, 5.63.

Dehydrobromination [6α-Fluoro-16-dehydroprogesterone (VIII)]

A solution of 144 mg of 6α-fluoro-17α-bromoprogesterone (IV), m.p. 162–164° decomp., in 25 cc of dimethylformamide was refluxed with 25 mg of lithium chloride for 1 hour. The cooled mixture was extracted with ether, the ethereal solution was washed with dilute hydrochloric acid, sodium bicarbonate solution, and water and dried over sodium sulphate. Removal of the solvent gave 108 mg of yellowish crystals, m.p. 142–146°. The product

was dissolved in benzene – ethyl acetate (97:3) and filtered through 4 g of silica gel. The colorless crystalline fractions (70 mg) were recrystallized twice from ether to afford pure $\Delta^{4,16}$-6α-fluoro-3,20-dioxopregnadiene (VIII), m.p. 162–163°, $[\alpha]_D^{26}$ +158.4° (*c*, 0.5 in $CHCl_3$), λ_{max}^{EtOH} 238 mμ (log ϵ 4.34); ν_{max}^{KBr} 1592 and 1662 cm^{-1} (Δ^{16}-20-ketone doublet), 1628 and 1678 cm^{-1} (Δ^4-3-ketone doublet). Anal. Calc. for $C_{21}H_{27}O_2F$: C, 76.33; H, 8.24; F, 5.75. Found: C, 76.22; H, 8.34; F, 5.61.

ACKNOWLEDGMENTS

We express our sincere thanks to Mr. D. Capitaine and Mrs. J. Capitaine for their devoted assistance in these experiments and to Drs. M. Eisler and P. Perlman, Bloomfield, New Jersey, for the preliminary biological tests. We are greatly indebted to the National Research Council of Canada, the Schering Corporation, Bloomfield, New Jersey, and the Schering Corporation Ltd., Montreal, for financial support of this project.

REFERENCES

1. R. Deghenghi and Ch. R. Engel. J. Am. Chem. Soc. In press. (1960).
2. Ch. R. Engel and H. Jahnke. Can. J. Biochem. and Physiol. **35**, 1047 (1957).
3. K. Revesz, R. Herne, and C. I. Chappel. Proc. Can. Federation Biol. Socs. **1**, 41 (1958); and personal communications by the authors.
4. A. David, F. Hartley, D. R. Millson, and V. Petrow. J. Pharm. and Pharmacol. **9**, 929 (1957).
5. H. J. Ringold, E. Batres, and G. Rosenkranz. J. Org. Chem. **22**, 99 (1957).
6. J. C. Babcock, E. S. Gutsell, M. E. Herr, J. A. Hogg, J. C. Stucki, L. E. Barnes, and W. E. Dulin. J. Am. Chem. Soc. **80**, 2904 (1958).
7. J. A. Campbell, J. C. Babcock, and J. A. Hogg. J. Am. Chem. Soc. **80**, 4717 (1958).
8. H. J. Ringold, J. Pérez Ruelas, E. Batres, and C. Djerassi. J. Am. Chem. Soc. **81**, 3712 (1959).
9. A. Bowers and H. J. Ringold. J. Am. Chem. Soc. **80**, 4423 (1958).
10. J. A. Hogg, G. B. Spero, J. L. Thompson, B. J. Magerlein, W. P. Schneider, D. H. Peterson, O. K. Sebek, H. C. Murray, J. C. Babcock, R. L. Pederson, and J .A. Campbell. Chem. & Ind. 1002 (1958).
11. A. Bowers, L. C. Ibáñez, and H. J. Ringold. J. Am. Chem. Soc. **81**, 3707 (1959).
12. S. P. Barton, B. Ellis, and V. Petrow. J. Chem. Soc. 478 (1959).
13. P. B. Sollman, R. L. Elton, and R. M. Dodson. J. Am. Chem. Soc. **81**, 4435 (1959).
14. H. J. Ringold, E. Batres, A. Bowers, and J. Zederic. J. Am. Chem. Soc. **81**, 3485 (1959).
15. L. Fieser and M. Fieser. Steroids. Reinhold Publishing Corp., New York; and Chapman and Hall, Ltd., London. 1959. pp. 564–566.
16. A. Bowers and H. J. Ringold. Tetrahedron, **3**, 14 (1958).
17. H. B. Henbest and T. I. Wrigley. J. Chem. Soc. 4765 (1957).
18. R. U. Schock and W. J. Karpel. U.S. Patent No. 2,684,963 (1954).
19. Ch. R. Engel, G. Just, and R. G. Buttery. Unpublished data from this laboratory.
20. J. Fried and F. Sabo. J. Am. Chem. Soc. **74**, 3849 (1952).
21. H. Heusser, Ch. R. Engel, P. Th. Herzig, and Pl. A. Plattner. Helv. Chim. Acta, **33**, 2229 (1950).
22. K. Bowden, J. M. Heilbron, E. R. H. Jones, and B. C. L. Weedon. J. Chem. Soc. 3911 (1946).
23. C. Djerassi, R. R. Engle, and A. Bowers. J. Org. Chem. **21**, 1547 (1956).
24. H. E. Zimmerman and Wen-Hsuan Cheng. J. Am. Chem. Soc. **81**, 3634 (1959).
25. R. P. Holysz. J. Am. Chem. Soc. **75**, 4432 (1953).

REACTION OF *syn*-BENZALDOXIME WITH CARBON MONOXIDE AND HYDROGEN TO YIELD SUBSTITUTED UREAS

A. ROSENTHAL AND J. P. O'DONNELL

Our previous successful application of a modified oxo reaction to aromatic ketoximes (1) led us to subject an aromatic aldoxime to the action of carbon monoxide and hydrogen in the presence of preformed dicobalt octacarbonyl. Although *syn*-benzaldoxime is generally known to be resistant to dehydration, there is mention in the recent literature (2) that this isomer, when subjected to a pressure of 38,400 atm at a temperature of 200°, underwent an explosive decomposition to ammonia and a carbonaceous material.

When a benzene solution of *syn*-benzaldoxime was subjected to a mixture of carbon monoxide and hydrogen (98.5:1.5) at 300 atm and at about 220° in the presence of a high concentration of preformed dicobalt octacarbonyl, *sym*-dibenzylurea and monobenzylurea were formed. The ureas were accompanied by a small amount of benzaldehyde, as well as two crystalline compounds (A and B) which possessed no carbonyl (by infrared analyses).

$$\mathrm{Ph{-}C{-}H \;\overset{CO + H_2}{\longrightarrow}\; PhCH_2NHCONHCH_2Ph + PhCH_2NHCONH_2}$$
$$\mathrm{\underset{\|}{N}{-}OH}$$
(C) 35% (D) 10%

+ PhCHO + A + B
3%

The reaction mixture was separated chromatographically on alumina. Gas-chromatographic fractionation of the gaseous product of the reaction showed that all of the hydrogen had been consumed, and only unused carbon monoxide was present.

By analogy with our previously described work (1), phthalimidine could be expected as a product of this reaction. That this was not realized is further proof that aromatic aldoximes are more unstable than aromatic ketoximes. The presence of benzaldehyde in the product implies that some hydrolysis might have taken place, though it does not preclude the possibility that a complex formed by the reaction of *syn*-benzaldoxime with dicobalt octacarbonyl might have decomposed to yield benzaldehyde. In support of this speculation, it is to be noted that Greenfield and co-workers (3) have found that diphenylacetylene formed an unstable complex with dicobalt octacarbonyl, which decomposed at room temperature to yield benzil. Unfortunately, our attempts to form a complex of the aldoxime and the catalyst in open systems at moderate temperatures were fruitless. An unstable cobalt-containing material was isolated chromatographically from the original reaction mixture.

Monobenzyl and *sym*-dibenzylurea were identified by mixed melting point using authentic samples (4). These compounds also possessed infrared spectra identical with those of the authentic samples. *sym*-Dibenzylurea was also characterized by oxidation with sodium dichromate in glacial acetic acid to yield *sym*-dibenzoylurea.

The only tentative mechanism which the authors are able to advance in order to explain the formation of dibenzylurea is one deduced from the work of Natta and co-workers (5). When styrene, aniline, and carbon monoxide were reacted, the latter authors reported the presence of an abnormally high amount of diphenylurea and the reduction of styrene to ethylbenzene.

It was suggested that the cobalt carbonyl acted as a hydrogen-transfer agent by formation and decomposition of the hydrocarbonyl. Such a hypothesis might also apply to our reaction. Part of the *syn*-benzaldoxime might be expected to be reduced to benzylamine by the hydrogen present in the original gaseous reactants. The latter primary amine might then react with carbon monoxide and unreacted oxime in some type of hydrogen-transfer process to yield dibenzylurea.

$$PhCH{=}NOH + H_2 \rightarrow PhCH_2NH_2 + H_2O$$

$$2PhCH_2NH_2 + CO + PhCH{=}NOH \rightarrow PhCH_2NHCONHCH_2Ph + PhCH_2NH_2 + H_2O$$

EXPERIMENTAL

General Considerations

The equipment was described previously (1).

Reaction of syn-Benzaldoxime with Carbon Monoxide and Hydrogen

A mixture of 6.5 g (0.054 mole) of *syn*-benzaldoxime (6), 85 ml of catalyst solution containing 0.02 mole of dicobalt octacarbonyl in benzene and carbon monoxide containing 1.5% by volume of hydrogen (2300 p.s.i. at 11°) was placed in the high pressure bomb. The reactants were heated with rocking at 190–220° for 40 minutes. An observed pressure drop of 210 p.s.i. at 11° (2.1 moles per mole of substrate) was obtained. Vapor phase chromatography of the product gases showed carbon monoxide only to be present. After decomposition of the catalyst and removal of the benzene under vacuum, the residue was dissolved in 51 ml of benzene. A 3-ml aliquot of this solution was placed on an alumina column (125×30 mm diameter) for chromatography. The following mixtures of developer were then added consecutively.

(1) 125 ml of benzene gave 0.040 g of crystalline A which was recrystallized from light petroleum ether, m.p. 239–242°. Infrared (KBr): 3050 (w), 1589 (w), 1523 (s).

(2) 50 ml of benzene yielded nothing.

(3) 150 ml of benzene eluted 0.040 g of crystalline B which after two recrystallizations from light petroleum ether melted at 280–282°. Infrared (KBr): 3055 (w), 1601 (w), 1579 (w), 1507 (w).

(4) 450 ml of benzene removed no material.

(5) 300 ml of benzene–ethanol (99:1) yielded 0.120 g of compound C.

(6) 150 ml of benzene–ethanol (98:2) eluted no material.

(7) 50 ml of benzene–ethanol (98:2) gave 0.027 g of compound D.

Chromatography of an aliquot of the original reaction mixture on alumina using benzene eluted a red zone (not dicobalt octacarbonyl) which decomposed rapidly on standing. Addition of light petroleum ether to the red material produced a benzene-insoluble brown substance.

All attempts to form a complex between *syn*-benzaldoxime and preformed dicobalt octacarbonyl in benzene in open systems at different temperatures from 20° to 45° were fruitless.

Extraction of Benzaldehyde from the Reaction Mixture

After evaporation of the benzene from the reaction mixture under reduced pressure at 40°, the residue was extracted with light petroleum ether. Removal of the petroleum ether yielded impure benzaldehyde which was purified by conversion to the bisulphite salt. Reaction of the purified benzaldehyde with 2,4-dinitrophenylhydrazine gave the hydrazone (0.54 g), m.p. 235–237°, undepressed on admixture with an authentic sample of benzaldehyde 2,4-dinitrophenylhydrazone.

Characterization of Compound C (*sym-Dibenzylurea*)

Compound C was twice recrystallized from benzene – light petroleum ether, m.p. 168–169°. The mixed melting point of compound C and an authentic sample of *sym*-dibenzylurea (4) was 167–169°. The infrared spectra of both compounds were identical. Anal. Found: C, 74.87; H, 6.79; N, 11.91; mol. wt. (Rast), 263. Calc. for $C_{15}H_{16}N_2O$: C, 75.00; H, 6.67; N, 11.67; mol. wt., 240. Infrared of C (KBr): 3337 (s), 3043 (w), 2922 (w), 1625 (s), 1591 (s), 1575 (s), 1497 (w).

Oxidation of sym-Dibenzylurea (Compound C*) to sym-Dibenzoylurea*

Compound C (63 mg) was dissolved in 25 ml of glacial acetic acid, and sodium dichromate (0.3 g) was added to the solution. After the solution was refluxed for 4 hours, the reaction mixture was poured into 50 ml of water. Extraction of the aqueous solution with chloroform gave on evaporation 42 mg of product. Recrystallization of the latter from ethanol yielded *sym*-dibenzoylurea, m.p. 202–203°. The literature (7) melting point of *sym*-dibenzoylurea is 203°. Infrared spectrum (KBr): 3240 (w), 1753 (s), 1670 (s), 1603 (w), 1577 (w), 1534 (m), 1506 (m), 1480 (m), 1288 (m), 1266 (s), 1200 (m).

Characterization of Compound D *(Monobenzylurea)*

Several recrystallizations of compound D from benzene – light petroleum ether gave pure monobenzylurea, m.p. 147–149°. The mixed melting point of an authentic sample of monobenzylurea (4) and compound D was 147–149°. The infrared spectrum of compound D was identical with that of the authentic sample. Infrared of D (KBr): 3440 (s), 3328 (s), 3035 (w), 2922 (w), 1651 (s), 1601 (s), 1564 (s), 1499 (w), 1471 (m), 1458 (m).

ACKNOWLEDGMENTS

Grateful acknowledgment is made to the National Research Council for financial support of this work.

This research was also supported in part by a grant from the Petroleum Research Fund administered by the American Chemical Society. Grateful acknowledgment is hereby made to the donors of said fund.

The authors wish to thank Dr. S. Ryce and Mr. S. Ruzicka of this department for vapor phase chromatography.

1. A. Rosenthal, R. F. Astbury, and A. Hubscher. J. Org. Chem. **23**, 1037 (1958).
2. I. S. Bengelsdorf. J. Am. Chem. Soc. **80**, 1442 (1958).
3. H. Greenfield, H. W. Sternberg, R. A. Friedel, J. H. Wotiz, R. Markby, and I. Wender. J. Am. Chem. Soc. **78**, 120 (1956).
4. T. L. Davis and K. C. Blanchard. J. Am. Chem. Soc. **45**, 1819 (1923).
5. G. Natta, P. Pino, and R. Ercoli. J. Am. Chem. Soc. **74**, 4496 (1952).
6. E. Beckmann. Ber. **23**, 1685 (1890).
7. H. Biltz. Ber. **40**, 2635 (1907).

Received October 23, 1959.
Department of Chemistry,
University of British Columbia,
Vancouver 8, B.C.

SEPARATION OF SOME HEAVY METALS BY SOLVENT EXTRACTION AND BY PAPER CHROMATOGRAPHY

Gerhard Weidmann*

The partition of the chlorides of Fe, Co, and Cu between tri-*n*-butyl phosphate and an aqueous HCl solution of different concentrations was determined. Tri-*n*-butyl phosphate

**Present address: Coburg, Kanonenweg 83, West Germany.*

was also used as an extraction agent to separate the chlorides of Fe, Ni, and Co or Fe, Ni, and Cu. The R_F values of Mn, Fe, Co, Ni, and Cu were determined using as a solvent tri-*n*-butyl phosphate adjusted with HCl of different concentrations.

Tri-*n*-butyl phosphate (TBP) is well known as an extraction agent for uranium, plutonium, and some other actinides from nitrate solutions (1, 2).

Other authors have investigated the extraction of zirconium (3), copper, and cobalt (4) from concentrated chloride or aqueous solutions using TBP. McKay and Hesford (5) and Healy and Kennedy (6) reported the extraction of nitrates of metals. Peppard and co-workers (7, 8) first showed that a feasible extraction of actinides, lanthanides, scandium, and zirconium from HCl solutions is possible using TBP and TBP – dibutyl ether mixtures and aqueous solutions of different HCl concentration.

In this work we have investigated the dependence of the partition of $FeCl_3$, $CoCl_2$, and $CuCl_2$ between pure TBP and aqueous HCl solutions as a function of HCl concentration. Referring to the obtained distribution coefficients and the fact that Ni is not extracted by pure TBP, a separation of Ni, Fe, and Co or Ni, Fe, and Cu can be realized. TBP was also used as a solvent in paper chromatography to separate a mixture of $MnCl_2$, $FeCl_3$, $CoCl_2$, $NiCl_2$, and $CuCl_2$.

Determination of the Distribution Coefficients of Fe, Co, Cu

Commercially available TBP was purified by washing with a 5% sodium carbonate solution and then by distillation at about 178° C, 25 mm Hg. All other reagents were of analytical grade.

Previous qualitative tests have shown that the chlorides of Fe, Co, Cu are extracted by TBP from an aqueous HCl solution, while Ni is not extracted.

EXPERIMENTAL

Before determination of the distribution coefficients the organic solvent was saturated with water. After separation 200-ml portions of the organic phase were shaken at 20° C with the following molarities of HCl: 1, 2, 3, 4, 5, 6, 7, 8, 9, 10, 11. Each portion was shaken so often with quantities of the corresponding HCl molarity that finally the HCl concentration in the aqueous phase remained constant. For this reason the distribution coefficients and R_F values in the following figures and tables are plotted as a function not of the actual HCl concentration in TBP but of the HCl concentration in the aqueous solution.

The chlorides corresponding to about 100 mg of each element were separately dissolved in 50 ml HCl of different molarity and shaken with an equal volume of TBP adjusted with HCl of the corresponding molarity. After the separation of the two phases, aliquots were taken and analyzed. Before analysis, the metals dissolved in the TBP phase were re-extracted completely by water. Concentrations higher than about 10 mg per 100 ml water of Co and Cu were transformed into sulphates and were determined by electrolysis. Fe was determined by redox titrations. Lower concentrations of Fe, Co, and Cu were determined colorimetrically using sulphosalicylate ($5HO \cdot C_6H_3 \cdot (COOH)SO_3H$) for Fe, ammonium thiocyanate for Co, and tetramine copper-II-chloride for Cu (10). Measurements were made with an ELKO Photo II colorimeter.*

Figure 1 shows the distribution coefficients (D) of $FeCl_3$, $CoCl_2$, and $CuCl_2$ and Fig. 2

**Carl Zeiss, Oberkochem/Württ.*

shows the per cent of metal extracted ($\%E$) as a function of the molarity of aqueous HCl. $\%E$ is related to D by the following equation:

$$\%E = \frac{100D}{D+(V_{aq}/V_{TBP})},$$

where V_{TBP} and V_{aq} represent respectively the volumes of the organic and the aqueous phases.

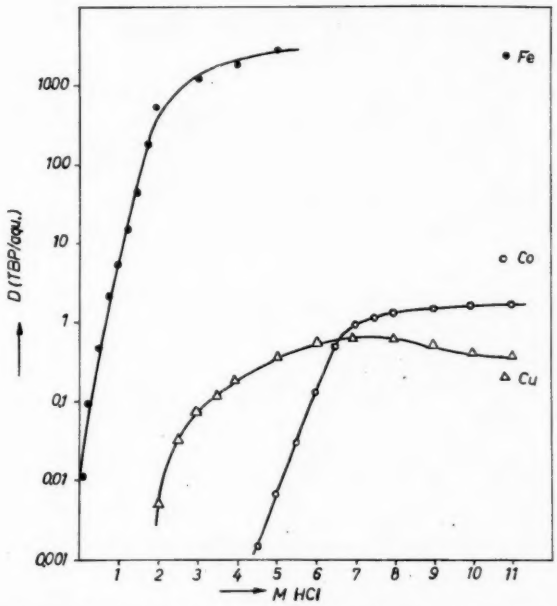

FIG. 1. Distribution of $FeCl_3$, $CoCl_2$, and $CuCl_2$ into TBP using HCl solutions of different molarity.

Separation of Ni, Fe, *and* Co *or* Ni, Fe, *and* Cu *Using* TBP *as an Extraction Agent*

As seen from Figs. 1 and 2 Fe can be easily separated from Co and Cu at about 2 *M* HCl, while a separation of Co and Cu is possible in the range from 2 to 4, 5 *M* HCl at a distribution coefficient$_{max}$ of Cu 0.288. The distribution coefficients of Co and Cu are greatest at high acid concentrations.

Procedure

The chlorides of Ni, Fe, and Co or Ni, Fe, and Cu each in portions of about 100 mg metal were dissolved in 2 *M* HCl. Fe was extracted quantitatively by adding TBP adjusted with 2 *M* HCl as described before, whereas Co(Cu), under these conditions, remains in the aqueous phase. After the acidity of the aqueous solution was increased to 10 *M* HCl for Co, or 8 *M* HCl for Cu, Co(Cu) was separated from Ni in stages by adding 30-ml portions of TBP. As mentioned before, Ni remains nearly completely in the aqueous phase. The chlorides of the metals in the TBP were re-extracted by water and were determined as described before. The procedure was repeated with four single samples and averages of the four results obtained for each element are recorded in Table I for Ni, Fe, Co and for Ni, Fe, Cu in Table II.

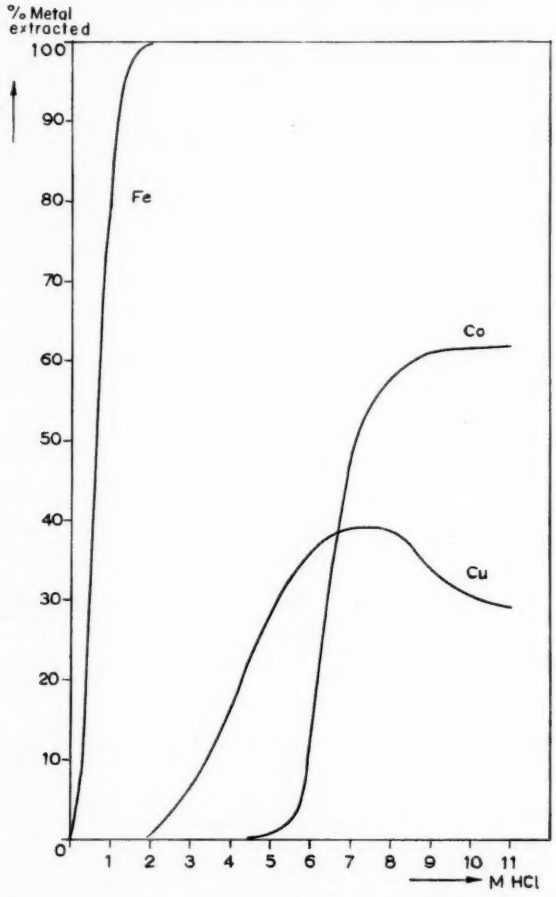

FIG. 2. Effect of hydrochloric acid concentration on the extractability of Fe-, Co-, and Cu-chlorides by TBP.

TABLE I

Separation of Ni, Fe, Co using TBP as an extraction agent

Solution of chlorides	Micrograms applied	Metal found	Recovery (%)
Ni	100.0	98.9	98.9
Fe	99.5	98.7	99.2
Co	98.9	98.0	99.1

Separation of Mn, Fe, Co, Ni, *and* Cu *by Paper Chromatography*

In another publication the author stated that TBP served as a solvent in paper chromatography to separate Ni and Co (11). Further on, TBP was tested also for other elements.

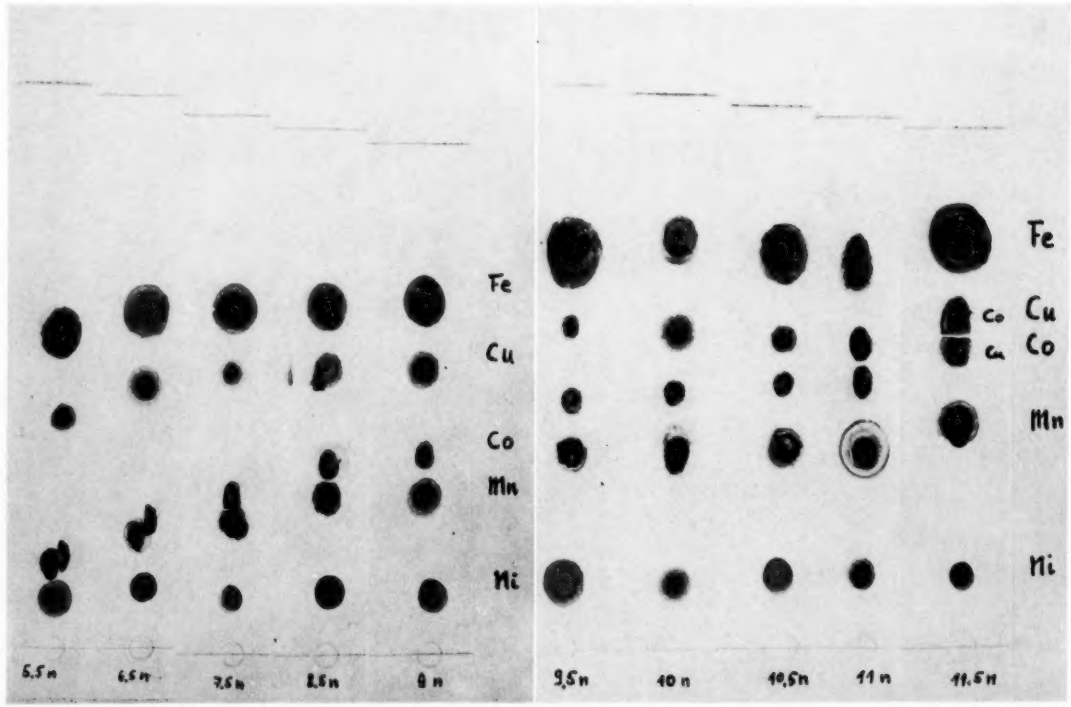

FIG. 3. Flow of Mn, Fe, Co, Ni, and Cu using a TBP/methanol mixture in the ratio 2:1 as a solvent.

The efficiency of TBP proved to be at least equal to that of other agents in the separation of Mn, Fe, Co, Ni, and Cu (12, 13, 14).

TABLE II

Separation of Ni, Fe, Cu using TBP as an extraction agent

Solution of chlorides	Micrograms applied	Metal found	Recovery (%)
Ni	100.0	98.9	98.9
Fe	99.5	98.6	99.0
Cu	101.2	100.1	98.9

Before use TBP was purified and then adjusted with HCl of different molarity as described above. The organic phase was separated and mixed with methanol (reagent grade) in the ratio of two volumes of TBP to one volume of methanol.

Procedure

The chromatograms were developed by ascending chromatography. The paper used was Schleicher and Schüll No. 4023*b* (Whatmann No. 1). Solutions of Mn-, Fe-, Ni-, Co-, and Cu-chlorides each in quantities of about 10 γ per 1 mm^3 were put on the paper. The process took 4 hours at a temperature of 22° C. Fe and Cu were easily identified by their yellow color and Co by its blue color.

In Fig. 3, Fe was marked with $K_4Fe(CN)_6$, Cu with an acetic acid – α-benzoinoxime solution, and Co with α-nitroso-β-naphthol. Ni was identified with an alcoholic solution of dimethyl glyoxime; Mn was first oxidized with sodium peroxide then marked with an acetic acid – benzidine solution (15).

RESULTS

The R_F values of Co, Mn, and Cu recorded in Table III show a significant dependence on the concentration of HCl used to equilibrate TBP. Increasing the concentration of HCl reduces the distance of Co, Mn, and Cu from the liquid front, i.e. the R_F values increase.

TABLE III

R_F values of Mn, Co, and Cu using TBP/methanol mixtures in the ratio 2:1

	TBP adjusted with HCl (molarity)									
	5.5	6.5	7.5	8.5	9.0	9.5	10.0	10.5	11.0	11.5
R_F Mn	0.15	0.20	0.24	0.30	0.31	0.34	0.35	0.36	0.38	0.42
R_F Co	0.16	0.23	0.28	0.35	0.38	0.43	0.46	0.48	0.51	0.61
R_F Cu	0.42	0.48	0.52	0.54	0.56	0.57	0.57	0.57	0.58	0.59

At low concentrations of HCl similar R_F values are obtained for Co and Mn. However, this is optimum for the separation of Cu from Co and Mn. Increasing the concentration of HCl reduces the distance of Co from Cu and at a concentration of 11.5 *M* HCl the R_F value of Co is a little higher than the R_F of Cu.

The flow rates of Ni and Fe are independent of the HCl concentration and roughly proportional to the quantity of methanol present. Fe is always next to the liquid front (see Fig. 3).

SUMMARY

The chlorides of Fe, Co, and Cu were extracted by TBP from an aqueous HCl solution, while Ni was not extracted. Because of the different distribution coefficients of Fe, Co, and Cu, a separation of Ni, Fe, and Co or Ni, Fe, and Cu was possible. Fe can be easily separated from Ni, Co, and Cu at about 2 *M* HCl. After the acidity of the aqueous solution is increased to 10 *M* HCl for Co or 8 *M* HCl for Cu, Co or Cu can be separated from Ni.

TBP also served in paper chromatography as a solvent. Sharp chromatographic separations of the chlorides of Mn, Fe, Co, Ni, and Cu can be obtained using HCl-adjusted TBP. It is recommended that TBP is to be treated with 9 to 10 *M* HCl and mixed with methanol in the proportion 2:1.

With acknowledgments to Diplom-Chemiker H. G. Zimmermann and G. J. Weidmann for their help in translation and scientific discussion and to Mr. U. Mattern for experimental work.

1. K. ALCOCK, G. F. BEST, E. HESFORD, and H. A. C. MCKAY. J. Inorg. & Nuclear Chem. **6**, 328 (1958).
2. H. A. C. MCKAY and T. V. HEALY. Tri-*n*-butyl phosphate as an extracting agent. Anon. Progress in nuclear energy, Series 3, 546–556. Pergamon Press. 1959.
3. A. E. LEVITT and H. FREUND. J. Am. Chem. Soc. **78**, 1545 (1956).
4. M. CHATELETT and C. NICAUD. Chem. Revs. **242**, 1471, 1891 (1956).
5. E. HESFORD, E. E. JACKSON, and H. A. C. MCKAY. J. Inorg. & Nuclear Chem. **9**, 279 (1959).
6. T. V. HEALY, J. KENNEDY, and G. M. WAIND. J. Inorg. & Nuclear Chem. **10**, 137 (1959).
7. D. F. PEPPARD *et al.* J. Phys. Chem. **57**, 294 (1953).
8. D. F. PEPPARD, G. W. MASON, and J. L. MAIER. J. Inorg. & Nuclear Chem. **3**, 215 (1956).
9. J. J. GAL and A. RUVARAC. Bull. Inst. Nuclear Sci. "Boris Kidrich", **8**, 67 (1958).
10. B. LANGE. Kolorimetrische Analyse. Verlang Chemie G.m.b.H., Weinheim/Bergstr. 1956.
11. G. R. WEIDMANN. Can. J. Chem. **37**, 830 (1959).
12. W. J. FRIERSON and D. A. REARICK. Anal. Chem. **30**, 468 (1958).
13. F. H. BURSTALL *et al.* J. Chem. Soc. (London), 1497 (1952).
14. R. A. GUEDES DE CARVALHO. Anal. Chim. Acta, **16**, 555 (1957).
15. F. FEIGL. Spot tests in inorganic analysis. Elsevier Press, Inc., New York. 1958.

RECEIVED JUNE 19, 1959.
PRIVATE CONTRIBUTION.

THE YIELD OF Ba^{140} IN THE THERMAL NEUTRON FISSION OF U^{235} *

D. C. SANTRY† AND L. YAFFE

The fission product Ba^{140} has often been used as a standard in fission yield determinations. These determinations were usually subject to a large error due to uncertainties in the measurement of the various disintegration rates. In 1954, Yaffe *et al.* (1), using 4π β-counting methods, reported a value of $(6.32\pm0.24)\%$ for the yield of Ba^{140} in the thermal neutron fission of U^{235}.

The measurement consisted of a simultaneous, long-term irradiation of natural uranium and boron trifluoride. The Ba^{140} was estimated radiochemically and the depletion in the B^{10} content of the boron was determined mass spectrometrically. The Ba^{140} yield was estimated relative to a value of $\sigma_f/\sigma_B = 0.1456$ where σ_f is the fission cross section of U^{235} and σ_B is the cross section for the reaction $B^{10}(n,\alpha)Li^7$.

**Financial assistance was received from the Atomic Energy Control Board of Canada and the Defence Research Board.*

†*Present address: Chemistry Branch, Atomic Energy of Canada Limited, Chalk River, Ontario.*

Petruska *et al.* (2) introduced an additional self-shielding correction to the above value which they suggested should raise the value of the Ba^{140} yield to 6.55%. The uranium in the above-mentioned irradiation was in fairly massive form. This, coupled with the unpredictable nature of the geometrical arrangement, suggested to the present authors that the experiment be repeated under more favorable circumstances.

Accordingly, an irradiation was performed in a No. 1 self-serve position in the NRX Chalk River nuclear reactor. The uranium trioxide (63.67 mg) was placed in a quartz vial. Into similar tubes were sealed weighed amounts (1.348 and 1.174 mg) of "spec-pure" cobalt wire (0.005-in. diameter) which acted as flux monitors. The material was irradiated for 2.247 days. The neutron attenuations in the uranium and cobalt samples were calculated to be 1.0 and 2.1% respectively. The latter agreed with a similar value which R. E. Jervis of A.E.C.L., Chalk River, was kind enough to give to us for the same type of wire.

On removal from the reactor, the cobalt wires were dissolved and made up to a known volume. Measurements of the quartz vials after the removal of the cobalt wire indicated that the loss by recoil was negligible. A small aliquot of the cobalt solution was placed on a VYNS film and the Co^{60} disintegration rate determined in a 4π β-counter (3). Very small corrections were necessary for absorption in the very thin source and thin VYNS film. A thermal neutron flux value of 9.42×10^{11} n/cm^2 sec was obtained using 36.3 barns (4, 5) for the cross section of the reaction $Co^{59}(n,\gamma)Co^{60}$. Auxiliary measurements showed that the contribution by epicadmium neutrons in this irradiation position to the production of both Co^{60} and Ba^{140} was less than $\frac{1}{2}$%. The fission rate was then determined to be 5.220×10^8 fissions per second using σ_f equal to 571 barns (6). The reactor power was constant during this irradiation, so the normal saturation correction could be used.

The uranium trioxide was dissolved in dilute nitric acid and Ba^{140} was separated using standard methods. Agreement between theoretical and experimental growth and decay curves attested to the fact that both Ba^{140} with its soft β-component and La^{140}, the daughter with its hard β-component, were being measured with equal efficiency.

It can be shown that, if U_0 atoms of U^{235} were irradiated in a thermal flux I of a nuclear reactor for a time T, then at some time t, after removal from the reactor, the following equation would apply:

$$[1] \qquad N\lambda = U_0 I\sigma_f Y_f(1-e^{-\lambda T})e^{-\lambda t}.$$

In the above equation λ is the disintegration constant of the fission product being studied and N is the number of atoms of that nuclide present at time t. Thus $N\lambda$ is the disintegration rate. The fission cross section of U^{235} is represented by σ_f, and Y_f is the probability of formation, or the fission yield of the nuclide under study.

If some cobalt were irradiated simultaneously with and under the same conditions as the U^{235}, then the following equation would obtain:

$$[2] \qquad N_1\lambda_1 = N_{Co} I\sigma_c(1-e^{-\lambda_1 T})e^{-\lambda_1 t}.$$

As before, $N_1\lambda_1$ would be the disintegration rate of Co^{60}, N_{Co} the number of cobalt atoms placed in the reactor, and σ_c the thermal neutron cross section for the reaction $Co^{59}(n,\gamma)Co^{60}$.

If equations [1] and [2] are now divided, the term I cancels, all other quantities are easily measurable, and Y_f, the fission yield, can be determined in terms of σ_f/σ_c.

The fission yield of Ba^{140} was calculated in this manner and found to be (6.36 ± 0.12)%, in excellent agreement with that obtained earlier (1).

ACKNOWLEDGMENT

One of us (D.C.S.) gratefully acknowledges the receipt of a National Research Council Studentship.

1. L. YAFFE, H. G. THODE, W. F. MERRITT, R. C. HAWKINGS, F. BROWN, and R. M. BARTHOLOMEW. Can. J. Chem. **32**, 1017 (1954).
2. J. A. PETRUSKA, H. G. THODE, and R. H. TOMLINSON. Can. J. Phys. **33**, 693 (1955).
3. B. D. PATE and L. YAFFE. Can. J. Chem. **33**, 610 (1955).
4. R. S. CARTER, H. PALEVSKY, V. W. MYERS, and D. J. HUGHES. Phys. Rev. **92**, 716 (1953).
5. L. YAFFE, R. C. HAWKINGS, W. F. MERRITT, and J. A. CRAVEN. Phys. Rev. **82**, 553 (1951).
6. G. J. SAFFORD and E. MELKONIAN. Phys. Rev. Letters, **2**, 189 (1959).

RECEIVED NOVEMBER 27, 1959.
RADIOCHEMISTRY LABORATORY,
DEPARTMENT OF CHEMISTRY,
MCGILL UNIVERSITY,
MONTREAL, QUE.

THE PRIMARY PROCESS IN THE MERCURY-6($^3P_1$)-PHOTOSENSITIZED POLYMERIZATION OF ACETYLENE

ALDEN G. SHERWOOD AND HARRY E. GUNNING

In the reaction of Hg 6($^3P_1$) atoms with acetylene, LeRoy and Steacie (1) have suggested the following possible primary processes:

$$\text{Hg } 6(^3P_1) + C_2H_2 \rightarrow \text{Hg } 6(^1S_0) + H + C_2H \quad [1]$$

$$\rightarrow HgH + C_2H \quad [2]$$

$$\rightarrow HgC_2H + H. \quad [3]$$

An excited molecule mechanism has also been recently suggested (2). However such a sequence could not explain the observed consumption of mercury during the reaction. In the present study, the technique of monoisotopic mercury photosensitization in natural mercury vapor (3, 4, 5, 6, 7, 8) has been employed to determine the extent to which mercury consumption occurs in the primary reaction.

The apparatus used for the investigation was similar to that described in reference 5. The mercury in the electrodeless discharge source contained 95.0% ^{202}Hg. All runs were made at an acetylene pressure of 6.7 mm of Hg. The solid product of the reaction was a yellow deposit which formed on the walls of the spiral quartz reaction cell. The yellow product was treated in separate runs with a variety of reagents to convert the chemically combined mercury to a solution of mercuric ion, from which the mercury was extracted, after neutralization, by electrodeposition. Isotopic analysis of the mercury was carried out on a Metropolitan–Vickers, type MS-2, mass spectrometer. The results are summarized below:

Run No.	Treatment of product	% ^{202}Hg in recovered mercury
A	Solution in hot HNO_3–H_2SO_4	39.3
B	Solution in hot, conc. HCl	33.8
C	Solution in 0.1 *N* HCl	64.0
D	Solution in boiling water	62.7
E	Evacuation for 8 hours followed by solution in hot HNO_3–H_2SO_4	63.0
F	Solution in 2 *N* KI, 0.1 *N* in $Na_2S_2O_3$	32.4
	Natural abundance	29.8

The results show conclusively that there is a primary process involving the formation of a mercury compound. The effects of the various methods of product treatment on the ^{202}Hg-content of the recovered mercury is instructive. In run A the hot HNO_3–H_2SO_4 reagent dissolved both the mercury compound and the cuprene polymer, together with any adsorbed natural mercury. The enrichment in ^{202}Hg was 32%. In run E the system, after reaction, was evacuated for 8 hours to pump off adsorbed natural mercury. The mercury recovered from this run, using the same reagent as in run A, was found to be enriched by 111% in ^{202}Hg. Previous experience has shown that it is very unlikely that all of the adsorbed natural mercury could be removed by this simple evacuation technique. The isotope-diluting effect of adsorbed natural mercury is also shown in run B. The hot, concentrated HCl reagent dissolved only the mercury compound and the adsorbed natural mercury. The cuprene was found to be insoluble under these conditions. The highest ^{202}Hg-enrichment was obtained by treating the product with dilute HCl as in run C. It is likely, however, that exchange reactions are occurring to some extent between dissolved natural mercury and $^{202}Hg^{+2}$ ions in the treatment with dilute HCl in run C and with boiling water in run D. The isotope-diluting effect of adsorbed natural mercury is obviously very extensive in the KI reagent used in run F.

The fact that mercury can be recovered from solution of the mercury product in boiling water would suggest that the primary product is readily hydrolyzed by water. This behavior is in consonance with the primary formation of a mercury carbide, as proposed in step [3].

As a result of this preliminary study it can be said that a mercury compound, probably a mercury carbide, is formed in the primary reaction between Hg $6(^3P_1)$ atoms and acetylene. A detailed investigation is currently underway in this laboratory to determine the specific primary processes operative in the acetylene reaction, and their relative importance.

The authors are indebted to The National Research Council, for financial assistance, and to the Associated Electrical Industries Export, Ltd., for performing the Mass Spectrometric Analyses.

1. D. J. LeRoy and E. W. R. Steacie. J. Chem. Phys. **12**, 117 (1944).
2. S. Shida, Z. Kuri, and T. Furuoya. J. Chem. Phys. **28**, 131 (1958).
3. K. R. Osborn, C. C. McDonald, and H. E. Gunning. J. Chem. Phys. **26**, 124 (1957).
4. H. E. Gunning. Can. J. Chem. **36**, 89 (1958).
5. R. Pertel and H. E. Gunning. Can. J. Chem. **37**, 35 (1959).
6. C. C. McDonald, J. R. McDowell, and H. E. Gunning. Can. J. Chem. **37**, 930 (1959).
7. K. R. Osborn and H. E. Gunning. Can. J. Chem. **37**, 1315 (1959).
8. J. R. McDowell, C. C. McDonald, and H. E. Gunning. Can. J. Chem. **37**, 1432 (1959).

Received November 16, 1959.
Department of Chemistry,
University of Alberta,
Edmonton, Alberta.

SENSITIVE FREQUENCIES. V. THE SENSITIVE AMMINE FREQUENCIES AND ELECTRONEGATIVITIES OF COMPLEX TRANSITION METAL ION RADICALS

J. K. Wilmshurst

The internal vibrational frequencies of the methyl group in the CH_3X derivatives are known to vary (1, 2, 3, 4) with the nature of the substituent X and as these variations are greater than those due to mass effects alone (5), they can be considered to reflect

changes in the potential energy of the system. However, of the eight internal methyl group modes only three, the symmetrical deformation and the rocking modes, vary by a sufficiently large factor with changing X to make any empirical correlations meaningful and it has been shown in a previous publication (4) that the squares of these "sensitive" frequencies depend linearly on the electronegativity of X. Similar results would be expected for other series of the type MH_3X and, in fact, have been observed for the silyl (SiH_3X) derivatives (4).

In the present paper empirical plots of the squares of the symmetrical deformation and rocking frequencies in the ammine series (NH_3X) have been obtained against the electronegativity of X. The sensitive frequencies in the complex transition metal ammine ions have been fitted to these plots and estimates made for the electronegativity of the transition metal in its particular environment. A number of internal and external frequency relations in the MH_3X series are discussed and two are illustrated.

The Electronegativity Relation

In the ammine series, just as in the methyl and silyl series, only the symmetrical deformation (ν_d) and rocking frequency (ν_r) vary by a sufficiently large factor to warrant any reliable empirical correlation to be made. Only two simple NH_3—X molecules, in which the electronegativity of X is known (6) and for which the vibrational spectrum has been completely analyzed (7), are known, $[NH_3 \cdot OH]Cl$ and $[NH_3 \cdot NH_2]Cl$. If the assumption is made that the electronegativity of the mercury atom in $[Hg(NH_3)_2]Cl_2$ is

TABLE I

The ammine rocking and symmetrical deformation frequencies[a]

Compound	ν_d	ν_r	χ_x[b]	Ref.
$[NH_3 \cdot OH]Cl$	1478	1195, 1171	3.83[c]	7
$[NH_3 \cdot NH_2]Cl$	1414	1125, 1105	3.47[c]	7
$[Hg(NH_3)_2]Cl$	1268	719	1.93[d]	8
$[Co(NH_3)_6]Cl_2$	1158	650	1.39	10
$[Co(NH_3)_6]Cl_3$	1325	827	2.32	10
$[Co(NH_3)_5OH]Br_2$	1303	806	(2.19)	10
$[Co(NH_3)_5Cl]Br_2$	1310	840	(2.29)	10
$[Co(NH_3)_5Br]Br_2$	1312	832	(2.29)	10
$[Co(NH_3)_5H_2O]Cl_3$	1325	835	(2.33)	10
$[Co(NH_3)_5NO_2]Cl_2$	1315	850	2.33	10
Trans-$[Co(NH_3)_4(NO_2)_2]Cl$	1300	840	2.25	10
$[Co(NH_3)_3(NO_2)_3]$	1290	815	2.16	10
$K[Co(NH_3)_2(NO_2)_4]$	1265	790	2.02	10
$[Cr(NH_3)_6]Cl_3$	1314	757	(2.13)	10
$[Cr(NH_3)_5Cl]Cl_2$	1290	724	(2.07)	10
$[Cr(NH_3)_5NO_2]Cl_2$	1305	768	(2.11)	10
$[Ni(NH_3)_6]Cl_2$	1175	678	1.50	10
$[Cu(NH_3)_4]SO_4 \cdot H_2O$	1285	732	2.10	10
$[Pt(NH_3)_4]Cl_2$	1350	850	2.46	10
$[Pt(NH_3)_5Cl]Cl_2$	1355	935	2.70	10
Trans-$[Pt(NH_3)_2Cl_2]$	1295	815	(2.21)	10
$[Pd(NH_3)_4]Cl_2$	1304	827	2.25	10
Trans-$[Pd(NH_3)_2Cl_2]$	1250	756	1.90	10
$[Ag(NH_3)_2]_2SO_4$	1215	738	1.74	10
$[Na(NH_3)_4]Cl$	1105	500	1.00	[e]

[a] In cm^{-1}.

[b] Unless otherwise noted, electronegativity values were derived by fitting the sensitive frequencies to Fig. 1. Parentheses imply that compound is not shown in Fig. 1.

[c] Mean value of observed (refs. 9, 13) and calculated (ref. 11).

[d] Assumed the same as that for $Hg(CH_3)$.

[e] G. W. Leonard, E. R. Lippincott, R. D. Nelson, and D. E. Sellers. J. Am. Chem. Soc. 77, 2029 (1955).

the same as that in $Hg(CH_3)_2$, then the infrared spectral data for $[Hg(NH_3)_2]Cl_2$, which have been analyzed (8), can also be used. One further point at zero electronegativity is available if the effect of decreasing electronegativity (χ_X) of X on the rocking frequency in NH_3—X is considered. As $\chi_X \to 0$ the N—X bond strength must go to zero, the molecule falling apart and the rocking frequency going over into a pure rotation. The corresponding deformation frequency is just that for the ammonia molecule (9). The sensitive frequencies, ν_d, ν_r, for these molecules are given in Table I, together with the electronegativity, χ_X, of X.

As discussed elsewhere (4), the pair of lines ν_d^2 versus χ_X and ν_r^2 versus χ_X should be parallel and they are fitted to the four sets of points above* under this condition, the resulting plots being shown in Fig. 1. The analytical expressions for the pair of lines are

$$\nu_d^2 = 3.66\chi + 8.12$$

$$\nu_r^2 = 3.66\chi - 0.78$$

and these can be compared with the expressions for the corresponding lines obtained in the methyl (4), silyl (4), and germanyl† series:

$$CH_3X\begin{cases}\nu_d^2 = 4.21\chi+5.72\\ \nu_r^2 = 4.05\chi-1.78\end{cases}$$

$$SiH_3X\begin{cases}\nu_d^2 = 1.41\chi+4.83\\ \nu_r^2 = 1.40\chi+0.20\end{cases}$$

$$GeH_3X\begin{cases}\nu_d^2 = 1.22\chi+3.54\\ \nu_r^2 = 1.22\chi.\end{cases}$$

If the sensitive ammine frequencies observed (10) in the complex transition metal ions (Table I) are plotted on Fig. 1 in such a way that the deviation of ν_d^2 and ν_r^2 from their respective lines is equal for any molecule, estimates of the electronegativity of the transition metal ion in that configuration can be obtained‡ and these are given in Table I. Of interest is the fact that the electronegativity of the transition metal ion increases with increasing charge, e.g. cobalt and platinum, and that in the series $[Co(NH_3)_n(NO_2)_{6-n}]$ the electronegativity of the cobalt ion increases smoothly as n increases. Electronegativities of the transition metals and ions are only poorly known at present (11) and the method of calculating electronegativities for these elements from a consideration of the nuclear charge at the covalent boundary (12) is not applicable without some modification. Likewise, the method of calculation of group electronegativities (6) would not be applicable to the complex transition metal radicals without modification.

The scatter of the experimental points about the two lines in Fig. 1 is greater than that observed (4) in the methyl and silyl series. However, it must be remembered that in the latter two cases all compounds discussed were in the gaseous state whereas here all the ammines are solid. Thus, in the present case, the sensitive frequencies do not depend on electronegativity alone, but will also depend, though to a much lesser extent, on the type

**For molecules of symmetry C_{3v} the rocking modes are degenerate. For molecules of lower symmetry the average of the squares of the two rocking frequencies is plotted.*

†The pair of lines for the germanyl series was obtained from the data of R. C. Lord and C.M. Steese (J. Chem. Phys. **22**, *542 (1954)) for* GeH_3Cl *with the consideration that in* GeH_3^- *($\chi_X = 0$) the rocking frequency is zero. The line for ν_d^2 versus χ_X was drawn parallel to that for ν_r^2 versus χ_X and gave a deformation frequency for* GeH_3^- *of 595 cm^{-1}.*

‡The meaning of such group electronegativities is, of course, dependent upon the reality of the empirical correlation (but see reference 5 for a more complete discussion).

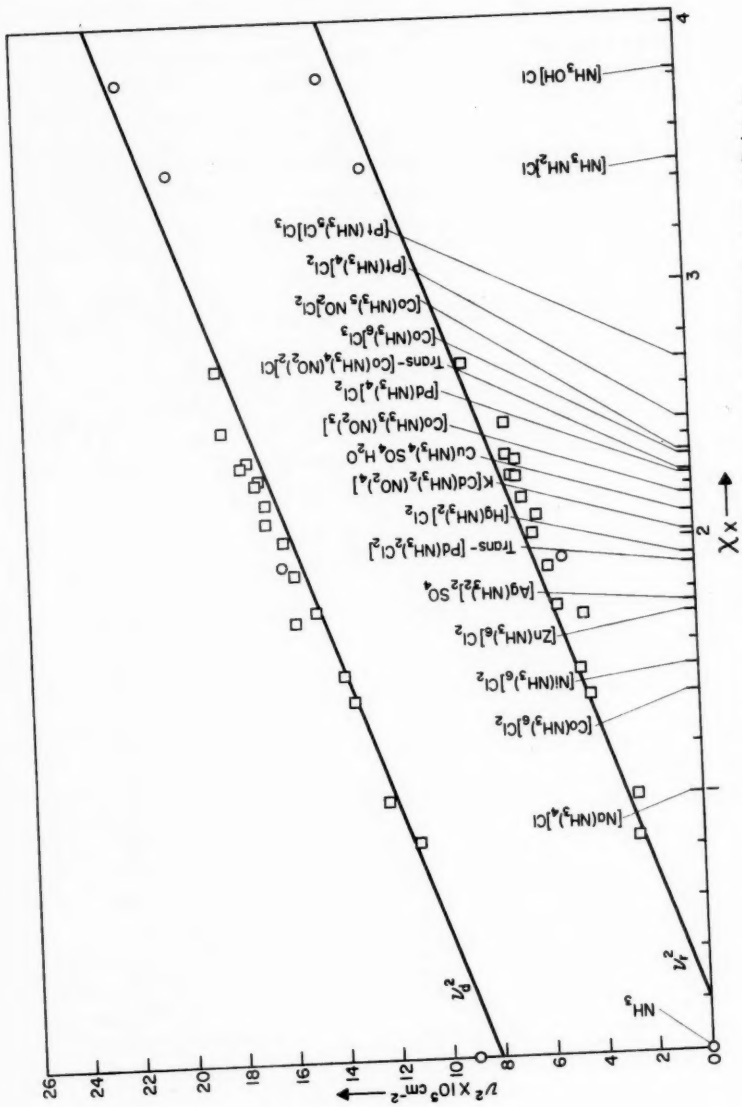

FIG. 1. The plot of ν_r^2 and ν_d^2 against electronegativity for the series of ammine derivatives. ○ Points to which the pair of parallel lines were fitted. □ Points that were fitted to the pair of lines.

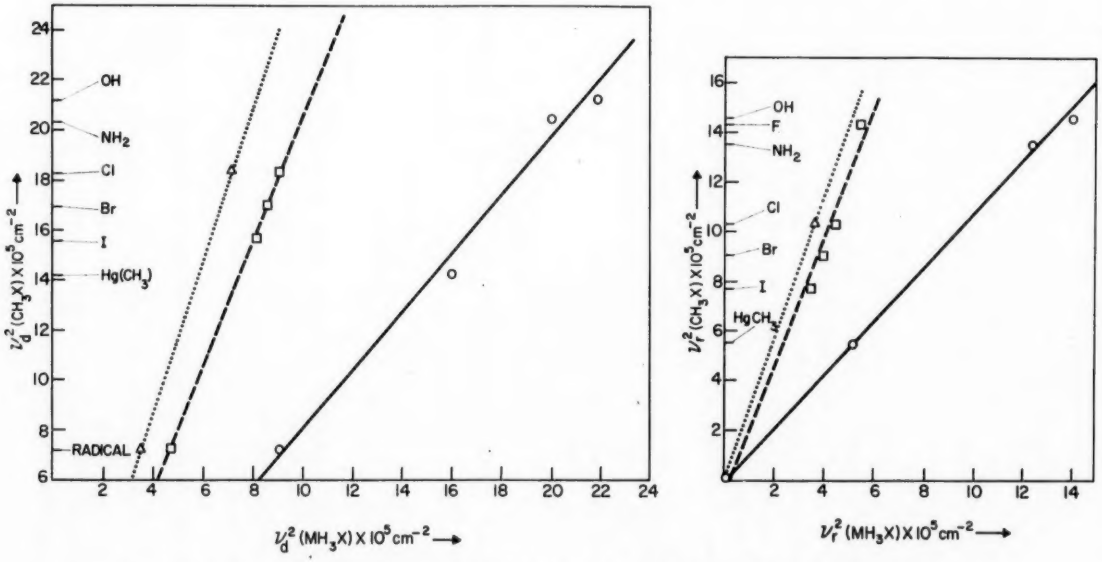

FIG. 2. Plots of ν_d^2 (CH_3X) against ν_d^2 (MH_3X) and of ν_r^2 (CH_3X) against ν_r^2 (MH_3X). —— Amine frequencies. – – – – Silyl frequencies. . . . . Germanyl frequencies.

of inter- and intra-molecular bonding occurring. As this bonding will not, in general, be the same in every system the agreement obtained in Fig. 1 is considered reasonable.*

Frequency–Frequency Relations

It was illustrated in the methyl series that since both ν_d^2 and ν_r^2 depended linearly on electronegativity they would be linearly related to each other. Similar relations must hold between ν_r^2 and ν_d^2 in other MH_3X series.

Since the H—X stretching frequency depends (13) on the electronegativity of X, it would be expected that external relationships exist between it and the internal frequencies of the MH_3-group in the MH_3X series and this has been shown to hold true for the eight internal methyl group frequencies in the CH_3X series (1). Similar relationships would also be expected for the silyl, germanyl, and ammine series. Again, of course, since all the internal frequencies in the MH_3-groups are related to electronegativity, relations must exist between the internal frequencies of one MH_3-group with those of any other and this is illustrated in Fig. 2 for the symmetrical deformation and rocking frequencies.

It can be appreciated that the frequency–frequency relations suggested here are of use to the spectroscopist enabling him to predict the internal vibrational frequencies of any MH_3-group in MH_3X if the internal frequencies of the YH_3-group in YH_3X are known, or even more simply, if the HX stretching frequency is known.

1. L. J. Bellamy and R. L. Williams. J. Chem. Soc. 2753 (1956).
2. G. Herzberg. Infrared and Raman spectra of polyatomic molecules. D. Van Nostrand Company, Inc., New York. 1951. p. 315.
3. J. K. Wilmshurst. J. Chem. Phys. **23**, 2463 (1955).
4. J. K. Wilmshurst. J. Chem. Phys. **26**, 426 (1957).
5. J. K. Wilmshurst. Can. J. Chem. **37**, 1896 (1959).
6. J. K. Wilmshurst. J. Chem. Phys. **27**, 1129 (1957).
7. J. K. Wilmshurst. To be published.
8. E. P. Bertin, I. Nakagawa, S. Mizushima, J. J. Lane, and J. V. Quagliano. J. Am. Chem. Soc. **80**, 525 (1958).
9. G. Herzberg. Infrared and Raman spectra of polyatomic molecules. D. Van Nostrand Company, Inc., New York. 1951. p. 295.
10. G. F. Svatos, D. M. Sweeny, S. Mizushima, C. Curran, and J. V. Quagliano. J. Am. Chem. Soc. **79**, 3313 (1957).
11. W. Gordy and W. J. O. Thomas. J. Chem. Phys. **24**, 439 (1956).
12. W. Gordy. Phys. Rev. **69**, 604 (1946).
13. J. K. Wilmshurst. J. Chem. Phys. **28**, 733 (1958).

Received September 14, 1959.
Research Laboratories,
Parma, P.O. Box 6116,
Union Carbide Corporation,
Cleveland 1, Ohio.

DECARBOXYLATION OF DIMETHYLTRIFLUOROACETOXYARSINE

W. R. Cullen and L. G. Walker

This paper includes the preparation of the new compound dimethyltrifluoroacetoxyarsine and the characterization of fluorodimethylarsine. These compounds are best obtained as follows:

$$(CH_3)_2AsCl + AgOOCCF_3 \rightarrow (CH_3)_2AsOOCCF_3 + AgCl,$$

$$(CH_3)_2AsI + AgF \rightarrow (CH_3)_2AsF + AgI.$$

**Further, some coupling might be expected between the rocking modes when more than one ammine group is attached to the same metal atom, although this would, in general, be slight for the rather large central metal atoms experienced here.*

Dimethyltrifluoroacetoxyarsine is a colorless mobile liquid stable in nitrogen at its boiling point of 136 to 137°. It is moderately stable in the absence of air at 150° but decomposes at 205° to give, among other products, the known compound dimethyltrifluoromethylarsine (1) and carbon dioxide.

$$(CH_3)_2AsOOCCF_3 \rightarrow (CH_3)_2AsCF_3 + CO_2$$

Organometallic haloacetates have been prepared by this method previously (2, 3) and the trifluoroacetates are unusually stable in comparison with other haloacetates (3, 4), probably because of the stability of the C—F bond. The actual mode of decomposition of the haloacetates has been incompletely studied and such decarboxylation reactions may be useful in synthesizing other perfluoroalkyl derivatives of the metals and metalloids. This is now being investigated.

Fluorodimethylarsine is a very reactive liquid isolated by Bunsen (5) but not characterized. The fluorodimethylarsine attacks glass very readily and is unstable to oxygen and moisture. It boils in a nitrogen atmosphere at 75°, a value in good agreement with the estimated 72° (6). The yield of the fluorodimethylarsine from silver fluoride and chlorodimethylarsine is very low. The reaction of iododimethylarsine with the appropriate silver salt gives good yields of dimethylchloro-, dimethylbromo-, and dimethylcyanoarsine. The bromide is not obtainable from the chloride by this method. Similar reactions are known in the bis(trifluoromethyl)arsine series (6) and previous workers have obtained cyanodimethylarsine from chlorodimethylarsine and silver cyanide in benzene solution (7).

A reinvestigation of the reaction between chlorodimethylarsine and dimethylamine has led to the characterization of dimethylaminodimethylarsine, first isolated by Cullen and Emeléus (8).

$$(CH_3)_2AsCl + 2HN(CH_3)_2 \rightarrow (CH_3)_2As{-}N(CH_3)_2 + (CH_3)_2NH_2Cl$$

The amino compound boils at 112° and is unstable to oxygen and moisture. The compounds $(CH_3)_2P{-}N(CH_3)_2$ and $(CF_3)_2M{-}N(CH_3)_2$ (M = As or P) are obtained by similar reactions (8, 9, 10).

EXPERIMENTAL

Apparatus and Technique

Conventional vacuum techniques were used for the manipulation of volatile reactants and products out of contact with moisture and oxygen. Reactions were carried out in sealed Pyrex tubes (50-ml capacity) in the absence of air and light. Infrared spectra were measured on a Perkin–Elmer Model 21 double-beam instrument with rock-salt optics.

Dimethyltrifluoroacetoxyarsine

Chlorodimethylarsine (10.5 g) and silver trifluoroacetate (22 g) were heated to 60° for 15 hours. Trap-to-trap distillation of the volatile products followed by distillation of the least volatile fraction in a nitrogen atmosphere at 760 mm gave dimethyltrifluoroacetoxyarsine, b.p. 136–137° (4.5 g, 32% yield). Anal. calc. for $C_4H_6AsF_3O_2$: As, 34.3%. Found: As, 33.7%.

Decarboxylation of Dimethyltrifluoroacetoxyarsine

The arsine (1.919 g) was heated to 150° for 17 hours and little decomposition was detected. When the same sample was heated to 205° a black solid was slowly deposited, and after 17 hours at this temperature trap-to-trap distillation of the volatile products

gave a fraction condensing at −196° (0.194 g), a fraction condensing at −98° (0.354 g), and a fraction condensing at −64°. Spectroscopic examination showed the most volatile fraction to be mainly carbon dioxide together with traces of silicon tetrafluoride and fluoroform, and the least volatile fraction to contain no unchanged dimethyltrifluoroacetoxyarsine. The middle fraction was dimethyltrifluoromethylarsine (23% yield). Anal. found: mol. wt., 173. Calc.: mol. wt., 174. The infrared spectrum was identical with that of the pure compound (11, 12).

Preparation of Fluorodimethylarsine

Iododimethylarsine (12.5 g) and silver fluoride (12 g) were left at 20° for 48 hours. Distillation of the volatile products in a nitrogen atmosphere at 760 mm gave a 1-g (15% yield) fraction, b.p. 75°, identified as fluorodimethylarsine. Anal. calc. for C_2H_6AsF: As, 60.6%. Found: As, 61.2%.

Reaction of Iododimethylarsine with Silver Chloride

The arsine (8.5 g) and silver chloride (28 g) were heated to 60° for 14 hours. The volatile products were distilled in a nitrogen atmosphere to give 4.5 g (90% yield) of chlorodimethylarsine, b.p. 107° (published b.p. 106.5–107° (13)).

Reaction of Iododimethylarsine with Silver Bromide

The arsine (9.0 g) and silver bromide (38 g) were heated to 60° for 14 hours. The contents of the tube gave in the usual manner 6.0 g (81% yield) of bromodimethylarsine, b.p. 129° (published b.p. 128–129° (13)).

Reaction of Iododimethylarsine with Silver Cyanide

The arsine (12 g) and silver cyanide (13 g) were left at 20° for 48 hours. The solid cyanodimethylarsine (5 g, 76% yield) was sublimed *in vacuo* from the reaction tube. On distillation in a nitrogen atmosphere, the cyanodimethylarsine boiled at 162° (770 mm) (published b.p. 158–160° (730 mm) (7)).

Reaction of Chlorodimethylarsine with Dimethylamine

The arsine (4.8 g) and anhydrous dimethylamine (5.6 g) were left at 20° for 7 days. After removal of the excess dimethylamine by trap-to-trap distillation the least volatile fraction was distilled at 760 mm in a nitrogen atmosphere at 112°, with a middle cut of 2.1 g. This 2.1-g fraction on redistillation again boiled at 112° and was dimethylaminodimethylarsine. Anal. calc. for $C_4H_{12}AsN$: As, 50.3%. Found: As, 50.8%. The infrared spectrum showed the following absorption bands: liquid film: 2980(s), 2890(s), 2860(s), 2820(s), 2780(s), 2480(w), 1453(s), 1423(s), 1259(m), 1237(m), 1177(vs), 1140(m), 1095(w), 1054(s), 946(vs), 880(s), 813(s), 805(m), 775(w), 735(m) cm^{-1}.

ACKNOWLEDGMENT

The authors wish to acknowledge financial assistance from the National Research Council of Canada.

1. R. N. HASZELDINE and B. O. WEST. J. Chem. Soc. 3631 (1954).
2. H. H. ANDERSON and H. FISCHER. J. Org. Chem. **19**, 1296 (1954).
3. H. H. ANDERSON. J. Org. Chem. **20**, 536 (1955).
4. H. H. ANDERSON. J. Org. Chem. **22**, 147 (1957).
5. R. W. BUNSEN. Ann. **37**, 1 (1841).
6. H. J. EMELÉUS, R. N. HASZELDINE, and E. G. WALACHEWSKI. J. Chem. Soc. 1552 (1953).
7. C. S. HAMILTON *et al.* J. Am. Chem. Soc. **69**, 927 (1947).
8. W. R. CULLEN and H. J. EMELÉUS. J. Chem. Soc. 372 (1959).

9. G. S. HARRIS. J. Chem. Soc. 512 (1958).
10. A. B. BURG and P. J. SLOTA. J. Am. Chem. Soc. **80**, 1107 (1958).
11. H. J. EMELÉUS, R. N. HASZELDINE, and R. C. PAUL. Chemical Society No. 93.
12. B. O. WEST. Ph.D. Thesis, Cambridge. 1954.
13. G. W. RAIZISS and J. L. GAVRON. Organic arsenical compounds. The Chemical Catalog Co., Inc., New York. 1923.

RECEIVED NOVEMBER 17, 1959.
CHEMISTRY DEPARTMENT,
UNIVERSITY OF BRITISH COLUMBIA,
VANCOUVER, B.C.

NOTES TO CONTRIBUTORS

Canadian Journal of Chemistry

MANUSCRIPTS

General.—Manuscripts, in English or French, should be typewritten, double spaced, on paper 8½×11 in. **The original and one copy are to be submitted.** Tables and captions for the figures should be placed at the end of the manuscript. Every sheet of the manuscript should be numbered. Style, arrangement, spelling, and abbreviations should conform to the usage of recent numbers of this journal. Greek letters or unusual signs should be written plainly or explained by marginal notes. Characters to be set in bold face type should be indicated by a wavy line below the characters. Superscripts and subscripts must be legible and carefully placed. Manuscripts and illustrations should be carefully checked before they are submitted. Authors will be charged for unnecessary deviations from the usual format and for changes made in the proof that are considered excessive or unnecessary.

Abstract.—An abstract of not more than about 200 words, indicating the scope of the work and the principal findings, is required, except in Notes.

References.—These should be designated in the text by a key number and listed at the end of the paper, with the number, in the order in which they are cited. The form of the citations should be that used in this journal; in references to papers in periodicals, titles should not be given and only initial page numbers are required. The names of periodicals should be abbreviated in the form given in the most recent *List of Periodicals Abstracted by Chemical Abstracts.* All citations should be checked with the original articles and each one referred to in the text by the key number.

Tables.—Tables should be numbered in roman numerals and each table referred to in the text. Titles should always be given but should be brief; column headings should be brief and descriptive matter in the tables confined to a minimum. Vertical rules should not be used. Numerous small tables should be avoided.

ILLUSTRATIONS

General.—All figures (including each figure of the plates) should be numbered consecutively from 1 up, in arabic figures, and each figure referred to in the text. The author's name, title of the paper, and figure number should be written in the lower left corner of the sheets on which the illustrations appear. Captions should not be written on the illustrations.

Line drawings.—Drawings should be carefully made with India ink on white drawing paper, blue tracing paper, or co-ordinate paper ruled in blue only; any co-ordinate lines that are to appear in the reproduction should be ruled in black ink. Paper ruled in green, yellow, or red should not be used. All lines must be of sufficient thickness to reproduce well. Decimal points, periods, and stippled dots must be solid black circles large enough to be reduced if necessary. Letters and numerals should be neatly made, preferably with a stencil (**do NOT use typewriting**), and be of such size that the smallest lettering will not be less than 1 mm high when the figure is reduced to a suitable size. Many drawings are made too large; originals should not be more than 2 or 3 times the size of the desired reproduction. Wherever possible two or more drawings should be grouped to reduce the number of cuts required. In such groups of drawings, or in large drawings, full use of the space available should be made; the ratio of height to width should conform to that of a journal page (5½×7¾ in.) but allowance must be made for the captions. **The original drawings and one set of clear copies (e.g. small photographs) are to be submitted.**

Photographs.—Prints should be made on glossy paper, with strong contrasts. They should be trimmed so that essential features only are shown and mounted carefully, with rubber cement, on white cardboard, with no space between those arranged in groups. In mounting, full use of the space available should be made. **Photographs are to be submitted in duplicate;** if they are to be reproduced in groups one set should be mounted, the duplicate set unmounted.

REPRINTS

A total of 100 reprints of each paper, without covers, are supplied free. Additional reprints, with or without covers, may be purchased at the time of publication.

Charges for reprints are based on the number of printed pages, which may be calculated approximately by multiplying by 0.5 the number of manuscript pages (double-space typewritten sheets, 8½×11 in.) and including the space occupied by illustrations. Prices and instructions for ordering reprints are sent out with the galley proof.

Contents

Yoshio Matsunaga—Magnetic properties of mesonaphthodianthrene - - - 323

Catherine Haggart and C. A. Winkler—The reactions of active nitrogen with cyanogen and CN radicals - - - - - - - - - - - - - - - 329

R. A. Westbury and C. A. Winkler—The reactions of active nitrogen with hydrogen sulphide and carbon disulphide - - - - - - - - - - - - 334

A. F. McKay, D. L. Garmaise, G. Y. Paris, and S. Gelblum—Bacteriostats. III. Oxyamines and their derivatives - - - - - - - - - - - - - 343

R. F. Grant and B. A. Dunell—Proton magnetic resonance absorption in the C-form of stearic acid - - - - - - - - - - - - - - - 359

G. W. King—Electronic potential surfaces of acetylene in LCAO/MO approximation - 365

A. R. G. Lang and S. G. Mason—Tritium exchange between cellulose and water: Accessibility measurements and effects of cyclic drying - - - - - - 373

C. T. Bishop and F. P. Cooper—Separation of carbohydrate derivatives by gas–liquid partition chromatography - - - - - - - - - - - - 388

A. V. Robertson and Léo Marion—The biogenesis of alkaloids. XXV. The role of hygric acid in the biogenesis of stachydrine - - - - - - - - - - 396

Ross Stewart and R. Van der Linden—The acidity of some aromatic fluoro alcohols and ketones - - - - - - - - - - - - - - - - - 399

D. C. Frost and C. A. McDowell—The ionization and dissociation of some halogen molecules by electron impact - - - - - - - - - - - - 407

D. C. Santry and L. Yaffe—Absolute thermal neutron fission yields of U^{235} - - 421

W. R. Cullen—Perfluoroalkyl arsenicals. Part I. The preparation of alkyl perfluoroalkyl arsenicals - - - - - - - - - - - - - - - - - 439

W. R. Cullen—Perfluoroalkyl arsenicals. Part II. The preparation and properties of aryl perfluoroalkyl arsenicals - - - - - - - - - - - - - 445

Ch. R. Engel and R. Deghenghi—Steroids and related products. XIII. The synthesis of 6α-fluoro-17α-bromoprogesterone - - - - - - - - - 452

Notes:

A. Rosenthal and J. P. O'Donnell—Reaction of *syn*-benzaldoxime with carbon monoxide and hydrogen to yield substituted ureas - - - - - - - 457

Gerhard Weidmann—Separation of some heavy metals by solvent extraction and by paper chromatography - - - - - - - - - - - - - - 459

D. C. Santry and L. Yaffe—The yield of Ba^{140} in the thermal neutron fission of U^{235} - 464

Alden G. Sherwood and Harry E. Gunning—The primary process in the mercury-6($^3P_1$)-photosensitized polymerization of acetylene - - - - 466

J. K. Wilmshurst—Sensitive frequencies. V. The sensitive ammine frequencies and electronegativities of complex transition metal ion radicals - - - 467

W. R. Cullen and L. G. Walker—Decarboxylation from dimethyltrifluoroacetoxyarsine - - - - - - - - - - - - - - - - - - 472

Printed in Canada *by* University of Toronto Press